The role of Galectin-3 in the differentiation of neural stem cells

A thesis submitted for the degree of

Doctor of Philosophy

by

Luana Campos Soares



St. Peter's College, University of Oxford

Michaelmas Term 2020

Supervisors:
Prof. Eric O'Neill (University of Oxford)
Prof. Francis Szele (University of Oxford)

The work presented in this thesis was performed at the Department of Oncology, University of Oxford. This study was funded by a Medical Sciences Graduate School Studentship composed of Cancer Research UK (CRUK) and Clarendon Studentships.

Abstract

The role of Galectin-3 in the differentiation of neural stem cells

Luana Campos Soares, St Peter's College

Michaelmas Term 2020

Stem cell therapy harbours a great potential for treating neurodegenerative disorders. However, it is not a commonly used approach due to the complexity of neural stem cell regulatory mechanisms. Galectin-3 is a lectin that activates cellular signalling via interacting with glycoconjugates. Although Galectin-3 is strongly expressed in the subventricular zone neurogenic niche in the brain, its specific functions remain to be elucidated. Here, I show that Galectin-3 is an important regulator of neural differentiation. I found that Galectin-3 depletion *in vivo* altered the number of glia generated from postnatal neural stem cells, indicating an active role in gliogenesis. Using an *in vitro* model of early neural differentiation, I established that Galectin-3 regulates cell polarisation but not expression of neural markers. Finally, I studied the developmental Hippo pathway in this context. I observed that Galectin-3-mediated cell polarisation influences the delivery of the Hippo pathway's main effector, the co-transcriptional factor YAP, to the apical region of neural stem cells. Collectively, these results show that Galectin-3 not only participates in gliogenesis, but also regulates neural differentiation via a mechanism that impacts on cell polarisation and YAP localisation. The findings presented in this thesis help to clarify how neurodevelopment is regulated by offering a new set of integrated molecular mechanisms involved with neural differentiation.

COVID-19 Disruption Statement

This work was affected by COVID-19 lockdown imposed in the UK during the months of March until July of 2020. During that period, I did not have access to the laboratory to conduct the last experiments, compromising the finalisation of important aspects of the thesis.

After the opening of the laboratory, work was resumed but with limited time and access. Unfortunately, this scheme made it particularly difficult to conduct experiments with stem cells, which require daily media change and treatments.

Therefore, the remaining aspects and experiments missing are highlighted in Chapter 6.

Authorship Statement

I confirm that the work presented in this thesis is my own unless indicated. I designed the project with inputs from my supervisors Prof Eric O'Neil and Prof Francis Szele.

Chapter 3 was developed in collaboration with Dr Osama Al-Dalahmah. Electroporations were conducted with the help and guidance of Dr Bin Sun. Victor Lu assisted with free-floating immunohistochemistry, and with the acquisition and quantification of confocal images for Gal-3 KD validation and microglia activation.

Viviana Macarelli helped throughout the establishment of hESCs culture in Chapter 4, with the characterisation of Gal-3 in this model and authored Figure 7.1 B.

All other experiments, quantifications and analyses were done by me with experimental advice from colleagues in both departments.

Copyright © 2020 by Luana Campos Soares

All rights reserved

Acknowledgements

I can still remember the feeling I had when I arrived in Oxford for the first time, after flying (and crying) for 12 hours. I looked out the bus' windows and saw English houses, just as I had imagined them so many times. The realisation that this was my dream coming true hit me intensely. I remembered how far I had travelled for that moment and all the amazing people who had supported me along the way. For those who encouraged me to try when I did not dare, and for those who held my hand when I needed it the most: thank you.

To my supervisors, Prof. Eric O'Neill and Prof. Francis Szele. What a privilege to have the guidance and the experience of both of you throughout these years. Thank you for trusting me since the beginning. You have always valued my opinion and heard what I had to say, which I appreciate above everything. Thank you for the discussions, support, and for offering me the opportunity to nourish and become the scientist I am today.

My gratitude also goes to Florian, Dr Frances Willenbrock, and Dr Asmita Thapa, for proofreading and providing invaluable feedback on the thesis writing. Thank you to Dr Blanca Torroba, Dr Julie Davies, Dr Maria Laura Tognoli, Dr Fiona Bangs, Dr Anna Hoerder-Suabedissen, and many other for the precious advice and input throughout my DPhil. To Dr Bin Sun, for being the most patient instructor. I appreciate the collaboration with Dr. Osama Al Dalahmah, which has opened so many doors for this project. I would like to thank the contributions of Victor Lu and Viviana Macarelli for the conclusion of this work. Vivana, thank you for the almost one year of partnership and friendship, seeing your career progress will always make me proud.

I have had the greatest luck of having the support of two amazing groups of people: the Szele lab and the EON lab. To my dearest Blanca, Ksenia, Penny, Julie, Farah, Bin, Yichen, Martin and many other past and present members of the Szele lab, thank you for teaching me what living in Oxford would feel like. To my friends, Blanca and Ksenia, I share many of the happiest memories of these years with you, and I will bring you in my heart forever. I would also like to thank Asmita, Sophie, Maria, Daniela, Frances, Mary, Dafni, Simone, Michael, Dan, and many other past and present EON

lab members. Sharing my daily routine (and coffees) with you was what kept me going until the end. There has never been such a great group as ours, and that is a fact. Each one of you, at some point, has offered me a hand and gave me words of encouragement, for which I will be eternally grateful. Thank you also to all my friends, colleagues and staff of DPAG and Department of Oncology, in special to Javier, Giuliana, Florian, Ashwin, Sovan, Rafael, Kay, Jen, and Sam.

To my family in Oxford: Sergio, Asmita, and Nico. To have formed such strong bonds worthy of the name family was the most unexpected and precious present that Oxford has given me. Having had people to come back to and a place to call home is perhaps what I value the most about my years here. Sergio, you have always been my safe harbour. From the beginning to the end, and for the years still to come – my life is better since you have joined it. Asmita, you are the most caring and generous person I have ever met, and the best friend I could have ever asked for. Nico, thank you for always listening to me and for the precious memories I have of us. There are no words to describe how lucky I am for having you three next to me.

I am also so grateful for other friends that Oxford has brought to me. Florian, you more than anyone else has helped me to see the light in the end of the tunnel, and I will be forever grateful for your support. To my new housemates who have endured me during this stressful time with so much kindness: thank you. Charlotte, Ashwin and Prashanti: thank you for the cookies, the food, the cheering me up that made absolutely all the difference. To my St. Peter's college and Clarendon friends, who were the first ones to receive me in Oxford, in special to Jen, Jamie, Oly, Arne and Chris, thank you for welcoming me with such an open hearth. Thank you also to my Brazilian in Oxford friends, in special to Nati, Vinicius, Barbara, Giuliana, Ivan, Darlan and Mari, for never giving up on our friendship even at times when I was more distant.

I would like to thank some people in Brazil who have believed in me and supported me along the way. To dear colleagues and professors from the UNESP Botucatu Bio XLV class, thank you for sharing those precious years of professional and personal growth. A special thank you to my brilliant past supervisors, Prof. Maeli Dal Pai, Dr Glaucia Hajj and Dr Martin Roffe. In the name of my dearest friends Fernanda and Gabi, thank you to all the wonderful past lab friends, colleagues and staff from

LBME UNESP and CIPE ACCamargo. I simply would not have gotten this far without you. To my friends now and ever: Carol, Regis, Marcela, Lucas and Marcelo, and all my beloved friends in Brazil, may we continue to cherish our friendship as we have done for all these years we were kept apart.

During my years in Oxford, I would frequently be confronted with the greatest feeling of “saudades”, of my country, my friends and above all, my family. To my mother Lucia, thank you for teaching me how to be brave and for always pushing me forward and never letting me down, no matter what. Thank you to my grandma (Vó Sonia, *in memoriam*) and to my grandpa (Vô Paulo, *in memoriam*), for teaching me to always look up. To my auntie Heloisa Galvão for having trusted and supported me since the very beginning of my career. To my dearest sister Luiza; my loved aunties Mina, Soninha, Bia (*in memoriam*), Claudia and Lilian; cousins Renata, Thais, Cassio, Nicole, De, Tiz, Sofia; my grandparents Vó Ilma and Vô João; my father Luiz and my brother Cristian – thank you for being the most amazing family in the world. I love you all.

Finally, thank you to CRUK and Clarendon for funding my studies in Oxford. This DPhil would have not been possible without your support.

Thank you all!

Table of contents

Abstract ..... **II**
COVID-19 Disruption Statement ..... **III**
Authorship Statement ..... **IV**
Acknowledgements ..... **V**
Table of contents ..... **VIII**
List of Tables ..... **XI**
List of Figures ..... **XII**
List of Abbreviations ..... **XIV**

Chapter 1
Introduction **1**
1.1 Stem cells and neural development 2
1.1.1 Stem cells 2
1.1.2 Pluripotent stem cells as an *in vitro* research model 3
1.1.3 Development of the Central Nervous System 7
1.1.4 Neurulation overview 8
1.1.5 Cellular and molecular mechanisms of neurulation 11
1.1.6 Neural stem cell lineage progression 17
1.1.7 The subventricular zone 20
1.1.8 *In vitro* differentiation of neural stem cells 23
1.2 Galectin-3 26
1.2.1 Introduction to glycoconjugates and lectins 26
1.2.2 Galectin-3 overview 28
1.2.3 Gal-3 expression during embryogenesis 36
1.2.4 Gal-3 in the brain and neural development 37
1.3 The Hippo pathway 41
1.3.1 Pathway overview 41
1.3.2 Hippo pathway in neural development 43
1.4 Research question 46

Chapter 2
Material and Methods 47
2.1 General laboratory reagents 48
2.2 *In vivo* brain electroporation 48
2.3 Tissue collection and microtomy 51
2.4 Brains sections provided 52
2.5 Immunofluorescence of free-floating brain sections 52
2.6 Image analysis and quantifications of brain sections 53
2.7 Cell lines and culture 54
2.8 Differentiation assay 57
2.9 Transient transfections 57
2.10 Cell treatments 59
2.11 Western Blotting 60
2.12 Immunoprecipitation 63
2.13 Immunofluorescence of hESCs 64
2.14 Statistics 66

Chapter 3
The role of Galectin-3 in SVZ gliogenesis in mice 67
3.1 Introduction 68
3.2 *In vivo* brain electroporation 70
3.3 Galectin-3 Knockdown validation 73
3.4 Galectin-3 is necessary for postnatal striatal gliogenesis 76
3.5 Study of cell fate shift upon Galectin-3 modulation 78
3.6 Galectin-3 overexpression did not induce apoptosis or inflammation 79
3.7 Discussion 85

Chapter 4
The role of Galectin-3 in neural differentiation of hESCs 89
4.1 Introduction 90
4.2 Neural differentiation of H9 stem cells 91
4.3 Galectin-3 during neural differentiation 96
4.4 Modulation of Galectin-3 did not alter expression of neural markers 97
4.5 Galectin-3 extracellular inhibition disturbed rosette formation 100
4.6 Galectin-3 interaction with integrins 103

4.7 Discussion 106

Chapter 5

The role of the Hippo pathway in neural differentiation of hESCs and its involvement with Galectin-3-induced polarisation 110

5.1 Introduction 111
5.2 Galectin-3 localises towards the apical region in early neural induction 112
5.3 Expression and localisation of YAP during neural differentiation 114
5.4 Galectin-3 depletion does not affect YAP expression 118
5.5 YAP remains nuclear upon Galectin-3 blocking during neural induction 120
5.6 Expression and localisation of RASSF1A during neural induction 122
5.7 Discussion 124

Chapter 6

Discussion 128

6.1 Gal-3 role in pSVZ gliogenesis 129
6.2 Gal-3 role in hESCs neural differentiation 131
6.3 Conclusion 135
6.4 Remaining aspects 136

References 137

Appendices 176

Appendix A. Neural differentiation using EB protocol 176
Appendix B. Gal-3 and YAP at the junctional complex 179
Appendix C. ReNCell® as an *in vitro* model of neural differentiation 181
Appendix D. Galectin-3 and cancer 183
Appendix E. Free-floating antibodies specificity shown via secondary-only controls 187

List of Tables

Table 1. Short-hairpin sequences 49

Table 2. Antibodies used for free-floating immunohistochemistry 53

Table 3. siRNA sequences used 58

Table 4. Antibodies used for hESCs experiments 65

List of Figures

Figure 1.1. Early embryonic development.....4

Figure 1.2. Primary and secondary neurulation. 10

Figure 1.3. Mechanism of neurulation. 11

Figure 1.4. Neural stem cell progression.....19

Figure 1.5. Neural rosettes resemble neurulation. 24

Figure 1.6. Galectin subtypes.....28

Figure 1.7. Galectin-3 structure and carbohydrate recognition. 30

Figure 1.8. Galectin-3 extracellular interactions. 32

Figure 1.9. The Hippo pathway. 42

Figure 3.1. *In vivo* brain electroporation. 71

Figure 3.2. Plasmids used for Gal-3 *in vivo* modulation. 73

Figure 3.3. Validation of Gal-3 knockdown.....75

Figure 3.4. Gal-3 knockdown decreases striatal gliogenesis at 17 DPE. 76

Figure 3.5. Gal-3 knockout decreases striatal gliogenesis at 17 DPE. 77

Figure 3.6. Gal-3 knockout could not be used for cell fate at 17 DPE. 79

Figure 3.7. Gal-3 OE did not induce apoptosis at 3 DPE. 81

Figure 3.8. Microglia morphological classification. 83

Figure 3.9. Gal-3 OE did not activate microglia in the pSVZ. 84

Figure 4.1. Neural induction in H9 cells.....92

Figure 4.2. Monolayer culture of H9 form neural rosettes. 94

Figure 4.3. Rosette formation follows multiple steps. 95

Figure 4.4. Gal-3 levels during neural induction. 96
Figure 4.5. Recombinant Gal-3 did not affect neural markers 98
Figure 4.6. Gal-3 depletion did not affect levels of Pax6. 99
Figure 4.7. Secreted Gal-3. 100
Figure 4.8. Gal-3 inhibition disturbed the formation of rosettes. 102
Figure 4.9. Integrin isoforms during neural induction. 103
Figure 4.10. Gal-3 interaction with integrins. 105
Figure 5.1. Gal-3 localisation during first days of neural induction. 113
Figure 5.2. YAP expression during neural induction. 115
Figure 5.3. YAP and P-YAP localisation during neural differentiation. 117
Figure 5.4. Effect of Gal-3 modulation on YAP expression and phosphorylation. 119
Figure 5.5. YAP localisation is affected by inhibition of Gal-3. 121
Figure 5.6. R1A expression during neural induction. 123
Figure 6.1. Gal-3 in early neural differentiation. 134
Figure 7.1. Generation of astrocytes using the EB protocol. 177
Figure 7.2. R1A during EB neural induction 178
Figure 7.3. Gal-3 is not at the junctional complex. 180
Figure 7.4. Gal-3 and the Hippo pathway in ReNCell® 182
Figure 7.5. Gal-3 and Cancer 186
Figure 7.6. Free-floating antibodies specificity. 187

List of Abbreviations

%	Percentage
°C	Celsius degree
^{14}C	Carbon-14
A.caspase3	Activated caspase 3
AIM	Astrocyte induction media
AJ	Adherent junction
Akt	RAC-alpha serine/threonine-protein kinase
aPKC	Protein kinase C
ARL13B	ADP-ribosylation factor-like protein 13B
aSVZ	Adult SVZ
AU	Arbitrary units
AURKA	Aurora kinase A
BB	Basal body of the cilium
Bcl-2	Bcl2-associated agonist of cell death
BMP	Bone morphogenetic protein
BMPR	BMP receptor
BrdU	Bromodeoxyuridine
BSA	Bovine serum albumin
Ca++	Calcium
Cadherin	Calcium dependent adhesion protein
CEACAM3	Carcinoembryonic antigen-related cell adhesion molecule 3
CNS	Central nervous system
CO_2	Carbon dioxide
Crb2	Crumbs homolog 2
CRD	Carbohydrate-recognition domain
Cre	Causes recombination
CX	Cortical ReNcell®
DAPI	4’,6-diamidino-2-phenylindole
DLHP	Dorsolateral hinge point
DMEM	Dulbecco's modified eagle medium
DMEM/F-12	Dulbecco's modified eagle medium/nutrient mixture f-12
DNA	Deoxyribonucleic acid
DPBS	Dulbecco’s phosphate-buffered saline
DPE	Days post electroporation
DTT	Dithiothreitol
EB	Embryoid body
ECM	Extracellular matrix

EDTA	Ethylenediaminetetraacetic acid
EGF	Epidermal growth factor
EGFR	EGF receptor
EGTA	Ethylene glycol tetraacetic acid
ER	Endoplasmic reticulum
ESCRT	Endosomal sorting complex required for transport
ESCRT-I	Endosomal sorting complex required for transport I
ESCs	Embryonic stem cells
Fas	Fas cell surface death receptor
FAK	Focal adhesion kinases
FAT1	Protocadherin fat 1
FceRI	High-affinity IgE receptor
FcγRII	IgG Fc receptor II-b
FGF	Fibroblast growth factor
flox/flox	Flanking/flanked by LoxP (locus of X-over P1)
g	Grams
Gal	Galactose
Gal-3	Galectin-3
GAPDH	Glyceraldehyde-3-phosphate dehydrogenase
Gemin4	Gem-associated protein 4
GFAP	Glial fibrillary acidic protein
GFP	Green fluorescent protein
Glc	Glucose
GlcNAc	N-Acetylglucosamine
GRB2	Growth factor receptor-bound protein 2
GSK3β	Glycogen synthase kinase-3 beta
Gαi	Heterotrimeric G protein αi-subunit
h	Hour
H3	Histone 3
HDAC6	Histone Deacetylase 6
hESCs	Human embryonic stem cells
HRP	Horseradish peroxidase
Iba1	Ionized calcium-binding adapter molecule 1
ICM	Inner cell mass
IF	Immunofluorescence
IgG	Immunoglobulin G
$IDH1^{R132H}$	Isocitrate dehydrogenase R132H mutation
IP	Immunoprecipitation
IP/LB	Immunoprecipitation lysis buffer
iPSCs	Induced pluripotent stem cells

IVC	Ventilated cages
JAK/STAT	Janus kinase/signal transducer and activator of transcription
KH_2PO_4	Potassium dihydrogen phosphate
Klf4	Kruppel-like factor 4
KRas	GTPase KRas
L	Liter
Lac	Lactose
LacNAc	N-Acetyllactosamine
LAMP	Lysosome-associated membrane glycoproteins
LATS1/2	Large tumour suppressor 1 and 2
LB	Lysogeny broth media
LGALS3	Gal-3 gene
LiCl	Lithium-chloride
LIF	Leukaemia inhibitory factor
LIN28	Lin-28 homolog
lox	Locus of X-over P1
LRRK2	Leucine-rich repeat serine/threonine-protein kinase 2
LV	Lateral ventricle
M	Molar
MDCK	Madin-Darby canine kidney
MEFs	Mouse embryonic fibroblasts
mg	Milligram
Mg++	Magnesium
Mgat5	B1,6-N-acetylglucosaminyl transferase
MHP	Medial hinge point
min	Minutes
ml	Millilitre
mm	Millimetres
mM	Millimolar
MMS	Medial migratory stream
MOB1	Mps one binder
ms	Millisecond
MST1/2	Mammalian STE20-like protein kinase 1 and 2
MUC4	Mucin-4
n	Sample size
Na_2HPO_4	Sodium phosphate dibasic anhydrous
NaCl	Sodium chloride
NaH_2PO_4	Sodium phosphate monobasic
Nanog	Homeobox protein NANOG
NC	Notochord

NCPr	Notochordal precursor
NEP	Neuroepithelial cells
ng	Nanogram
NIM	Neural induction media
nM	Nanomolar
nm	Nanometre
Notch	Neurogenic locus notch homolog protein
NP40	Nonidet P-40
NPHP	Nephrocystin
NSC	Neural stem cell
OB	Olfactory bulb
Oct4	Octamer-binding protein 4
OE	Overexpression
Olig2	Oligodendrocyte transcription factor 2
OligPr	Oligodendrocyte progenitors
p	P-value
P-YAP	Phosphorylated YAP at S127
P2	Postnatal day 2
p73	Tumor protein p73
PAR	PDZ scaffold proteins
Pax6	Paired box protein Pax-6
PB	Phosphate buffer
PBS	Phosphate buffered saline
PBS-T	PBS-tween
PBS+	Blocking solution for free-floating sections
PCP	Planar cell polarisation
PDGF	Platelet-derived growth factor
PDGFR	PDGF receptor
PFA	Paraformaldehyde
pH	Potential of hydrogen
PINS	Partner of inscuteable
PI3K	Phosphoinositide 3-kinase
PrE	Primitive endoderm
PSI	Pounds per square inch
pSVZ	Postnatal SVZ
R1A	RASSF1A
RASSF1A	Ras association domain-containing protein 1 A
rcf	Relative centrifugal force
RG	Radial glia
RMS	Rostral migratory stream

RNA	Ribonucleic acid
ROCK	Rho-associated kinase
ROI	Region of interest
rpm	Rotation per minute
RT	Room temperature
RTK	Receptor tyrosine/kinase
RUNX	Runt-related transcription factor
S-phase	Synthesis phase
S100β	S100 calcium binding protein B
S127	Serine 127
SARAH	SAv/RAssf/Hippo domain
SAV1	Salvador homolog 1
scRNAseq	Single cell RNA sequencing
sec	Seconds
SEM	Standard error of the mean
Ser	Serine
SFK	Src-family kinase
shGal-3	Short hairpin RNA targeting Gal-3
Shh	Sonic hedgehog
shNT	Non-target sequence
shRNA	Short hairpin RNA
siGal-3	Small interfering RNA targeting Gal-3
siNT	Non-target sequence
siRNA	Small interfering RNA
SMAD	Mothers against decapentaplegic homolog
SMADi	SMAD inhibitor
snRNPs	Small nuclear ribonucleoproteins
Sox2	Transcription factor SOX2
ssDNA	Single strand DNA
STR	Striatum
SVZ	Subventricular zone
Tam-IDH1-KI	Tamoxifen-inducible $IDH1^{R132H}$ knockin
TAP	Transit amplifying progenitor
TAZ	PDZ-binding motif
TCF3	Transcription factor 3
TCR	T-cell receptors
TE	Trophectoderm
TEAD	TEA domain transcription factors
TF	Transcriptional factors
TFEB	Transcription factor EB

TFRC	Transferrin receptor protein 1
TGFβ	Transforming growth factor beta
TJ	Tight junction
TLR4	Toll like receptor 4
TRIM 16	Tripartite motif-containing protein 16
Tris-HCl	Tris hydrochloride
Tsg101	Tumor susceptibility gene 101 protein
V	Volt
V1	Vector 1
V2	Vector 2
VM	Midbrain ReNcell®
Vps4	Vacuolar protein sorting-associated protein 4A
WB	Western blotting
YAP	Yes-associated protein
ZO1	Zonula occludens 1
αGal-3	Antibody anti-Gal-3
αIgG	Antibody anti-IgG
µg	Microgram
µl	Microliter
µm	Micrometre
µM	Micromolar

Chapter 1

Introduction

1.1 Stem cells and neural development

1.1.1 Stem cells

The ability of an organism to regenerate backdates to primitive phyla such as sponges and cnidarians (Bosch, 2009; Funayama, 2018). This fascinating capability is preserved in some vertebrates, for example, salamanders that can regrow a limb after amputation (Joven et al., 2019). Humans and other mammals no longer possess such outstanding plasticity. Still, a more limited potential of tissue repair exists, to a greater or lesser extent, including in those regions presumed less likely to renovate such as the brain.

We know that this regenerative ability is provided by stem cells, which have been the focus of developmental and regenerative research for many years. Studying them is not only important for understanding the normal process of development and embryogenesis but it is also essential for uncovering possible targets of regenerative therapy (Gurusamy et al., 2018; Kelava and Lancaster, 2016).

Although the search for a complete understanding of stem cells is still ongoing, they can quite simply be defined by the ability to self-renew multiple times and to give rise to daughter cells that differentiate into several phenotypes (Potten and Loeffler, 1990). Stem cells self-renew through symmetric division generating two identical daughter cells. This is a process essential for amplification and maintenance of the stem cell pool, especially at the early stages of organ development. Alternatively, stem cells can divide asymmetrically, generating one stem cell and one more specialised cell that can continue to divide and then differentiate or that can undergo differentiation directly. Asymmetric division occurs when specific factors acquire a polarised intracellular distribution before

mitosis, resulting in unequal segregation of cell fate determinants in the daughter cells. Likewise, extrinsic factors can orientate the direction of mitosis causing spatial separation of the daughter cells where only one will continue to receive influence from the stem cell niche. In both cases, the two daughter cells will have different fates with one of them being more specialised or differentiated (Knoblich, 2010).

Stem cells can be categorised according to their differentiation potential, a feature called potency. The potency grade corresponds to the number of possible cell types generated from a given cell. Totipotent stem cells, from the Latin *totipotentia* - the ability for all the things, carry the highest potential grade possible, since they can generate all the cells of the organism as well as placental cells that arise during development. Totipotent cells can only be found from the zygote to the end of the cleavage period of embryogenesis, or morula stage. Another class of stem cells, pluripotent stem cells, from the Latin *pluripotentia*- the ability for many things, are found in the inner cell mass (ICM) of the blastocyst and can differentiate into the three germ layers of the embryo (Figure 1.1 A). Finally, multipotent stem cells give rise to daughter cells that are committed to the fate of their tissue of origin (Fortier, 2005; Weissman, 2000).

1.1.2 Pluripotent stem cells as an *in vitro* research model

Five days after fertilisation, the blastocyst is formed consisting of an inner cell mass (ICM) of pluripotent stem cells surrounded by an outer layer trophectoderm (TE) which will generate extra-embryonic cells (De Paepe et al., 2014) (Figure 1.1 A). The ICM retains the ability to generate the entire organism, which characterises its pluripotency

(De Los Angeles et al., 2015). Due to this potential, *in vitro* culture of pluripotent cells has proven to be of vital importance for research in development and regenerative biology.

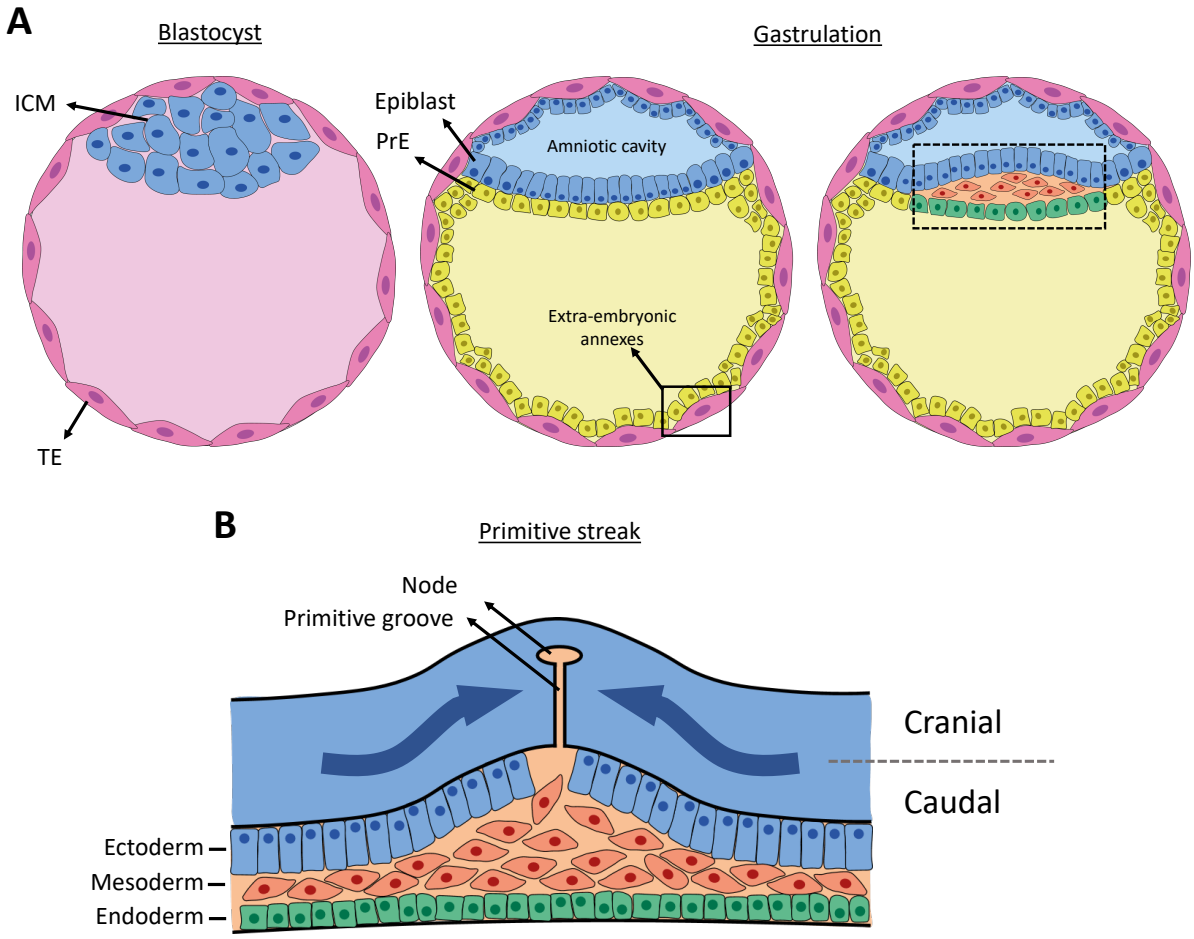


Figure 1.1. Early embryonic development

A) Schematic of early stages of embryonic development. The blastocyst in composed of an inner cell mass (ICM) of pluripotent stem cells and an external layer of cells called trophectoderm (TE). During Gastrulation, the ICM differentiate into the epiblast and the primitive endoderm (PrE). While TE and PrE are responsible for generating extra-embryonic annexes, the epiblast generates the embryo. B) Amplified detail of the dashed box in A, showing the differentiation of epiblast. A thickening of the epiblast generates a structure called the primitive streak, which is the first to define body axes. This structure develops a depression called primitive groove and a primitive node at the most cranial portion. Cells from the epiblast move in the direction indicated by blue arrows into the primitive groove and node to generate cells of the three germ layers: ectoderm, mesoderm and endoderm. Adapted from (Barresi and Gilbert, 2020).

Pluripotent cells derived from the mouse ICM were successfully isolated for the first time in 1981, opening the way for similar following attempts in primates and humans (Evans and Kaufman, 1981; Thomson et al., 1998; Thomson and Marshall, 1998). The North American developmental biologist James Thomson was the pioneer in establishing human embryonic stem cells (hESCs) derived from the ICM of human blastocysts in 1998. This study described five different cell lines, with H1 and H9 still being the most commonly used hESCs in developmental research, over 20 years after the initial publication (Guhr et al., 2018; Scott et al., 2009).

Embryonic stem cell studies helped to elucidate the main functional players and markers of pluripotency, which included the transcription factors Homeobox protein NANOG (NANOG), POU domain, class 5, transcription factor 1 (POU5F1, also known as Octamer-binding protein 4 or Oct4), and Transcription factor SOX2 (SOX2). These factors not only share many target genes but also act in combination to maintain pluripotency and self-renew, and to block differentiation. (Boiani and Scholer, 2005; Boyer et al., 2005). In fact, the subsequent breakthrough in stem cell research was the establishment of induced pluripotent stem cells (iPSCs), generated upon the introduction of specific transcription factors in somatic cells which then return to pluripotency: Oct4, SOX2, c-Myc and Kruppel-like factor 4 (Klf4). Surprisingly, NANOG was not required for iPSCs production but it was indeed expressed by them (Takahashi et al., 2007; Takahashi and Yamanaka, 2006). Thomson's group have also described four alternative factors for cell reprograming: Oct4, SOX2, NANOG and lin-28 homolog (LIN28) (Yu et al., 2007). Patient-derived or disease-specific iPSCs hold enormous promise for regenerative medicine research.

Many pathways are known to promote expression of NANOG, Oct4, or SOX2 and therefore, regulate pluripotency. The fibroblast growth factor (FGF) was one of the first factors identified as required for the undifferentiated proliferation of hESCs (Amit et al., 2000; Levenstein et al., 2006; Xu et al., 2005a). Additionally, components of the transforming growth factor beta (TGFβ) superfamily have been extensively implicated in pluripotency maintenance. For example, the secretory proteins TGFβ, Nodal and Activin promote self-renewal and block neural differentiation through activation of Mothers against decapentaplegic homolog (Smads) 2/3, which can bind to promoters resulting in the upregulation of genes essential for pluripotency (James et al., 2005; Park, 2011; Vallier et al., 2009; Xu et al., 2008). The Wnt canonical pathway is also important to maintain hESCs self-renewal (Sato et al., 2004). Wnt acts through the inhibitory phosphorylation of Glycogen synthase kinase-3 beta (GSK3β) causing β-catenin nuclear localisation and transcription of target genes (Moon et al., 2002). All the three pathways described above, FGF, TGFβ, and Wnt, can block bone morphogenetic protein (BMP) signalling, which has been reported to induce differentiation and impair pluripotency in hESCs (Haegele et al., 2003; Pera et al., 2004; Xu et al., 2008; Xu et al., 2002; Xu et al., 2005b). BMP ligands act upon binding to serine/threonine kinase receptors (BMPR) type I and II, which dimerise and become active. Activated type I receptors are phosphorylated and regulate Smads 1/5/8, which, in combination with the co-mediator Smad4, translocate to the nucleus to promote gene transcription (Wang et al., 2014a).

Collectively, these molecules and their signalling pathways are essential to support pluripotency during the culture of hESCs *in vitro*. Initially, hESCs were co-cultured with a feeder layer of mouse embryonic fibroblasts (MEFs), which release growth factors in the

media (Villa-Diaz et al., 2013). However, there were other factors secreted which, although important to sustain mouse ESCs, did not support human ESCs, for example, leukaemia inhibitory factor (LIF) and BMP4 (Ludwig et al., 2006b). It was evident that a defined media for hESCs was needed, leading the research group of Thomson to develop a feeder-free media largely used nowadays known as mTeSR (Ludwig et al., 2006a; Ludwig et al., 2006b). This media contains, among others, three main components: FGF, TGFβ, and the Wnt signalling activator Lithium-chloride (LiCl). The latter causes β-catenin accumulation by directly inhibiting (GSK3β) via magnesium competition. It also has an indirect effect by increasing GSK3β inhibitory phosphorylation (Hedgepeth et al., 1997; Jope, 2003; Ryves and Harwood, 2001). A layer containing extracellular matrix components was used to provide the cell anchorage, a role previously offered by MEFs.

Pluripotent stem cells are an important model used to investigate several aspects of embryogenesis. They have been increasingly used for studies on neural stem cells and pathways regulating brain development. In order to do that, hESCs go through a process of neural induction, which mimics the natural process of neurulation, as discussed below.

1.1.3 Development of the Central Nervous System

During embryogenesis, pluripotency ends when cells from the ICM further specialise into the primitive endoderm (PrE; or hypoblast) and epiblast (Figure 1.1 A). While the PrE contributes to the formation of extra-embryonic tissues, it is from the epiblast that three germ layers derive, that are responsible for the formation of the entire organism: endoderm, mesoderm, and ectoderm. The embryologic period when the germ layers are formed is known as gastrulation (Figure 1.1 A) (Barresi and Gilbert, 2020).It is

during gastrulation that a structure known as the primitive streak defines the body axes (cranial/caudal and right/left). This structure derives from a thickening and depression of the epiblast and is the basis for the formation of the germ layers. In addition, it contains the primitive node at its most cranial end, an important structure that participates in notochord formation and induction of the next steps of neural development (Figure 1.1 B) (Stemple, 2005; Sulik et al., 1994).

At the end of Gastrulation, two major systems will derive from the ectoderm: The central nervous system (CNS) and the epidermis (Barresi and Gilbert, 2020). Concurrently, neural crest cells arise from the junction of the neural and non-neural ectoderm and migrate elsewhere to generate many derivatives throughout the body (Knecht and Bronner-Fraser, 2002). The process leading to CNS development is known as Neurulation and consists of the formation of the Neural Tube, the basis from which the nervous tissue derives. Neurulation can be divided into two phases, primary and secondary (Figure 1.2) (Harrington et al., 2009).

1.1.4 Neurulation overview

Perhaps the most studied phase of CNS development, primary neurulation involves many steps that culminate in the closure of the neural tube (Figure 1.2). In short, this phase starts with the differentiation of ectodermal cells into a columnar neuroepithelium localised over the notochord (Barresi and Gilbert, 2020). The middle part of the neural plate bends towards the notochord forming the medial hinge point (MHP). At the same time, the edges thicken and elevate, leading to the formation of bilateral neural folds and a neural groove. Dorsolateral hinge points (DLHPs) will be formed from

the approximation of neural folds, which finally come into contact and fuse, resulting in a closed neural tube located underneath the newly formed epidermis. In humans, this fusion occurs in a zippering style from several different closure sites (Nikolopoulou et al., 2017). Induction, bending and closure depend on the morphogenetic movement of convergent extension, where cells narrow towards the mediolateral axis (convergent) and expand along at the anteroposterior direction of the embryo (extension) (Zohn et al., 2003). This movement is dependent on cytoskeletal reorganisation which is directed by planar cell polarisation (PCP), resulting in a regulated cellular movement within the same plane. The Wnt non-canonical PCP pathway is known to control this process (Gray et al., 2011).

Conversely, secondary neurulation does not involve a tube closure. Instead, undifferentiated mesenchymal cells from the tail bud, a residual structure of the primitive node, condensate into a solid cord and undergo epithelial transition (Griffith et al., 1992). This tube will form a lumen trough the coalescence of many cavities, creating the most caudal part of the neural tube which will merge into its anterior portion (Figure 1.2) (Dady et al., 2014; Lowery and Sive, 2004). Mechanisms controlling primary and secondary neurulation are distinct and an imbalance in any of the steps could lead to neural tube defects, such as anencephaly and spina bifida (Greene and Copp, 2014).

Even before neurulation ends, the neural tube starts to differentiate into precursor structures that will form the CNS. The anterior portion enlarges and specialises in the three primary brain vesicles: prosencephalon (precursor of the forebrain), mesencephalon, and rhombencephalon. By the end of tube closure, secondary vesicles are formed and the neural tube undergoes flexures to form the brain (Barresi and Gilbert, 2020).

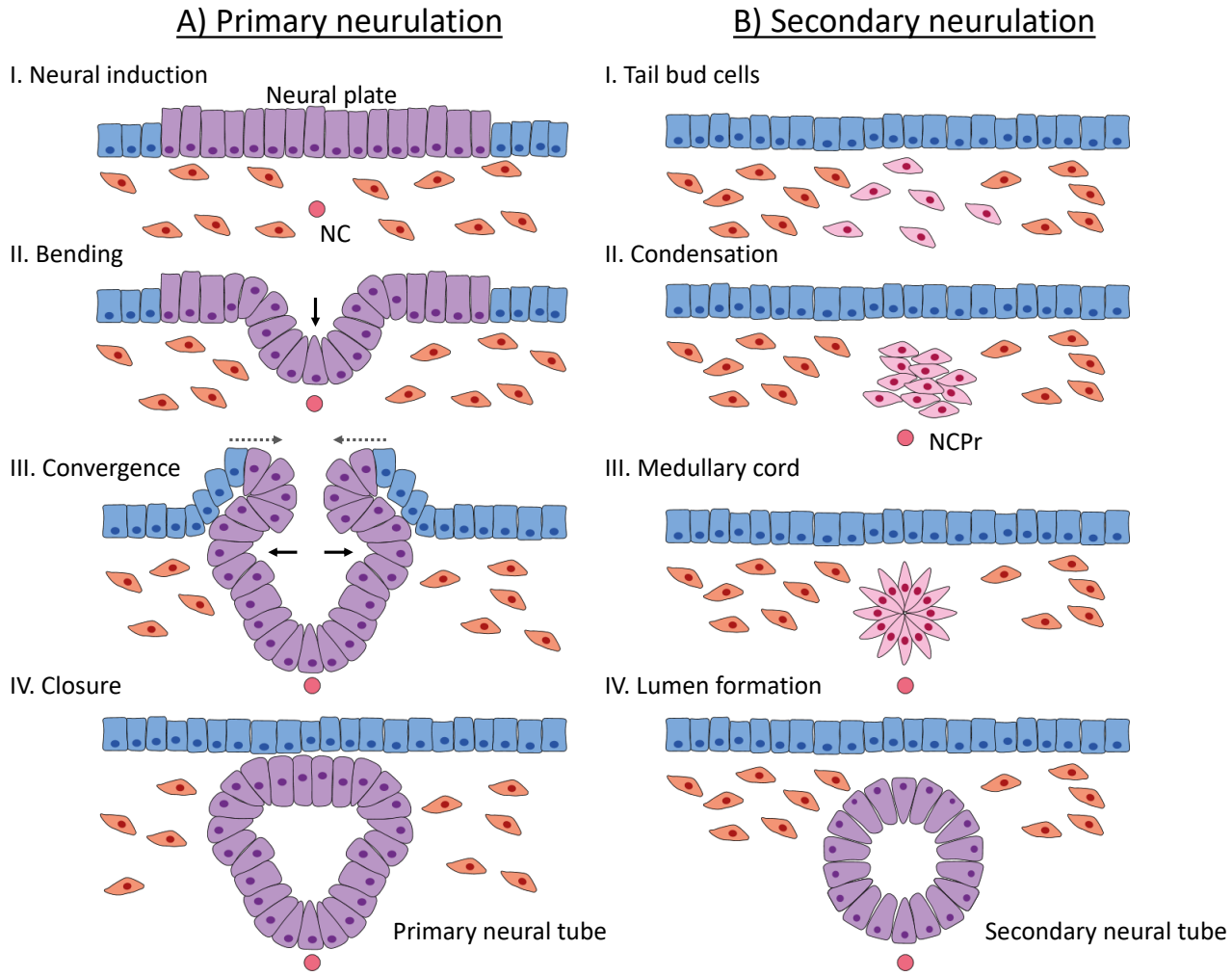


Figure 1.2. Primary and secondary neurulation.

Schematic of the two phases of neurulation. A) Primary neurulation starts with the neural induction of the ectoderm which differentiate into the neural plate (I). The neural plate bends inwards towards the notochord forming the neural grove (II). The laterals (neural folds) elevate and converge towards each other forming a second hinge point (III). Finally, both neural folds fuse forming a closed neural tube underneath the epidermis (IV). Black arrows: formation of hinge points; Grey dashed arrow: convergence movement; NC: notochord. B) Differently, the secondary neural tube differentiates from the tail bud cells (I). This cells first condensate (II) and then organise in circular structures known as the medullary chord (III). The medullary chord undergoes epithelialisation to form a closed tube containing a lumen. NCPr: notochordal precursor. Adapted from (Lowery and Sive, 2004).

1.1.5 Cellular and molecular mechanisms of neurulation

The process of neurulation requires cellular and molecular modifications that are tightly coordinated by morphogens (Figure 1.3). They act through specific canonical or non-canonical pathways to regulate the sequence of steps that ultimately lead to neural tube closure.

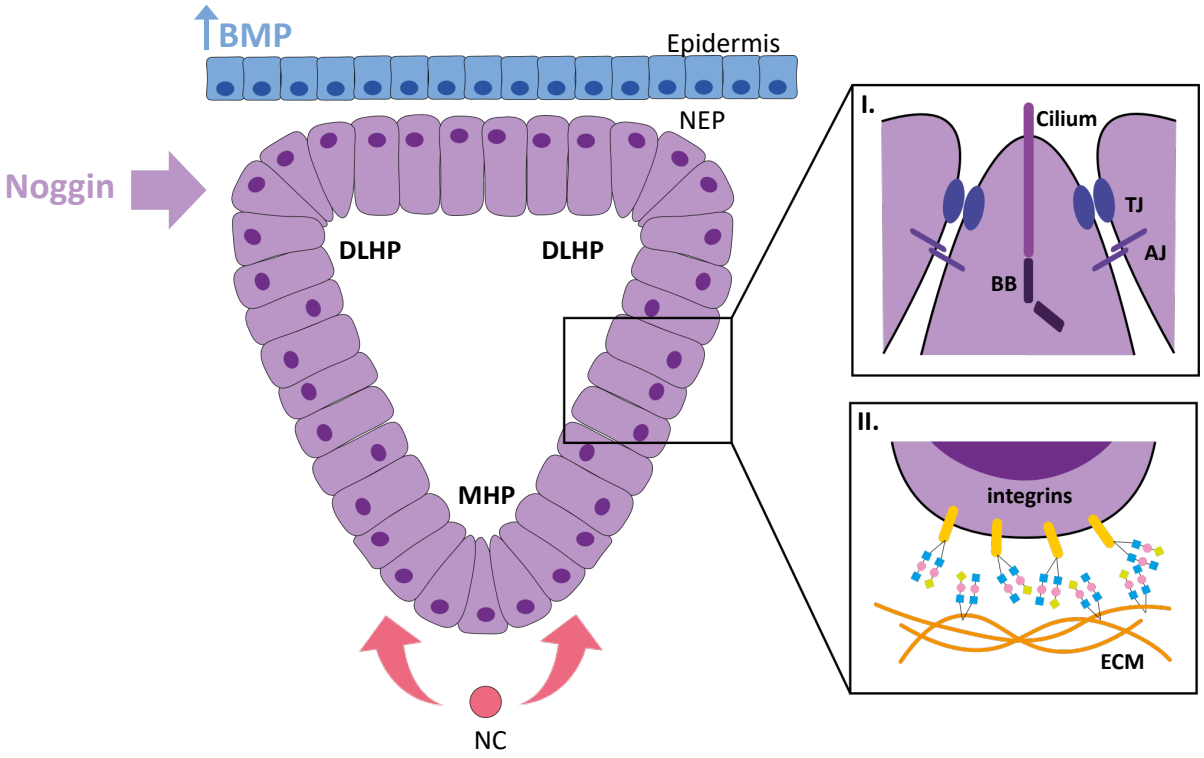


Figure 1.3. Mechanism of neurulation.

Schematic representing the main cellular and molecular modifications during neurulation. Noggin is a BMP inhibitor that promotes the neural fate. Under influence of this and other morphogens, such as signals released from the notochord (represented in pink), cells bend forming hinge points. Polarised cells also respond to cell-cell (I) and cell-matrix (II) interactions. NEP: neuroepithelial cells; MHP: medial hinge point; DLHP: dorsolateral hinge point; NC: notochord. TJ: tight junction; AJ: adherent junction; BB: basal body of the cilium; ECM: extracellular matrix. Adapted from (Nikolopoulou et al., 2017).

Under the influence of morphogens, the medial epiblast differentiates into the neuroepithelium. The central player in this process of neural induction is BMP, an inhibitor of the neural fate. This observation is part of the default theory, which claims that cells isolated from the epiblast become neural by default but BMP induce epidermis formation instead. Therefore, the neural fate is only possible due to secretion of BMP inhibitors such as Noggin, from the primitive node (Munoz-Sanjuan and Brivanlou, 2002). This inhibition is important for neural induction and for the expression of neural markers (Chang and Harland, 2007).

Other pathways regulate the process of neurulation, although many also act through BMP inhibition (Wilson and Edlund, 2001). FGF plays a role in neural induction not only by inhibiting BMP signalling in the medial epiblast, but also by sensitizing cells in the region to subsequent induction signals (Cohen et al., 2010; Delaune et al., 2005; Pownall and Isaacs, 2010; Streit et al., 2000; Wilson et al., 2000). Additionally, Wnt signalling weakens the response of cells to FGF (Wilson et al., 2001). As a result, the lateral epiblast commits to the epidermal fate under the influence of Wnt signals while in the medial epiblast its inhibition allows FGF and BMP antagonist to promote neural fate.

1.1.5.1 Apical-basal polarity

The neuroepithelium is composed of columnar cells that present apical-basal polarity. Therefore, cells are divided into two specialised subcellular domains, apical and basal, which contain different molecules, organelles and cytoskeleton components. Polarity impacts on several cellular events such as barrier protection, migration, neuronal signalling and presentation of antigens (Piroli et al., 2019). In the neuroepithelium, this

feature is particularly important for asymmetric cell division and formation of hinge points, as will be discussed. The disruption of polarity can lead to neurodevelopmental disorders such as neural tube defects, Down syndrome, autism spectrum disorders and schizophrenia (Arai and Taverna, 2017; Copp and Greene, 2010).

The junctional complex, formed by tight and adherent junctions, plays an essential role in both asymmetric cell division and formation of hinge points. Tight junctions are composed of membrane associated proteins, such as claudins, cytoplasmic adaptor proteins such as zonula occludens 1 (ZO1) and intracellular associated scaffold complexes. One example is the PAR complex, formed by the PDZ scaffold proteins PAR3 and PAR6, and the key effector atypical protein kinase C (aPKC) (Macara, 2004; Zihni et al., 2016). On the other hand, adherent junctions are formed by transmembrane calcium dependent adhesion proteins (Cadherins) complexed with intracellular catenins (McEwen et al., 2012). Tight and adherent junctions are interdependent, and the formation of one is dependent on the other (Campbell et al., 2017). The neuroepithelium loses junctional components as cells differentiate into more specialised types (Aaku-Saraste et al., 1996; Lechler, 2012; Medelnik et al., 2018; Watters et al., 2015).

Polarity is important for asymmetric cell division for two main reasons. First because the unequal distribution of fate determinants in the daughter cells allows tissue specialisation and their differentiation into other cell types. This was originally observed for the protein Numb in the *Drosophila melanogaster* external sensory organ (Rhyu et al., 1994). The junctional protein aPKC participates in this process by phosphorylating and inhibiting the interaction of Numb with the apical membrane. As a result, the protein is accumulated in the basal compartment of the sensory organ precursor cell, determining

daughter cell fate (Smith et al., 2007). Second, asymmetry is important for directing the mitotic spindle during cell division, ensuring the correct inheritance of molecular components by the daughter cells. Components of the PAR complex participate in this process by recruiting adaptor and microtubule binding proteins to the apical region. This is possible upon interaction with the adaptor protein Inscuteable (Kraut et al., 1996), which in turn recruits a mitotic spindle formation complex formed by Partner of inscuteable (PINS), heterotrimeric G protein αi-subunit (Gαi) and the microtubule-associated dynein-binding protein NuMa (Bowman et al., 2006). The assembly of these complexes will direct the site for microtubule biding, orienting mitotic spindle formation (Knoblich, 2010). In the mammalian brain, the orientation of the mitotic spindles coordinates the generation of intermediate progenitors via inscuteable. The absence of this protein leads to generation of neurons via direct differentiation affecting neurogenesis and the formation of cortical layers (Postiglione et al., 2011).

Additionally, the morphological polarisation of the neuroepithelium, where the apical region of the cell is constricted compared to the base, is essential for neural tube closure (Eom et al., 2013). The dismantling of junctions is required for the apical constriction that happens during formation of hinge points (Sawyer et al., 2010), and the BMP cascade impairs this process by stabilizing junctions through PAR3 recruitment (Eom et al., 2012). Therefore, formation of hinge points is possible upon BMP inhibition: MHP formation is possible due to Chordin released by the notochord (Patten and Placzek, 2002); and DLHP occurs under the influence of Noggin (Ybot-Gonzalez et al., 2007).

Localised in the apical pole, the primary cilium is an important organelle for polarisation of epithelial cells. The primary cilium is different from motile cilia due to the

absence of a central pair of microtubules. Primary cilia are formed after mitosis, when the mother centriole becomes the basal body from which the ciliary structure is derived (Pan and Snell, 2007). Junctional and cilia proteins interact and together participate in the establishment of polarisation (Gerdes et al., 2009). Their interaction has been shown in both ways. First, the protein inversin from the ciliary inversin compartment has been described to interact with N-cadherin and catenins, in a cell-cell contact depend manner (Nurnberger et al., 2002). Then, components of the PAR complex where observed to be localised at the cilia and interact with microtubles via KIF3A/Kinesin II complex (Fan et al., 2004). Moreover, the estabilishment of polarisation and functional juntions is required for correct ciliogenesis. For example, abrogation of the membrane sorting protein FAPP2 and the tight junction component aPKC were both shown to impair ciliogeneis (Fan et al., 2004; Vieira et al., 2006). Importanly, it possible to speculate that the contrary is also true, as deffects on ciliary proteins such as KIF3A and Polaris have been shown to affect polarisation causing ephitelium defects (Lin et al., 2003; Taulman et al., 2001). The primary cilium participates in developmental signalling such as Sonic hedgehog (Shh) and Wnt, acting in response to morphogens and growth factors (Gerdes et al., 2009). Primary cilia can be found in neural stem cells and are important for brain patterning and cortex development (Han and Alvarez-Buylla, 2010; Higginbotham et al., 2013; Park et al., 2019).

1.1.5.2 Interaction with the extracellular matrix

In addition to responding to soluble ligands and cell-cell contact, neuroepithelial cells respond to components of the extracellular matrix (ECM), such as the glycoproteins fibronectin and laminin.

The major proteins responsible for cell contact with the ECM are integrins, transmembrane proteins formed of α and β subunits. Activation of integrins results in conformational changes in the cytoskeleton and activation of signalling cascades of proliferation and survival (Hynes, 2002). Integrins participate in cytoskeleton remodelling at sites of focal adhesions. There, integrin activation results in the recruitment of intracellular protein complexes that bind to actin microfilaments. These complexes are formed for proteins such as paxillin, talin, vinculin and the focal adhesion kinases (FAK) and Src-family kinase (SFK) (Lawson and Schlaepfer, 2012). Additionally, pathways regulating cell growth, proliferation, and apoptosis can be regulated by integrins. Firstly, many receptor tyrosine/kinase (RTK) activities are dependent on integrin-mediated anchorage. For example, lack of integrin-mediated anchorage results in degradation of Platelet-derived growth factor (PDGF) receptor (PDGFR) (Baron and Schwartz, 2000). Additionally, integrins can activate these pathways directly. For example, integrins can regulate apoptosis through Phosphoinositide 3-kinase (PI3K)-RAC-alpha serine/threonine-protein kinase (Akt) pathway (Stupack and Cheresh, 2002), and promote cell cycle progression via ERK and cyclins (Schwartz and Assoian, 2001).

The various α and β isoforms combine to form integrin receptors that have specific affinity for different components of the ECM. Therefore, during different phases of development, stem cells and progenitors modulate the expression of subtypes of integrins

accompanying distinct cellular needs and the dynamic changes in the matrix composition (Schmid and Anton, 2003). The fibronectin receptor α5β1 plays important roles during neural development. It is highly expressed in neural progenitors, and decreases as cells differentiate into neurons (Jacques et al., 1998; Yoshida et al., 2003). ECM anchorage mediated by integrins α5β1 is important for neural tube closure in a zippering fashion and its absence can result in spina bifida (Molè et al., 2020). The same isoform regulates migration of neurons and cortical expansion during brain development (Marchetti et al., 2010). *In vitro*, integrin signalling mediates hESCs neural differentiation in response to mechanical forces (Topal et al., 2019). The distribution of β1 integrin in hESCs-derived neural stem cells is polarised towards the basal portion (Banda et al., 2015), which has also been described *in vivo* (Fietz et al., 2010).

1.1.6 Neural stem cell lineage progression

The first population of embryonic neural progenitors that form the CNS are the neuroepithelial cells (NEP) (Figure 1.4). One of the most important neuroepithelial transcriptional factor and marker described is SOX2. In contrast to its role in pluripotency, in the context of neural induction SOX2 switches co-factor binding partners to override BMP signalling, promote neuroepithelial commitment and regulate the maintenance of the neural stem cell pool (Archer et al., 2011; Graham et al., 2003; Zhang and Cui, 2014). NEPs also express the Paired box protein Pax-6 (Pax6), essential for neural fate by regulating cell proliferation, differentiation and adhesion (Osumi et al., 2008; Thakurela et al., 2016; Zhang et al., 2010). Pax6 and SOX2 act in coordination to promote expression of many factors, including the neuroepithelial stem cell protein Nestin, a

cytoskeletal intermediate filament first described in neural stem cells. (Thakurela et al., 2016). As part of the cytoskeleton, Nestin participates in essential stem cell remodelling functions, such as asymmetrical division, polarity and migration (Bernal and Arranz, 2018).

As brain development progresses, the lumen of the neural tube originates lateral ventricles filled with cerebrospinal fluid. At the tissue level, neuroepithelial cells proliferate, increasing their pool, and gradually transform into a more specialised population of elongated periventricular stem cells (Figure 1.4). These cells are called radial glia (RG) due to their resemblance to astrocytes, including the expression of markers such as the intermediate filaments vimentin and glial fibrillary acidic protein (GFAP) (Alvarez-Buylla et al., 2001; Merkle and Alvarez-Buylla, 2006). Although their molecular characteristics differ, RGs possess great similarity to NEPs such as the contact with the ventricular surface, expression of markers such as Pax6 and Nestin, apical-basal polarisation and primary cilia (Alvarez-Buylla et al., 2001).

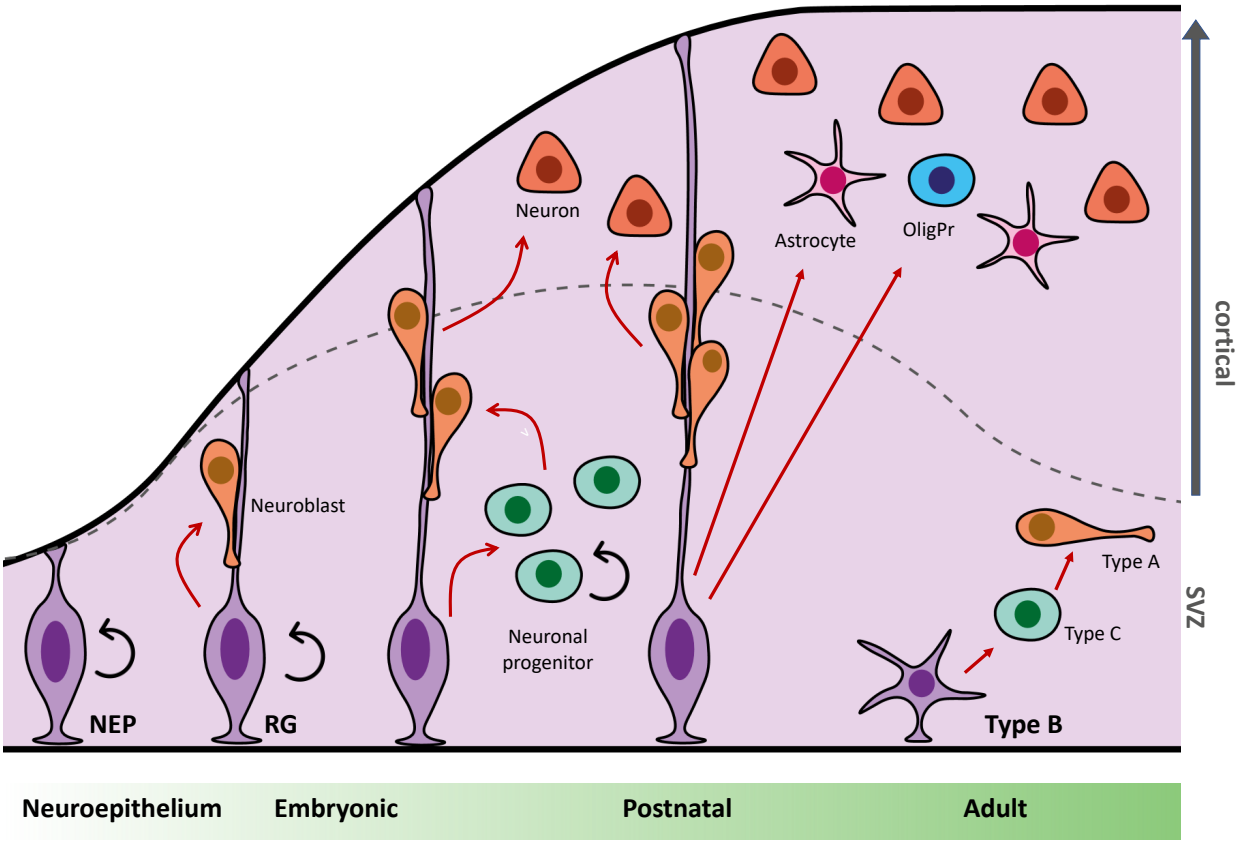


Figure 1.4. Neural stem cell progression.

Representation of the progression of neural stem cells from the neuroepithelium to adulthood. Neuroepithelial cells (NEP) directly progresses to become Radial glia (RG). During embryonic development, RG generate the first population of neuronal progenitors and neuroblast. Neuroblast migrate using the RGs' processes towards the forebrain where they generate neurons. As development progresses, progenitors accumulate in the region surrounding the ventricles generating a niche known as the Subventricular zone (SVZ), which is indicated as a dashed grey line. The SVZ is at its largest size during the postnatal period, where postnatal RGs also generate astrocytes and oligodendrocyte progenitors (OligPr). The neural stem cell during adulthood is also known as Type B cells. Type B cells do not have a basal process and are similar to astrocytes in morphology. Adult stem cells can generate neuronal progenitors and neuroblasts which are also known as Type C and Type A cells. Black arrows: self-renewal; Red arrows: differentiation. Adapted from (Alvarez-Buylla et al., 2001; Kriegstein and Alvarez-Buylla, 2009).

RGs give rise to two cell populations vital for the brain to function: neurons and glia. Initial RGs asymmetric divisions result in the first population of neuronal progenitors and neuroblasts. These neuroblasts use the long RGs process as a guide and scaffold

during their migration towards the outer cortical layers. As progenitors are generated, the layer of cells surrounding the lateral ventricle expands generating the subventricular zone (Malatesta et al., 2008). Later, RGs start originating glial cells upon the so called 'gliogenic switch'. This is a timing regulated process that involves blocking of the neurogenic fate, for example through BMPs, and activation of gliogenic factors, such as IL-6 cytokine family which acts through the Janus Kinase/Signal Transducer and Activator of Transcription (JAK/STAT) pathway promoting transcription of the astrocytic factors GFAP and S100 calcium binding protein B (S100β). (Miller and Gauthier, 2007).

Beyond embryonic development, neural stem cells lineage continues to progress, generating a population of astrocyte-like cells that surround the lateral ventricles of postnatal and even adult brains (Figure 1.4). These neural stem cells are capable of generating glia and neurons throughout life, and have been the focus of research aiming treatment of diseases such as Alzheimer's and Parkinson's.

1.1.7 The subventricular zone

The remarkable finding of the existence of postnatal and adult neural stem cell populations that supports neurogenesis in humans originates from studies of post-mortem brains of cancer patients treated with bromodeoxyuridine (BrdU) (Eriksson et al., 1998). This thymidine analogue is incorporated in the DNA during the synthesis phase (S-phase), and therefore indicates newly born cells. BrdU was detected in brain regions enriched for stem cells and also in neurons. These results were later confirmed by carbon-14 (^{14}C) dating studies, where the concentration of the radioactive form of carbon that was incorporated in the DNA of humans after the Cold War's nuclear bomb testing, was

assessed offering a date of birth for the neurons (Spalding et al., 2013). These studies in humans further emphasised what was already known for other mammals, that there is a postnatal and adult neural stem cell population capable of generating neurons and glia (Altman and Das, 1965; Gould et al., 1998; Gueneau et al., 1982; Kuhn et al., 1996).

The maintenance of this population is dependent on the existence of specialised microenvironments. Therefore, postnatal and adult neural stem cells (NSC) can be found in a limited number of specialised niches, one of them being the subventricular zone (SVZ). The SVZ is localised underneath the ependymal cell layer surrounding the lateral ventricles. The niche is composed of three main types of cells: neural stem cells (type B cells), which generate transit amplifying progenitors (TAPs or type C cells) that in turn differentiate into neuroblasts (type A cells) (Figure 1.4). Neuroblasts migrate from the SVZ through the rostral migratory stream (RMS) towards the olfactory bulb (OB) to finally differentiate into interneurons (Ihrie and Alvarez-Buylla, 2011). In humans, an additional corridor of neuroblasts, the medial migratory stream (MMS), travels to the prefrontal cortex (Sanai et al., 2011), at the same time that sparse neuroblasts migrate tangentially towards the cortex (Paredes et al., 2016). Additionally, in one of the final waves of gliogenesis, SVZ cells generate astrocytes and oligodendrocytes that migrate out into the cortex and striatum, in a time and space-dependent way (Levison et al., 1993; Levison and Goldman, 1993).

It is important to note that, although there is a continuum in the development of the postnatal and adult SVZ (pSVZ and aSVZ, respectively), these two temporarily spaced regions present significant differences in regards to activity and cell composition. Overall, the pSVZ exists during the first 2 to 3 weeks after birth, when the SVZ is not only

approximately three times thicker than the aSVZ, but also still contains RGs, which gradually start to retract their basal process to become type B NSC (Fiorelli et al., 2015). The pSVZ is also more active than the aSVZ in the production of interneurons in the OB (Bayer, 1983), and in generating cortical and striatal neurons and glia (Paredes et al., 2016). In fact, pSVZ harbours a high gliogenic potential, generating astrocytes and oligodendrocytes that migrate radially into the forebrain (Marshall et al., 2003). This process creates a gliogenesis peak, which is temporally regulated: astrogenesis preceding oligodendrogenesis (Lyck et al., 2007; Parnavelas, 1999).

Specific factors control NSC maintenance and differentiation in the pSVZ and aSVZ. Growth factors such as Epidermal growth factor (EGF) and FGF promote expansion of the SVZ (Marshall et al., 2003), and are commonly used for the *in vitro* maintenance of undifferentiated NSC, and withdrawal of these two components promotes spontaneous differentiation (Pastrana et al., 2011). Very interestingly, BMP is expressed together with its receptor in the pSVZ, where it plays a role in astrogenesis. In contrast, due to the strong influence of the BMP inhibitor Noggin, secreted from ependymal cells, the aSVZ is essentially neurogenic during healthy homeostasis, although it can become gliogenic during demyelination (Lim et al., 2000). Finally, a subpopulation of type B NSC that expresses PDGFR can acquire the oligodendrocyte fate (Jackson et al., 2006).

Recent studies on single cell RNA sequencing (scRNAseq) have shed light on the complexity of SVZ neurogenesis and gliogenesis. One of the studies suggested that the SVZ contains more than 20 different cell types (Zywitza et al., 2018). Cells from the SVZ generate OB neurons of nine distinct identities, which are specifically distributed in the different OB layers (Mizrak et al., 2020). We have also learnt that there is a regional

difference of the SVZ with regards to cell composition and gene expression (Mizrak et al., 2019). For example, the lateral SVZ is more proliferative and neurogenic compared to septal SVZ. The latter has an oligodendrogenic identity, which is significatively more prominent in males than in females, revealing that sex can play a role in neural differentiation. The ventral SVZ has been shown to be enriched for intermediate cell type expressing NOTUM, an Wnt signalling agonist that blocks proliferation (Mizrak et al., 2020). ScRNAseq has also indicated that age plays a role in neurogenesis, not for altering the molecular characteristics of the neural stem cells, but for keeping those in a quiescent stage as a result of local inflammation (Kalamakis et al., 2019).

Although much is already known about postnatal neural differentiation, many aspects about the regulation of this process remains to be elucidated and this is the subject of the first part of my thesis (Chapter 3).

1.1.8 *In vitro* differentiation of neural stem cells

Neural stem cells can be obtained *in vitro* through the neural induction of pluripotent stem cells. In order to carry out the induction, it is necessary to mimic signals existing during neurulation. Two Smad inhibitors are the main components of the most successful defined media used for that purpose: Noggin and SB431542 (Chambers et al., 2009). While Noggin acts by inhibiting BMP signalling as previously described, SB431542 blocks Activin/Nodal receptors (Smith et al., 2008). This dual-Smad inhibition not only suppresses stimuli for pluripotency, such as the expression of NANOG, but also impedes the acquisition of other fates that are not neural.

Fascinatingly, cells in such conditions not only acquire the expression of neuroepithelial cell markers but also present polarisation, apical constriction, and cytoskeletal reorganisation greatly resembling what is observed during neurulation (Figure 1.5) (Abranches et al., 2009; Banda et al., 2015; Ying et al., 2003). The apical domain presents tight and adherent junction-associated proteins such as ZO-1, PAR, aPKC, N-cadherin, and β-catenin; as well as primary cilia with active Shh signalling. In the basal compartment, β1 integrin interacts with the extracellular matrix. The similarity with neurulation goes as far as the spontaneous formation of a lumen around which cells organise in a structure known as neural rosettes (Hribkova et al., 2018). The process of lumen formation led some researchers to believe that *in vitro* formation of neural rosettes is controlled by mechanisms that resemble secondary neurulation rather than primary (Fedorova et al., 2019).

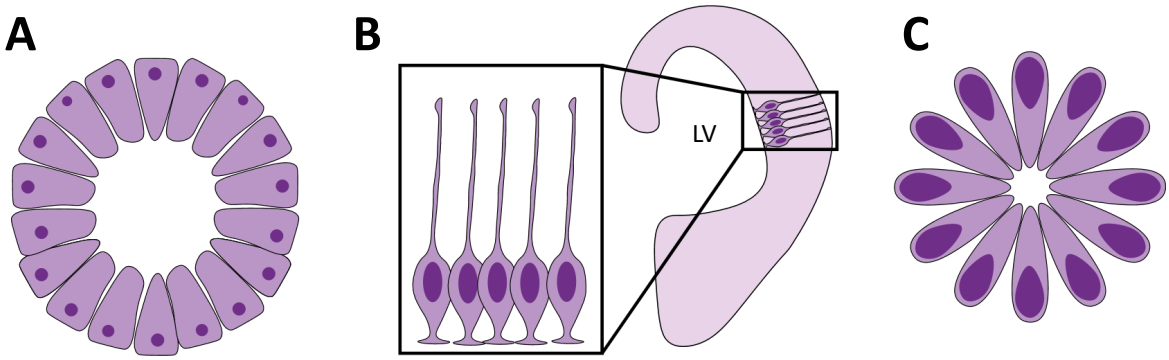


Figure 1.5. Neural rosettes resemble neurulation.

Schematic of the similarities between the neural tube (A), the postnatal cortex (B) and the *in vitro* model of neural differentiation (C). All these structures are composed of apical-basal polarised cells that organise around a lumen. LV: lateral ventricle. Adapted from (Banda et al., 2015).

Nevertheless, these structures preserve molecular and morphological characteristics of embryonic neural differentiation, and, as such, are a remarkable tool for

studying this process. Neural rosette disruption leads to impaired differentiation and neuronal fate (Hribkova et al., 2018). Therefore, this model can help to uncover mechanisms behind neurodevelopment disorders and help to find targets for neural stem cell therapy. In this thesis, I took advantage of this approach to address the questions proposed in Chapter 4 and 5.

1.2 Galectin-3

1.2.1 Introduction to glycoconjugates and lectins

Such an intricate process as the development of the CNS involves a plethora of coordinated cellular and molecular reorganisation. Many aspects of cell communication and signalling during neurodevelopment requires glycosylated molecules. These molecules are glycoproteins, glycolipids, and proteoglycans, collectively known as glycoconjugates, which can be found in the nervous tissue both in the cell surface and extracellular matrix and participate in several aspects of development (Bhavanandan and Gowda, 2014; Yu and Itokazu, 2014). Neurodevelopmental events and different neural cell types can be determined by the expression of different glycoconjugates (Ngamukote et al., 2007; Yanagisawa and Yu, 2007). Glycolipids and glycoproteins often organise in clusters, forming specialised membrane microdomains (Chen et al., 2016). The coalescence of glycoconjugates such as transmembrane receptors in these regions can result in activation of intracellular signalling. This is the case of the EGF receptor (EGFR), that upon formation of clusters, become active and bind to Growth factor receptor-bound protein 2 (GRB2) and activate downstream Ras pathway (Kaszuba et al., 2015; Wang et al., 2014b). Modulation of the glycosylated chains in glycoconjugates adds another level of regulation for intracellular cellular signalling. Although this modulation mainly happens by glycosyltransferases and other glycan-modifying enzymes during glycosylation at the endoplasmic reticulum (ER) and Golgi, it has also been shown that glycan chains can be remodelled by extracellular glycosidases and sulfatases (Parker and Kohler, 2010).

Glycoconjugates act in biological processes in several ways, including through interaction with complementary proteins released from other cells or in the ECM. A major

class of carbohydrate-binding proteins that recognise glycoconjugates are known as lectins. Lectins are an ancient class of protein that have important bacterial and viral defence functions through glycosylation pattern recognition (Taylor et al., 2015). They are found in many microorganisms, plants, and animals, and are expressed in several organs including the brain (Sharon and Lis, 2004). There are a variety of families of lectins based on the carbohydrate-recognition domain (CRD), in which some are transmembrane while others are soluble proteins. These many different types of lectins are involved in triggering intracellular signalling and mediating cell-cell and cell-matrix adhesion through their interaction with a variety of glycoconjugates (Taylor et al., 2015).

Galectins comprise a group of soluble lectins that have affinity for β-galactose-containing glycans (Barondes et al., 1994a; Barondes et al., 1994b). The presence of sulfhydryl groups, or thiols, causing free cysteine residues in their composition led these proteins to be previously known as S-type lectins. Galectins lack a transmembrane domain and, although deficient of a signal sequence, can be secreted by non-classical mechanisms. Galectins are, therefore, not only expressed intracellularly, but can also can be found in the extracellular environment and attached to glycoconjugates in the cell membrane.

There are 15 galectins described in vertebrates, numbered respectively in the order of discovery, and they can be classified into three groups according to their structure: prototypical, tandem-repeat, and chimeric galectins (Figure 1.6). Prototypical galectins organise in homodimers of the same CRD, while tandem-repeat galectins are heterodimers of distinct CRD connected by a linker region. In contrast, the chimeric galectins group consists of a single member, Galectin-3, which contains only one CRD.

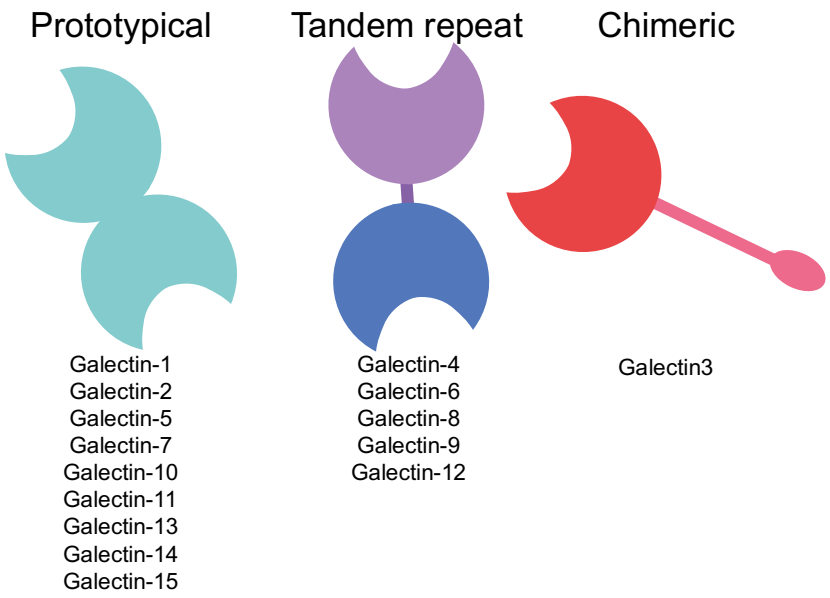


Figure 1.6. Galectin subtypes.

Among the fifteen galectins described in vertebrates, Gal-3 is the only member of the chimeric group. Other galectins are divided in prototypical, with two homologous CRD, and tandem repeat, formed by two heterodimers of CRD connected by a linker region. Adapted from (Cummings et al., 2015).

1.2.2 Galectin-3 overview

Galectin-3 (Gal-3) was first characterised in 1982 and given the name of Mac-2, as it was thought to be a macrophage specific marker (Ho and Springer, 1982). Since then, it has been independently isolated by different research groups under various names, CBP35, εBP, RL-29, HL-29, L-34, and LBP, until in 1994 these were acknowledged as the same protein and finally called Gal-3 (Barondes et al., 1994a; Cerra et al., 1985; Liu and Orida, 1984; Raz et al., 1987; Roff and Wang, 1983; Sparrow et al., 1987; Woo et al., 1990).

Gal-3 is encoded by the *LGALS3* gene and is the sole member of the chimeric group of galectins. Therefore, the protein is composed of two functional domains, a CRD

and a proline, glycine, tyrosine enriched amino-terminal domain (Figure 1.7 A). The N-terminal domain of Gal-3 monomers interact forming pentamers in a concentration dependent manner (Chiu et al., 2020). The ability to organise in oligomers and cross-link different glycoconjugates confers a multivalent functionality to Gal-3 (Ahmad et al., 2004). Interestingly, Gal-3 has two sites for phosphorylation in the N-terminal tail, Serine (Ser) 6 and Ser 12, which have been shown to impair its glycan binding, possibly by hampering its oligomerisation (Huflejt et al., 1993; Mazurek et al., 2000).

The CRD of Gal-3 binds to carbohydrate ligands containing galactoside, such as the disaccharides Lactose [Lac – composed of the monosaccharides galactose (Gal) and glucose (Glc)] and N-acetyllactosamine [LacNAc – composed of Gal and N-acetylglucosamine (GlcNAc); 3Galβ1-4GlcNAcβ] (Seetharaman et al., 1998). These basic recognition structures compose more complex saccharides for which Gal-3 has even greater affinity, such as poly-LacNAc [$(3Gal\beta1\text{-}4GlcNAc\beta)_n$] and other polysaccharides (Figure 1.7 B) (Hirabayashi et al., 2002; Ochieng et al., 2002). In fact, the glycosyltransferase responsible for adding LacNAc residues in glycan chains, the β1,6-N-acetylglucosaminyl transferase (Mgat5), is needed for Gal-3's ability to bind to receptors (Demetriou et al., 2001). More recently, it was described that some large polysaccharides, such as galactomannans, strongly interact with Gal-3 via a noncanonical binding site of the CRD (Miller et al., 2016). Glycan chains containing the saccharides described above can be found in the cell membrane attached to proteins and lipids. Gal-3 has been described to interact with glycoproteins containing N- and O-glycans (glycans linked to an asparagine or serine/threonine, respectively), as well as glycosphingolipids (Collins et al., 2014; Flowers et al., 2019; Nielsen et al., 2018).

Intriguingly, Gal-3 can also interact with many intracellular partners through protein-protein interactions independent of carbohydrate recognition (Dumic et al., 2006; Liu et al., 2002; Wang et al., 2004).

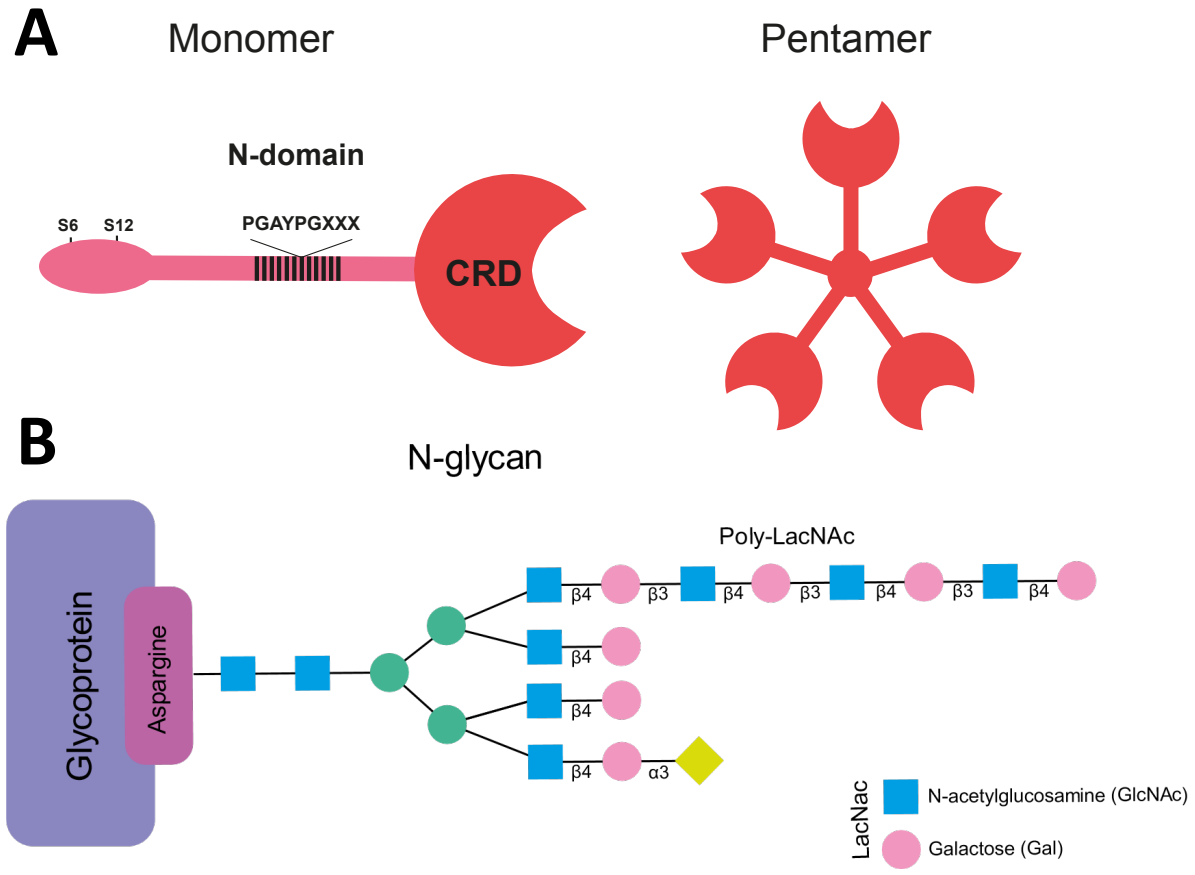


Figure 1.7. Galectin-3 structure and carbohydrate recognition.

A) Galectin-3 is a chimeric galectin composed of a carbohydrate recognition domain (CRD) and a N-terminal tail that contains a proline, glycine, tyrosine enriched region (7-14 repeats of Pro-Gly-Ala-Tyr-Pro-Gly-X-X-X or PGAYPGXXX). Galectin-3 can be phosphorylated at Ser 6 and 12. Monomers of Galectin-3 associate through the N-domains to form pentamers. Adapted from (Fortuna-Costa et al., 2014). B) Structure of a N-glycan containing a Poly-LacNAc chain. Poly-LacNAc is formed upon connection of LacNAc by β bonds. LacNAc is a disaccharide formed by the monosaccharides Gal and GlcNAc. Adapted from (Lee et al., 2018).

1.2.2.1 Gal-3 extracellular functions

Gal-3 is secreted by a mechanism that is independent of ER-Golgi compartments (Sato et al., 1993). Once in the extracellular environment, Gal-3 acts in many cell processes through recognition of N-glycan chains in a variety of cell transmembrane receptors (Figure 1.8). This binding creates clusters of Gal-3 and its ligands in the cell membrane known as lattices. These microdomains are very important for receptor activation by promoting crosstalk and avoiding receptor turnover (Garner and Baum, 2008; Rabinovich et al., 2007). Some RTK that respond to growth stimuli present branched N-glycans and their activation can be regulated by Gal-3 binding (Lau et al., 2007).

Gal-3 has been extensively studied in the immune response, since it is usually considered a pro-inflammatory molecule. Previous names for Gal-3, Mac-2, was given to describe a macrophage differentiation marker, and εBP means IgE binding protein. Gal-3 is expressed and secreted by many immune cells such as microglia, having autocrine or paracrine effects. For example, by cross-linking receptors such as Carcinoembryonic antigen-related cell adhesion molecule 3 (CEACAM3), High-affinity IgE receptor (FcεRI) and Toll like receptor 4 (TLR4), Gal-3 activates monocytes/macrophages, neutrophils, mast cells and microglia (Burguillos et al., 2015; Feuk-Lagerstedt et al., 1999; Frigeri et al., 1993; Jeng et al., 1994; Liu et al., 1995; Yamaoka et al., 1995). Gal-3 has also been reported to be a chemoattractant and increases monocyte and macrophage infiltration (Hsu et al., 2000; Sano et al., 2000). Additionally, Gal-3 has the ability to bind to glycoconjugates in the membrane of pathogens and thus activate an immune response (Beatty et al., 2002; Sato and Nieminen, 2002). Nevertheless, in certain contexts, there

are reports of an anti-inflammatory role of Gal-3. For example, Gal-3 can inhibit eosinophils by its interaction with the IgG Fc receptor II-b (FcyRII), or bind T-cell receptors (TCR) impairing its activity (Cortegano et al., 2000; Demetriou et al., 2001).

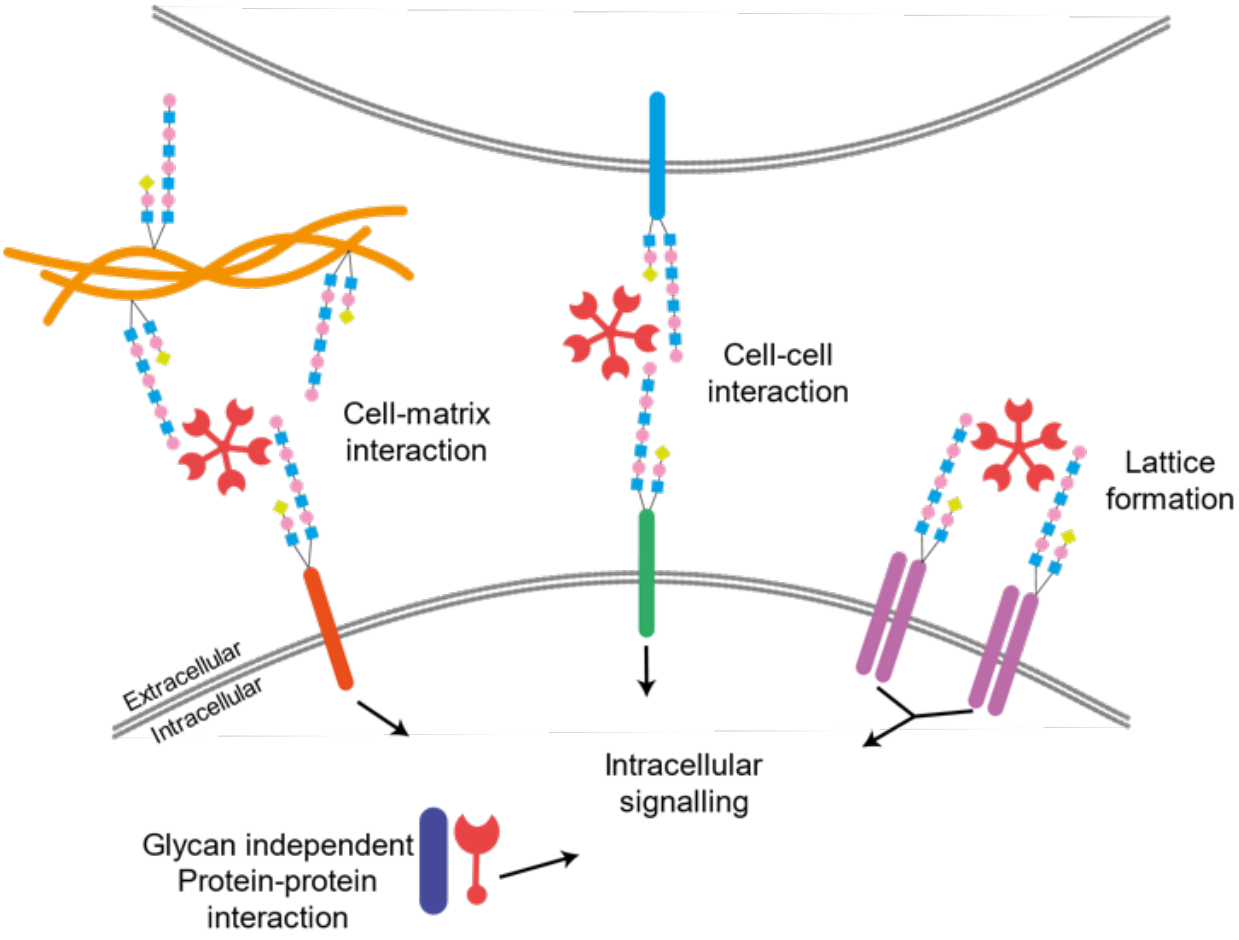


Figure 1.8. Galectin-3 extracellular interactions.

Extracellular Gal-3 binds to several glycoconjugates found in the ECM and in the cellular membrane. Because it forms pentamers, Gal-3 intermediate interactions between cells and the matrix. Additionally, intracellular Gal-3 interacts with protein in a glycan independent way. In both extracellular and intracellular compartments, Gal-3 interactions results in activation of intracellular signalling. Adapted from (Cummings et al., 2015).

Gal-3 participates in cell adhesion, having a stimulatory or inhibitory role depending on the context. In cell-matrix adhesion, Gal-3 can act as a bridge between adhesion molecules in the cell membrane, such as integrins, and components of the cellular matrix, such as laminin and fibronectin (Kuwabara and Liu, 1996; Matarrese et al., 2000; Sato et al., 2002; Swarte et al., 1998). The reverse effect has also been described, where Gal-3 impair cell adhesion by blocking adhesive molecules which then cannot attach (Ochieng et al., 1998; Villa-Verde et al., 2002). In cancer cells, Gal-3 can bind and activate integrin signalling independently of anchorage, promoting tumorigenesis (Seguin et al., 2017; Seguin et al., 2014). Gal-3 also participates in cell-cell interaction, for example, via binding to glycans on N-cadherins promoting junction destabilization (Argüeso et al., 2015; Boscher et al., 2012). In addition, Gal-3 binds to the extracellular domain of the desmosome protein desmoglein-2 increasing cell-cell attachment (Hrdlickova-Cela et al., 2001; Jiang et al., 2014).

1.2.2.2 Gal-3 intracellular functions

Besides its ability to recognise glycoconjugates, Gal-3 is largely encountered in the cytosol and participates in several intracellular processes in a carbohydrate-independent manner (Figure 1.8). Gal-3 binds to a number of cytoplasmic and nuclear proteins mainly through the CRD, though the exact motif that mediates this interaction is not clear (Dumic et al., 2006; Liu et al., 2002; Wang et al., 2004). Gal-3 intracellular distribution is influenced by its interaction with other proteins and by its phosphorylation state (Cowles et al., 1990; Takenaka et al., 2004).

In the cytoplasm, Gal-3 participates in pro-survival processes, such as cell growth and inhibition of apoptosis. For example, Gal-3 not only shares a sequence similarity with the antiapoptotic protein Bcl2-associated agonist of cell death (Bcl-2), the NWGR motif (Akahani et al., 1997; Yang et al., 1996), but it regulates apoptosis through binding to several proteins such as Bcl-2, Fas cell surface death receptor (Fas, or CD95), Nucling and synexin (Fukumori et al., 2004; Liu et al., 2004; Yu et al., 2002). Additionally, Gal-3 mediates cell growth by activating GTPase KRas (KRas) and PI3K pathways (Elad-Sfadia et al., 2004; Oka et al., 2005; Seguin et al., 2017; Shalom-Feuerstein et al., 2005).

Gal-3 is involved with several steps of intracellular protein trafficking (Bänfer and Jacob, 2020). Gal-3 is internalised and required for non-clathrin mediated endocytosis of proteins such as β1-integrin and CD44 (Lakshminarayan et al., 2014; Straube et al., 2013). Interestingly, the recycling of β1-integrin upon Gal-3 binding to it affects cell adhesion (Furtak et al., 2001). The GL-Lect theory (from GlycoLipids and Lectins) explains that the oligomerization of Gal-3 upon its binding with membrane receptors allows its interactions with glycosphingolipids promoting membrane curvature and the formation of vesicular carriers (Johannes et al., 2016). Internalised Gal-3 was identified in early endosomes and in the recycling compartment, co-localised with the markers Rab-4, Rab-8 and Rab-11 (Furtak et al., 2001; Schneider et al., 2010; Straube et al., 2013). There, it participates in apical trafficking and protein sorting, and its absence promotes aberrant protein distribution and loss of polarity, which ultimately impairs epithelial morphogenesis (Delacour et al., 2006; Delacour et al., 2008; Honig et al., 2018; Torkko et al., 2008; Yamamoto et al., 2013).

Gal-3 has been also found in extracellular vesicles. Gal-3 was initially described to be secreted via microvesicles blebbing (Mehul and Hughes, 1997; Sato et al., 1993). It is now largely acknowledged that Gal-3 is present in the exosome of many cell types (Bänfer and Jacob, 2020). The mechanism of Gal-3 recruitment to late endosomes has started to be elucidated. For example, a conserved motif in Gal-3's N-domain was shown to interact with the endosomal sorting complex required for transport I (ESCRT-I) component Tumor susceptibility gene 101 protein (Tsg101) to promote a Vacuolar protein sorting-associated protein 4A (Vps4)-mediated secretion, very similar to the mechanism of secretion of some viruses (Bänfer et al., 2018).

In infections, Gal-3 is recruited to damaged vesicles, such as *Shigella*-containing phagosomes and adenovirus-containing endosomes upon their rupture (Maier et al., 2012; Paz et al., 2010). This is important for targeting the content of these vesicles for selective autophagy (Chen et al., 2014b; Hong et al., 2019; Maejima et al., 2013). Recently it was shown that Gal-3 associated with the ESCRT component Alix is recruited to site of lysosomal damage by Transferrin receptor protein 1 (TFRC) glycoprotein. There it quickly promotes endomembrane repair (Jia et al., 2020). Gal-3 then switches interactions to associate with Tripartite motif-containing protein 16 (TRIM16), removing damaged lysosomes via autophagy (Chauhan et al., 2016; Jia et al., 2020). Gal-3 also promotes lysosome replacement via Transcription factor EB (TFEB) activation (Jia et al., 2020). Interestingly, it has been recently reported that, in human macrophages, the Parkinson's disease-related Leucine-rich repeat serine/threonine-protein kinase 2 (LRRK2) participates in the decision for membrane damage repair, while Gal-3 regulates destruction via autophagy (Herbst et al., 2020).

Another described function of Gal-3 is its participation on ciliogenesis. Gal-3 transiently localises to the basal body of the cilia, where it interacts with specific proteins such as Centrin-2 and is needed for the correct cilia morphology (Chiu et al., 2006; Hafsia et al., 2020; Koch et al., 2010). Gal-3 also binds to the mitotic regulator NuMa to establish spindle poles and ensure correct cell division (Magescas et al., 2017).

In the nucleus, Gal-3 can promote cell growth by binding to transcriptional factors and by participating in the assembly of transcriptional complexes (Lin et al., 2002; Paron et al., 2003). It has also been associated with the process of RNA splicing through directly binding to single strand DNA (ssDNA) and RNA (Dagher et al., 1995; Wang et al., 1995). This process can also be mediated by its interaction with proteins, such as Gem-associated protein 4 (Gemin4) to regulate spliceosome assembly (Park et al., 2001). More recent studies have shown the interaction of Gal-3 with small nuclear ribonucleoproteins (snRNPs) in early spliceosome complexes (Fritsch et al., 2016; Haudek et al., 2016). Gal-3 interacts with Heterogeneous nuclear ribonucleoprotein L to promote stability of *Mucin-4 (MUC4)* mRNA (Coppin et al., 2017). The only intracellular interaction dependent on carbohydrate recognition that has been described for Gal-3 is with cytokeratin, though its function is unclear (Goletz et al., 1997).

1.2.3 Gal-3 expression during embryogenesis

As previous described, glycoconjugates play a crucial role during embryogenesis and neural development (Ngamukote et al., 2007; Yanagisawa and Yu, 2007). Glycoconjugate-binding galectins have been described to mediate processes such as cell polarisation, adhesion, migration, differentiation and ciliogenesis, which are required for

the normal development of the CNS. This raises the question of the specific role of galectins, and particularly Gal-3, in embryogenesis and neural development.

It is known that Galectin-3 has a specific distribution in the embryo which changes as development progresses, indicating an active role during this process. During the first days after fertilisation, Gal-3 is expressed in the trophectoderm and was suggested to participate in embryo implantation through its interaction with integrins (Bojić-Trbojević et al., 2019; Colnot et al., 1996; Poirier and Robertson, 1993). Studies in mouse and human embryo reveal that Gal-3 expression first appears at the notochord during the neural tube folding stage, persisting until it disappears (Fowlis et al., 1995; Van den Brûle et al., 1997). While the role of Gal-3 at the notochord remains to be elucidated, it indicates the participation of Gal-3 in neural induction and neural tube patterning. Later, Gal-3 expression is restricted to epithelial cells and to chondrocytes that will form the skeleton, indicating a role in osteogenesis (Colnot et al., 2001). Gal-3 null mice exhibit viable embryogenesis with only a subtle change in phenotype, which could be explained by redundancy with other galectins (Colnot et al., 1998).

1.2.4 Gal-3 in the brain and neural development

Gal-3 participates in local inflammation and has been extensively studied in brain damage, which usually increase its expression. For example, Gal-3 activates microglia in a model of ischemic injury (Lalancette-Hebert et al., 2007). Also, in response to demyelination, increased levels of Gal-3 promote infiltration of leukocytes in the SVZ in a model of Multiple Sclerosis (James et al., 2016). Gal-3 has been linked with brain cancer aggressiveness, not only due its pro-inflammatory role, but because it upregulates several

pro-tumorigenic pathways, and its expression levels are corelated with tumour grade and worse prognosis (Bresalier et al., 1997; Camby et al., 2001; Gordower et al., 1999; Kuklinski et al., 2000; Wang et al., 2019).

In the healthy postnatal and adult brain, the only region where Gal-3 can be detected is the SVZ. There, it is expressed in type B NSC, type C TAPs and ependymal cells, but not in neuroblasts (Comte et al., 2011). Remarkably, the SVZ is naturally a semi-inflamed region, which could partially explain Gal-3 overexpression (Bardella et al., 2018; Goings et al., 2006). The role of Gal-3 in these cells during homeostasis remains largely unknown. One study has shown that Gal-3 is required for neuroblast migration to the OB, while being dispensable for NSC proliferation (Comte et al., 2011). There is also evidence that Gal-3 induces oligodendrocyte differentiation and maturation (Pasquini et al., 2011; Thomas and Pasquini, 2018). I focused the Chapter 3 of my thesis in investigating Gal-3 role in postnatal gliogenesis.

Gal-3 has been described to regulate developmental pathways. For example, secreted Gal-3 has been shown to activate Neurogenic locus notch homolog protein (Notch) signalling in a carbohydrate-dependent manner impairing differentiation of cancer cells (Kang et al., 2016; Nakajima et al., 2014). Also, Gal-3 binds to N-glycan residues of tyrosine/kinase receptors such as EGFR preventing their endocytosis, which ultimately results in the upregulation of progenitor genes such as SOX2 (Kuo et al., 2016; Partridge et al., 2004). In contrast, Gal-3 does not bind to EGFR in SVZ cells (Comte et al., 2011). Interestingly, Gal-3 modulates Wnt signalling in opposite directions in cancer and in the postnatal SVZ. While Gal-3 sequesters β-catenin, downregulating Wnt signalling in postnatal SVZ gliogenesis (Al-Dalahmah et al., 2020b), the contrary is observed in

cancer. In those cases, Gal-3 activates the Wnt signalling pathway by mediating β-catenin nuclear localisation, by translocating with it, and enhancing the transcription of Wnt target genes (Shimura et al., 2004; Song et al., 2009). This mediation was described in breast cancer cells to take place through a direct interaction of β-catenin with Gal-3's C-domain (Shimura et al., 2004), or indirectly by the downregulation of Akt and GSK3β activity, as described in colon (Song et al., 2009), pancreatic (Kobayashi et al., 2011) and tongue cancer (Zhang et al., 2013). In addition, Gal-3 might take part in regulating the β-catenin destruction complex since it contains a GSK3β phosphorylation motif and has been described to associate with axin (Shimura et al., 2005). Additionally, our group has shown that BMP signalling, which is required for adult SVZ neurogenesis and astrocytic fate (Bonaguidi et al., 2005; Colak et al., 2008; Gomes et al., 2003), can be activated by Gal-3 in the postnatal SVZ, promoting gliogenesis through BMPR binding and increasing Smad phosphorylation (Al-Dalahmah et al., 2020a).

Not only does Gal-3 regulate developmental pathways, but it has also been described to regulate other important features required for the maintenance of epithelial cells, such as the establishment of cell polarity (Delacour et al., 2006; Delacour et al., 2008; Honig et al., 2018; Torkko et al., 2008; Yamamoto et al., 2013), ciliogenesis (Chiu et al., 2006; Hafsia et al., 2020; Koch et al., 2010) and spindle pole formation (Magescas et al., 2017). The development of neural rosettes *in vitro* can be compared to these models of epithelialisation with regards to the apical-basal polarity and structure. However, the involvement of Gal-3 in polarity in the context of neural differentiation has never been investigated.

Even though Gal-3 has many described roles that could be implicated with neural development, its role in that process has never been investigated before. Hence, this is the main subject of investigation of Chapters 4 and 5.

1.3 The Hippo pathway

1.3.1 Pathway overview

The tumour suppressor Hippo pathway is a protein signalling cascade well known to regulate stem cell pool maintenance and tissue regeneration. The Hippo pathway is evolutionarily conserved and it was first described as an organ size regulator in Drosophila (Harvey et al., 2003; Jia et al., 2003; Pantalacci et al., 2003; Udan et al., 2003; Wu et al., 2003).

In mammals, the core of the pathway is composed of two kinases, the mammalian STE20-like protein kinase 1 and 2 (MST1/2) and the large tumour suppressor 1 and 2 (LATS1/2) (Figure 1.9). The catalytic activity of these kinases depends on their interaction with regulatory proteins: while MST1/2 complexes with Salvador homolog 1 (Sav1) (Callus et al., 2006; Chan et al., 2005), LATS1/2 binds to Mps one binder (MOB1) (Praskova et al., 2008). When active, MST1/2 phosphorylates and enhances activity of LATS1/2-MOB1 (Chan et al., 2005; Praskova et al., 2008). Activation of the core kinase cascade results in the phosphorylation of the transcriptional co-activator Yes-associated protein (YAP) or its paralogue transcriptional co-activator with PDZ-binding motif (TAZ) by LATS (Hao et al., 2008; Zhao et al., 2007). Phosphorylation of YAP (Ser 127) or TAZ (Ser 89) creates a docking site for the adaptor protein 14-3-3 resulting in its cytoplasmic retention or degradation through the proteasome (Kanai et al., 2000; Oh and Irvine, 2008; Zhao et al., 2010). Alternatively, it can promote a shift in YAP/TAZ binding partners as in the case of Tumor protein p73 (p73) interaction (Matallanas et al., 2007). When the Hippo pathway is off, YAP/TAZ is localised in the nucleus where it binds to transcription factors such as TEA domain transcription factors (TEAD), Smads, Runt-related transcription

factor (RUNX) and β-catenin to regulate expression of genes related to cell proliferation, survival and regeneration (Alarcón et al., 2009; Heallen et al., 2011; Passaniti et al., 2017; van der Weyden et al., 2012; Varelas et al., 2008; Varelas et al., 2010; Vassilev et al., 2001).

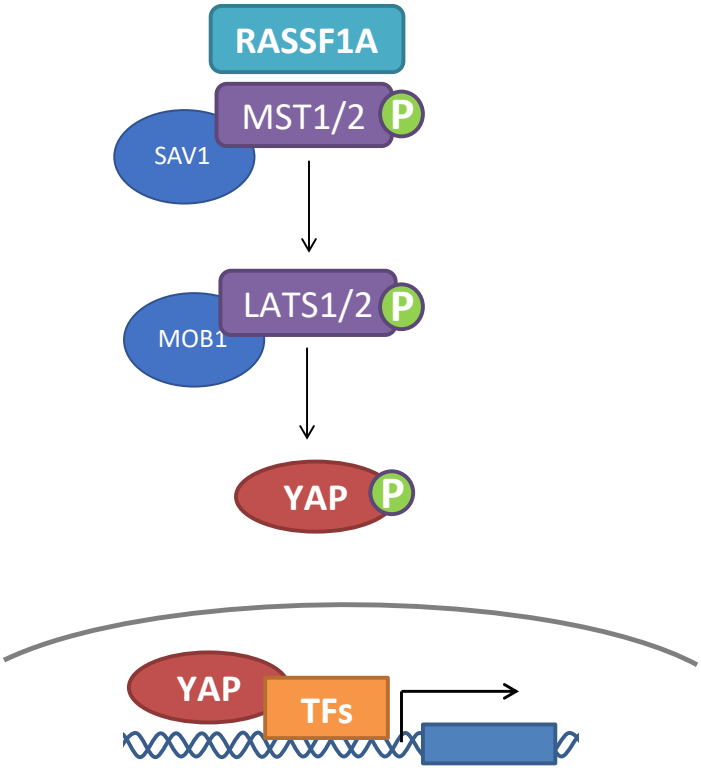


Figure 1.9. The Hippo pathway.

Simplified schematics of the mammalian Hippo pathway. The co-transcriptional factor YAP is the main effector of the pathway. In the nucleus, YAP associates with transcription factors (TF) upregulating transcription of target genes. MST1/2 and LATS1/2 kinases compose the core of the pathway, and are activated upon interaction with SAV1 and MOB1, respectively. Upstream components such as RASSF1A can regulate activation of the pathway resulting in YAP phosphorylation. Adapted from (Taha et al., 2018).

Many upstream proteins act through Hippo pathway-mediated YAP phosphorylation, including Ras association domain-containing protein 1 A (RASSF1A). RASSF1A is a scaffold protein product of the *RASSF1* gene that is commonly methylated

in cancer (Dammann et al., 2000). RASSF1A (R1A) interacts with and activates MST1/2 through its SAv/RAssf/Hippo (SARAH) domain (Avruch et al., 2006; Guo et al., 2007; Oh et al., 2006). It has also been described to mediate phosphorylation-dependent YAP interaction with p73, resulting in the expression of lineage specific genes (Papaspyropoulos et al., 2018). YAP also responds to mechanical cues through direct interaction with component of adherent junctions, such as Angiomotin and α-catenin, which are known to cause its cytoplasmic retention (Chan et al., 2011; Wang et al., 2011; Zhao et al., 2011).

1.3.2 Hippo pathway in neural development

The Hippo pathway and its main effector YAP/TAZ have been implicated in many aspects of stem cell maintenance and differentiation. Put simply, YAP is nuclear and promotes self-renewal and proliferation of stem cells, while it is targeted by the Hippo pathway and downregulated during differentiation. Additionally, a switch in YAP binding partners promotes a balance between pluripotency and cell specification.

During early embryogenesis, YAP/TAZ play a role in fate decision between ICM and TE cells in the blastocyst (Nishioka et al., 2009). Nuclear YAP in combination with TEAD promotes pluripotency, and its absence affect expression of NANOG, Oct4 and SOX2 (Lian et al., 2010). YAP-TEAD complexes with β-catenin-Transcription factor 3 (TCF3) to promote Oct4 expression (Papaspyropoulos et al., 2018). Additionally, the complexing of YAP/TAZ with components of the TGFβ/BMP signalling regulates both pathways to inhibit neural fate in favour of pluripotency (Alarcón et al., 2009; Beyer et al., 2013; Varelas et al., 2008). However, once neural fate is acquired, YAP/TAZ play a role

in the proliferation of neural stem cells as well. YAP-TEAD promotes expansion of the neural tube by increasing the neural stem cell pool (Cao et al., 2008; Gee et al., 2011). Additionally, YAP inhibits neurogenesis, and is downregulated during neuronal differentiation (Zhang et al., 2012).

Upstream to YAP, R1A participates in neural differentiation of pluripotent stem cells. This is mediated through phosphorylation of YAP which disables its interaction with TEAD and β-catenin-TCF3 complexes. Moreover, this event does not target YAP for degradation. Instead, it enables YAP interaction with p73, ultimately resulting in transcription of neural differentiation genes (Papaspyropoulos et al., 2018).

The Hippo pathway also participates in apical-basal polarity and it is localised to the junctional complex, responding to several mechanical cues such as cell-cell adhesion. It is well known that high cell density causes YAP/TAZ cytoplasmic retention, which is reverted if junctional proteins are blocked (Varelas et al., 2010; Zhao et al., 2007). More specifically, YAP directly interacts with the adherent junction proteins Angiomotin and α-catenin (Chan et al., 2011; Schlegelmilch et al., 2011; Silvis et al., 2011; Wang et al., 2011; Zhao et al., 2011). Core components of the Hippo pathway, such as Mst1/2 and Lats1/2, are also recruited to adherent junctions by the angiomotin family (Hirate et al., 2013; Paramasivam et al., 2011). Therefore, the junctional complex and scaffold proteins play a role in clustering components of the Hippo pathway together at the junctional complex. This process happens in response to cell density and results in YAP inactivation and inhibition of proliferation.

As previously described, the establishment of apical-basal polarity through the formation of a junctional complex is an essential step during neural development. The

Hippo pathway has been described to participate in that process. For example, disruption of the apical Protocadherin Fat 1 (Fat1) increased cell proliferation in the neuroepithelium through YAP activity (Cappello et al., 2013; Van Hateren et al., 2011). Angiomotin also participates in neuronal differentiation by responding to stiffening of the extracellular matrix. Stiff matrix promotes high polymerisation of intracellular F-actin, which sequester and inactivates angiomotin allowing Yap translocation to the nucleus. Conversely, soft matrix results in the release of angiomotin which then targets YAP to degradation resulting in neuronal differentiation (Zaltsman et al., 2019). Interestingly, the same authors observed two pools of YAP in NSC, a nuclear pool that regulates proliferation, and a pool localised at the junction complex.

Finally, signalling in the cilia can also be regulated by the Hippo pathway (Rausch and Hansen, 2020). Indeed, Mst1/2 is localised to the basal body of the cilium and together with Sav1 promote ciliogenesis (Kim et al., 2014). It does that by impairing the formation of the cilia-disassembly complex Aurora kinase A (AURKA)/Histone Deacetylase 6 (HDAC6) via AURKA phosphorylation. Additionally, cilia associated proteins such as Nephrocystin (NPHP) have been describe to associate with Mst1/2 and Lats1/2, thus acting as an antagonist to the signalling and promoting proliferation through nuclear localisation of TAZ (Habbig et al., 2011; Habbig et al., 2012).

The Hippo pathway has not only been implicated with development, but also is known to respond to several cues that are crucial for the establishment of apical-basal polarity. Therefore, in the Chapter 5 of this thesis I investigated the role of its components in epithelialisation of NEPs using the neural rosette model.

1.4 Research question

Although great effort has been directed towards finding better treatments for neurodegenerative disorders, such treatments are still not very efficient. Stem cell therapy harbours a great potential for such cases; however, it is not commonly used due to the complexity of this approach. There are still many uncertainties regarding how neurodevelopment is regulated.

The aim of this thesis is to help clarify molecular pathways involved with different aspects of neural differentiation. I focus on the role of Galectin-3, a lectin that has been studied in the context of development but for which specific functions remain to be elucidated.

Firstly, due to the strong expression of Gal-3 in the SVZ, I questioned whether this molecule participates in the pSVZ-derived striatal gliogenesis *in vivo*. For that, I used *in vivo* brain electroporation as a method to modulate Gal-3 in SVZ-stem cells.

In light of these new evidences, I moved on to an i*n vitro* model of hESCs-derived neural induction, studying the role of Gal-3 in early neural commitment. I tested if Gal-3 modulation affected neural progenitors' markers expression. Sequentially, two hypotheses were raised to address the molecular mechanism by which Gal-3 participates during that process: the activation of integrin pathway, and the polarisation of neural rosettes. In this context, components of the developmental Hippo pathway, that participate in polarisation, were analysed.

The results presented in this thesis will help in the comprehension of which factors regulate neural stem cell differentiation and the contribution of Galectin-3 and the Hippo pathways to this process.

Chapter 2

Material and Methods

2.1 General laboratory reagents

All chemicals were purchased from either Sigma-Aldrich or Thermo Fisher Scientific, unless stated otherwise. Tissue culture plastic was purchased from Corning and Sarstedt. Glassware was purchased from VWR and Fisher.

2.2 *In vivo* brain electroporation

2.2.1 Animals

All animal studies were performed under UK Home office Project License (PPL) number 30/3096 and personal licenses (PIL) number IBE52FC90, which were approved by the UK Home Office and the University of Oxford ethical review committee and were in accordance with the Animal (Scientific Procedure) Act of 1986. Mice of the strain C57BL/6 were housed in individually ventilated cages (IVC), in a group of maximum 5 animals per cage with free access to certified food and tap water. Pups were maintained with their mother until the end of the experiment (maximum of 17 days). Cages were environmentally enriched with an activity wheel, nesting material and chew sticks. Light cycle was of 12 h day-night, temperature was maintained at 22°C and humidity at 50%.

2.2.2 Preparation of plasmids for electroporation

The plasmids containing short hairpin vector targeting Gal-3 (V1 shGal-3 and V2 shGal-3) used for electroporation were made in the Szele lab (Dr Osama Al Dalahmah) through inserting the annealed Gal-3 short-hairpin sense and antisense sequences of vectors V1 and V2 into the pSilencer 2.0-U6 plasmid (Ambion, #AM7209) (Table 1). A non-target sequence (shNT) was used as a control. To allow cell tracking, vectors were

co-electroporated with pCAG_tdTom_2A_H2BGFP, which was a gift from Dr. Shankar Srinivas's lab (Trichas et al., 2008).

Table 1. Short-hairpin sequences

Sequence name	Sequence
shGal3_v1- sense	GATCCGATGTTGCCTTCCACTTTA**TTCAAGAGA**TAAAGT GGAAGGCAACATCTTTTTTGGAAA
shGal3_v1- antisense	GCTACAACGGAAGGTGAAAT**AAGTTCTCT**ATTTCACCTT CCGTTGTAGAAAAAACCTTTTCGA
shGal3_v2- sense	GATCCGCAGACAGCTTTTCGCTTA**TTCAAGAGA**TAAGC GAAAAGCTGTCTGCTTTTTTGGAAA
shGal3_v2- antisense	GCGTCTGTCGAAAAGCGAAT**AAGTTCTCT**ATTCGCTTTT CGACAGACGAAAAAACCTTTTCGA

Loop-sequences are represented in bold.

The plasmids obtained were amplified and purified after bacterial transformation. Briefly, One Shot TOP10 Chemically Competent *E. coli* (Thermo Fisher Scientific) were thawed and incubated with the plasmids on ice for 15 min (2 µl plasmid + 50 µl bacteria). A heat-shock was performed by transferring the cells to a heat block at 42°C for 30 sec and then to ice for 5 min. Bacteria was allowed to recover in 1 ml of Lysogeny broth media (LB – 31 g/L of LB both base in Milli-Q® water; autoclaved at 121°C, 15 psi for 30 min) for 1 h while shaking at 750 rpm (Eppendorf heat block). Bacterial cells were then seeded in LB agar ampicillin plates (40 g/L of LB agar in Milli-Q® water; autoclaved at 121°C, 15 psi for 30 min, supplemented with 100 µl/ml of ampicillin, allowed to solidify into plates) and incubated overnight at 37°C. Successfully transformed bacteria grow in colonies on the agar plate, which were collected with sterile pipette tips into starter cultures of 3 ml of LB media supplemented with 100 µl/ml of Ampicillin and amplified for 6 to 8 h at 37°C

while shaking at 225 rpm (Innova 44 Incubator). Starter cultures were transferred to expansion cultures of 250 ml of the same media and incubated overnight at 37°C while shaking. In the next day, cells were harvested by centrifugation at 6000 rcf for 15 min at 4°C and the DNA extraction took place according to the EndoFree® Plasmid Maxi Kit (Qiagen) manufacturer's instruction. In short, cells were resuspended and lysed with Buffers P1 + LyseBlue® and P2 and precipitated with Buffer P3 until completely colourless. Lysates was cleaned out using a QIAfilter Cartridge and endotoxins were removed from the solution after a 30 min incubation on ice with Buffer ER. The DNA was collected upon binding to a QIAGEN-tip 500 column, washed and then eluted with Buffer QN. Isopropanol was added to the solution for DNA precipitation, and a DNA pellet was obtained after a 15,000 rcf centrifugation for 30 min at 4°C. The pellet was air dried for 30 min and dissolved in endotoxin-free water.

In preparation for electroporation, plasmids were diluted to a final concentration of 2 µg/µl (1 µg vector or control + 1 µg pCAG_tdTom_2A_H2BGFP in Endotoxin-free water). Fast Green dye at a final concentration of 0.1% was added to facilitate visualisation of the solution during the procedure.

2.2.3 Electroporation

The *in vivo* brain electroporation methodology was previously described (Boutin et al., 2008; Fernandez et al., 2011; Platel et al., 2010). Firstly, C57BL/6 mice on the postnatal day 2 (P2) were anaesthetised by hypothermia (ice-immersion for 2 min). Approximately 2 µl of the solution containing the plasmid (total of 4 µg DNA) was injected into the right lateral ventricle using pulled glass pipettes. The exact point of injection was

calculated at around 2/3 of the distance between the Lambda suture and the right eye. Visual assessment of the dye ensured the correct delivery of the solution. Electroporation was then carried out using CUY650-P5 tweezer electrodes (Sonidel), which were coated with electroconductive gel and connected to an electroporator (BTX ECM830). Five 100 V pulses were conducted, each lasting 50 milliseconds (ms) with 850 ms interval in between. The whole procedure took no longer than 5 min, and the pups were allowed to recover for 20 min in a heated box (36°C) before returning to the dam. Animals were perfused 17 days post electroporation (DPE) for posterior sectioning of the brain. Approximately 70% of the procedures were successful. Successful procedures were defined by the presence of several dozen or more tdTomato+ or GFP+ cells in the SVZ. The survival rate was higher than 99%.

2.3 Tissue collection and microtomy

Animals were first overdosed with intraperitoneal pentobarbital and the tissue was fixed by perfusion with 4% paraformaldehyde (PFA) in 0.1 M Phosphate Buffer [PB – 28 mM Sodium phosphate monobasic (NaH_2PO_4) + 72 mM Sodium phosphate dibasic anhydrous (Na_2HPO_4) in distilled water, pH 7.4]. The brains were dissected and transferred to a 15 ml tube containing 4% PFA for post-fixation overnight at 4°C. The next day, brains were transferred to a cryoprotective solution (300 g sucrose + 300 ml ethylene glycol/L in PB) at 4°C and kept that way until they sank (approximately 2 days). Brains were then frozen in dry ice and stored at -80°C.

Serial coronal sections of approximately 30 µm were obtained using a sliding microtome (Leica). Sections from the olfactory bulb until the hippocampus were kept in 48-well plates in cryoprotectant solution at -20°C.

2.4 Brains sections provided

Brain sections of Gal-3 overexpression and Cre-induced Gal-3 knockout at different time points were generated in the Szele lab (Dr. Osama Al Dalahmah). Those sections were obtained from Gal-3$^{flox/flox}$ mice which were electroporated with of pCAGIG (control) (Addgene #11159) or pCAG-Cre-IRES2-GFP (Cre) (Addgene #26646) plasmids; and C57BL/6 mice electroporated with pCAGIG (control) or pCAG-Gal-3-IRES-GFP (Gal-3 OE) (Al-Dalahmah et al., 2020a).

2.5 Immunofluorescence of free-floating brain sections

For immunofluorescence (IF), free-floating SVZ sections (up to 6/animal) were placed in plates of 12-wells containing phosphate buffered saline [PBS – 8 g Sodium chloride (NaCl) + 240 mg Potassium dihydrogen phosphate (KH_2PO_4) + 1.44 g Sodium phosphate dibasic anhydrous (Na_2HPO_4) in distilled water, pH 7.4] for an initial wash of the cryoprotectant. All the washes were performed on a rotating shaker. Porous well inserts (Sigma-Aldrich) were used to facilitate transference of the sections between wells. In order to avoid possible background caused by the fixation process, a step of 15 min incubation with 50 mM glycine in PBS was conducted, followed by another round of PBS washes (3 times of 10 min each). Unspecific sites of antibody recognition were blocked with PBS+ solution (PBS + 10% Donkey serum + 0.1% Triton-X-100) for 1 h at room temperature (RT). Primary antibody incubation was conducted overnight at 4°C with

antibodies diluted in PBS+ at different concentrations (Table 2). The next day, the excess antibody was washed away with a set of PBS washes (3 times of 10 min each), which preceded the 1 h RT incubation with secondary antibodies diluted at 1:500 in PBS+. Secondary antibodies were species-specific and conjugated with Alexa Fluor 488, 568, 594, or 647 fluorophores (Invitrogen and Sigma-Aldrich). This step and the following ones were conducted in darkness to protect fluorophores from bleaching. After washes with PBS (3 times of 10 min each), the nuclei were stained with 4',6-diamidino-2-phenylindole (DAPI, Sigma-Aldrich). For DAPI staining, cells were incubated for 10 min RT with 10 µg/ml DAPI diluted in PB. A final set of 3 times 10 min wash with PB was conducted before sections were mounted on Superfrost Plus™ slides (Thermo Fisher Scientific). After airdrying for approximately 30 min, slides were mounted with FluorSave mounting media (Calbiochem) and stored at 4°C in darkness.

Table 2. Antibodies used for free-floating immunohistochemistry

Antigen	Host	Clonality	Dilution	Supplier	Catalogue
A.caspase3	Rabbit	Polyclonal	1:500	Cell Signalling	#9661
Galectin-3	Rat	Monoclonal	1:100	Santa Cruz	#SC 23938
GFAP	Rat	Monoclonal	1:400	Invitrogen	#13-0300
GFP	Chicken	Polyclonal	1:500	Aves-lab	#GFP 10-10
Iba1	Goat	Monoclonal	1:300	Abcam	#ab5076
Olig2	Rabbit	Polyclonal	1:1000	Millipore	#AB9610

2.6 Image analysis and quantifications of brain sections

A ZEISS LSM 710 Laser Scanning Confocal Microscope was used to take images of at least 3 SVZ sections per brain (technical replicates). Z-stacks with 1.0 µm interval were acquired using a 20X (Zeiss Plan-Neofluar 20X/0.50) or 40X (Zeiss Plan-NeoFluar 40X1.3 Oil DIC) objective lens. To allow quantification, a minimum of 3 images of the SVZ

and adjacent striatum were acquired per section, which were analysed using the FIJI (NIH ImageJ) software package.

At least 100 cells per animal were quantified whist I was blinded to the experimental conditions. Gal-3 knockdown validation was measured by the proportion of Gal-3 positive cells that were also positive for tdTomato in the SVZ divided by the total number of tdTomato positive cells in the SVZ (tdTom+Gal-3+/tdTom+). Striatal gliogenesis was obtained from the proportion of GFP+ cells in the striatum divided by the total number of GFP+ cells [GFP+STR/ Total GFP+ (STR plus SVZ)]. Microglia density was calculated by counting Ionized calcium-binding adapter molecule 1 (Iba)+ cellular bodies in the SVZ or striatum divided by the region's volume [volume = area o region of interest (ROI) calculated in FIJI (NIH ImageJ) multiplied by the number of z-stacks]. The activation state of microglia was calculated as a percentage of microglia classified as activated, intermediate or resting against total Iba1+ cells per region.

Non-specific binding was always assessed with a secondary antibody-only negative control for immunofluorescence staining. Only experiments that lacked non-specific binding were used.

2.7 Cell lines and culture

2.7.1 H9

The human embryonic pluripotent stem cell line H9 (WA009) was acquired from WiCell. Cells were maintained in a humidifying incubator at 37°C and 5% CO_2 and kept in a feeder-free culture using defined medium mTeSR™Plus (StemCell Technologies) (Ludwig et al., 2006a; Ludwig et al., 2006b). Media was completely replaced every two

days. Cells were kept in plates of either 60 mm or 100 mm diameter coated with Matrigel™ [Corning, diluted to 83.33 µg/ml in Dulbecco's Modified Eagle Medium/Nutrient Mixture F-12 (DMEM/F-12, Gibco)], which was allowed to polymerise for 1 h at RT before being aspirated. Matrigel™-coated plates were immediately used or filed with fresh DMEM/F-12 and kept at 4°C for maximum 7 days.

Cell were allowed to grow until aggregates reached high density through visual assessment and then split in a ratio of 1:5 using ReLeSR™ (StemCell Technologies) according to the manufacture's protocol. Briefly, cells were washed once with D-PBS (without Ca++ and Mg++) (StemCell Technologies). ReLeSR™ was added to the plate and aspirated within 1 min allowing only a thin layer to remain. After 8 min in the incubator, mTeSR™Plus was added and aggregates were detached by few firm hand taps on the lateral of the plate. Cell were carefully transferred to a new Matrigel™-coated plate containing fresh mTeSR™Plus using a 5 ml pipette to avoid further breakage of aggregates.

Pluripotent H9 cells were cryopreserved after splitting as previously described and centrifuged at 300 rcf for 5 min. The pellet was cautiously resuspended with mFreSR™ Medium (StemCell Technologies) and directly frozen down with a standard slow rate-controlled cooling protocol (Mr. Frosty™ Freezing Container, Thermo Fisher Scientific) in a -80°C freezer and then transferred to liquid nitrogen for long term storage. Vials were thawed at 37°C in a water bath for a few minutes, the content was transferred to a 15 ml Falcon tube and mTeSR™Plus slowly added. Sequentially, cells were spun down at 300 rcf for 5 min and resuspended in mTeSR™Plus supplemented with the ROCK (Rho-associated kinase) inhibitor Y-27632 (StemCell Technologies) to a concentration of 10

μM. Y-27632 was used only in the first day to reduce anoikis and removed afterwards (Li et al., 2009; Watanabe et al., 2007).

2.7.2 ReNcell® CX and VM

The human neural progenitor cell lines ReNcell® CX and VM (Donato et al., 2007) were acquired from Merck Millipore. Cells were maintained in ReNcell® NSC Medium (Merck Millipore) supplemented with FGF and EGF (Merck Millipore) to a final concentration of 20 ng/ml each, and cultured in a humid incubator at 37°C and 5% CO_2.

Cells grew in tissue culture flasks coated with laminin (Sigma-Aldrich). For that, laminin was thawed at 4°C for approximately 1 h, diluted to 20 μg/ml in DMEM/F-12 and added to the flask for at least 4 h in the incubator (37°C). After aspiration of laminin, flasks were immediately used. Cells were split with Accutase™ (Merck Millipore) once culture reached approximately 80% confluency. Briefly, cells were washed once with Oxoid™ PBS (Thermo Fisher Scientific) and incubated with Accutase™ for 4 min in the incubator. Cells were then added of ReNcell® NSC Medium and resuspended, transferred to a 15 ml tube and centrifuged at 300 rcf for 5 min. The pellet was resuspended in fresh media and seeded in laminin-coated plates.

A similar procedure was followed for cells cryopreservation. In that case, the pellet was resuspended in a concentration of approximately 3 x 10^6 cells/ml in ReNcell® freezing medium (Merck Millipore) and added to cryovials which followed a rate-controlled cooling protocol with Mr. Frosty™ Freezing Container. Cell were thawed in a water bath at 37°C for a few minutes, until almost entirely thawed, then transferred to a 15 ml tube and 5 ml ReNcell® NSC Medium added. Cells were then pelleted down and resuspended

in fresh ReNcell® NSC Medium supplemented with growth factors and transferred to laminin-coated flask.

2.8 Differentiation assay

Pluripotent H9 cells were induced to commit to the neural lineage using a dual SMAD inhibition methodology (Chambers et al., 2009). For that, cells were detached upon incubation with Versene™ (Thermo Fisher Scientific) for 5 min in the incubator. Cells were then resuspended with a 5 ml pipette until a single-cell suspension was obtained. The density of cells in the suspension was calculated using a haemocytometer and cells were pelleted down at 300 rcf for 5 min. Cell pellets were resuspended in STEMdiff™ Neural Induction Medium (StemCell Technologies, also called NIM in this thesis) supplemented with SMAD inhibitors (STEMdiff™ SMADi Neural Induction Supplement, provided in the STEMdiff™ Neural Induction Medium Kit) and seeded on Matrigel™-coated plates of either 6, 24, 48 wells. In order to obtain a confluent monolayer culture, the density seeded was of 1 x 10^6 cells/ml. Y-27632 (10 μM) was added on the first day to increase survival rate and media was changed daily. Cells were allowed to differentiate for a maximum of 7 days.

2.9 Transient transfections

2.9.1 H9 transfection

To promote transient knockdown of Gal-3 in H9 cells, a pool of small interfering RNAs targeting Gal-3 (siGal3) was acquired from Dharmacon (siGal-3) and a sequence targeting luciferase was acquired from Eurofins MWG and used as a non-target control

(siNT) (Table 3). siRNAs were diluted in nuclease-free water to100 µM and stocked at -20°C.

Reverse lipid transfection was performed using Lipofectamine 3000 (Invitrogen). Briefly, siRNAs were diluted in OptiMEM™ (Gibco) to a reach a final concentration of 100 nM. The solution was distributed in wells of 24 well Matrigel™-coated plates (100 µl) and 1 µl of Lipofectamine was then added on this solution, gently mixed, and incubated in the plate for 15 min, allowing the formation of lipid droplets containing siRNA. Pluripotent H9 aggregates were detached using Versene™ as previously described and a single cell suspension of 1.6 x 10^6 cells/ml was generated in mTeSR™Plus. The suspension containing the cells was then added to the wells (500 µl/well) already containing the lipid droplets and incubated for 24 h. The media was changed in the next day to STEMdiff™ Neural Induction Medium plus SMADi and renewed daily. Cells were collected at different time points.

Table 3. siRNA sequences used

Target gene	siRNA target sequence	Supplier
siLuciferase (siNT)	GCCAUUCUAUCCUCUAGAGGAUG	Eurofins MWG
siGal3 human (siGenome SMARTpool)	GAAGAAAGACAGUCGGUUU (1) GCAAUACAAAGCUGGAUAA (2) GUACAAUCAUCGGGUUAAA (3) CAGUACAAUCAUCGGGUUA (4)	Thermo (Dharmacon)

2.9.2 ReNcell® transfection

ReNcell® CX and VM were nucleofected with the shGal-3 sequences described in Table 1 for validation of the knockdown. For that, an 4D-Nucleofector™ X Unit (Lonza) was used according to the P3 Primary Cell 4D-NucleofectorTM X Kit (Lonza)

manufacturer's instruction. For that, ReNcell® were passaged with Accutase™ as previously described and cells were centrifuged for 5 min at 300 rcf. The pellet containing 2.5 x 10^6 cells per reaction was resuspended in 20 µl of Nucleofector™ Solution already added of Supplement 1. Plasmid (0.5 µg) were added to the solution and then transferred to a well of a 16-well Nucleocuvette™ strip, which was gently tapped to avoid bubbles, and immediately transferred to the 4D-Nucleofector™ X Unit. The program CD100 was used for ReNcell® CX and CM162 for ReNcell® VM. After nucleofection, cells were incubated for 10 min at RT and finally fresh ReNcell® NSC Medium was added. Cells were seeded in laminin-coated 6-well plate and collected 48 h after transfection to assess Gal-3 depletion.

The plasmids used were the same as described for the *in vivo* brain electroporation (shNT and shGal3 V1). The pmaxGFP™ vector (Lonza) was used to assess the efficiency of nucleofection through the quantity of GFP+ cells in culture, which was always more than 90%.

2.10 Cell treatments

Carrier-free human recombinant Gal-3 (R&D systems, #1154-GA-050/CF) was diluted in D-PBS at 100 µg/ml, aliquoted and kept in -20°C for not longer than 3 months. For H9 treatment, STEMdiff™ Neural Induction Medium media already containing SMADi was supplemented with Gal-3 at the final concentration of 1 µg/ml and added to cells. This process was repeated every other day. The control group was treated with the same quantity of D-PBS. Cells were collected at different days.

For Gal-3 activity inhibition experiments, H9 cells were treated every day with 1 or 5 µg/ml of rat Gal-3 antibody clone M3/38 (Santa Cruz, #sc-23938) diluted in STEMdiff™ Neural Induction Medium + SMADi. The same quantity of species specific IgG was used as a control (Cell Signalling Technology). Cells were collected at different days.

2.11 Western Blotting

2.11.1 Protein extraction

For protein extraction, cells were first washed once with PBS and detached from the plate with Accutase™ for 4 min in a 37°C cell culture incubator. Cells were transferred to a 1.7 ml microtube and pelleted down for 5 min at 500 rcf at 4°C. The pellet was washed once with cold PBS and spun down in the centrifuge with the same settings. After discarding the supernatant, the pellet was immediately frozen down in dry ice and kept in a -80°C freezer. Alternatively, pellets were immediately lysed using protein lysis buffer [50 mM Tris hydrochloride (Tris-HCl) pH 8.0 + 150 mM NaCL + 1 mM Ethylenediaminetetraacetic acid (EDTA) + 1 mM Ethylene glycol tetraacetic acid (EGTA) + 1% Nonidet P-40 (NP40) + 0.5% Sodium deoxycholate + 10% Pierce™ Phosphatase Inhibitor (Thermo Fisher Scientific) + 10% cOmplete™ Protease Inhibitor Cocktail (Roche) in Milli-Q® water], which was added in quantity according to the approximate size of the pellet (50 µl for a 30 mm diameter plate, for example). In order to avoid DNA contamination, samples were sonicated for approximately 10 sec in amplitude 10% in Branson 450 Digital Sonifier® (Emerson). Finally, lysates were centrifuged at maximum speed for 15 min and the supernatant containing proteins was transferred to a new microtube. Samples were always kept at 4°C.

2.11.2 Protein quantification

Samples were quantified through the Bradford colorimetric methodology (Bradford, 1976) in a 96-well plate using Pierce™ Bovine Serum Albumin Standard Ampules (Thermo Fisher Scientific) as a standard. In brief, 1 µl of each sample was loaded in triplicates and 200 µl of Pierce™ Coomassie Plus (Bradford) Assay Reagent was added on top. Sample and reagent were carefully mixed with a micropipette avoiding bubbles. The absorbance was read with 595 nm wavelength in a microplate reader (BMG POLARstar Omega). Protein concentration was calculated based on the linear equation generated from the standard curve.

At the end, 30 to 50 µg of proteins per sample were treated with NuPAGE™ LDS Sample Buffer (Invitrogen) added of 100 mM of the reducing reagent dithiothreitol (DTT), and then denatured by boiling at 97°C for 5 minutes.

2.11.3 SDS Page and Immunoblotting

Samples were loaded in NuPAGE™ 4 to 12%, Bis-Tris, 1.5 mm, Mini Protein Gel (Invitrogen) and separated according to the molecular weight through electrophoresis using PowerPac™ HC High-current power supply (Bio-Rad). Electrophoresis was conducted upon controlled voltage at 100 V for approximately 2 h using NuPAGE™ MOPS SDS Running Buffer (Invitrogen). The PageRuler™ Prestained Protein Ladder (Thermo Fisher Scientific) was used as a base for the molecular weight distribution in the gel. After electrophoresis, proteins were transferred from the gel to an Immobilon®-FL PVDF membrane of pore size 0,45 µm (Merck Millipore) using controlled voltage of 100 V and cold transfer buffer (25 mM Tris-HCl + 190 mM glycine + 20% methanol in distilled

water) for 90 min. An ice block and a magnetic stirrer were used to avoid solution overheating. After transfer, proteins were briefly visualised in the membrane using Ponceau S Solution (Sigma-Aldrich), according to the manufacturer's protocol, which offered an indication of the quality of the procedure until that point. Membranes were washed in PBS-Tween (PBS-T – 0.1% Tween® 20 in PBS) and then blocked in Milk 5% (5% skimmed milk powder in PBS-T) for 1 h at RT. Primary antibodies diluted at different concentrations (Table 4) in Milk 5% or BSA 5% [5% BSA (Sigma-Aldrich) in PBS-T] were incubated with the membranes overnight at 4°C while shaking. In the next day, 3 times of 10 min washes with PBS-T preceded and followed a 1 h incubation with species-specific secondary antibodies (Cell Signalling Technology). Secondary antibodies were horseradish peroxidase (HRP)-labelled and were diluted to 1:2500 in Milk 5%. Protein bands were obtained in X-ray film (Fujifilm) and developed in ECOMAX™ X-ray Processor (Raytech Diagnostics) after 1 min incubation with Pierce™ ECL Western Blotting Substrate (Thermo Fisher Scientific). In some cases, secondary antibodies were de-activated by 30 min incubation with 0.02% sodium azide and membranes were re-incubated with other antibodies.

Densitometry quantification of bands were obtained in the FIJI (ImageJ) software and are given in arbitrary units (AU). Graphs were generated with GraphPad Prism 8 software and express quantity of protein relative to a loading control such as glyceraldehyde-3-phosphate dehydrogenase (GAPDH) or Histone 3 (H3).

2.12 Immunoprecipitation

For immunoprecipitation (IP), cells were lysed using the Immunoprecipitation lysis buffer [IP/LB – 150 mM NaCl + 0.5 mM EDTA + 20 mM Hepes pH 7.5 + 1% NP40 0.5% Pierce™ Phosphatase Inhibitor (Thermo Fisher Scientific) + 0.5% cOmplete™ Protease Inhibitor Cocktail (Roche) in Milli-Q® water] and proteins were extracted as described above at 2.11.1. Approximately 300 µl of the lysis buffer was used per 60 mm diameter plate. After centrifugation, extracts were similarly quantified via Bradford colorimetric methodology as described in 2.11.1. Samples were normalised and the same quantity of protein was taken from each condition, aiming for at least 1 µg of protein per sample. Samples were kept in the ice for all times.

Protein G Magnetic Beads (Millipore) was used for IP. Firstly, 30 µl of beads per sample were cleaned using a magnet (Thermo Fisher Scientific) and resuspended in the same volume of IP/LB. Samples were then pre-cleaned with 10 µl of beads/sample for 30 min at 4°C while rotating. Beads bound to non-specific protein were discarded using a magnet. Approximately 30 µl/sample (10%) was saved as input control and treated with NuPAGE™ LDS Sample Buffer + DTT. Cleaned samples were then incubated with 20 µl/sample of beads plus antibodies at various quantities (Table 4). A species-specific anti-IgG1 antibody (Cell Signalling Technology) was used as a negative control. Samples were incubated overnight at 4°C while rotating. In the next day, beads containing the antibody conjugated with the protein of interest were collected using a magnet. After 3 washes with IP/LB to avoid unspecific contamination, beads were treated with approximately 50 µl of NuPAGE™ LDS Sample Buffer + DTT. All samples were boiled and used to run a Western blot as described in 2.11.3.

2.13 Immunofluorescence of hESCs

For immunofluorescence of H9 cells, 13 mm circular coverslips were added to the culture plates before incubation with Matrigel™. Cover slips with attached cells were collected from the plate and fixed with PFA 4% (Thermo Fisher Scientific) for 15 min at RT in darkness. Alternatively, for visualisation of ciliary structures, cover slips were fixed with PFA 4% for 5 min, washed with PBS once and fixed for another 20 min in Methanol at -20°C. After fixation, cover slips were kept at 4°C in PBS or immediately permeabilised for 15 min with 0.5% Triton™ X-100 (Sigma-Aldrich) in PBS. Cover slips were blocked at RT for 1 h with blocking solution (5% BSA + 0.2% Triton™ X-100 in PBS) and then incubated with primary antibodies at RT for 2 h. Primary antibodies were diluted in antibody solution (1% BSA + 0.2% Triton™ X-100 in PBS) at different concentrations (Table 4) and a volume of 50 µl was enough to completely cover the area of the cover slips. After washing by an approximately 30 sec immersion in PBS, cover slips were incubated for 1 h at RT with secondary antibodies diluted in antibody solution at 1:500, 1:1000 or 1:2000 plus 10 µg/ml DAPI (Thermo Fisher Scientific). Secondary antibodies were species-specific and conjugate with Alexa Fluor 488, 568, or 647 fluorophores (Invitrogen). Following the incubation with secondary antibodies, coverslips were washed with PBS as described. For F-actin staining, cover slips were incubated for another 15 min at RT with Alexa Fluor™ 568 Phalloidin (Invitrogen) diluted to 1:20 in PBS. Cover slips were mounted using ProLong™ Gold Antifade Mountant (Invitrogen), sealed with nail polish and air-dried overnight at 4°C in darkness. Images were acquired using Nikon Eclipse Ni-E Microscope or ZEISS LSM 780 Laser Scanning Microscope and processed in FIJI (ImageJ) software. Non-specific binding was always assessed with a secondary

antibody-only negative control for immunofluorescence staining. Only experiments that lacked non-specific binding were used.

Table 4. Antibodies used for hESCs experiments

Antigen	Host	Clonality	Dilutions (WB)	(IF)	(IP)	Supplier	Catalogue
Acetyl-α-Tubulin	Mouse IgG2b	Monoclonal	-	1:500	-	Sigma-Aldrich	#T6793
ARL13B	Rabbit	Polyclonal	-	1:50	-	Proteintech	#17711-1-AP
ARL13B	Mouse	Monoclonal	-	1:50	-	Santa Cruz	#sc-515784
Galectin-3	Rat	Monoclonal	1:1000	1:50	-	Santa Cruz	#sc-23938
Galectin-3	Rabbit	Polyclonal	-	-	1 μg/sample	Santa Cruz	#sc-20157
GAPDH	Mouse	Monoclonal	1:1000	-	-	Cell Signalling	#5174
γTubulin	Mouse IgG1	Monoclonal	-	1:500	-	Sigma-Aldrich	#T6557
H3	Mouse	Monoclonal	1:2000	-	-	Cell Signalling	#14269
Integrin α5	Rabbit	Polyclonal	1:1000	-	-	Cell Signalling	#4705
Integrin β1	Rabbit	Polyclonal	1:1000	-	1:50	Cell Signalling	#4706
Integrin β1	Mouse	Monoclonal	1:1000	-	-	Santa Cruz	#sc-59829
Integrin β3	Rabbit	Monoclonal	1:1000	-	-	Cell Signalling	#13166
NANOG	Rabbit	Monoclonal	1:1000	1:100	-	Cell Signalling	#4903
Nestin	Goat	Polyclonal	1:1000	1:100	-	Santa Cruz	#sc-21248
Oct4	Rabbit	Monoclonal	1:1000	1:100	-	Cell Signalling	#2840
Pax-6	Rabbit	Polyclonal	1:1000	1:100	-	Bio Legend	#901301
RASSF1A	Rabbit	Polyclonal	1:500	1:50	-	Atlas	#HPA040735
RASSF1A	Mouse	Monoclonal	1:100	-	-	Santa Cruz	#sc-58470
SOX2	Rabbit	Monoclonal	1:1000	1:100	-	Cell Signalling	#3579
P(S127)YAP	Rabbit	Polyclonal	1:1000	1:50	-	Cell Signalling	#4911
YAP	Mouse	Monoclonal	1:1000	1:50	-	Santa Cruz	#sc-101199
ZO-1	Mouse	Monoclonal	-	1:50	-	Invitrogen	#33-9100

WB: Western blotting; IF: Immunofluorescence; IP: Immunoprecipitation.

2.14 Statistics

All experiments were conducted at least three time, unless stated otherwise. n numbers represent independent biological replicates, unless stated otherwise. Independent biological replicates in Chapter 3 are different animals; independent biological replicates in Chapter 4 and 5 are neural inductions from different plates, seeded in different days, from cells at different passages or batches. Analyses and graphs were acquired using GraphPad Prism 8 software and data is presented as mean ± standard error of the mean (SEM). Student's t-test was used to assess difference between two groups. Significant difference is presented as * for $p < 0.05$, ** for $p < 0.01$, and *** for $p < 0.001$.

Chapter 3

The role of Galectin-3 in SVZ gliogenesis in mice

3.1 Introduction

During the first weeks after birth, the region surrounding the lateral ventricles of the brain contains neural stem cells that continue to generate neurons and glia. This is the postnatal subventricular zone (pSVZ), which originates from the embryonic neuroepithelium of the forebrain (Ihrie and Alvarez-Buylla, 2011).

The pSVZ is associated with high rates of neurogenesis, generating neuroblasts that both migrate to the OB to generate interneurons, and migrate out tangentially to the cortex (Bayer, 1983; Paredes et al., 2016). But it is during this period of development that the SVZ produces a peak of glial cells after birth (Levison et al., 1993; Levison and Goldman, 1993). Astrocytes and oligodendrocytes arise and populate the cortex and the adjacent striatum (Brazel et al., 2003; Marshall et al., 2003). Astrogenesis happens before oligodendrogenesis, with the latter process continuing in young adults (Lyck et al., 2007; Parnavelas, 1999). Understanding the mechanisms that regulates gliogenesis in the SVZ is of great therapeutic potential for brain damage. Some molecular pathways have been investigated in the context of pSVZ gliogenesis. For example, it is known that, while BMP regulates astrogenesis, PDGF promotes oligodendrocytic fate (Jackson et al., 2006; Lim et al., 2000). However, many aspects of the regulation of this process remains to be elucidated.

As described above, Galectin-3 (Gal-3) is a galactoside binding lectin that have affinity for branched poly-LacNAc containing N-glycans (Hirabayashi et al., 2002; Seetharaman et al., 1998). Due to the ability to form pentamers, Gal-3 can bind and bring together different glycoproteins (Ahmad et al., 2004). Secreted Gal-3 can bind to components of the extracellular matrix and to transmembrane receptors to participate in

cell adhesion, migration and signalling transduction (Ochieng et al., 2002). Alternatively, intracellular Gal-3 plays a role in several cellular signalling pathways through protein-protein interaction (Dumic et al., 2006; Liu et al., 2002; Wang et al., 2004). Among the signalling that Gal-3 regulates, many are related to neural development and maintenance of stem cells potency (Kuo et al., 2016; Nakajima et al., 2014). Remarkably, in the healthy brain, the only region where Gal-3 is readily detectable is the pSVZ. In this region, Gal-3 is expressed in NSC, TAPs and ependymal cells, and has been implicated in neuroblast migration, overall neurogenesis and oligodendrogenesis (Comte et al., 2011; Pasquini et al., 2011; Thomas and Pasquini, 2018). However, the role of Gal-3 in the pSVZ gliogenesis remains elusive.

In this chapter, I started investigating the role of Gal-3 in neural differentiation by studying its role in pSVZ gliogenesis *in vivo*. In order to do that, I modulated Gal-3 expression levels in the pSVZ and questioned if this would have an effect on the quantity of glial cells that migrated out to populate the striatum. I then attempted to determine the fate of those cells to assess Gal-3's possible involvement in cell fate decisions. Finally, I investigated if overexpression of Gal-3 resulted in increased apoptosis or inflammation, which could signify an off-target effect of the protein rather than a direct effect on gliogenesis.

The results presented in this chapter considerably increase our knowledge on endogenous function of Gal-3 in neural differentiation, specifically of NSC from the pSVZ, and contributed to a publication in a peer-review journal (Al-Dalahmah et al., 2020a)

3.2 *In vivo* brain electroporation

In order to study the role of Galectin-3 in postnatal SVZ (pSVZ) gliogenesis, I used postnatal *in vivo* brain electroporation, which allowed the modulation of Gal-3 in NSCs by promoting the incorporation of plasmids of interest. The technique consisted of injecting the DNA in the lateral ventricle and posteriorly using electrical tweezers to stimulate DNA incorporation into the adjacent cells. The electrical current applied directs the DNA towards the positive electrode, resulting in gene expression modulation in the pSVZ (Boutin et al., 2008; Chesler et al., 2008; Fernandez et al., 2011).

In this study I was interested in postnatal gliogenesis, therefore the electroporation was conducted in P2 animals and gliogenesis was allowed to happen for 3, 7 or 17 days (DPE – days post electroporation) (Figure 3.1 A). After this period, the brains were collected and cells that had incorporated the plasmid could be tracked using a fluorescent reporter. The reporter used, pCAG-tdTom-2A-H2BGFP, allowed distinction between the nucleus and the cytoplasm by different fluorophores, with the nuclear staining in green (GFP) and the cytoplasmic in red (tdTomato) (Trichas et al., 2008). At 17 DPE, it was possible to observe a good number of labelled cells in the pSVZ, which were self-renewing and/or maintained NSCs, and a number of cells in the striatum (Figure 3.1 B). pSVZ cells have been described to migrate out to the striatum to generate glia (Levison et al., 1993; Levison and Goldman, 1993). The glial identity of these cells was further confirmed via morphological characterisation together with immunofluorescence staining of specific markers, conducted by a previous member of the lab (Al-Dalahmah et al., 2020a). Additionally, a portion of labelled NSC had become neuroblasts, migrated out to

the olfactory bulb and differentiated into interneurons, as expected (Bayer, 1983; Paredes et al., 2016) (Figure 3.1 C).

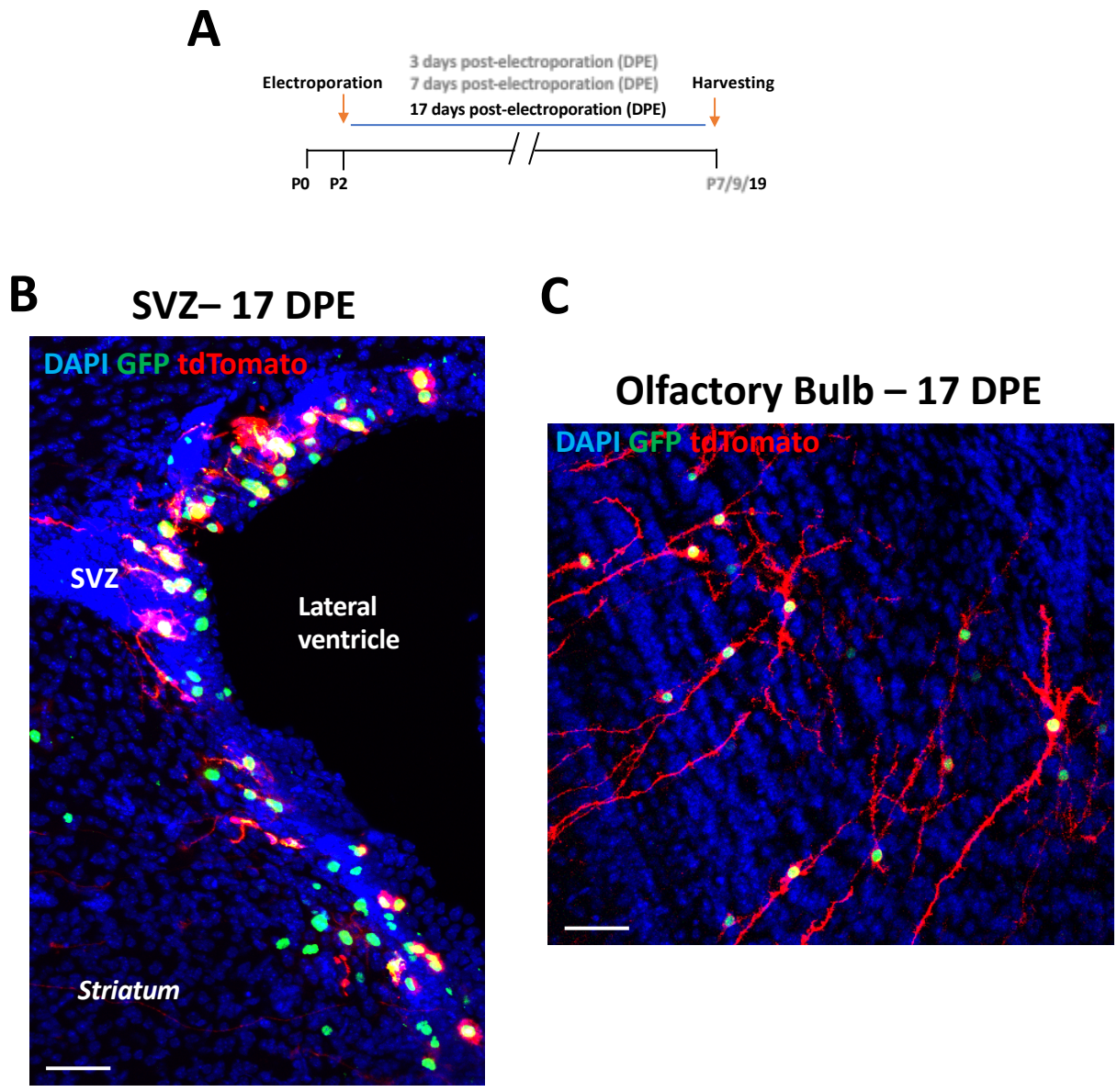


Figure 3.1. *In vivo* brain electroporation.

A) Timeline showing that electroporation was performed at postnatal day 2 (P2) and brains were collected at either 3, 7 or 17 days post electroporation (DPE). B) Confocal image illustrating how pSVZ stem cells are labelled and can be tracked after incorporation of plasmids. C) Confocal image showing that labelled neuroblasts migrated to the olfactory bulb to become interneurons. Scale bar 50 µm.

The efficiency of the technique was visually assessed via the presence of positive labelled cells in the pSVZ, and no difference in the quality of the technique (assessed via the number of cells and their morphology) between experimental conditions was observed. The rate of DAPI+ cells labelled by the fluorescent tracker in the pSVZ at 3 DPE was found to be 7.8±1.9% (n=3 animals), which was in accordance to the typical rates in the lab, which ranges around 10% efficiency of electroporation.

Using electroporation, I modulated the expression of Gal-3 in the pSVZ together with the expression of a cell tracker. To assess Gal-3 loss-of-function phenotype, I co-electroporated the fluorescent tracker pCAG-tdTom-2A-H2BGFP with plasmids containing two different short hairpin sequences against Gal-3 (shGal-3 V1 and shGal-3 V2), or with a non-targeting sequence (shNT) as a control (Figure 3.2 B, clear purple square). I also had access to brain sections of a conditional knockout experiment conducted by a previous member of the lab, where Gal-3 deletion was achieved by using a Cre/lox system. In this case, the site-specific recombinase Cre was delivered to pSVZ cells of Gal-$3^{flox/flox}$ mice through electroporation, resulting in deletion of Gal-3 through cleavage and recombination of the lox sites flanking its gene (Branda and Dymecki, 2004; Feil, 2007) (Figure 3.2 B – faint purple square). Additionally, Gal-3 was overexpressed in the pSVZ of wild type mice and cells were tracked using GFP as a reporter (Figure 3.2 A).

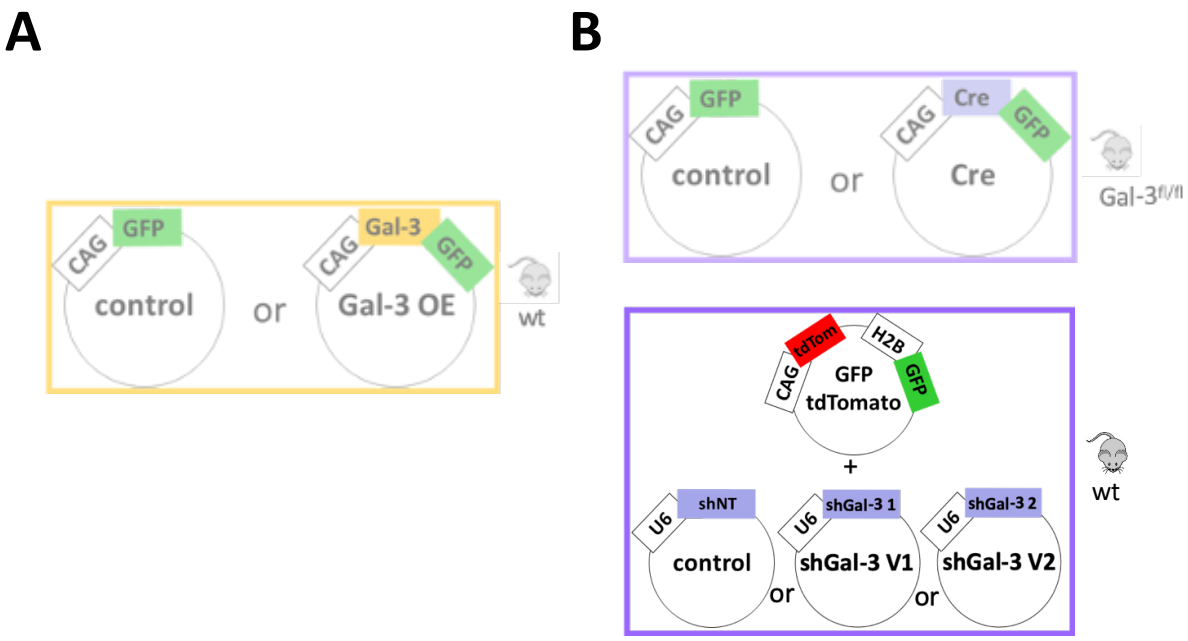


Figure 3.2. Plasmids used for Gal-3 *in vivo* modulation.

Plasmids used for A) Gal-3 overexpression (yellow) and B) depletion (purple) experiments. The faint figures represent experiments previously conducted by a member of the lab.

3.3 Galectin-3 Knockdown validation

The efficiency of the knockdown using short hairpin constructs against Gal-3 was obtained *in vivo* and *in vitro*. Gal-3 antibody specificity was assessed in control and Gal-3 OE mice at 3 DPE, and through a secondary-only control [Appendix E (A)].

17 days after electroporation, I assessed the percentage of labelled pSVZ cells that were also positive for Gal-3 immunostaining (%tdTom+Gal-3+) as an indication of the knockdown efficacy (Figure 3.3 A). I observed that, compared to the control which had 31.31±1.9% (n=3 animals), of double positive cells, both V1 and V2 sequences significantly decreased the number of tdTomato cells that also expressed Gal-3 to 17.19±2.8% (n=4 animals) and 14.42±1.4% (n=4 animals), respectively (Figure 3.3B).

These results indicate that the constructs used indeed decrease the levels of Gal-3 in cells of the pSVZ *in vivo*.

Additionally, I further confirmed that the efficiency by transfecting the human neural progenitor cell lines (ReNcell®) with the shGal-3 V1 plasmid. ReNcell® are derived from the cortical (CX) and midbrain (VM) regions of a 14- and 10-week-old embryo brain, respectively. Both cell lines have immature neural morphology and express Nestin (Donato et al., 2007). I detected high basal levels of Gal-3 in both cell lines, which was reduced by more than 70% two days after shGal-3 V1 transfection (Figure 3.3 C).

The efficiency of these constructs had also been previously assessed by a former member of the lab in HEK293T cells after overexpressing Gal-3. Nevertheless, the data presented in this thesis helped to validate these constructs, further showing their ability to deplete Gal-3 *in vivo* even at 17 DPE. Similarly, the efficiency of the Cre/lox system in promoting Gal-3 knockout, as well as Gal-3 overexpression, had been assessed beforehand (Al-Dalahmah et al., 2020a).

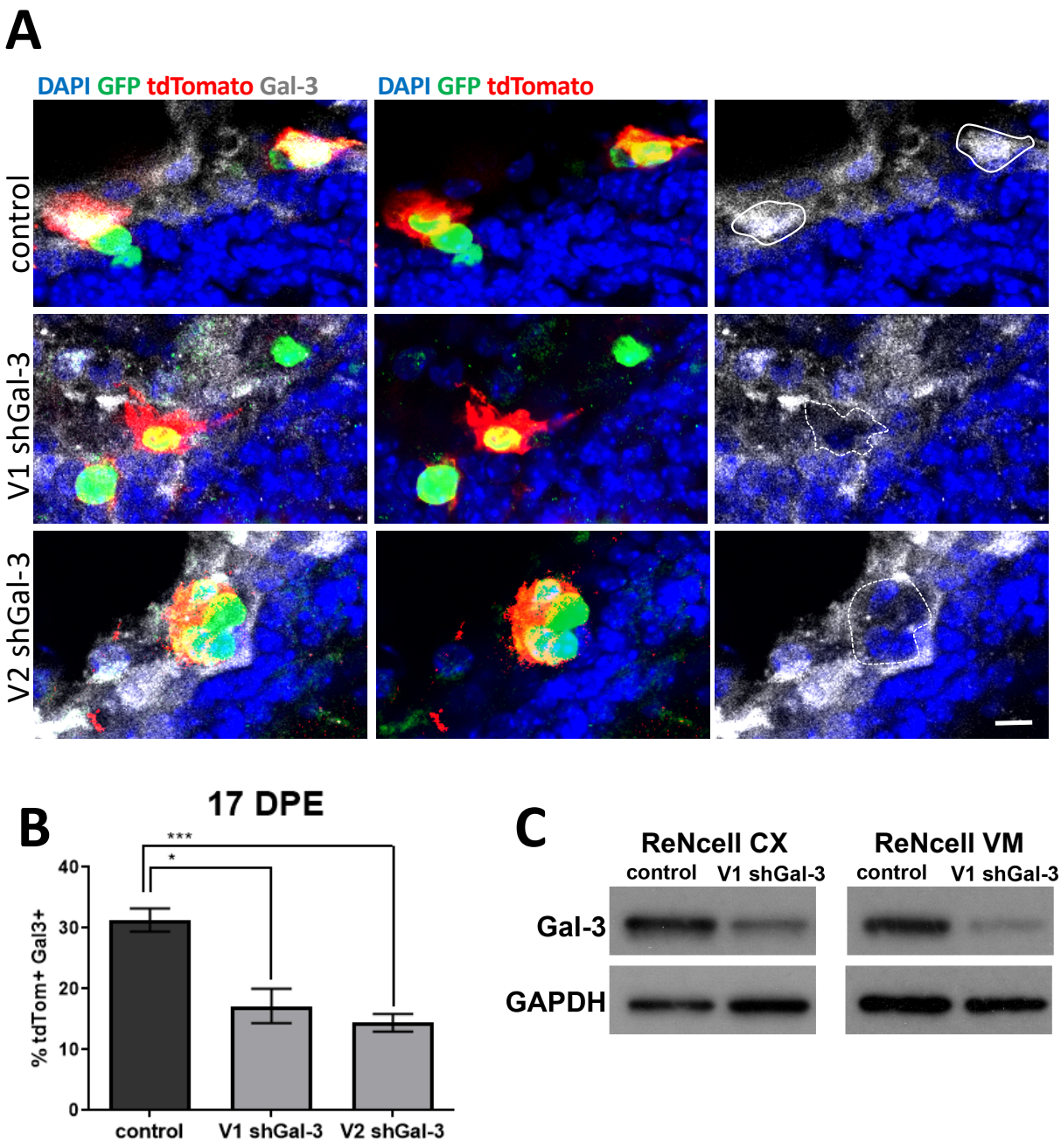


Figure 3.3. Validation of Gal-3 knockdown.

A) Confocal images exemplifying pSVZ cells positive for GFP and tdTomato which were also positive (white lines) or negative (dotted white lines) for Gal-3. Scale bar 10 μm. B) Quantification of cells in A showing that there were fewer tdTomato+ Gal-3+ cells in the pSVZ after 17 days of electroporation with the Gal-3 short-hairpin constructs. The graphs represent mean with SEM. At least 100 cells per animal (n=3 or 4) were quantified. *$p < 0.05$; ***$p < 0.001$. C) Western blotting showing decrease on the levels of Gal-3 after 2 days of nucleofection with V1 shGal-3 plasmid.

3.4 Galectin-3 is necessary for postnatal striatal gliogenesis

After validating the technique and the ability of the shGal-3 constructs to deplete Gal-3, I examined if Gal-3 loss-of-function impacts pSVZ-derived glial differentiation. In order to do that, I co-electroporated mice with pCAG-tdTom-2A-H2BGFP plus shNT (control), shGal-3 V1 or shGal-3 V2 and collected the brains at 17 DPE, to allow time for gliogenesis. As mentioned before, it was expected that glia generated in the pSVZ populate the striatum (Levison et al., 1993; Levison and Goldman, 1993). Therefore, I considered that the proportion of labelled cells in the striatum compared to the total number of fluorescent cells (in the striatum plus the pSVZ) indicates levels of gliogenesis. Using this proportion, it was possible to observe that 30.71±3.7% (n=5 animals), of labelled cells migrated to the striatum in control animals. However, the knockdown of Gal-3 through both shRNA sequences significantly decreased this percentage to 14.24±1.5% (n=6 animals) in V1 and 19.71±2.0% (n=6 animals) in V2 shGal-3 groups (Figure 3.4).

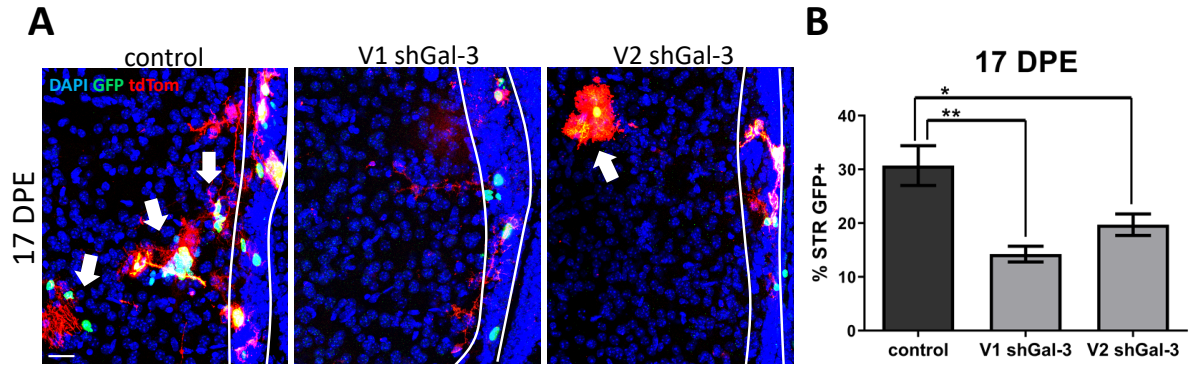


Figure 3.4. Gal-3 knockdown decreases striatal gliogenesis at 17 DPE.

A) Confocal images illustrating the decrease in the number of cells that migrate out from the pSVZ (delimited by white lines) to the adjacent striatum 17 days after co-electroporation of pCAG-tdTom-2A-H2BGFP plus shNT, shGal-3 V1 or shGal-3 V2. Those cells are highlighted with a white arrow. Scale bar 10 μm. B) Quantification of A: the number of cells in the striatum were calculated as a percentage of total number of labelled cells. Graphs represent mean with SEM. At least 100 cells per animal (n=5 or 6) were quantified. *p < 0.05; **p < 0.01.

I also had access to brain sections from a conditional Gal-3 knockout using the Cre/lox system and used them to analyse similar parameters in order to assess pSVZ striatal gliogenesis. Both control and Cre plasmids contained a sequence for GFP, allowing to track specific cells that had incorporated the DNA. Using that model, I observed that 9.08±2.0% (n=4 animals) of labelled cells were localised at the striatum of Gal3$^{flox/flox}$ mice electroporated with a control plasmid (Figure 3.5). A reduction to 3.23±1.3% (n=4 animals) was observed upon Gal-3 knockout in Cre-electroporated animals.

The results from both experiments led to the conclusion that Gal-3 is indeed necessary for pSVZ striatal gliogenesis, revealing a new role for the endogenous Gal-3 that is expressed in the pSVZ.

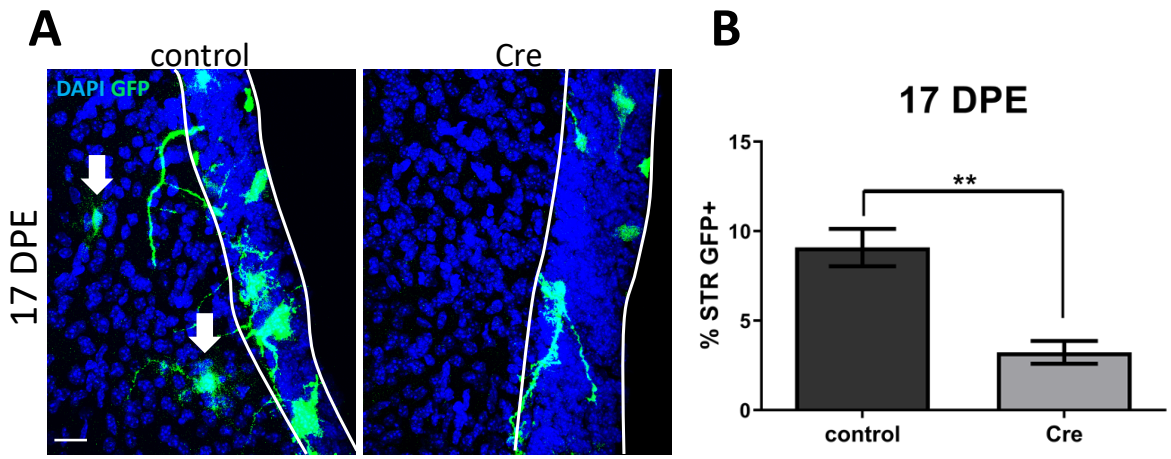


Figure 3.5. Gal-3 knockout decreases striatal gliogenesis at 17 DPE.

A) Confocal images illustrating the decrease in the number of cells that migrate out from the pSVZ (delineated by white lines) to the adjacent striatum 17 days after electroporation with control or Cre plasmids in Gal-3$^{flox/flox}$ mice. Those cells are highlighted with a white arrow. Scale bar 10 μm. B) Quantification of A: the number of cells in the striatum were calculated as a percentage of total number of labelled cells. Graphs represent mean with SEM. At least 100 cells per animal (n=4) were quantified. **p < 0.01.

3.5 Study of cell fate shift upon Galectin-3 modulation

The data shown above, collectively with previous data from Gal-3 overexpression (OE) experiments, opened the question of whether there was a specific glial subtype that was selectively influenced by Gal-3 in the postnatal SVZ (Al-Dalahmah et al., 2020a). Both astrocytes and oligodendrocytes have been described to originate from the pSVZ, with astrogenesis being the earlier event (Brazel et al., 2003; Lyck et al., 2007; Marshall et al., 2003; Parnavelas, 1999). Additionally, Gal-3 has been implicated with oligodendrogenesis in the adult (Pasquini et al., 2011). This function, however, has never been investigated in the postnatal SVZ.

For the reasons given before, I considered that virtually all the labelled cells in the striatum were glia, being either GFAP+ astrocytes or oligodendrocyte transcription factor 2 (Olig)2+ oligodendrocytes. Interestingly, previous Gal-3 OE experiments caused a cell fate shift towards astrocytes over oligodendrocytes, evidenced by an increase in the proportion of GFP-labelled cells in the striatum that were also positive for the astrocyte markers GFAP and S100β. Additionally, a decrease in labelled cells expressing Olig2 in the striatum was also observed (Al-Dalahmah et al., 2020a).

Here, I sought to determine if Gal-3 depletion would have a reverse effect over gliogenesis balance. In order to do that, I used 17 DPE brain sections obtained from the Cre/lox conditional knockout experiment. I analysed the presence of the markers GFAP and Olig2 in GFP-labelled cells localised in the striatum of control or Cre electroporated mice. Whilst I confirmed the positivity of these markers in GFP+ cells localised in the striatum of control animals (n=4 animals) (Figure 3.6 A and A'), unfortunately, the extremely limited number of striatal labelled cells in Cre animals impeded any conclusion

to be made with regards to cell fate (n=4 animals) (Figure 3.6 B). Antibody specificity was assessed in 17 DPE control mouse through a secondary-only control [Appendix E (B)].

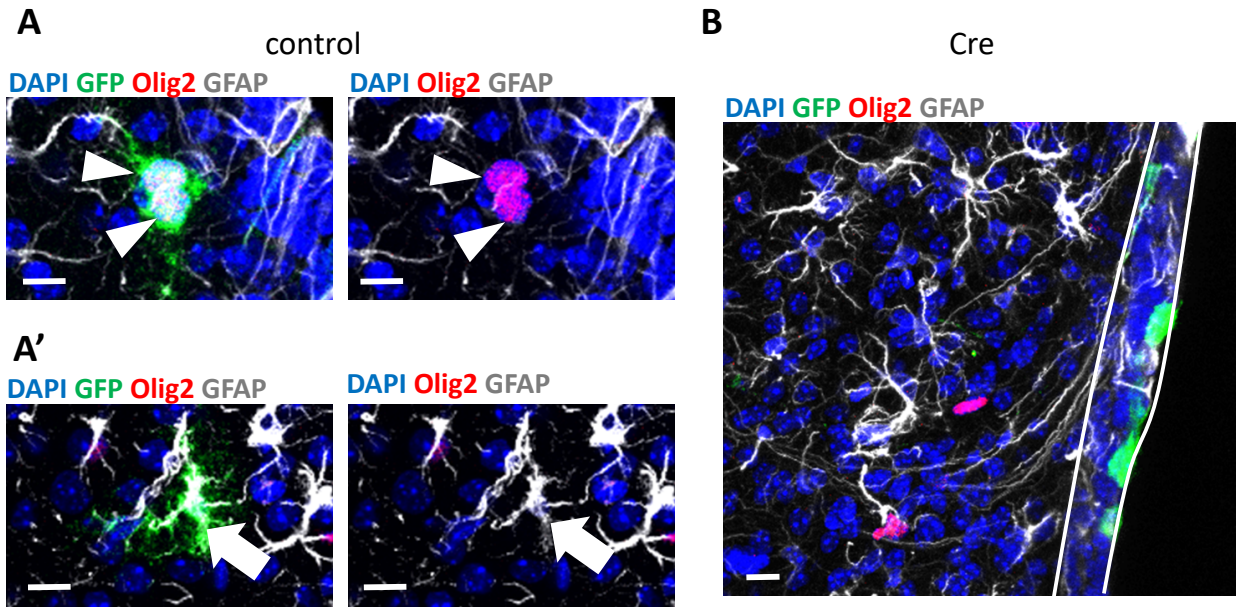


Figure 3.6. Gal-3 knockout could not be used for cell fate at 17 DPE.

Confocal image showing that GFP-labelled cells in the striatum of control animals at 17 DPE were either A) oligodendrocytes (Olig2+ cells, arrowhead) or A') astrocytes (GFAP+ cells, arrow). B) Confocal image exemplifying the lack of GFP-labelled cells in the striatum of Cre-electroporated animals at 17 DPE. Scale bar 10 µm.

3.6 Galectin-3 overexpression did not induce apoptosis or inflammation

In this chapter, I have shown and discussed the role of Gal-3 in pSVZ gliogenesis and cell fate decision. Gal-3 overexpression (OE) experiments that were previously conducted in the lab supported these findings, revealing that Gal-3 OE promoted pSVZ gliogenesis (Al-Dalahmah et al., 2020a). Interestingly, Gal-3 OE also resulted in a higher number of astrocytes and fewer oligodendrocytes, which suggest a role in cell fate decision. There was, however, the formal possibility that Gal-3 OE resulted in apoptosis

of oligodendrocytes, which would explain the lower number of Olig2+ cells. A previous overall analysis revealed that Gal-3 OE did not induce apoptosis in the pSVZ (Al-Dalahmah et al., 2020a). However, a more detailed observation of specific oligodendrocytes apoptosis was lacking.

I addressed this question by using brain sections of 3 DPE mice electroporated with control or Gal-3 OE plasmid. The time point was chosen in an attempt to detect apoptosis, which was expected to occur early on in the process. Apoptosis was assessed by immunostaining of cleaved caspase 3, which is the active from of the effector caspase 3 (McIlwain et al., 2013; Riedl and Shi, 2004); and oligodendrocytes were detected with Olig2. A.caspase3 and Olig2 antibody specificity were assessed in control mice cortex through a secondary-only control showing no signal [Appendix E (C)]. It was possible to observe only very few activated caspase 3+ cells (A.caspase3) in the brain and virtually no triple positive cells+ (GFP+A.Caspase3+Olig2+) (n=3 animals) (Figure 3.7). These results further confirm that Gal-3 specifically acts on cell fate decision but does cause oligodendrocyte apoptosis.

The converse experiment was performed by a previous member of the lab (Osama Al-Dalahmah) via flow cytometry assay ™ (Invitrogen). The percentage of live cells upon Gal-3 knockdown at 3 DPE (n=2 animals) did not differ from control.

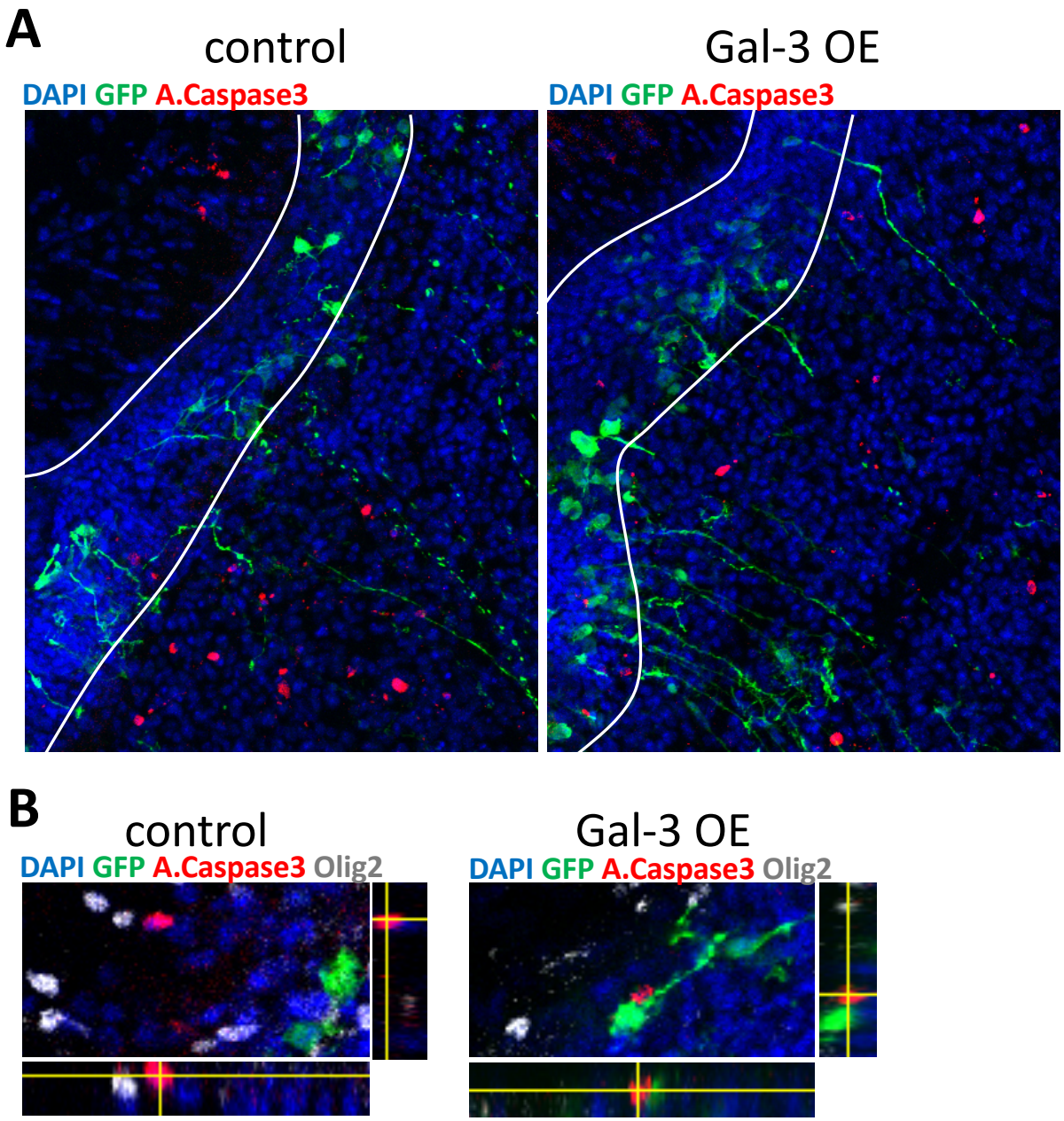


Figure 3.7. Gal-3 OE did not induce apoptosis at 3 DPE.

A) Confocal image showing that there were few A.caspase3 positive cells in the pSVZ and striatum of 3 DPE control or Gal-3 OE mice. Scale bar 50 μm. B) Orthogonal view showing the detail of A.caspase3 positive cells that are negative for GFP and Olig2. Scale bar 10 μm.

Moreover, Gal-3 is well-known for its role in causing inflammation, including in the brain (Burguillos et al., 2015; Feuk-Lagerstedt et al., 1999; Frigeri et al., 1993; Jeng et al., 1994; Liu et al., 1995; Yamaoka et al., 1995). Gal-3 is secreted by microglia and contributes to its paracrine activation via TLR4 (Burguillos et al., 2015). As inflammation can influence neurogenesis and generation of glial cells (Ekdahl et al., 2003; Monje et al., 2003; Ribeiro Xavier et al., 2015; Shigemoto-Mogami et al., 2014), it was important to address the question of whether Gal-3 OE promotes inflammation in the pSVZ or adjacent striatum.

To address this question, I indirectly assessed inflammation by studying the activation state of local microglia (Iba1+ cells) in control or Gal-3 OE mice at 3, 7 and 17 DPE. It is well known that microglia change cell shape in relation to their function (Kettenmann et al., 2011). Therefore, I classified microglia in three possible activation states based on morphology, according to previous studies (Cunningham et al., 2013; Rezaie and Male, 1999). While resting microglia are very ramified cells, with several thin processes and a small cell body; activated ones present the opposite morphology, being ameboid and having had completely retracted cellular processes. Microglia could also be classified in an intermediate state, which in fact composed the majority of cells at the pSVZ. At this stage, compared to resting microglia, cells are less ramified, with no more than 4 thick processes, attached to a larger cell body (Figure 3.8).

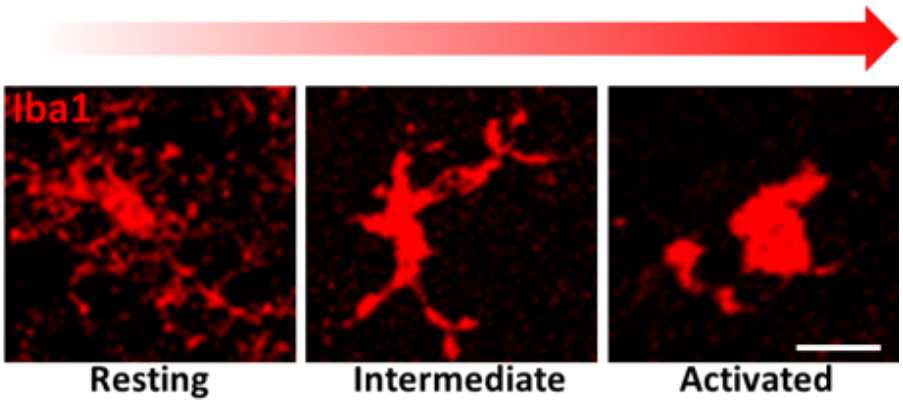


Figure 3.8. Microglia morphological classification.

Confocal image exemplifying how microglia (Iba1+) was classified on resting, intermediate and activated stages based on cell morphology. Scale bar 5 μm.

Using this classification, it was possible to observe that the proportion of resting/intermediate/activated microglia did not change in the Gal-3 OE group compared to control at any of the time points studied (Figure 3.9 A and B, lower graphs). The majority of cells were in the intermediate state, in both the pSVZ and in adjacent striatum, as well as in all experimental groups and time points. Additionally, activated microglia in the pSVZ of control and Gal-3 OE groups range around 15% at 3 DPE and 25% at 7 and 17 DPE (n=3 or 4 animals). This proportion is much smaller in the striatum, where all the groups had less than 8% cells in the activated state (n=3 or 4 animals). This fact can be explained by the well-known semi-activate state of the SVZ (Bardella et al., 2018).

Similarly, I quantified total numbers of microglia both in the pSVZ and adjacent striatum in an attempt to assess microglia recruitment. In all the time points studied, the numbers did not change with Gal-3 OE compared to control (Figure 3.9 A and B, upper graphs).

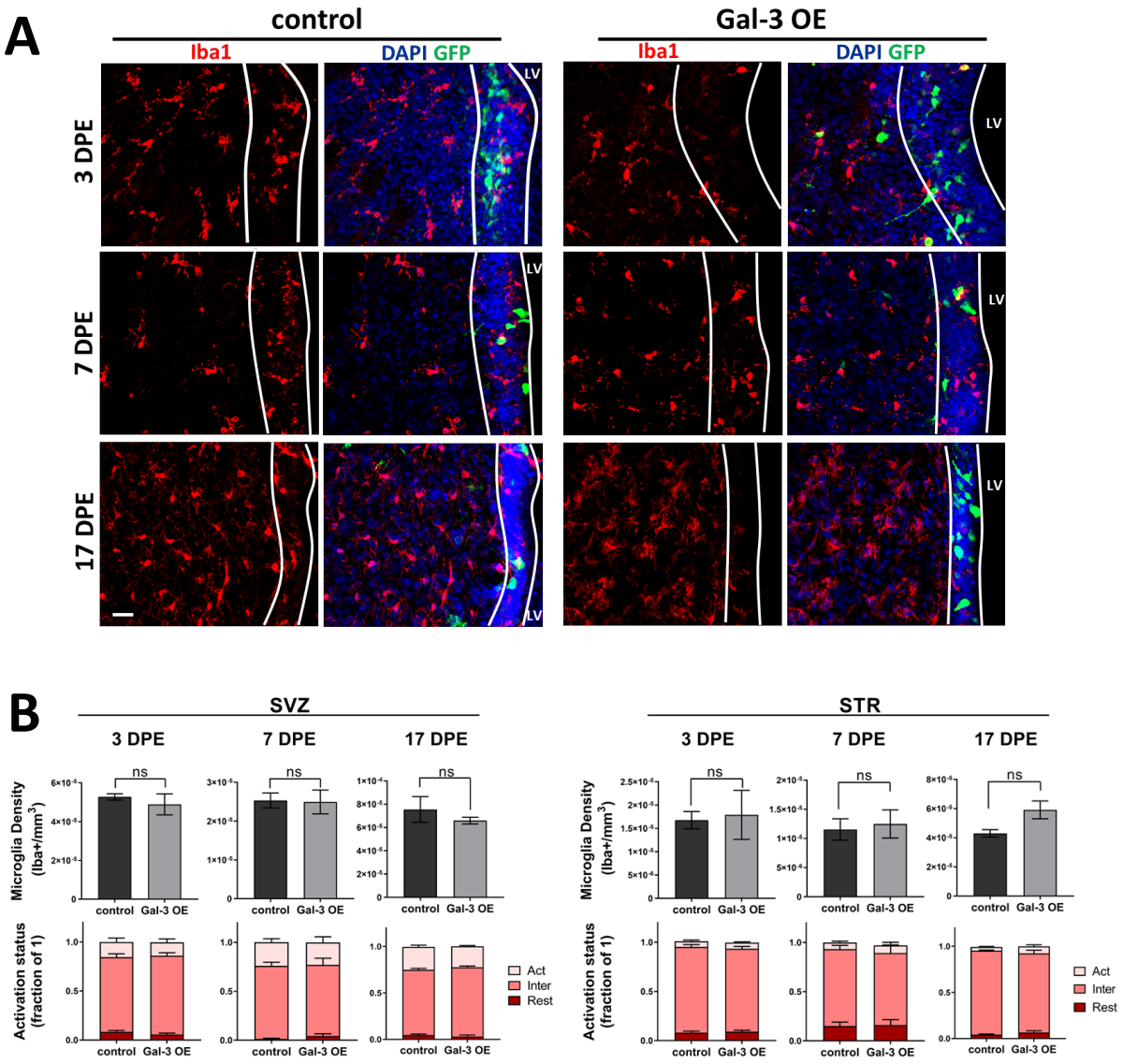


Figure 3.9. Gal-3 OE did not activate microglia in the pSVZ.

Representative confocal image showing no difference in quantity and activation state of microglia in the pSVZ (delimited by white lines) and the adjacent striatum upon overexpression of Gal-3 after 3, 7 and 17 days of electroporation. Scale bar 50 µm. B) Quantification of B. Graphs are mean with SEM. At least 100 cells per animal (n=3 or 4) were quantified. ns: non-significant. STR: striatum

3.7 Discussion

Postnatal SVZ is the region surrounding the lateral ventricles in the brain that contains active NSCs (Ihrie and Alvarez-Buylla, 2011). Great progress has been made towards understanding the pSVZ's role in neurogenesis (Alvarez-Buylla et al., 2020). However, there are still many open questions concerning pSVZ-derived gliogenesis, particularly understanding the molecular mechanism behind this process. Progenitors in the pSVZ express Galectin-3, a lectin that has been described to play a role in cell differentiation (Comte et al., 2011; Pasquini et al., 2011; Thomas and Pasquini, 2018). Therefore, in this Chapter, I investigated the role of Gal-3 in pSVZ gliogenesis.

Firstly, I optimised *in vivo* brain electroporation to knockdown Gal-3 specifically in the pSVZ. The technique was conducted as previously described, and consists of delivering the plasmid of interest using electrical tweezers. The electrical current applied promotes transient pores in the cell membrane at the same time that the negatively charged DNA is pushed towards the cathode (Boutin et al., 2008; Chesler et al., 2008; Fernandez et al., 2011). The success of the technique was assessed via observation of a fluorescent reporter (Trichas et al., 2008), which was correctly localised in cells at the region. After 17 days post electroporation (DPE), labelled neuroblasts had migrated to the olfactory bulb, where they generated interneurons, as expected (Bayer, 1983; Paredes et al., 2016). Moreover, the constructs used for the knockdown were efficient in promoting Gal-3 depletion, which was evaluated *in vivo* and *in vitro*.

Using this technique, I showed that Gal-3 depletion diminished the proportion of labelled cells in the striatum. This result was further supported by a parallel study using a conditional Gal-3 knockout model, which similarly showed a decrease in the proportion of

striatal cells upon Cre electroporation. The opposite effect had been observed in Gal-3 OE experiments previously conducted by another member of the lab, in which increased Gal-3 levels increased the proportion of labelled cells in the striatum (Al-Dalahmah et al., 2020a). Glial cells derived from the pSVZ are known to migrate to the striatum (Levison et al., 1993; Levison and Goldman, 1993). Additionally, a detailed characterisation using morphology and markers expression revealed that labelled cells that migrate out from the SVZ to the striatum during this interval of time are indeed either astrocytes or oligodendrocytes (Al-Dalahmah et al., 2020a). Therefore, it was possible to conclude that Gal-3 is required for pSVZ striatal gliogenesis.

The generation of astrocytes and oligodendrocytes are sequential events, each regulated by distinct molecular pathways. For example, while astrogenesis is an earlier event regulated by BMP signalling, the oligodendrocyte fate is acquired upon PDGFR activation and continues into young adulthood (Jackson et al., 2006; Lim et al., 2000; Lyck et al., 2007; Parnavelas, 1999). Therefore, the next question raised was if Gal-3 regulates the generation of different types of glia. In the adult SVZ, Gal-3 is known to play a role in oligodendrogenesis (Pasquini et al., 2011), but this role has never been investigated in the pSVZ. Therefore, I attempted to assess a possible fate shift upon conditional Gal-3 knockout by looking at the expression of GFAP and Olig2 markers in GFP-labelled cells at the stratum. Unfortunately, the proportion of striatal cells in the Cre group was near 3 times lower than in the control. This meant that the total number of cells in the striatum was bellow 5 per animal in the Cre group, impeding any meaningful statistical comparison between different glial cell types.

The conditional Gal-3 knockout did not provide any information related to the cell fate of pSVZ-derived glial cells. However, Gal-3 OE experiments evidenced its role in the acquisition of the astrocytic fate (Al-Dalahmah et al., 2020a). In order to discard the possibility of a nonspecific effect of Gal-3 OE in oligodendrocyte cell death, I analysed if there was evidence of apoptosis in this model. Apoptosis was evaluated via activated Caspase-3 (A.Caspase3) immunostaining, which is an effector Caspase that becomes active upon cleavage (McIlwain et al., 2013; Riedl and Shi, 2004). The study of apoptosis is challenging since A.Caspase3 is expected to be degraded as cells die. Nevertheless, few A.Capase3 positive cells could be observed in the brain at 3 DPE. However, no GFP labelled oligodendrocytes were found to be positive for A.Caspase3. This study was conducted in 3 DPE brain sections, as I believed that apoptosis would happen shortly after electroporation. Yet, an overall analysis of apoptosis did not show any evidence of Caspase-mediated cell death at the other time points (Al-Dalahmah et al., 2020a). Therefore, the data presented in this thesis supports that Gal-3 effect on gliogenesis and cell fate choice are not due to apoptosis.

Gal-3 is known to promote brain inflammation and activate microglia (Burguillos et al., 2015; Chen et al., 2014a), a process that can affect SVZ differentiation (Ekdahl et al., 2003; Monje et al., 2003; Ribeiro Xavier et al., 2015; Shigemoto-Mogami et al., 2014). The activation state of microglia can be accessed via its morphology (Cunningham et al., 2013; Rezaie and Male, 1999). Therefore, to evaluate if Gal-3 OE resulted in inflammation, I analysed the total number and activation state of microglia in different time points after electroporation. The higher proportion of activated microglia in the pSVZ can be explained by its semi-inflamed state (Bardella et al., 2018). Moreover, there was no

difference in the numbers and in the activation state of microglia at any time point studied in this thesis. Hence, this work supports that Gal-3 actions in pSVZ-derived gliogenesis is not mediated through inflammatory effects.

The results provided in this Chapter show a role for Gal-3 in cell differentiation. More specifically, Gal-3 promotes astrogenesis in the postnatal SVZ. These findings, together with previous data from another member of the lab, compose the core of a paper that was published in a peer-reviewed journal (Al-Dalahmah et al., 2020a).

Chapter 4

The role of Galectin-3 in neural differentiation of hESCs

4.1 Introduction

Pluripotent stem cells harbour great potential for stem cell therapy since they have the ability to differentiate into all three germ layers of the embryo (Barresi and Gilbert, 2020). Moreover, they are a great tool for developmental research. Human embryonic stem cells (hESCs) can be obtained from the ICM of the blastocyst and cultured *in vitro* using a defined media (Ludwig et al., 2006a; Ludwig et al., 2006b). These cells are pluripotent and, hence, express markers such as NANOG, Oct4, and SOX2, which are lost during differentiation (Boiani and Scholer, 2005; Boyer et al., 2005).

Multipotent neural stem cells (NSCs) can be obtained from hESCs through dual Smad inhibition (Chambers et al., 2009). In these conditions, cells acquire the neural fate and express Pax6, Nestin and SOX2, at the same that they lose the expression of NANOG and Oct4. Additionally, they undergo essential morphological changes similar to those that take place during neurulation (Abranches et al., 2009; Banda et al., 2015; Ying et al., 2003). Cells acquire a polarised morphology and organise around a lumen, forming a structure known as neural rosettes (Hribkova et al., 2018). The maintenance of this structure is essential for preserving stem cells and their differentiation potential. Although developmental research has made outstanding progress in recent years, there are still many uncertainties related to the mechanism that regulates the early steps of neural commitment.

Galectin-3 has been involved with several processes that are related to different steps of neural differentiation. Not only does it regulate developmental pathways such as Notch, EGFR, and Wnt (Al-Dalahmah et al., 2020b; Kang et al., 2016; Kuo et al., 2016; Nakajima et al., 2014; Partridge et al., 2004), but it is also essential for the establishment

of cell polarisation (Apodaca et al., 2012; Delacour et al., 2006; Delacour et al., 2008; Honig et al., 2018; Torkko et al., 2008; Yamamoto et al., 2013). During embryogenesis, it is strongly expressed in the notochord and in embryonic epithelia (Fowlis et al., 1995; Van den Brûle et al., 1997). However, its role in early embryogenesis is still unclear.

In the previous chapter, I observed that Gal-3 plays a role in postnatal gliogenesis derived from pSVZ stem cells, a role that is independent of apoptosis or inflammation. Here, I follow this finding focusing on the mechanisms by which Gal-3 promotes differentiation. In order to do that, I used NSCs derived from hESCs upon neural induction protocol. After assessing the expression of Gal-3 at that stage, I asked if its modulation affects expression of multipotency markers. I then investigated the involvement of Gal-3 in the formation of neural rosettes.

Finally, integrins are important transmembrane receptors composed of α and β subunits that regulate epithelial polarisation (Lee and Streuli, 2014). Specific subunits are expressed during neural development and are responsible for signalling of cell survival and differentiation (Hynes, 2002; Schmid and Anton, 2003). Therefore, based on previous studies showing Gal-3 involvement in morphogenesis via integrins (Honig et al., 2018), I tested the hypothesis that Gal-3 acts on neural rosette polarisation by interaction with β1 integrin.

4.2 Neural differentiation of H9 stem cells

In order to address these questions, I first characterised the neural differentiation process of the pluripotent hESCs line H9. These cells grow as clumps on Matrigel™-

coated-plates in mTeSR™Plus media, which contain components that sustain pluripotency such as FGF, TGFβ, and LiCl (Ludwig et al., 2006a; Ludwig et al., 2006b).

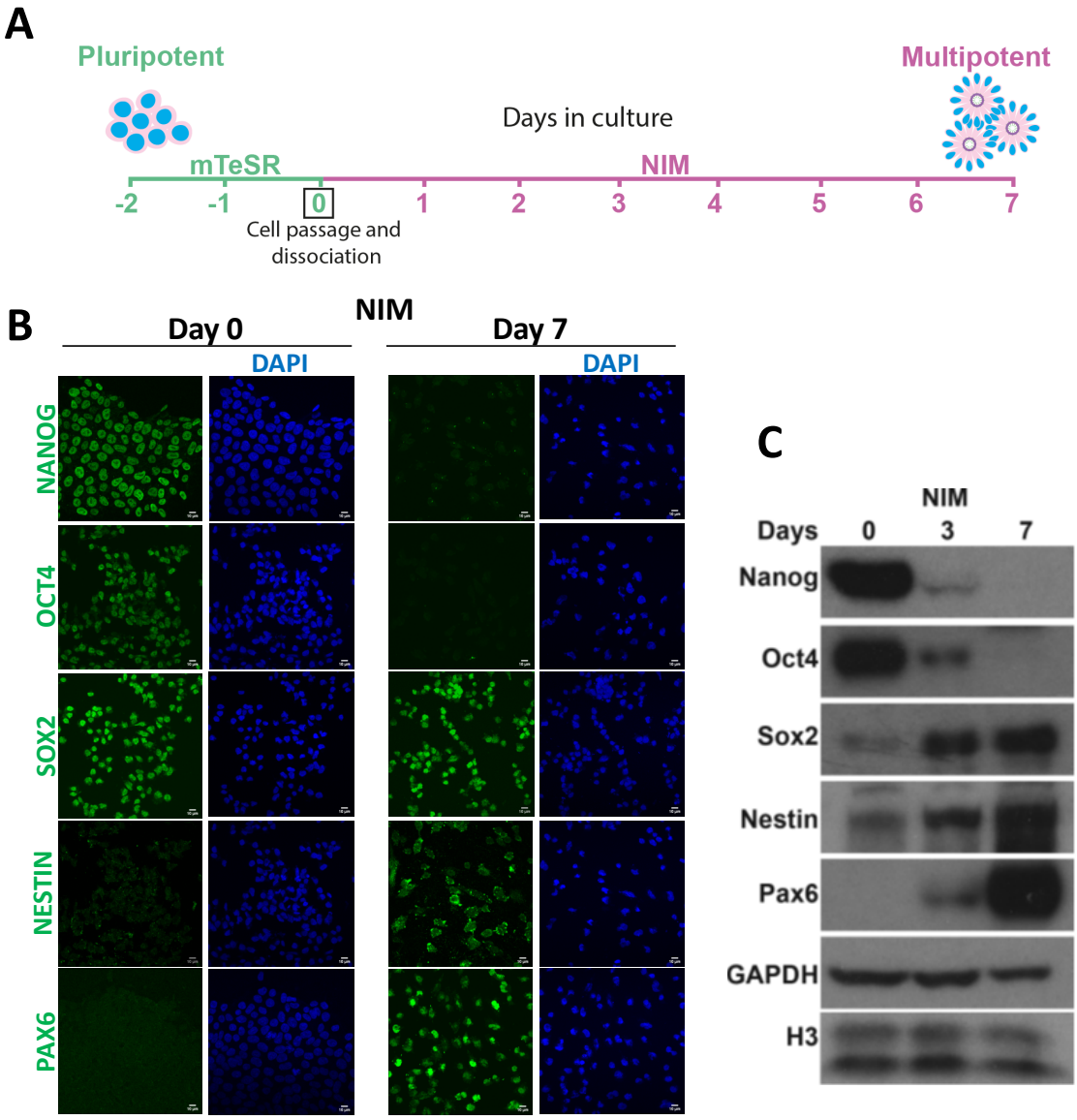


Figure 4.1. Neural induction in H9 cells.

A) Schematic of neural induction protocol in which pluripotent stem cells are treated with neural induction media for 7 days until acquisition of multipotent NSC. B) Immunofluorescence comparing the presence of pluripotency markers (NANOG and Oct4) at Day 0 and the acquisition of NSC markers (Nestin and Pax6) after 7 days of neural induction. Scale bar 10 μm. C) Western blot showing the transition from pluripotency to neural specific markers during neural induction progression. mTeSR: maintenance media for pluripotent stem cells (mTeSR™Plus). NIM: neural induction media.

Neural induction occurred upon dissociation of pluripotent hESCs clumps, which were then plated as monolayers in Matrigel™-coated plates and treated with STEMdiff™ neural induction media (NIM) for 7 days (Figure 4.1 A). This media contains two Smad inhibitors to block both BMP and Activin/Nodal receptors: Noggin and SB431542 (Chambers et al., 2009). After this period, cells successfully differentiated into the neural lineage as observed by the loss of the pluripotent markers NANOG and Oct4; and subsequent gain of expression of Nestin and Pax6. (Figure 4.1 B). SOX2 was expressed throughout the days of neural induction (Figure 4.1 B), which was expected since the molecule play a role in different stages of differentiation (Archer et al., 2011; Graham et al., 2003; Zhang and Cui, 2014). Western blot analysis revealed the gradual change in protein levels of markers as neural induction progressed (Figure 4.1 C).

After 7 days of neural induction, not only had cells acquired expression of neural progenitor markers, but also, they underwent important morphological changes. As previously described, NSC at this stage have polarised morphology, with apical and basal domains well defined by tight junctions (Hribkova et al., 2018). In my monolayer neural induction cultures, the apically-localised tight junctions could be identified through the expression of the intracellular scaffold protein ZO-1 (Figure 4.2 A). The cilium-specific protein ADP-ribosylation factor-like protein 13B (ARL13B) was also observed at the apical membrane, indicating the presence of primary cilia. Components of the cytoskeleton such as F-actin and αTubulin had a polarised distribution towards the apical side. This organised structure is known as neural rosette, and Figure 4.2 B shows a schematic of it.

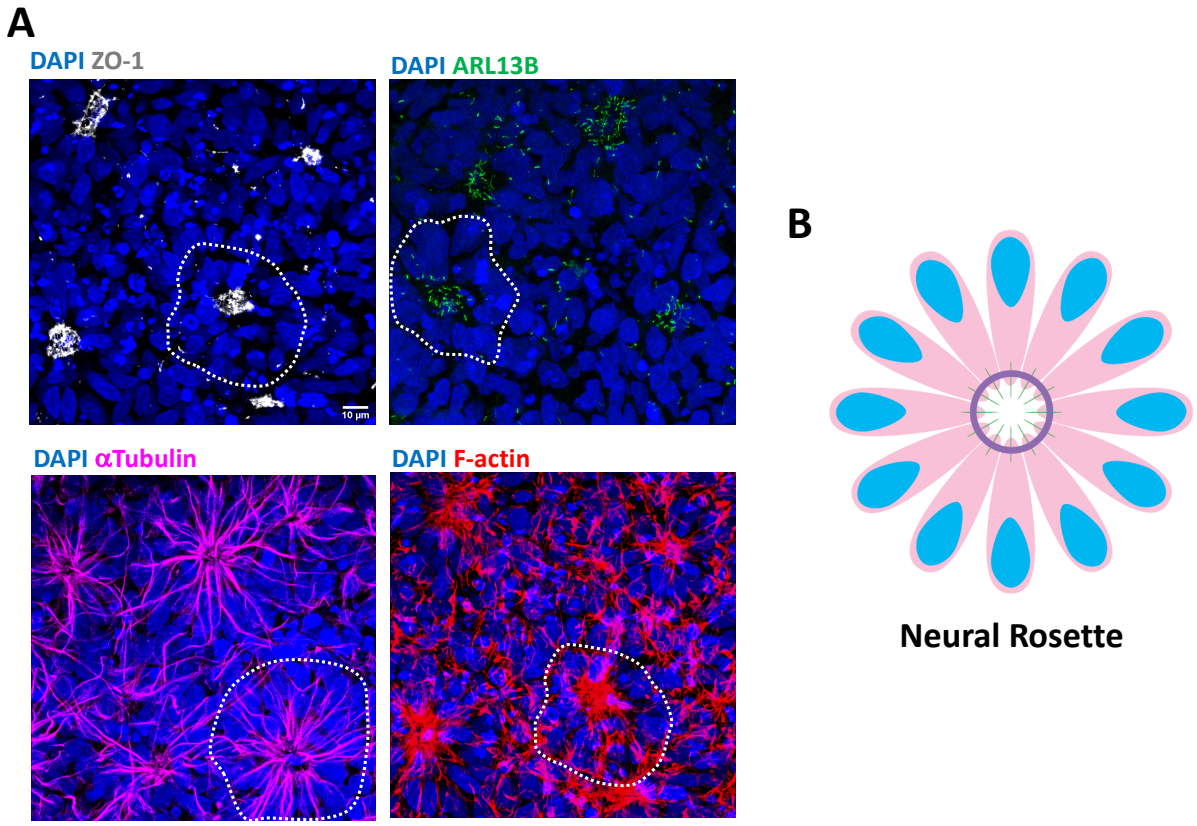


Figure 4.2. Monolayer culture of H9 form neural rosettes.

A) At Day 7, neural progenitor cells were organised in polarised rosettes (delimited by a dotted line) which can be seen through apical localisation of primary cilia (ARL13B), F-actin, αTubulin and tight junctions (ZO-1). Scale bar 15 µm. B) Neural rosettes schematic showing some of the components illustrated in A. Blue: DAPI; Magenta: ZO-1; Green: ARL13B.

Hribkova and colleagues described five steps that lead to the formation of rosettes in 9 days: cell intercaltion, cell constriction, cell polarisation, cell elongation and lumen formation (Hribkova et al., 2018). Here, I observed that all these main morphological features were acquired at the first 3 days of neural induction. Qualitative analysis after immunostaining with α and γTubulin revealed that, as early as Day 2, cells had already undergone constriction and elongation, as well as acquired polarisation. It was also evident that they started to organise in circular structures (Figure 4.3). At Day 3, almost

all cells in culture were distributed in circles containing a lumen. From that time point onwards, these structures increased in cell number and lumen size in a phase that I called maturation, which happened until the formation of mature neural rosettes at Day 7. The tight coordination of these steps is crucial for the correct formation of rosettes, and a disturbance in any of them could lead to malformation or complete abrogation of rosettes structures, which impairs NSC maintenance and their ability to further differentiate (Hribkova et al., 2018). Therefore, it is not only important to understand what determines neural commitment and expression of neural markers, but also it is essential to identify which cues are involved with rosettes formation at any possible step.

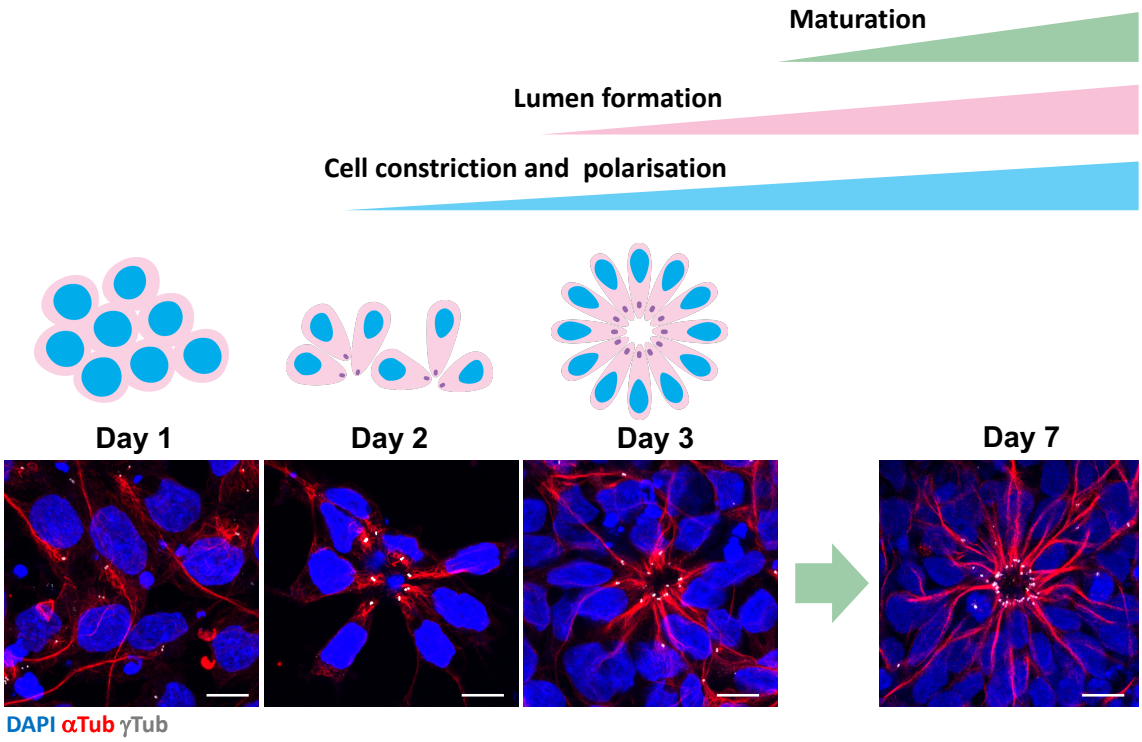


Figure 4.3. Rosette formation follows multiple steps.

Confocal images illustrating the progression of neural rosettes with a schematic representing the principal changes that happens along 7 days of neural induction. Scale bar 15 μm. In the schematic: Blue: DAPI; Magenta: γTubulin. Part of the schematic was adapted from (Hribkova et al., 2018).

4.3 Galectin-3 during neural differentiation

In the previous Chapter, I have shown that Galectin-3 is expressed in postnatal SVZ and participates in striatal gliogenesis. However, its role in embryonic neural development has never been investigated.

Here, I first looked at the protein levels of Galectin-3 through western blot (n=3 neural inductions) (Figure 4.4). Gal-3 expression significatively increased upon neural differentiation stimuli, peaking at Day 2 of neural induction, and then going back to basal levels at Day 5 (Figure 4.4 A and B). The sharp increase of Gal-3 levels preceded the expression of the NSC marker Pax6 (Figure 4.4 A). Considering that intracellular Gal-3 can activate signalling pathways, including been direct responsible for gene transcription (Liu et al., 2002), I raised the possibility of an involvement of Gal-3 in the regulation of Pax6 expression.

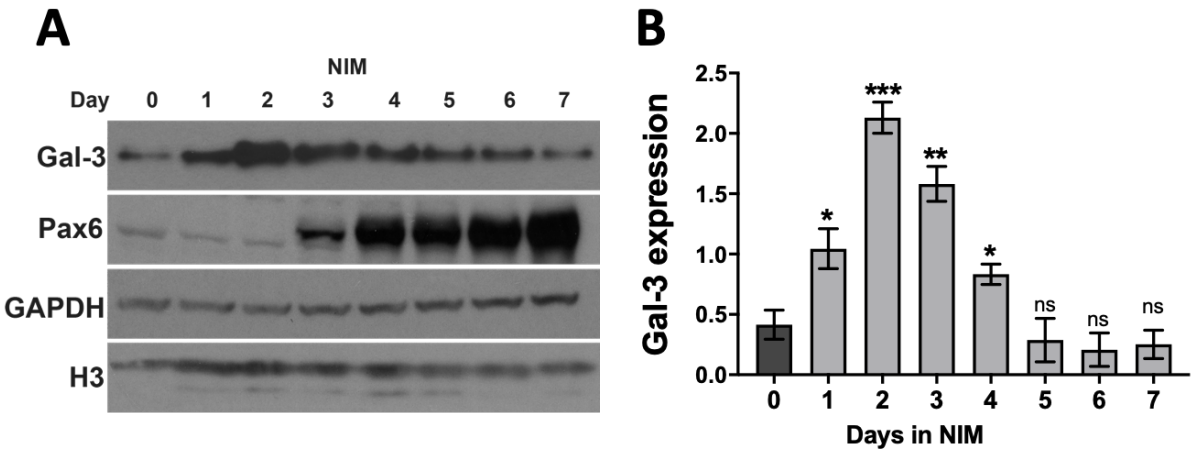


Figure 4.4. Gal-3 levels during neural induction.

A) Representative Western blot of 3 independent biological replicates showing that the levels of Gal-3 increase at Day 2 of neural induction. B) Quantification of Gal-3 levels from Western blot normalised to H3 and are represented in arbitrary units (AU). Graphs are mean with SEM; n=3. For statistical analysis, values were compared to Day 0. *$p < 0.05$; **$p<0.01$; ***$p < 0.001$; ns: non-significant. NIM: neural induction media.

4.4 Modulation of Galectin-3 did not alter expression of neural markers

The upsurge of Gal-3 expression at the initial steps of neural differentiation raised the question of its role in neural commitment. Therefore, I decided to address it by modulating Gal-3 and assessing the expression of neural markers. First, I treated H9 cells every other day with recombinant human Gal-3 for the 7 days of neural induction (Figure 4.5 A). As shown in the Western blot of Figure 4.5 B, the signal given by Gal-3 bands was much larger upon Gal-3 treatment at both time points, indicating that the protein was either largely incorporated by the cells or was strongly attached in the cell membrane. This, however, did not alter the expression of NANOG, Oct4, Pax6 and Nestin observed through Western blot (Figure 4.5 B). The quantification of one marker of pluripotency (NANOG; n=3 neural inductions) and one of NSC (Pax6; n=4 neural inductions) is shown in Figure 4.5 C and D, respectively, indicating no significant difference.

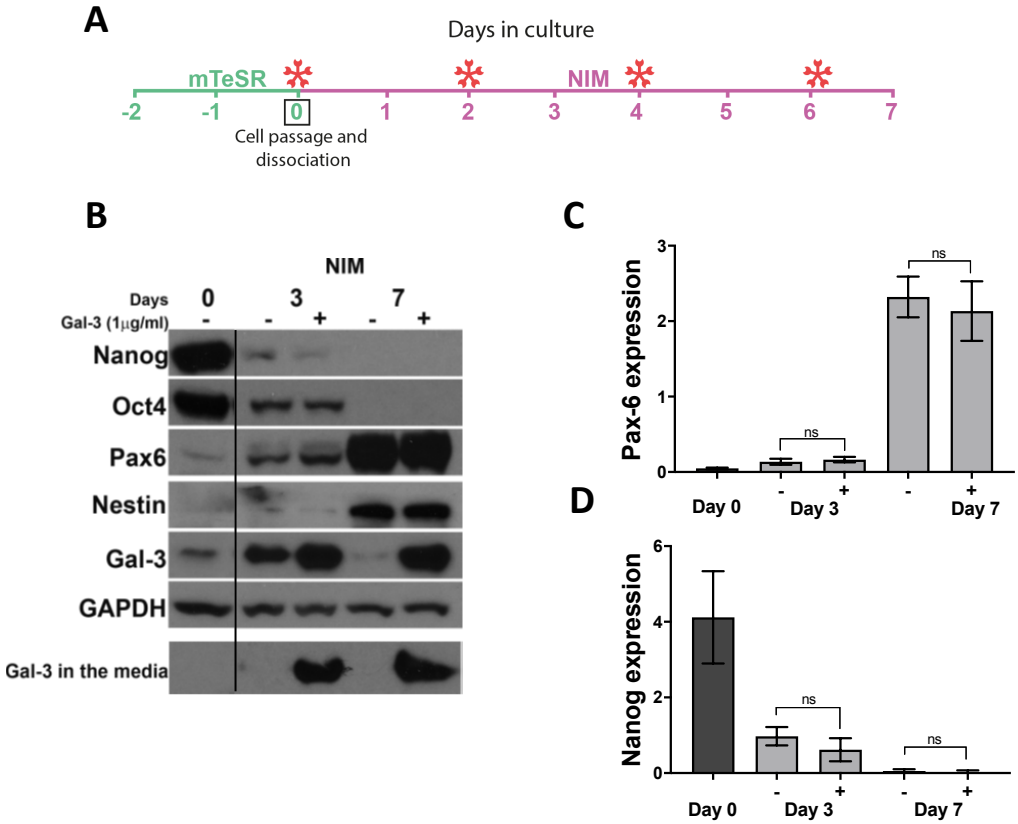


Figure 4.5. Recombinant Gal-3 did not affect neural markers.

A) Timetable of treatment with recombinant Gal-3, which was diluted on the NIM media every other day since the day of cell passaging. B) Representative Western blot of 3 independent biological replicates showing that the levels of pluripotency and multipotency markers remained unaltered upon treatment with 1 µg/ml recombinant Gal-3. NIM: neural induction media. Relative values of PAX-6 (n=4) and NANOG (n=3) are quantified in C and D, respectively. The values were normalised to GAPDH and are represented in arbitrary units (AU). Graphs are mean with SEM; ns: non-significant.

However, Gal-3 expression peaked very early during neural induction. Indeed, addition of recombinant protein at Day 3 only mildly increased its levels, whilst it had a more pronounced effect at Day 7. Hence, I decided to use another approach and test the effect of siRNA-mediated Gal-3 depletion (n=4 neural inductions) (Figure 4.6). The knockdown was performed in mTeSR^{TM}Plus media, and cells were allowed to recover for 2 days before neural induction. Cells in individual plates were collected daily (Figure 4.6 A). It is important to note that even in the control group (siNT), the increase in Gal-3 was

delayed by 2 days (Figure 4.6 B and C) compared to non-transfected cells (Figure 4.4). The knockdown was efficient in significantly decrease Gal-3 expression; however, it did not affect the levels of Pax6 (Figure 4.6 B, C and D). Collectively, these results suggest that Gal-3 does not participate in the acquisition of the neural fate with regards to the expression of neural markers such as Pax6.

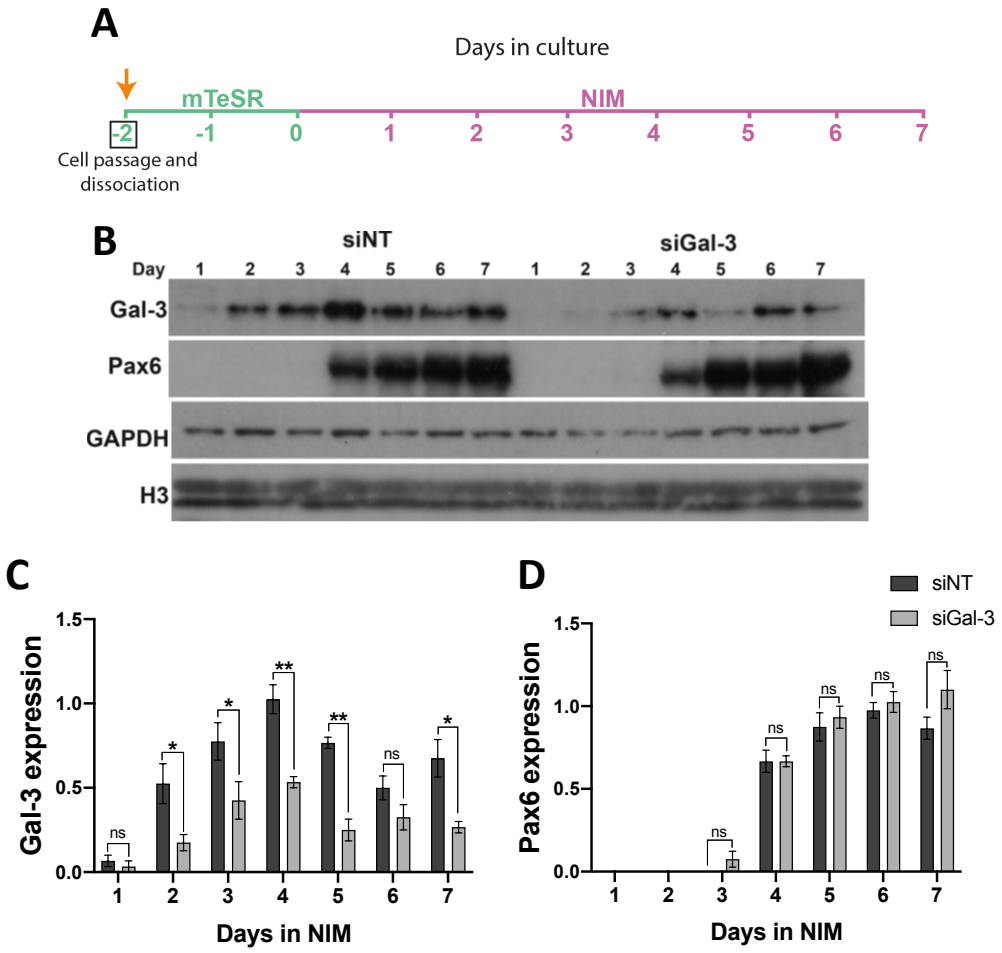


Figure 4.6. Gal-3 depletion did not affect levels of Pax6.

A) Timetable of H9 transfection, which happened 2 days before neural induction, indicated by an orange arrow. B) Representative Western blot of 4 independent biological replicates showing levels of Gal-3 and Pax6 upon Gal-3 depletion. The protein levels are quantified in C) for Gal-3 and D) for Pax6. The values were normalised to H3 and are represented in arbitrary units (AU). Graphs are mean with SEM; n=4. ns: non-significant; *p < 0.05; **p < 0.01. NIM: neural induction media.

4.5 Galectin-3 extracellular inhibition disturbed rosette formation

Gal-3 is known to be secreted by an alternative mechanism, and has several roles in the extracellular environment (Hughes, 1999; Menon and Hughes, 1999). Therefore, I decided to investigate if Gal-3 could be detected in the media during neural induction. Indeed, levels of Gal-3 in the media were low except at Day 1 (n=3 experimental replicates; different neural induction plates seeded from the same batch on the same day) (Figure 4.7). Interestingly, Gal-3 detected in the media at that day via western blot presented an extra band of higher molecular weight. Whether this band represents Gal-3 phosphorylation or another post-translational modification remains to be elucidated.

These observations mean a possible role for Gal-3 in the extracellular environment during early neural commitment.

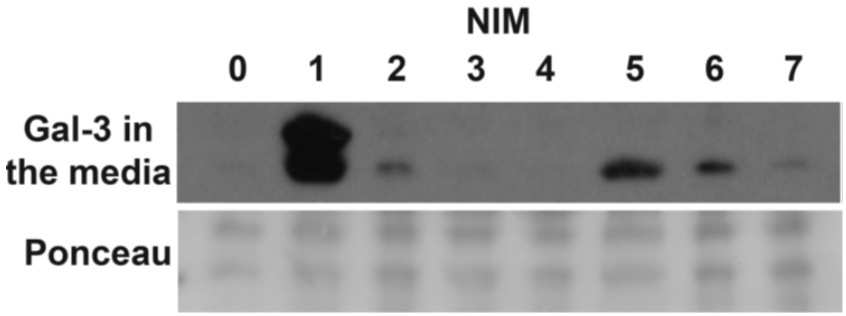


Figure 4.7. Secreted Gal-3.

Representative Western blot of 3 experimental replicates showing Gal-3 detected in the media during neural induction. NIM: neural induction media.

Extracellular Gal-3 has indeed been studied before in the context of cell polarisation and cyst formation (Honig et al., 2018; Torkko et al., 2008). Here, I observed that Gal-3 rises at Day 1 in the media (Figure 4.7) and at Day 2 in the cells (Figure 4.4), the same time point when rosettes start to be formed (Figure 4.3). Previous studies have shown that extracellular Gal-3 can be block by using antigen specific antibodies (Comte

et al., 2011; Inohara and Raz, 1995). Therefore, I studied the effects of blocking Gal-3 using an N-terminal specific antibody (clone M3/38) (Comte et al., 2011) on cell morphology and neural rosette formation during neural induction

Right at the beginning of neural induction (Day 2), cells treated with Gal-3 antibody (αGal-3) showed a substantial difference in their phenotype compared to cell treated with a control antibody (αIgG) (n=1 neural induction) (Figure 4.8). At this time point, cells organise in circular structures or “neural rosettes”, with cell-cell contact in the apical region. Upon treatment, rosettes seemed enlarged and less frequent resulting in a smaller number of rosettes per image analysed (Figure 4.8 A and B). Cells, which should have started to undergo size constriction by Day 2, appeared much larger than expected for that time point, which was assessed via nuclei length (Figure 4.8 A and C).

These dysmorphic rosettes were further characterised through several parameters. First, it was possible to observe that they were composed of several layers of cells aligned towards an apical centre. This feature was reflected in a larger number of cells per rosette (Figure 4.8 D) and rosette area (Figure 4.8 D’). Rosette’s edge was determined upon visual assessment of cells polarised towards the same centre. Additionally, upon treatment, there was an enrichment of actin between cells and not only in the apical region, indicating points of cell-cell contact. Indeed, the apical region itself was composed of cells attached to each other and it had an enlarged area when compared to control (Figure 4.8 D’’). As a result of those alterations at the initial days of neural induction, there was a complete abrogation of rosette formation at Day 6 (Figure 5.5). This result indicates the importance of Gal-3 for the cellular morphological alterations required for the formation of neural rosettes.

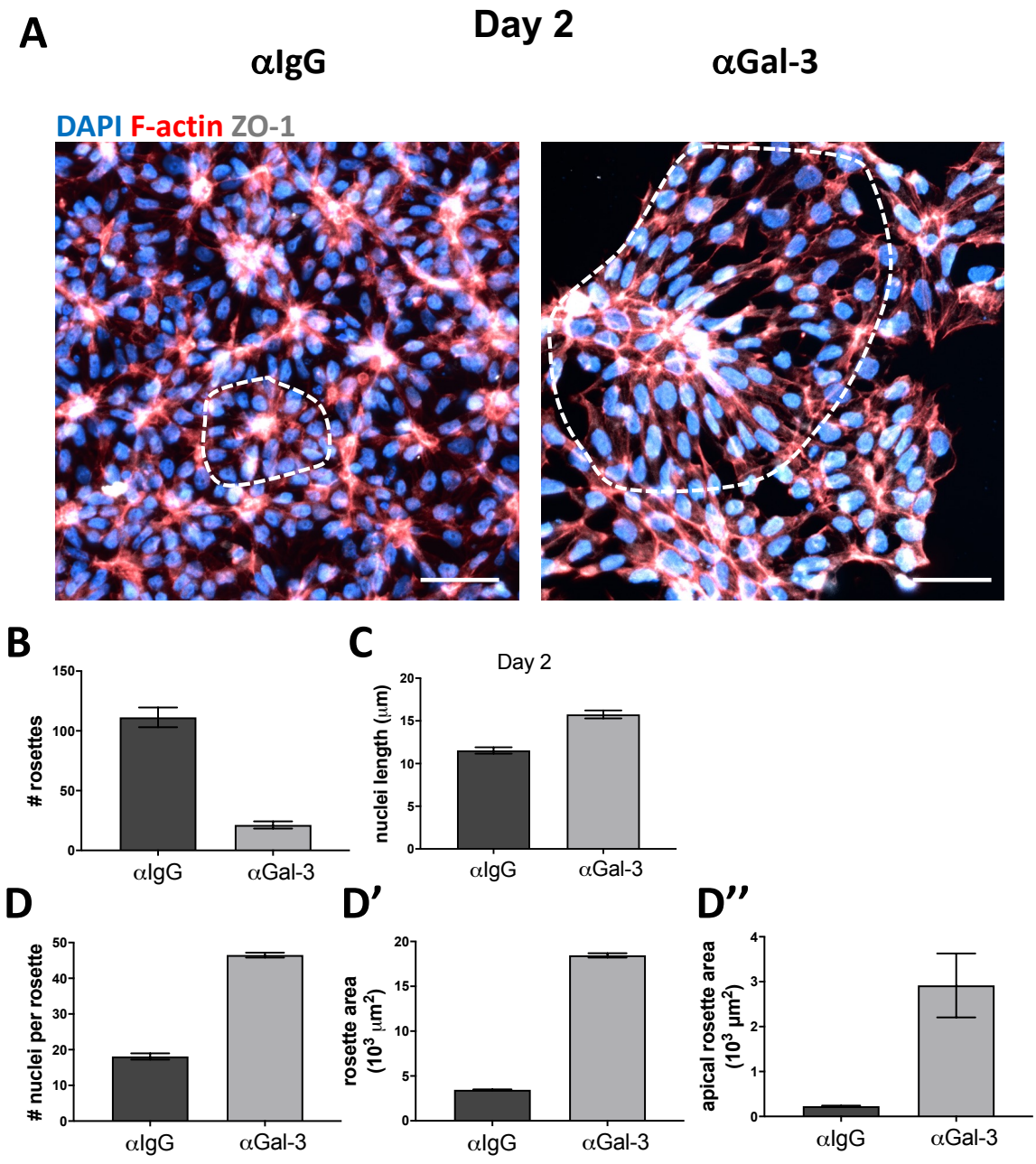


Figure 4.8. Gal-3 inhibition disturbed the formation of rosettes.

A) Immunofluorescence after 2 days of neural induction illustrating that the treatment with 5 μg/ml antibody against Gal-3 (αGal-3) disrupted the formation of polarised rosettes compared with the control treatment (αIgG). Dashed lines indicate a neural rosette. Scale bar 50 μm. n=1. B) Mean number of rosettes per analysed image (SEM of 3 images; n=1 neural induction). C) The mean of at least 100 nuclei length per image was analysed (SEM of 3 images; n=1 neural induction). Neural rosettes characteristics of at least 10 rosettes per image were analysed via mean with SEM (3 images; n=1 neural induction) in D) for number of cells per rosette D') for rosettes area, and D'") for apical rosette area.

4.6 Galectin-3 interaction with integrins

Because Gal-3 interacts with several extracellular receptors, it participates in many processes that could explain the phenotype observed. Therefore, for the next step, I decided to pursue a possible mechanism behind this result by looking at Gal-3 interaction with integrins. Localised at the basal surface of epithelial cells, where they interact with components of the ECM, integrins are known to maintain apical-basal polarity via regulating microtubule dynamics (Lee and Streuli, 2014). The same basal localisation has been observed in neural rosettes (Banda et al., 2015). In addition, not only Gal-3 has been implicated with cytoskeletal remodelling (Raz et al., 1990), but also it is capable of binding to integrins such as β1 and β3 (Honig et al., 2018; Seguin et al., 2014).

Among the variety of integrin subunits, α5 and β1 are known to be expressed in NSCs (Jacques et al., 1998; Yoshida et al., 2003), while β3 is not expressed in the brain (Pinkstaff et al., 1999). Indeed, hESCs presented a progressive increase in the α5 and β1 subunits upon neural induction. In contrast, β3 expression was completely abrogated as early as Day 2 (Figure 4.9).

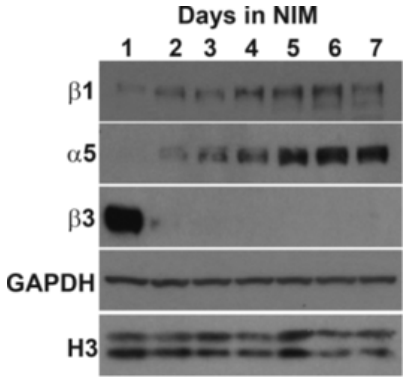


Figure 4.9. Integrin isoforms during neural induction.

Western blot (n=1) showing the variation of different integrin isoforms during neural induction. NIM: neural induction media.

Interestingly, Gal-3 regulates the polarised distribution of β1 integrin in MDCK cells, affecting cyst formation (Honig et al., 2018). I therefore hypothesised that extracellular Gal-3 interacts with integrins at the cell membrane in the basal compartment, regulating neural rosettes morphogenesis (Figure 4.10 A).

To test this possibility, I assessed Gal-3/β1 interaction through co-immunoprecipitation at different time points during neural induction. There was no evidence of interaction upon Gal-3 immunoprecipitation (n=1 neural induction) (Figure 4.10 B). To confirm this data, I did the reverse and immunoprecipitated β1 integrin instead (n=1 neural induction) (Figure 4.10 D). The Western blot showed that there was no band of Gal-3 in any of the time points, further suggesting that Gal-3 does not interact with β1 integrins. Considering that the peak of Gal-3 (Figures 4.4 and 4.7) as well as its role in neural rosettes polarisation (Figure 4.8) where described at the first 3 days of neural induction, it would be important to address Gal-3 interaction with β1 at earlier time points.

The results obtained in this Chapter support a role for Gal-3 in NSC polarisation and neural rosette formation. However, the presented data was not enough to demonstrate that this action is through Gal-3 interaction with integrins at the cell membrane. Therefore, moving forward, I will focus on a different hypothesis for the mechanism of action of Gal-3.

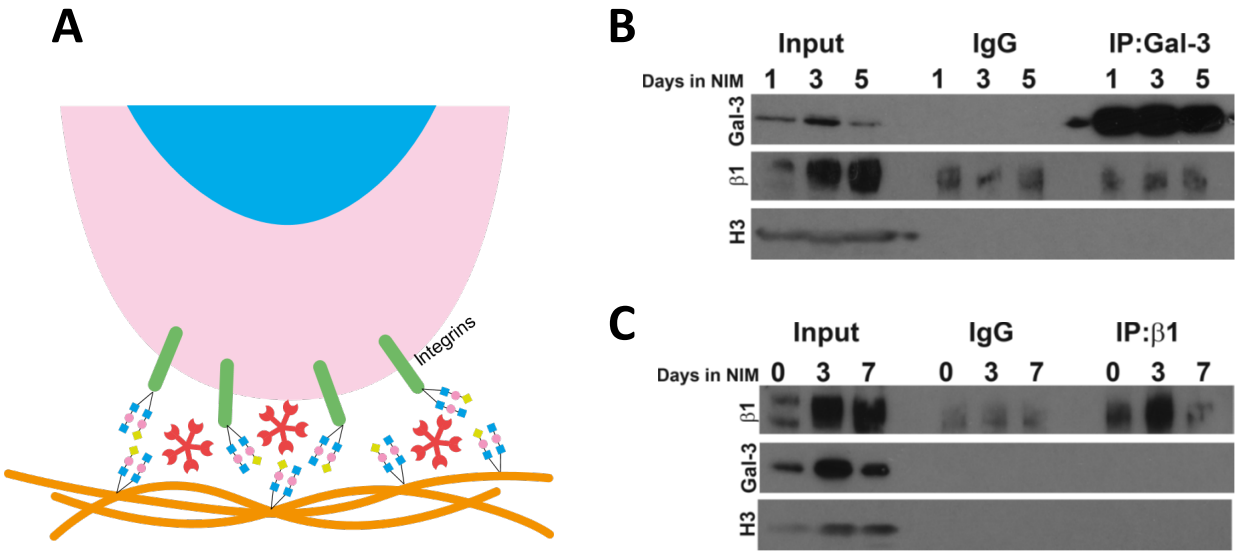


Figure 4.10. Gal-3 interaction with integrins.

A) Schematic representing the hypothesis that extracellular Gal-3 binds integrins in a glycan-dependent manner at the basal part of the cell membrane. B and C) Western blot (n=1) to test the interaction between Gal-3 and β1after Gal-3 (B) and β1 (C) immunoprecipitation. Different neural induction time points are shown. Antibody against the IgG of the same species was used as a negative control. NIM: neural induction media.

4.7 Discussion

In this Chapter, I analysed the expression and function of Galectin-3 in the context of early neural development. Following the findings which showed that Gal-3 has a role in differentiation of postnatal NSCs in the pSVZ *in vivo* (Chapter 3), I investigated if the protein also plays a role in early neural commitment. At the same time, I investigated possible molecular mechanisms behind the role Gal-3 in development.

Before assessing this, I first characterised the dual Smad inhibitor neural induction protocol to generate NSCs from hESCs, which has been previously established (Chambers et al., 2009). The hESCs successfully acquired expression of the neural markers Pax6 and Nestin. At the same time, they lost NANOG and Oct4, indicating loss of pluripotency and acquisition of the neural fate. Additionally, morphological alterations resulted in apical-basal polarity and neural rosettes could be observed from Day 2. Formation of neural rosettes, which has been described before in monolayer culture of pluripotent stem cells, is a very important step and resembles the formation of the neural tube (Banda et al., 2015; Chambers et al., 2009; Li et al., 2011).

Using the hESCs neural differentiation model, I observed by Western blot that Gal-3 was expressed during neural commitment, with the highest levels of expression at Day 2 followed by depletion to basal levels. NSCs and other progenitors in the pSVZ indeed express Gal-3 (Comte et al., 2011), which, as shown in Chapter 3, is important for cellular differentiation towards the glial lineage. Interestingly, here, the upsurge of Gal-3 preceded expression of neural markers such as Pax6, raising the question of whether both events were related. Gal-3 is known to activate a number of intracellular signalling pathways including direct upregulation of expression of target genes involved with cell survival (Lin

et al., 2002; Liu et al., 2002; Paron et al., 2003). Therefore, I modulated Gal-3 levels in the cells during neural differentiation to test if this could impact on the expression of neural markers. Both treatment with recombinant Gal-3 and siRNA mediated depletion of Gal-3 did not alter expression of markers such as Pax6. As I will show in the next Chapter, Gal-3 is not found in the nucleus during neural induction. Hence, the data collected in this thesis does not support the role of Gal-3 in the direct regulation of gene expression of neural markers. It is important to take into account that both methodologies used for Gal-3 modulation have limitations and a gene knockout would be needed to fully validate these results.

Interestingly, when hESCs were submitted to the neural differentiation protocol, they secreted Gal-3 in the media at Day 1. Secreted Gal-3 plays several roles in the extracellular compartment (Fortuna-Costa et al., 2014; Hughes, 1999; Menon and Hughes, 1999). Moreover, Gal-3 has been shown to form lattices in the cell membrane upon its interaction with transmembrane receptors (Garner and Baum, 2008; Rabinovich et al., 2007). This interaction often results in Gal-3 incorporation into carrier vesicles (Delacour et al., 2009). This could explain the observed increased levels of Gal-3 at Day 2. It is possible that the exogenous Gal-3 present in the media at Day 1 acts on neighbouring cells by binding to transmembrane receptors or by being incorporated by the cells themselves. Indeed, the recombinant Gal-3 treatment resulted in higher levels of Gal-3 protein in the Western blot when compared to non-treated cells, supporting that the exogenous Gal-3 might be interacting with the cell through transmembrane receptors and/or protein uptake into vesicles.

Since Gal-3 does not directly regulate expression of neural markers, and in the light of the evidences of its secretion and possible interaction with extracellular receptors, I questioned if Gal-3 plays a role in other aspects of the neural induction, such as morphological alterations required for neural rosette formation. This was supported by the results from the Gal-3 antibody treatment experiment. This antibody blocking altered morphogenesis of neural rosettes, leading to a complete abrogation of rosettes at Day 6. Treatment with antibody against Gal-3 has been described before and this specific clone that recognises the N-domain has been shown to block Gal-3-mediated neuroblast migration in explants (Comte et al., 2011; Inohara and Raz, 1995). Interestingly, it was at Day 2, when Gal-3 was at its highest levels, that rosettes started to be observed. Gal-3 promotes cytoskeletal remodelling and has been implicated in the formation of polarised cysts (Honig et al., 2018; Raz et al., 1990; Torkko et al., 2008), suggesting that the antibody treatment could have impaired this Gal-3 mediated cytoskeletal remodelling activity. The fact that Gal-3 inhibition affected polarisation but did not affect expression of neural markers is supported by previous studies showing that the expression of Pax6 can occur in the absence of rosette formation (Chambers et al., 2009; Li et al., 2011), which suggests that these are two unrelated and separate events.

Among the described binding partners of Gal-3, integrins are transmembrane proteins that localise at the basal membrane of neural rosettes. There, they regulate apical-basal polarity and microtubule dynamics (Banda et al., 2015; Honig et al., 2018; Lee and Streuli, 2014; Raz et al., 1990; Seguin et al., 2014). In fact, hESCs started expressing α5 and β1 integrins as neural differentiation progressed. However, no interaction between Gal-3 and β1 could be observed upon co-immunoprecipitation. Gal-

3 binding and function are context dependent. For example, Gal-3 binds to EGFR in cancer cells, but not in SVZ progenitors (Comte et al., 2011; Partridge et al., 2004). Nevertheless, it is important to consider that protein interactions, especially at the cell membrane, are difficult to preserve for immunoprecipitation and might need a more optimised protocol. Moreover, analysis of earlier time points would be required, since Gal-3 activity appear to mostly occur at the first 3 days of neural induction.

Other extracellular binding partners of Gal-3 could result in the observed phenotype, such as adhesion molecules. Gal-3 role in adhesion is also variable, and Gal-3 can either increase (Kuwabara and Liu, 1996; Matarrese et al., 2000) or impair it (Ochieng et al., 1998; Villa-Verde et al., 2002). Here, it is possible that Gal-3 blocking with antibody impeded its interaction with cell receptors and ECM, resulting in decreased cell adhesion to the matrix.

In the next Chapter, I will explore another possibility for Gal-3 mechanism of action in neural differentiation. Gal-3 participates in apical protein sorting, and it has been described to interact with junctional complex proteins (Boscher et al., 2012; Delacour et al., 2006; Delacour et al., 2008; Honig et al., 2018; Yamamoto et al., 2013). Therefore, I analysed if this could be the case in neural rosettes.

Chapter 5

The role of the Hippo pathway in neural differentiation of hESCs and its involvement with Galectin-3-induced polarisation

5.1 Introduction

Gal-3 is localised and secreted in the apical region of many epithelial cells, being important for the establishment of apical-basal polarity (Apodaca et al., 2012; Argüeso et al., 2015; Lindstedt et al., 1993; Vieira et al., 2006; Viguier et al., 2014). Therefore, I decided to explore another possible mechanism of action for Gal-3 in cell differentiation through participating in apical-basal establishment. In order to do that, I investigated its intracellular localisation during hESCs neural differentiation and how its inhibition could affect components of the junctional complex, such as the Hippo pathway.

Among the protein signalling cascades that regulate development, the Hippo pathway is well known for its role in cell growth and fate decision (Davis and Tapon, 2019; Varelas, 2014). Its mains effector, the co-transcriptional factor YAP, binds to several transcriptional factors to promote self-renewal and proliferation of NSCs (Cao et al., 2008; Gee et al., 2011). Upstream molecules can regulate development through the Hippo pathway. For example, activation of the pathway by the scaffold protein R1A results in YAP switching binding partners to promote differentiation (Papaspyropoulos et al., 2018). Additionally, the Hippo pathway and YAP respond to cell-cell interaction and are part of the junctional signalling. The junctional complex is a structure formed by adherent and tight junctions that divides polarised cells, including neuroepithelial cells, into apical and basal domains (Eom et al., 2013). The presence of the Hippo pathway at the junction is essential for the establishment and maintenance of apical-basal polarity (Genevet and Tapon, 2011; Karaman and Halder, 2018).

Although the Hippo pathway has been studied in context of neural development, its specific role and regulation remains to be clarified. Thus, I studied the involvement of

components of the Hippo pathway in early neural differentiation of hESCs. In particular, since the pathway can be regulated by changes in the localisation of its components (Genevet and Tapon, 2011; Hirate et al., 2013; Karaman and Halder, 2018), I characterised the expression and localisation of YAP and R1A as an indication of their function.

5.2 Galectin-3 localises towards the apical region in early neural induction

I started this investigation looking at Gal-3 cellular distribution during neural induction by immunostaining (Figure 5.1). Antibody specificity was assessed via a secondary-only control (Figure 5.1 A). Surprisingly, using this methodology, Gal-3 was not detected at Day 2 as strongly as what observed with the Western blotting in Figure 4.4. However, it was possible to see its localisation towards the luminal zone as early as Day 3, which persisted until Day 7 (Figure 5.1 A). Looking closely, Gal-3 immunostaining presented a spotted pattern resembling intracellular vesicles, which accumulate towards the apical region (Figure 5.1 B). Importantly, Gal-3 did not present a nuclear localisation at any time point studied, suggesting that Gal-3 indeed does not directly regulate gene expression, as previously hypothesised (Chapter 4).

This interesting result raised the possibility of Gal-3 playing a role at the endomembrane compartment of NPCs. Several quantifications would be interesting and help to elucidate Gal-3 roles during neural differentiation. For example, the fluorescence intensity, as well as number of puncta per cell could be quantified using FIJI (ImageJ) software, offering important information on Gal-3 expression as well as number of Gal-3 positive vesicles over time. Additionally, Gal-3 could be co-stained with widely used

protein markers for different endosomal compartments, focusing on those where Gal-3 has been already described, such as endosomes and lysosomes. For example, Rab GTPase proteins can be used to help distinguish among early endosomes (Rab5) and late endosomes (Rab7). For membrane recycling pathways it is possible to use Rab-4, Rab-8 and Rab-11. Lysosomes can be detected using Lysosome-associated membrane glycoproteins (LAMP) and the LysoTracker® dye. The secretory pathway can be also accessed via galactosyltransferases (Baba et al., 2020; Pfeffer, 2013; Schneider et al., 2010; Strous, 1986).

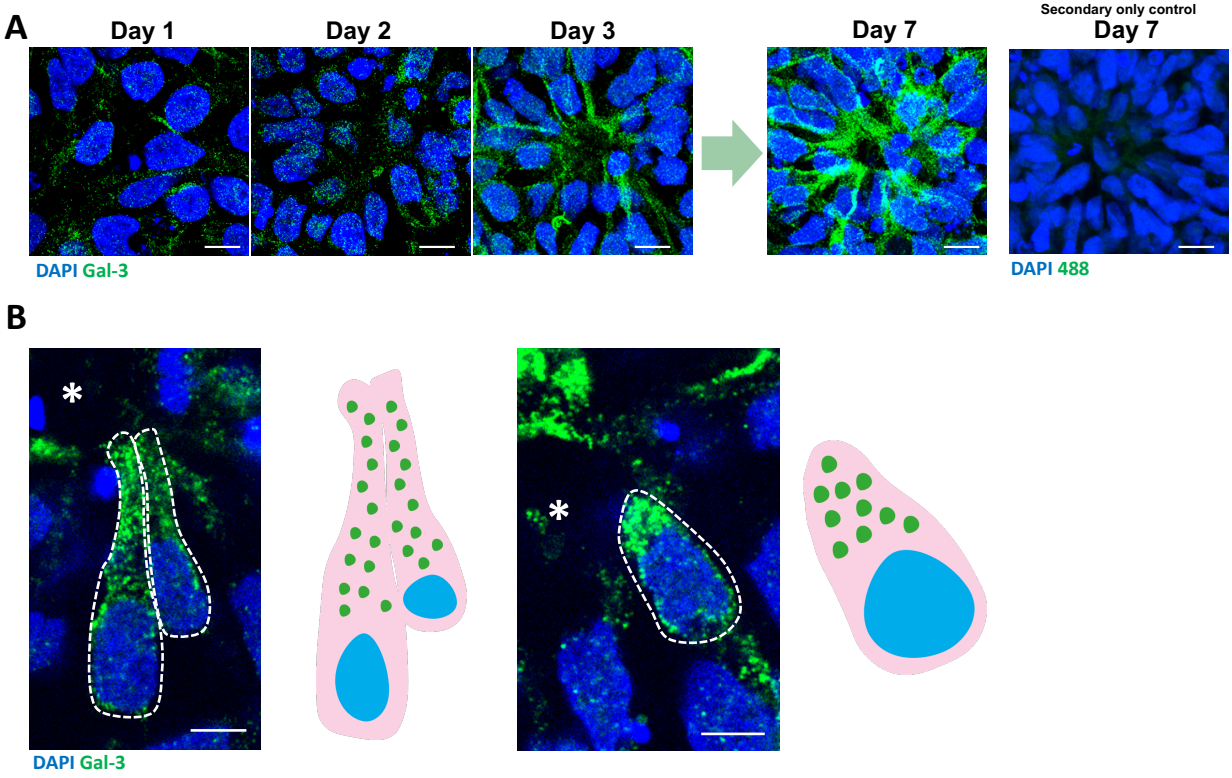


Figure 5.1. Gal-3 localisation during first days of neural induction.

A) Confocal image illustrating Gal-3 localisation during neural induction. An example of secondary-only control for Day 7 is shown. Scale bar 15 µm. B) Detail of 3 NSCs at Day 7 showing the spotted pattern of Gal-3 immunostaining which accumulates in the apical region. Lumen is shown with an asterisk (*) and cells are delimited in white dashed lines. Scale bar 5 µm. In the schematics: Green: Gal-3; Blue: DAPI.

5.3 Expression and localisation of YAP during neural differentiation

As mentioned before, the Hippo pathway is a developmental signalling cascade that is active in stem cells and participate in cell fate decision (Hirate et al., 2013; Papaspyropoulos et al., 2018; Varelas, 2014). The pathway responds to cell-cell contact stimuli from the junctional complex (Karaman and Halder, 2018). The junctional complex is localised in the intersection between the apical and basal domains and participates in the asymmetrical distribution of proteins (Eom et al., 2013). Therefore, I continued my studies investigating YAP, the main effector of the Hippo pathway, and its possible relationship with Gal-3 during neural differentiation.

The activity of the Hippo pathway during neural induction was assessed via expression and phosphorylation of YAP (n=3 neural inductions) (Figure 5.2). Western blot analysis showed that YAP levels initially dropped to less than 25% compared to pluripotency, although this was not statistically significant (Figures 5.2 A and B). This finding is in accordance with previous reports showing that YAP depletion is required to allow differentiation (Zhang et al., 2012). However, YAP started to be expressed again at Day 5 (Figures 5.2 A and B), suggesting a role in differentiated NSCs, which by Day 5 already expressed the neural markers Pax6, Nestin and Sox2 (Figure 4.1).

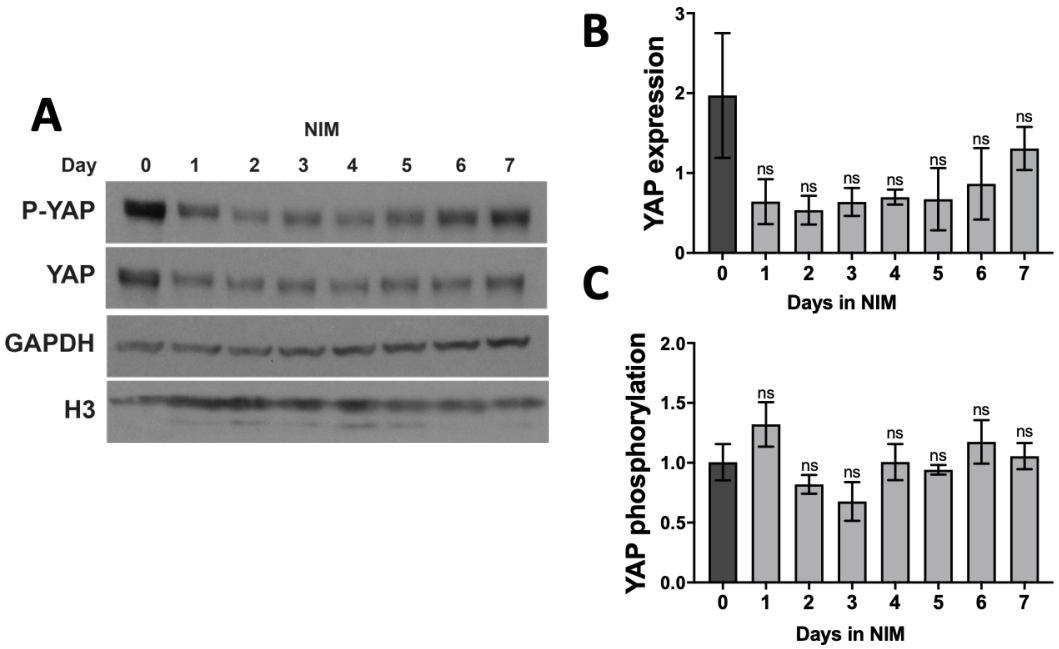


Figure 5.2. YAP expression during neural induction.

A) Representative Western blot of 3 independent biological replicates showing levels of YAP over days of neural induction and its phosphorylated form. B) Quantification of YAP and C) its phosphorylation at Ser 127 from Western blot. YAP was normalised to H3 and P-YAP was normalised to YAP. Values are represented in arbitrary units (AU). Graphs are mean with SEM; n=3. For statistical analysis, values were compared to Day 0. ns: non-significant. NIM: neural induction media.

YAP is targeted by the Hippo core kinase cascade and, upon its phosphorylation at the Ser127, is retained in the cytoplasm and degraded, or switches binding partners (Kanai et al., 2000; Matallanas et al., 2007; Oh and Irvine, 2008; Zhao et al., 2010). Therefore, studying the phosphorylation state of YAP offers important information about its function. Phosphorylation of YAP increased as hESCs differentiation progressed, as did total YAP (Figure 5.2 A). Quantification of western blot showed that, whilst YAP expression increased, the proportion of phosphorylated YAP remained constant during differentiation (Figure 5.2 C). This shows that at least part of the YAP being re-expressed in NSCs was also phosphorylated. The proportion of phosphorylated YAP slightly increased at Day 1, even though this was not statistically significant (Figure 5.2 C).

Interestingly, immunofluorescence images showed that YAP changed its localisation from nuclear to apical during the onset of neural differentiation (Figure 5.3 A). At Day 7, almost all YAP immunofluorescent signal was localised at the apical ring surrounding the lumen of neural rosettes, being co-localised with tight junction protein ZO-1 and the intracellular component cell-cell junction F-actin. Antibody specificity was assessed via a secondary-only control (Figure 5.3 C). The recruitment of YAP to the tight junction has been described before, and often results in its phosphorylation by the Hippo pathways core kinases (Paramasivam et al., 2011). I indeed observed phosphorylated YAP at the junctional region of neural rosettes co-localised with ZO-1 (n=1 neural induction) (Figure 5.3 B). The re-expression and specific localisation of YAP suggests an active role in NSCs, which could be by acting as a component of the junctional complex.

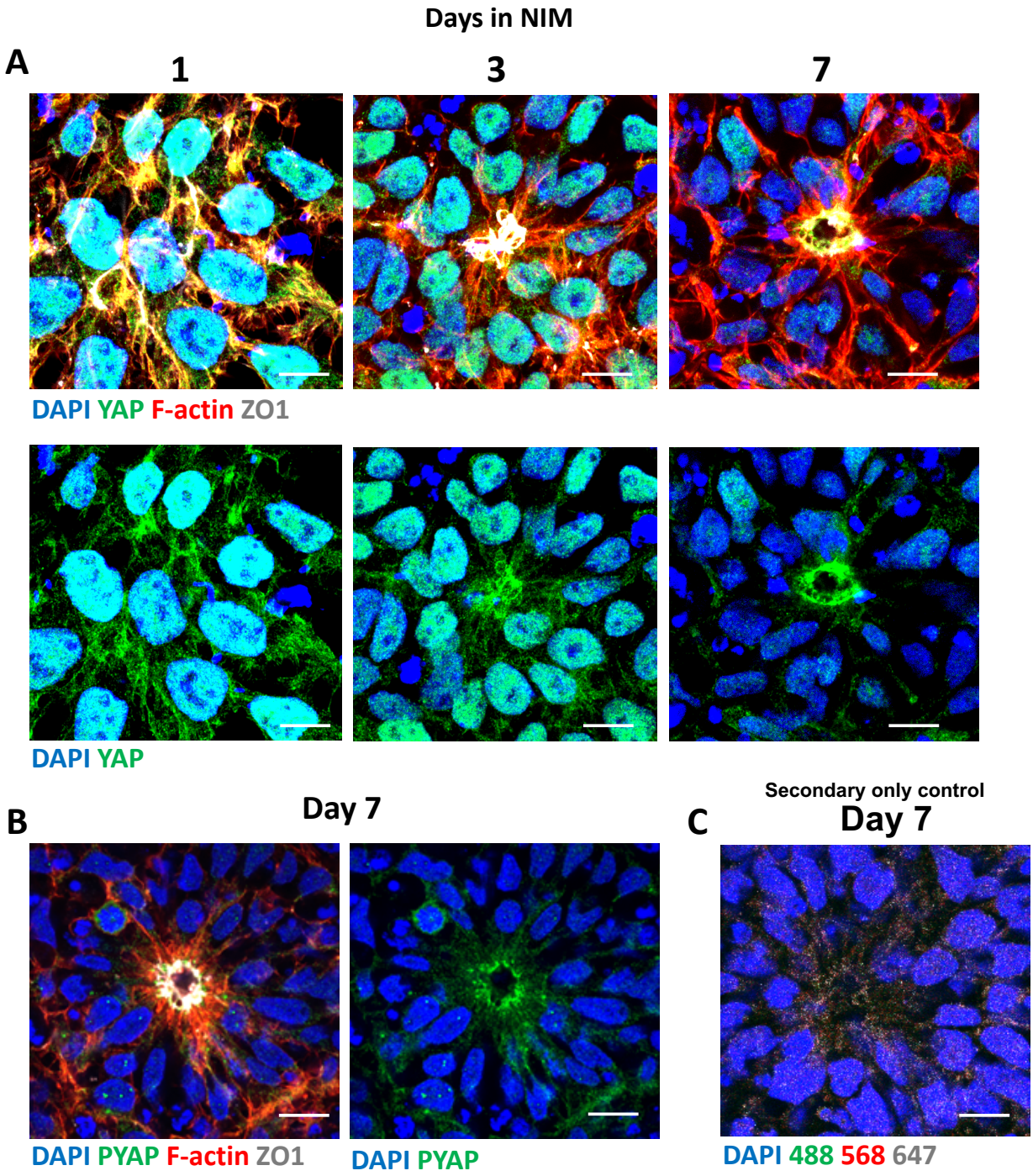


Figure 5.3. YAP and P-YAP localisation during neural differentiation.

A) Confocal images showing changes in localisation of YAP from nuclear to apical during neural induction. NIM: neural induction media. B) Confocal images illustrating P-YAP (Ser 127) localisation at apical region in neural rosettes. C) An example of secondary-only control for Day 7 is shown. Scale bar 15 μm.

5.4 Galectin-3 depletion does not affect YAP expression

As shown before, endogenous levels of Gal-3 increased at the beginning of neural induction while YAP is re-expressed and phosphorylated at Day 4. I decided to investigate if Gal-3 is affecting YAP expression or phosphorylation.

To do that, I initially treated the hESCs with recombinant Gal-3 during neural induction, following the same protocol as showed in Figure 4.5 A. Upon this treatment, neither YAP expression or phosphorylation was altered when quantified from the Western blot (n=4 neural inductions) (Figure 5.4 A, A' and A''). Therefore, I followed the same protocol as described in Figure 4.6 A to deplete Gal-3 with siRNA, and analysed YAP expression and phosphorylation daily. There was no difference in YAP (n=4 neural inductions) or its phosphorylated form (n=3 neural inductions) at any time point studied (Figure 5.4 B, B' and B''). These experiments evidenced that Gal-3 does not regulate YAP expression or phosphorylation.

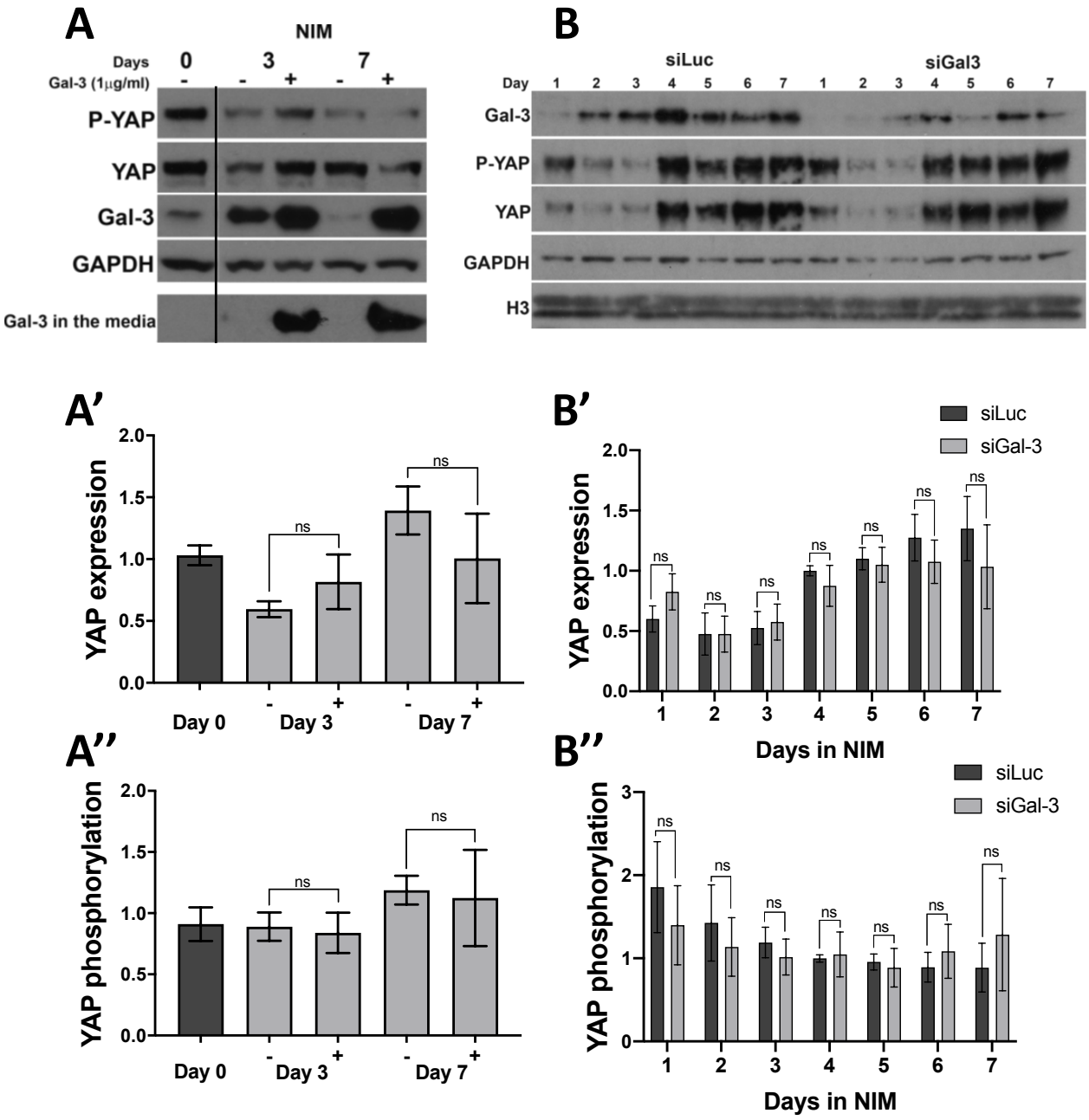


Figure 5.4. Effect of Gal-3 modulation on YAP expression and phosphorylation.

Representative Western blot of 3 or 4 independent biological replicates of expression and phosphorylation of YAP upon A) treatment with 1mg/ml recombinant Gal-3 and B) Gal-3 depletion during neural induction are shown. Western blot was quantified and YAP values after A') Gal-3 treatment and B') Gal-3 depletion were normalised to GAPDH and are represented in arbitrary units (AU). YAP phosphorylation at S127 was quantified and values after A'') Gal-3 treatment and B'') Gal-3 depletion were normalised to YAP and are represented in arbitrary units (AU). Graphs are mean with SEM; n=3 or 4. ns: non-significant. NIM: neural induction media.

5.5 YAP remains nuclear upon Galectin-3 blocking during neural induction

The data shown so far was not enough to indicate that Gal-3 regulates YAP expression and phosphorylation. However, YAP functions are also regulated by its localisation (Karaman and Halder, 2018). In the previous Chapter, I showed that the blocking of extracellular Gal-3 using a specific antibody disrupted formation of neural rosettes (Figure 4.8). I therefore questioned whether the same treatment would affect YAP's apical localisation. Indeed, it was possible to observe that, in the absence of polarisation caused by the treatment, YAP no longer formed an apical ring co-localised with F-actin. Instead, it remained nuclear even 6 days after the beginning of neural induction (n=2 neural inductions) (Figure 5.5).

This result showed that Gal-3 blocking abrogated rosettes formation, which is possibly a result from its functions on cell polarisation observed at Day 2 (Figure 4.8). Additionally, Gal-3 blocking caused YAP nuclear retention. Whether Gal-3 directly regulates YAP delivery to tight junctions or if this is a secondary result from Gal-3 actions in other pathways remains an open question that needs to be addressed.

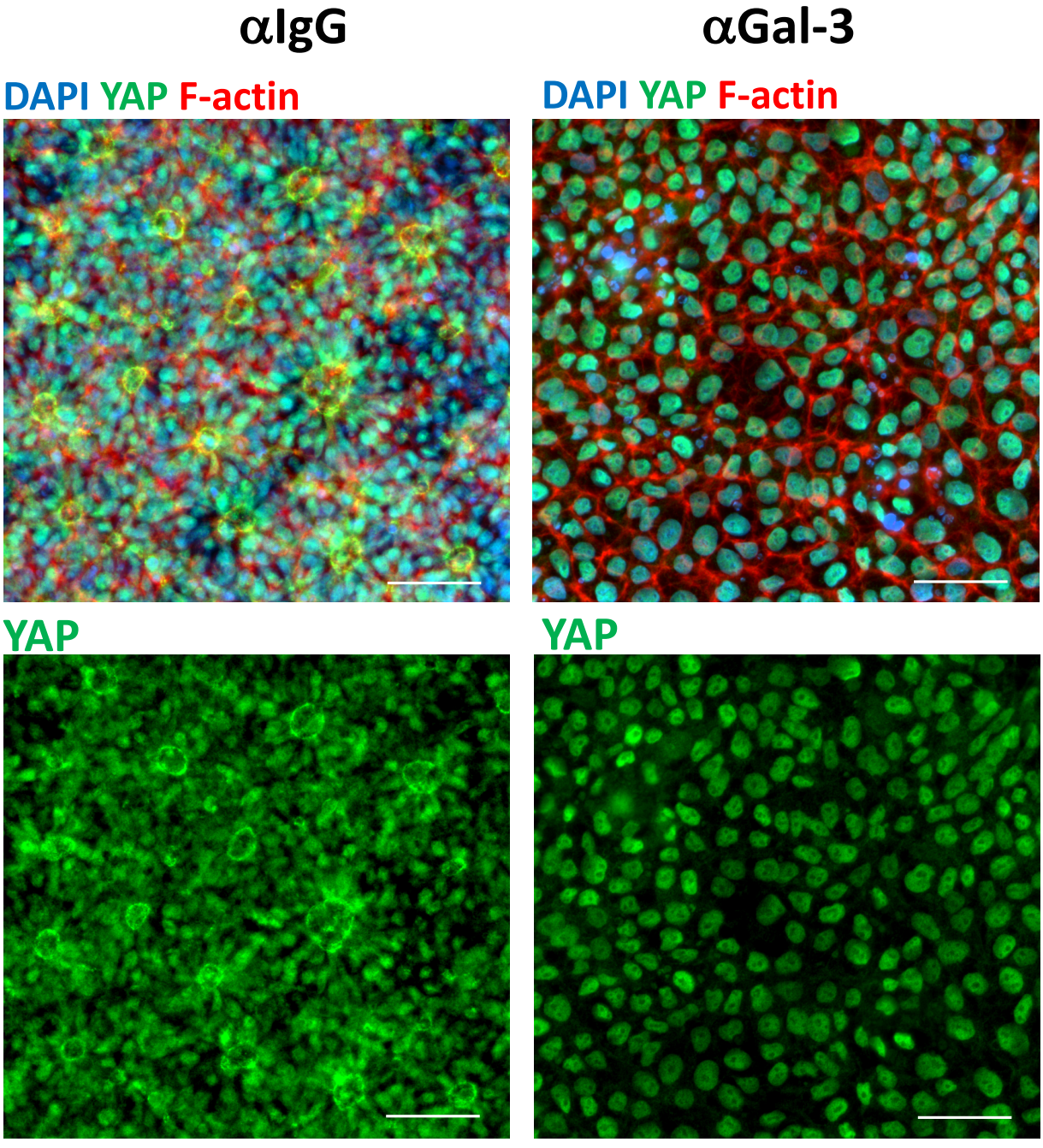


Figure 5.5. YAP localisation is affected by inhibition of Gal-3.

Treatment with an antibody against Gal-3 (1 μg/ml) prevented YAP to migrate to the junctional complex, resulting in YAP nuclear localisation after 6 days of neural induction. Scale bar 50 μm. n=2.

5.6 Expression and localisation of RASSF1A during neural induction

I have previously shown that Gal-3 loss affected formation of rosettes and polarity, as well as YAP delivery to the junctional complex (Figures 4.8 and 5.5). Upstream of YAP, RASSF1A (R1A) is a scaffold protein that activates Hippo by activating its core kinase cascade (Figure 1.9) (Avruch et al., 2006; Guo et al., 2007). Expression of R1A increases in differentiating pluripotent cells and results in YAP phosphorylation (Papaspyropoulos et al., 2018). Additionally, R1A is known to associate with components of the cytoskeleton (Dallol et al., 2004; Liu et al., 2003; Rong et al., 2004; Song et al., 2004; Vos et al., 2004), indicating that this protein could respond to signalling regulating cell reshaping and polarisation, such as from Gal-3. Therefore, I decided to investigate if R1A played a role in neural rosette formation.

First, I studied the expression and localisation of R1A during hESCs neural differentiation. Indeed, Western blot (n=1 neural inductions) and immunofluorescence (n=3 neural inductions) analysis showed that protein levels of R1A increased over time (Figure 5.6 A and B). Through immunofluorescence it was possible to see that R1A had a specific localisation in a structure that resembles the cytoskeleton (Figure 5.6 B). Antibody specificity was assessed via a secondary-only control (Figure 5.6 B'). A similar pattern was observed in NSC obtained from hESCs using an embryoid body protocol (Appendix A).

Interestingly, R1A accumulated at the apical region of neural rosettes (Figure 5.6 B, right panels), similar to YAP. R1A immunostaining, however, presented a peculiar spotted pattern comparable to what is expected for the primary cilia. I decided to investigate that studying the co-localisation of R1A with cilia markers. R1A

immunostaining was observed just under the cilia marker ARL13B but co-localised to the centrosome protein γTubulin, suggesting that R1A associates with the cilia basal body, as illustrated in the schematics.

The possibility of an interplay between R1A and Gal-3 remains an open question, and should be addressed. Proteins in the cilium participate in the junctional complex signalling (Gerdes et al., 2009). In the future, it will be important to analyse the interaction between R1A and YAP at the junction complex during neural differentiation.

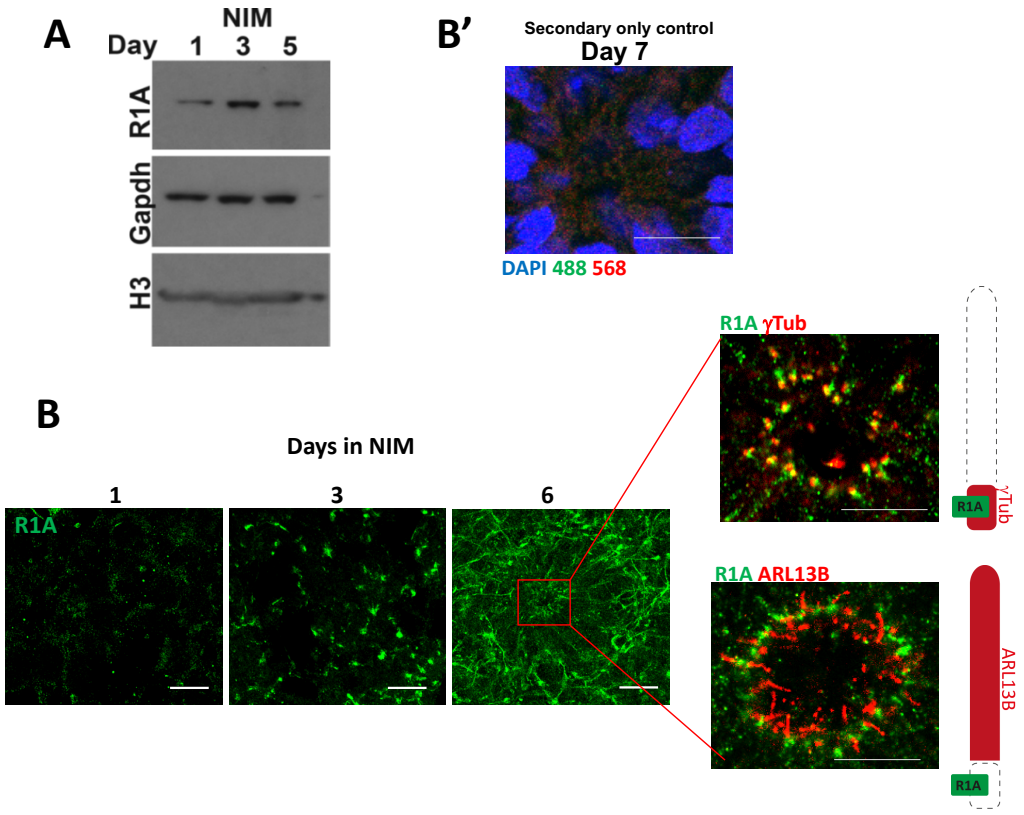


Figure 5.6. R1A expression during neural induction.

A) Western blot (n=1) and B) representative immunofluorescence of 3 independent biological replicates showing R1A levels and localisation during neural induction. The apical portion of a neural rosette at Day 6 is highlighted with a red box. Right panels: confocal images and schematic illustrating details of the apical portion of neural rosettes after R1A, ARL13B and γTubulin immunostaining. NIM: neural induction media. An example of secondary-only control for Day 7 is shown in B'. All scale bars 15 μm.

5.7 Discussion

I started this Chapter by investigating the cellular localisation of Gal-3 in the context of neural induction, which could offer an indication of its role. Firstly, the peak of Gal-3 at Day 2 of neural induction observed with Western blotting was not reproduced via immunofluorescence. In the previous Chapter, I discussed the possibility that exogenous Gal-3 binds to extracellular receptor forming lattices at the cell membrane. In fact, proteins at the cell surface might be difficult to preserve after immunofluorescence permeabilization (Vernay and Cosson, 2013). Therefore, an optimised protocol intending to preserve Gal-3 lattices would be required for visualisation of these structures. Still, after interaction with receptor, Gal-3 can be internalised in carrier vesicles and participate in apical protein sorting (Delacour et al., 2009). It is possible that this is the case in neural rosettes, since I observed that Gal-3 immunostaining presented a spotted pattern. However, this hypothesis requires further investigation.

Nevertheless, I observed that Gal-3 is distributed towards the luminal zone during neural induction. A similar localisation have been shown before in other models of epithelialisation (Vieira et al., 2006). In fact, Gal-3 is known to regulate tight and adherent junctions via, for example, interacting with cadherins (Argüeso et al., 2015; Boscher et al., 2012; Mauris et al., 2014). Although these reports have shown that Gal-3 promotes cell-cell detachment, Gal-3 actions in the same cellular process often diverge according to the context. Gal-3 also increases cell-cell attachment by binding to desmoglein-2 (Hrdlickova-Cela et al., 2001; Jiang et al., 2014). Hence, this finding opened the possibility that Gal-3 regulates polarisation via stabilising apical complexes and recruiting proteins that form junctions, such as components of the Hippo pathway.

The co-transcription factor YAP is the main effector of the Hippo pathway, and plays an important role in development (Varelas, 2014). Analysis of YAP expression and phosphorylation revealed that whilst the levels of total YAP decreased at the first day of neural induction, its phosphorylation at S127 increased. Phosphorylation of YAP at this specific site can lead to differentiation in two ways. P-YAP can either be targeted for subsequent degradation (Zhang et al., 2012; Zhao et al., 2010) or actively participates in gene regulation via binding to p73 (Papaspyropoulos et al., 2018). Degradation of YAP has indeed been described to be necessary for neuronal differentiation (Zhang et al., 2012). However, the observed strong nuclear presence of YAP in the beginning of neural induction and the detection of P-YAP in the Western blot indicates that there is indeed a pool of P-YAP that is not targeted for degradation and instead could be participating in transcription of developmental genes. At a later stage, YAP is re-expressed, implying that the protein has an active role in mature NSCs. Therefore, YAP phosphorylation could have different implications according to the stage of development: at first it participates in gene transcription and neural induction; later, it regulates cell-cell interaction signalling in mature neural rosettes. YAP loss- and gain-of-function experiments would be fundamental to properly address this question.

Immunostaining of YAP evidenced its presence towards the luminal side in mature neural rosettes, forming an apical ring in the apical region and co-localising with junctional markers such as ZO-1 and F-actin. This localisation, which can result in YAP phosphorylation, has been described before (Paramasivam et al., 2011; Zhao et al., 2011). The presence of YAP at epithelial junctions is more complex than only promoting its physical retention and, therefore, inactivation. It is rather a platform for receiving and

transducing mechanical and cell-cell contact signalling (Genevet and Tapon, 2011; Karaman and Halder, 2018; Zhao et al., 2011; Zhao et al., 2007). In fact, during early phases of development, YAP determines cell fate between trophectoderm and inner cell mass. In this case, YAP is nuclear in polarised cells where it, together with TEAD, promotes trophectoderm fate (Hirate et al., 2013; Nishioka et al., 2009).

Gal-3 depletion or recombinant protein treatment did not significantly alter YAP expression in hESCs under neural induction. Interestingly, treatment with Gal-3 antibody disturbed the formation of neural rosettes, affecting YAP delivery to the junctional complex. Collectively, these results suggest that Gal-3 effects on YAP signalling are not via regulation of the protein expression and phosphorylation, However, Gal-3 actions on polarisation are important for the correct delivery of YAP to the junctional complex. At this point, it is not possible to conclude if this effect is directly caused by Gal-3 or indirectly caused by the abrogation of rosettes formation.

Finally, the scaffold protein R1A has been shown to increase its levels during pluripotent stem cell specification, playing a role in its differentiation via YAP (Papaspyropoulos et al., 2018). Here, I observed that R1A increase in the onset of neural induction via Western blot and Immunofluorescence. R1A immunostaining resembles the cytoskeleton, which has been described in other models (Dallol et al., 2004; Liu et al., 2003; Rong et al., 2004; Song et al., 2004; Vos et al., 2004). Interestingly, R1A accumulated in the apical region of neural rosettes, similar to YAP. The spotted pattern observed resembled the basal body of primary cilia, which was further supported via staining with cilia markers. R1A has been described to associate with centrosomes participating in mitosis (Liu et al., 2008; Liu et al., 2003; Rong et al., 2004; Song et al.,

2004; Vos et al., 2004). Moreover, R1A activates Aurora-A (Liu et al., 2008), a protein essential for the primary cilium assembling (Pugacheva et al., 2007). Other components of the core cascade of the Hippo pathways and YAP have been involved with ciliogenesis (Rausch and Hansen, 2020). However, R1A direct association with cilia has never been described before, including in the context of NSC. Interestingly, ciliary proteins interact with the junctional complex, modulating activation of its components (Gerdes et al., 2009). Therefore, it is possible that R1A observed in the basal body of the cilia interacts and phosphorylate YAP at the junction.

The results presented in this Chapter revealed a possible role for Gal-3 in the establishment of apical polarity in neural rosettes. This mechanism might involve the recruitment of R1A and YAP to the junction, although the direct involvement of Gal-3 in this process needs to be addressed. The question now remains whether Gal-3 interacts with apical proteins to regulate assembly of apical junctions and polarisation.

Chapter 6

Discussion

In this thesis, I investigated the role of Gal-3 in neural differentiation. My results can be divided in two parts. Firstly, I investigated the contribution of Gal-3 for pSVZ-derived gliogenesis *in vivo* (Chapter 3). Then, I explored the mechanisms of action of Gal-3 during neural differentiation using an *in vitro* model of hESCs-induced neural commitment (Chapters 4 and 5).

6.1 Gal-3 role in pSVZ gliogenesis

In the first part of my thesis, I showed that the *in vivo* depletion of Gal-3 in postnatal SVZ reduced the number of glial cells in the striatum, demonstrating its role in pSVZ gliogenesis in an inflammation-independent manner.

In order to do that, I used *in vivo* brain electroporation technique to modulate Gal-3 in the pSVZ. This technique has been largely used in the literature, and it has been shown to promote plasmid delivery to progenitors in the SVZ (Boutin et al., 2008; Fernandez et al., 2011). Here, I indeed observed that labelled cells had migrated to the OB to generate interneurons, or to the striatum to generate glia, which is in accordance to cell fates produced the NSCs (Ihrie and Alvarez-Buylla, 2011; Levison et al., 1993; Levison and Goldman, 1993). However, other glial progenitor stages could result in similar phenotype (Levison et al., 1993; Miller and Gauthier, 2007). Therefore, a more controlled depletion of Gal-3 using cell type specific promoters to deliver Cre could offer a more precise indication of the stage in the cell line progression that Gal-3 acts. Additionally, Gal-3 knockdown happened from 3 DPE until 17 DPE. This interval of time is aligned with a later wave of gliogenesis. It would have been interesting to address if Gal-3 impacts gliogenesis at embryonic stages (Miller and Gauthier, 2007).

Collectively with previous data from Gal-OE experiments, I confirmed that Gal-3 modulation affects the number of cells in the striatum. Whilst we confirmed these cells are indeed glia, as expected (Levison et al., 1993; Levison and Goldman, 1993), other possible roles already described for Gal-3 would need to be ruled out. For example, Gal-3 leading to migration (Comte et al., 2011) or adhesion (Kuwabara and Liu, 1996; Matarrese et al., 2000) were not addressed and could have led to the observed phenotype.

Nevertheless, the evidences from OE experiments indeed show that Gal-3 gain-of-function leads to astrocyte progenitor proliferation and maturation (Al-Dalahmah et al., 2020a). This happens in detriment of oligodendrogenesis, which I have shown not to be because of promotion of oligodendrocytes cell death. Instead, the mechanism for Gal-3 astrogenesis was revealed to be via direct interaction with BMPR (Al-Dalahmah et al., 2020a). Unfortunately, loss-of-function experiments presented in this thesis could not help in providing evidence of fate choice shift due to the reduced number of glia cells generated. An *in vitro* model of astrogenesis upon Gal-3 depletion could be implemented in order to confirm the OE findings. This could be achieved after neural induction, when acquired NEPs can be further differentiated in the astrocytic lineage (Li et al., 2018). In that case, modulation of Gal-3 would need to be performed after the neural induction step to account for the role of Gal-3 on polarisation shown in this thesis.

Gal-3 is extensively studied in disease, when it is known to promote inflammation (Hillis et al., 2016; Hoyos et al., 2014; James et al., 2016; Lalancette-Hébert et al., 2012; Liu and Rabinovich, 2005). Although the levels of cytokines in the pSVZ were not

analysed, I have shown that the activation state of microglia was not altered upon Gal-3 OE. This indicates that Gal-3 actions in this context are independent of inflammation.

Therefore, in this chapter, I have helped revealing a novel role of Gal-3 in homeostasis. These findings helped to compose a paper that is published in a peer-review journal (Al-Dalahmah et al., 2020a).

6.2 Gal-3 role in hESCs neural differentiation

Following the *in vivo* finding of a role for Gal-3 in differentiation, I continued in the second part of my thesis to study Gal-3 involvement in neural commitment. Using an *in vitro* model of hESCs neural differentiation, I observed that Gal-3 expression peaks at Day 1 in the media and at Day 2 in the cell during neural induction, preceding the expression of the neural marker Pax6. However, the expression of examined neural markers was not affected by Gal-3 modulation. Interestingly, at Day 2, cells were organising in polarised circular structures from which neural rosettes originate. The formation of neural rosettes is an important step in neural differentiation and mechanisms regulating that process need to be clarified (Hribkova et al., 2018). I demonstrated that blocking Gal-3 at this time point affected this cellular re-organisation. Therefore, the role of Gal-3 in neural differentiation of hESCs is likely to be through regulation of morphological cellular alterations required for neural rosette formation. The fact that the treatment with specific antibody is expected to affect exogenous Gal-3 suggests a role for the protein in the extracellular environment. However, whether Gal-3 actions are extracellular or intracellular in this model remains to be fully elucidated. Previous studies have shown that secreted Gal-3 can activate signalling pathways through forming protein

lattices in the cell membrane (Garner and Baum, 2008; Rabinovich et al., 2007). The evidences presented in this thesis suggest that secreted Gal-3 at Day 1 interact with extracellular domain of transmembrane proteins at Day 2 and 3, which was preserved in the Western blot but not in the immunofluorescence. Still, this interaction was not directly shown and further immunofluorescence optimisation are required for a final conclusion (Vernay and Cosson, 2013).

Nevertheless, Gal-3 has been previously shown to affect epithelialisation and apical-basal compartmentalisation in other models (Honig et al., 2018; Torkko et al., 2008; Vieira et al., 2006). Therefore, I decided to continue pursuing this possibility. Among the already described Gal-3 receptors that could result in cell re-modelling, β1 integrin was selected as candidate because it is expressed in neural rosettes and participates in cell polarisation (Banda et al., 2015; Fietz et al., 2010; Hynes, 2002; Marchetti et al., 2010; Molè et al., 2020; Schmid and Anton, 2003; Topal et al., 2019). My results, however, did not support the hypothesis that these two proteins interact during neural induction. Other possibilities, such as the involvement of Gal-3 in cell adhesion to the ECM, would require future study.

Investigation of Gal-3 cellular localisation by immunostaining evidenced the protein accumulation at the apical region in forming and mature neural rosettes. In fact, Gal-3 has been reported to interact with components of cell-cell junction, promoting cell attachment or detachment depending on the context (Argüeso et al., 2015; Boscher et al., 2012; Jiang et al., 2014; Mauris et al., 2014). It is possible that Gal-3 participates in cell polarisation via interaction with extracellular domain of junctional proteins, as described in other models (Argüeso et al., 2015; Boscher et al., 2012; Jiang et al., 2014).

This binding would promote their stabilisation and the recruitment of intracellular components to the apical region, a possibility that remains to be investigated. The Hippo pathway localised at the junction where it participates in the response to mechanical and cell-cell contact signalling (Genevet and Tapon, 2011; Karaman and Halder, 2018; Zhao et al., 2011; Zhao et al., 2007). During neural induction, I observed that the main effector of the pathway, YAP, and the upstream scaffold protein R1A are localised towards the apical domain in neural rosettes. While YAP co-localises with junctional protein, such as ZO-1 and F-actin, R1A localises at the basal body of primary cilia. Ciliary and junctional proteins are known to interact during epithelisation (Gerdes et al., 2009). Moreover, R1A is known to phosphorylate YAP during development (Papaspyropoulos et al., 2018), however the interaction between these two proteins was not accessed in this thesis.

Gal-3 blocking affected YAP delivery to the junction in neural rosettes. This interesting finding raised the question of whether Gal-3 directly regulate YAP localisation, or if this is a secondary effect of Gal-3 actions in polarisation. If the hypothesis that Gal-3 stabilises components of the apical junction is proven right, it is possible that as a result of this stabilisation, R1A and YAP are recruited to the apical domain. This recruitment could possibly result in their interaction and YAP phosphorylation. Further experiments are required to clarify this mechanism.

Finally, the immunostaining pattern of Gal-3 indicated that the protein is internalised into carrier vesicles, although this possibility requires confirmation. Gal-3 internalisation has been described in other models and regulates protein apical sorting (Delacour et al., 2009). Further analyses would be required to rule out that the possible Gal-3 uptake results in its degradation; or if the observed carrier vesicles indeed play a

role in neural rosettes formation. Being that the case, Gal-3 might play a differential role according to the step of neural induction, being extracellular and promoting polarisation at first, and participating in apical protein sorting later.

These finding revealed the participation of Gal-3 in hESCs-derived neural differentiation, and led to the proposal of the following model for its mechanism of action:

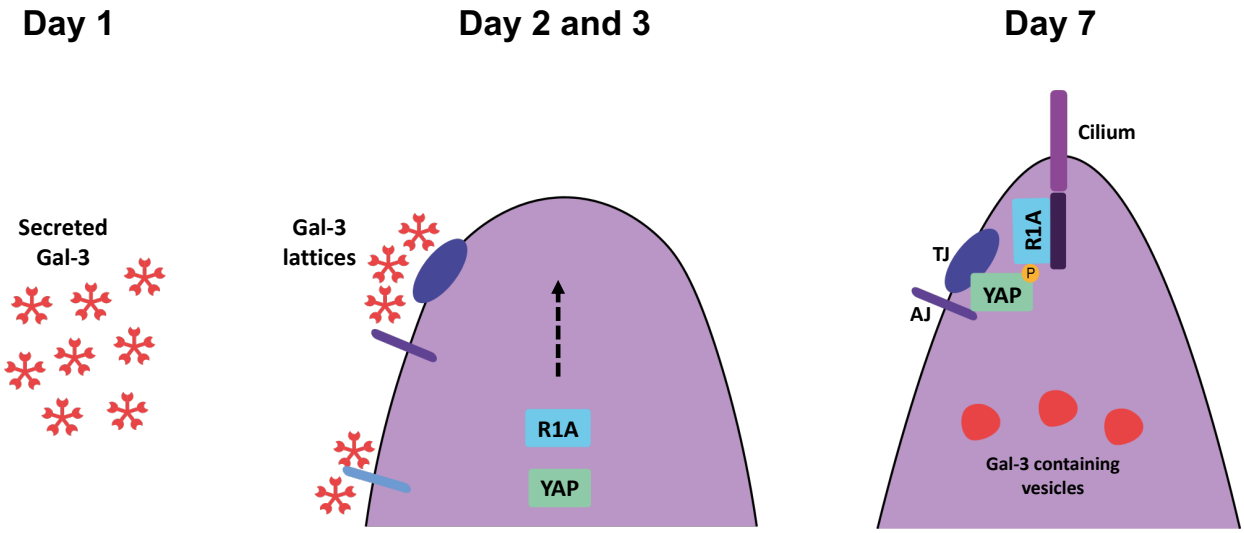


Figure 6.1. Gal-3 in early neural differentiation.

Schematic of the suggested actions of Gal-3 during neural induction. At Day 1, Gal-3 is secreted in the media. Secreted Gal-3 bind to extracellular domain of transmembrane proteins and form lattices at Day 2 and 3, which are not preserved in the immunofluorescence. These interactions result in polarisation and recruitment of apical proteins such as R1A and YAP. A portion of Gal-3 is then incorporated during the following days, possibly through carrier vesicles.

6.3 Conclusion

Gal-3 endogenous functions in the brain are poorly understood, being the lectin usually studied in the context of disease (Hillis et al., 2016; Hoyos et al., 2014; James et al., 2016; Lalancette-Hébert et al., 2012; Liu and Rabinovich, 2005). Yet, Gal-3 is expressed in regions of the brain containing NSCs, raising the question of a role that is unrelated to disease and inflammation. In this thesis, I used two different systems to shown that Gal-3 acts during healthy homeostasis, being important for neural differentiation.

The results presented here lead to the following main conclusions:

1. Gal-3 is required for *in vivo* glial differentiation in the pSVZ;
2. Gal-3 is expressed during early neural commitment;
3. Gal-3 does not regulate expression of neural markers;
4. Gal-3 participates in neural rosette polarisation;
5. YAP delivery to tight junction during neural induction is affected by Gal-3 blocking.

Therefore, Gal-3 not only participates in postnatal gliogenesis, but also in early neural commitment. The latter involves Gal-3-mediated establishment of polarity and neural rosettes formation. The mechanism is yet to be elucidated, but it impacts on YAP delivery to tight junctions. These findings reveal an important new molecule that plays a role in differentiation of neural stem cells, and help clarifying other possible regulatory mechanism that can be explored in stem cell therapy.

6.4 Remaining aspects

Although future work can be done in order to clarify specificities of Gal-3 actions in gliogenesis, the first part of this thesis has been already published (Al-Dalahmah et al., 2020a). The second part, however, contain several open questions that remains to be addressed.

Unfortunately, my work was interrupted by COVID-lockdown during the months of March until July of 2020, compromising the finalisation of important aspects of the hESCs neural differentiation study. Few experiments have to be repeated in order to reach a minimum of 3 biological replicates, and the n number of those experiments is indicated throughout the result chapters of the thesis. Additionally, the mechanism of action of Gal-3 needs to be confirmed. For example, a clarification of Gal-3 extracellular actions and possible receptor, as well as its direct association with R1A and YAP recruitment to the apical junctions, is lacking. A possible role for Gal-3 in protein apical sorting in this model is yet to be investigated.

References

Aaku-Saraste, E., A. Hellwig, and W.B. Huttner. 1996. Loss of Occludin and Functional Tight Junctions, but Not ZO-1, during Neural Tube Closure—Remodeling of the Neuroepithelium Prior to Neurogenesis. *Developmental Biology*. 180:664-679.

Abranches, E., M. Silva, L. Pradier, H. Schulz, O. Hummel, D. Henrique, and E. Bekman. 2009. Neural differentiation of embryonic stem cells in vitro: a road map to neurogenesis in the embryo. *PLoS One*. 4:e6286.

Adeberg, S., L. König, T. Bostel, S. Harrabi, T. Welzel, J. Debus, and S.E. Combs. 2014. Glioblastoma Recurrence Patterns After Radiation Therapy With Regard to the Subventricular Zone. *International Journal of Radiation Oncology*Biology*Physics*. 90:886-893.

Ahmad, N., H.J. Gabius, S. André, H. Kaltner, S. Sabesan, R. Roy, B. Liu, F. Macaluso, and C.F. Brewer. 2004. Galectin-3 precipitates as a pentamer with synthetic multivalent carbohydrates and forms heterogeneous cross-linked complexes. *J Biol Chem*. 279:10841-10847.

Akahani, S., P. Nangia-Makker, H. Inohara, H.R. Kim, and A. Raz. 1997. Galectin-3: a novel antiapoptotic molecule with a functional BH1 (NWGR) domain of Bcl-2 family. *Cancer Res*. 57:5272-5276.

Al-Dalahmah, O., L. Campos Soares, J. Nicholson, S. Draijer, M. Mundim, V.M. Lu, B. Sun, T. Tyler, I. Adorjan, E. O'Neill, and F.G. Szele. 2020a. Galectin-3 modulates postnatal subventricular zone gliogenesis. *Glia*. 68:435-450.

Al-Dalahmah, O., J. Nicholson, S. Draijer, L.C. Soares, and F.G. Szele. 2020b. Galectin-3 diminishes Wnt signaling in the postnatal subventricular zone. *STEM CELLS*. 38:1149-1158.

Alarcón, C., A.-I. Zaromytidou, Q. Xi, S. Gao, J. Yu, S. Fujisawa, A. Barlas, A.N. Miller, K. Manova-Todorova, and M.J. Macias. 2009. Nuclear CDKs drive Smad transcriptional activation and turnover in BMP and TGF-β pathways. *Cell*. 139:757-769.

Altman, J., and G.D. Das. 1965. Autoradiographic and histological evidence of postnatal hippocampal neurogenesis in rats. *J Comp Neurol*. 124:319-335.

Alvarez-Buylla, A., J.M. García-Verdugo, and A.D. Tramontin. 2001. A unified hypothesis on the lineage of neural stem cells. *Nat Rev Neurosci*. 2:287-293.

Alvarez-Buylla, A., F.T. Merkle, L. Fuentealba, and A. Cebrián-Silla. 2020. Chapter 22 - Neurogenesis in the postnatal V-SVZ and the origin of interneuron diversity. *In* Patterning and Cell Type Specification in the Developing CNS and PNS (Second Edition). J. Rubenstein, P. Rakic, B. Chen, and K.Y. Kwan, editors. Academic Press. 505-522.

Amit, M., M.K. Carpenter, M.S. Inokuma, C.P. Chiu, C.P. Harris, M.A. Waknitz, J. Itskovitz-Eldor, and J.A. Thomson. 2000. Clonally derived human embryonic stem cell lines maintain pluripotency and proliferative potential for prolonged periods of culture. *Dev Biol*. 227:271-278.

Apodaca, G., L.I. Gallo, and D.M. Bryant. 2012. Role of membrane traffic in the generation of epithelial cell asymmetry. *Nat Cell Biol*. 14:1235-1243.

Arai, Y., and E. Taverna. 2017. Neural Progenitor Cell Polarity and Cortical Development. *Frontiers in cellular neuroscience*. 11:384-384.

Archer, T.C., J. Jin, and E.S. Casey. 2011. Interaction of Sox1, Sox2, Sox3 and Oct4 during primary neurogenesis. *Dev Biol*. 350:429-440.

Argüeso, P., J. Mauris, and Y. Uchino. 2015. Galectin-3 as a regulator of the epithelial junction: Implications to wound repair and cancer. *Tissue barriers*. 3:e1026505-e1026505.

Arnette, C., N. Efimova, X. Zhu, G.J. Clark, and I. Kaverina. 2014. Microtubule segment stabilization by RASSF1A is required for proper microtubule dynamics and Golgi integrity. *Mol Biol Cell*. 25:800-810.

Arnold, K.M., L.M. Opdenaker, D. Flynn, and J. Sims-Mourtada. 2015. Wound healing and cancer stem cells: inflammation as a driver of treatment resistance in breast cancer. *Cancer growth and metastasis*. 8:1-13.

Avruch, J., M. Praskova, S. Ortiz-Vega, M. Liu, and X.F. Zhang. 2006. Nore1 and RASSF1 Regulation of Cell Proliferation and of the MST1/2 Kinases. *In* Methods in Enzymology. Vol. 407. Academic Press. 290-310.

Baba, K., S. Kuwada, A. Nakao, X. Li, N. Okuda, A. Nishida, S. Mitsuda, N. Fukuoka, H. Kakeya, and T. Kataoka. 2020. Different localization of lysosomal-associated membrane protein 1 (LAMP1) in mammalian cultured cell lines. *Histochemistry and Cell Biology*. 153:199-213.

Banda, E., A. McKinsey, N. Germain, J. Carter, N.C. Anderson, and L. Grabel. 2015. Cell polarity and neurogenesis in embryonic stem cell-derived neural rosettes. *Stem Cells Dev*. 24:1022-1033.

Bänfer, S., and R. Jacob. 2020. Galectins in Intra- and Extracellular Vesicles. *Biomolecules*. 10:1232.

Bänfer, S., D. Schneider, J. Dewes, M.T. Strauss, S.-A. Freibert, T. Heimerl, U.G. Maier, H.-P. Elsässer, R. Jungmann, and R. Jacob. 2018. Molecular mechanism to recruit galectin-3 into multivesicular bodies for polarized exosomal secretion. *Proceedings of the National Academy of Sciences*. 115:E4396-E4405.

Bardella, C., A.R. Al-Shammari, L. Soares, I. Tomlinson, E. O'Neill, and F.G. Szele. 2018. The role of inflammation in subventricular zone cancer. *Prog Neurobiol*. 170:37-52.

Baron, V., and M. Schwartz. 2000. Cell adhesion regulates ubiquitin-mediated degradation of the platelet-derived growth factor receptor β. *Journal of Biological Chemistry*. 275:39318-39323.

Barondes, S.H., V. Castronovo, D.N. Cooper, R.D. Cummings, K. Drickamer, T. Feizi, M.A. Gitt, J. Hirabayashi, C. Hughes, K. Kasai, and et al. 1994a. Galectins: a family of animal beta-galactoside-binding lectins. *Cell*. 76:597-598.

Barondes, S.H., D.N. Cooper, M.A. Gitt, and H. Leffler. 1994b. Galectins. Structure and function of a large family of animal lectins. *J Biol Chem*. 269:20807-20810.

Barresi, M.J.F., and S.F. Gilbert. 2020. Developmental biology. Oxford University Press, New York, United States of America.

Bayer, S.A. 1983. 3H-thymidine-radiographic studies of neurogenesis in the rat olfactory bulb. *Exp Brain Res*. 50:329-340.

Beatty, W.L., E.R. Rhoades, D.K. Hsu, F.-T. Liu, and D.G. Russell. 2002. Association of a macrophage galactoside-binding protein with Mycobacterium-containing phagosomes. *Cellular Microbiology*. 4:167-176.

Bernal, A., and L. Arranz. 2018. Nestin-expressing progenitor cells: function, identity and therapeutic implications. *Cell Mol Life Sci*. 75:2177-2195.

Beyer, Tobias A., A. Weiss, Y. Khomchuk, K. Huang, Abiodun A. Ogunjimi, X. Varelas, and Jeffrey L. Wrana. 2013. Switch Enhancers Interpret TGF-β and Hippo

Signaling to Control Cell Fate in Human Embryonic Stem Cells. *Cell Reports*. 5:1611-1624.

Bhavanandan, V.P., and D.C. Gowda. 2014. Introduction to the Complexity of Cell Surface and Tissue Matrix Glycoconjugates. *In* Glycobiology of the Nervous System. R.K. Yu and C.-L. Schengrund, editors. Springer New York, New York, NY. 1-31.

Boiani, M., and H.R. Scholer. 2005. Regulatory networks in embryo-derived pluripotent stem cells. *Nat Rev Mol Cell Biol*. 6:872-884.

Bojić-Trbojević, Ž., M. Jovanović Krivokuća, A. Vilotić, N. Kolundžić, I. Stefanoska, F. Zetterberg, U.J. Nilsson, H. Leffler, and L. Vićovac. 2019. Human trophoblast requires galectin-3 for cell migration and invasion. *Scientific reports*. 9:2136-2136.

Bonaguidi, M.A., T. McGuire, M. Hu, L. Kan, J. Samanta, and J.A. Kessler. 2005. LIF and BMP signaling generate separate and discrete types of GFAP-expressing cells. *Development*. 132:5503-5514.

Bosch, T.C. 2009. Hydra and the evolution of stem cells. *Bioessays*. 31:478-486.

Boscher, C., Y.Z. Zheng, R. Lakshminarayan, L. Johannes, J.W. Dennis, L.J. Foster, and I.R. Nabi. 2012. Galectin-3 protein regulates mobility of N-cadherin and GM1 ganglioside at cell-cell junctions of mammary carcinoma cells. *J Biol Chem*. 287:32940-32952.

Boutin, C., S. Diestel, A. Desoeuvre, M.C. Tiveron, and H. Cremer. 2008. Efficient in vivo electroporation of the postnatal rodent forebrain. *PLoS One*. 3:e1883.

Bowman, S.K., R.A. Neumüller, M. Novatchkova, Q. Du, and J.A. Knoblich. 2006. The Drosophila NuMA Homolog Mud regulates spindle orientation in asymmetric cell division. *Dev Cell*. 10:731-742.

Boyer, L.A., T.I. Lee, M.F. Cole, S.E. Johnstone, S.S. Levine, J.P. Zucker, M.G. Guenther, R.M. Kumar, H.L. Murray, R.G. Jenner, D.K. Gifford, D.A. Melton, R. Jaenisch, and R.A. Young. 2005. Core transcriptional regulatory circuitry in human embryonic stem cells. *Cell*. 122:947-956.

Bradford, M.M. 1976. A rapid and sensitive method for the quantitation of microgram quantities of protein utilizing the principle of protein-dye binding. *Anal Biochem*. 72:248-254.

Branda, C.S., and S.M. Dymecki. 2004. Talking about a revolution: The impact of site-specific recombinases on genetic analyses in mice. *Dev Cell*. 6:7-28.

Brazel, C.Y., M.J. Romanko, R.P. Rothstein, and S.W. Levison. 2003. Roles of the mammalian subventricular zone in brain development. *Prog Neurobiol*. 69:49-69.

Bresalier, R.S., P.-S. Yan, J.C. Byrd, R. Lotan, and A. Raz. 1997. Expression of the endogenous galactose-binding protein galectin-3 correlates with the malignant potential of tumors in the central nervous system. *Cancer*. 80:776-787.

Burguillos, Miguel A., M. Svensson, T. Schulte, A. Boza-Serrano, A. Garcia-Quintanilla, E. Kavanagh, M. Santiago, N. Viceconte, Maria J. Oliva-Martin, Ahmed M. Osman, E. Salomonsson, L. Amar, A. Persson, K. Blomgren, A. Achour, E. Englund, H. Leffler, Jose L. Venero, B. Joseph, and T. Deierborg. 2015. Microglia-Secreted Galectin-3 Acts as a Toll-like Receptor 4 Ligand and Contributes to Microglial Activation. *Cell Reports*. 10:1626-1638.

Callus, B.A., A.M. Verhagen, and D.L. Vaux. 2006. Association of mammalian sterile twenty kinases, Mst1 and Mst2, with hSalvador via C-terminal coiled-coil domains, leads to its stabilization and phosphorylation. *Febs j*. 273:4264-4276.

Camby, I., N. Belot, S. Rorive, F. Lefranc, C.-A. Maurage, H. Lahm, H. Kaltner, Y. Hadari, M.-M. Ruchoux, J. Brotchi, E. Zick, I. Salmon, H.-J. Gabius, and R. Kiss. 2001. Galectins Are Differentially Expressed in Supratentorial Pilocytic Astrocytomas, Astrocytomas, Anaplastic Astrocytomas and Glioblastomas, and Significantly Modulate Tumor Astrocyte Migration. *Brain Pathology*. 11:12-26.

Campbell, H.K., J.L. Maiers, and K.A. DeMali. 2017. Interplay between tight junctions & adherens junctions. *Experimental cell research*. 358:39-44.

Cao, X., S.L. Pfaff, and F.H. Gage. 2008. YAP regulates neural progenitor cell number via the TEA domain transcription factor. *Genes & development*. 22:3320-3334.

Cappello, S., M.J. Gray, C. Badouel, S. Lange, M. Einsiedler, M. Srour, D. Chitayat, F.F. Hamdan, Z.A. Jenkins, and T. Morgan. 2013. Mutations in genes encoding the cadherin receptor-ligand pair DCHS1 and FAT4 disrupt cerebral cortical development. *Nature genetics*. 45:1300-1308.

Cerra, R., M. Gitt, and S. Barondes. 1985. Three soluble rat beta-galactoside-binding lectins. *Journal of Biological Chemistry*. 260:10474-10477.

Chambers, S.M., C.A. Fasano, E.P. Papapetrou, M. Tomishima, M. Sadelain, and L. Studer. 2009. Highly efficient neural conversion of human ES and iPS cells by dual inhibition of SMAD signaling. *Nat Biotechnol*. 27:275-280.

Chan, E.H., M. Nousiainen, R.B. Chalamalasetty, A. Schäfer, E.A. Nigg, and H.H. Silljé. 2005. The Ste20-like kinase Mst2 activates the human large tumor suppressor kinase Lats1. *Oncogene*. 24:2076-2086.

Chan, S.W., C.J. Lim, Y.F. Chong, A.V. Pobbati, C. Huang, and W. Hong. 2011. Hippo pathway-independent restriction of TAZ and YAP by angiomotin. *Journal of Biological Chemistry*. 286:7018-7026.

Chang, C., and R.M. Harland. 2007. Neural induction requires continued suppression of both Smad1 and Smad2 signals during gastrulation. *Development*. 134:3861-3872.

Chauhan, S., S. Kumar, A. Jain, M. Ponpuak, M.H. Mudd, T. Kimura, S.W. Choi, R. Peters, M. Mandell, and J.-A. Bruun. 2016. TRIMs and galectins globally cooperate and TRIM16 and galectin-3 co-direct autophagy in endomembrane damage homeostasis. *Developmental cell*. 39:13-27.

Chen, H.-L., F. Liao, T.-N. Lin, and F.-T. Liu. 2014a. Galectins and Neuroinflammation. *In* Glycobiology of the Nervous System. R.K. Yu and C.-L. Schengrund, editors. Springer New York, New York, NY. 517-542.

Chen, J., J. Gao, M. Zhang, M. Cai, H. Xu, J. Jiang, Z. Tian, and H. Wang. 2016. Systemic localization of seven major types of carbohydrates on cell membranes by dSTORM imaging. *Scientific Reports*. 6:30247.

Chen, L., K.L. Chaichana, L. Kleinberg, X. Ye, A. Quinones-Hinojosa, and K. Redmond. 2015. Glioblastoma recurrence patterns near neural stem cell regions. *Radiotherapy and Oncology*. 116:294-300.

Chen, X., B. Khambu, H. Zhang, W. Gao, M. Li, X. Chen, T. Yoshimori, and X.M. Yin. 2014b. Autophagy induced by calcium phosphate precipitates targets damaged endosomes. *J Biol Chem*. 289:11162-11174.

Chesler, A.T., C.E. Le Pichon, J.H. Brann, R.C. Araneda, D.J. Zou, and S. Firestein. 2008. Selective gene expression by postnatal electroporation during olfactory interneuron neurogenesis. *PLoS One*. 3:e1517.

Chiu, M.G., T.M. Johnson, A.S. Woolf, E.M. Dahm-Vicker, D.A. Long, L. Guay-Woodford, K.A. Hillman, S. Bawumia, K. Venner, R.C. Hughes, F. Poirier, and P.J.D. Winyard.

2006. Galectin-3 associates with the primary cilium and modulates cyst growth in congenital polycystic kidney disease. *The American journal of pathology*. 169:1925-1938.

Chiu, Y.P., Y.C. Sun, D.C. Qiu, Y.H. Lin, Y.Q. Chen, J.C. Kuo, and J.R. Huang. 2020. Liquid-liquid phase separation and extracellular multivalent interactions in the tale of galectin-3. *Nat Commun*. 11:1229.

Cohen, M.A., P. Itsykson, and B.E. Reubinoff. 2010. The role of FGF-signaling in early neural specification of human embryonic stem cells. *Developmental biology*. 340:450-458.

Colak, D., T. Mori, M.S. Brill, A. Pfeifer, S. Falk, C. Deng, R. Monteiro, C. Mummery, L. Sommer, and M. Gotz. 2008. Adult neurogenesis requires Smad4-mediated bone morphogenic protein signaling in stem cells. *J Neurosci*. 28:434-446.

Collins, P.M., K. Bum-Erdene, X. Yu, and H. Blanchard. 2014. Galectin-3 interactions with glycosphingolipids. *J Mol Biol*. 426:1439-1451.

Colnot, C., D. Fowlis, M.A. Ripoche, I. Bouchaert, and F. Poirier. 1998. Embryonic implantation in galectin 1/galectin 3 double mutant mice. *Dev Dyn*. 211:306-313.

Colnot, C., M.-A. Ripoche, F. Scaerou, D. Fowlis, and F. Poirier. 1996. Galectins in mouse embryogenesis. *Biochemical Society Transactions*. 24:141-146.

Colnot, C., S.S. Sidhu, N. Balmain, and F. Poirier. 2001. Uncoupling of chondrocyte death and vascular invasion in mouse galectin 3 null mutant bones. *Dev Biol*. 229:203-214.

Colotta, F., P. Allavena, A. Sica, C. Garlanda, and A. Mantovani. 2009. Cancer-related inflammation, the seventh hallmark of cancer: links to genetic instability. *Carcinogenesis*. 30:1073-1081.

Comte, I., Y. Kim, C.C. Young, J.M. van der Harg, P. Hockberger, P.J. Bolam, F. Poirier, and F.G. Szele. 2011. Galectin-3 maintains cell motility from the subventricular zone to the olfactory bulb. *J Cell Sci*. 124:2438-2447.

Copp, A.J., and N.D. Greene. 2010. Genetics and development of neural tube defects. *J Pathol*. 220:217-230.

Coppin, L., A. Vincent, F. Frénois, B. Duchêne, F. Lahdaoui, L. Stechly, F. Renaud, C. Villenet, I. Van Seuningen, E. Leteurtre, J. Dion, C. Grandjean, F. Poirier, M. Figeac, D. Delacour, N. Porchet, and P. Pigny. 2017. Galectin-3 is a non-classic

RNA binding protein that stabilizes the mucin MUC4 mRNA in the cytoplasm of cancer cells. *Scientific Reports*. 7:43927.

Cortegano, I., V.d. Pozo, B. Cárdaba, I. Arrieta, S. Gallardo, M. Rojo, E. Aceituno, T. Takai, S. Verbeek, and P. Palomino. 2000. Interaction between galectin-3 and FcγRII induces down-regulation of IL-5 gene: implication of the promoter sequence IL-5REIII. *Glycobiology*. 10:237-242.

Cowles, E.A., N. Agrwal, R.L. Anderson, and J.L. Wang. 1990. Carbohydrate-binding protein 35. Isoelectric points of the polypeptide and a phosphorylated derivative. *Journal of Biological Chemistry*. 265:17706-17712.

Cummings, R.D., F.T. Liu, and G.R. Vasta. 2015. Galectins. *In* Essentials of Glycobiology. rd, A. Varki, R.D. Cummings, J.D. Esko, P. Stanley, G.W. Hart, M. Aebi, A.G. Darvill, T. Kinoshita, N.H. Packer, J.H. Prestegard, R.L. Schnaar, and P.H. Seeberger, editors, Cold Spring Harbor (NY). 469-480.

Cunningham, C.L., V. Martínez-Cerdeño, and S.C. Noctor. 2013. Microglia Regulate the Number of Neural Precursor Cells in the Developing Cerebral Cortex. *The Journal of Neuroscience*. 33:4216-4233.

Dady, A., E. Havis, V. Escriou, M. Catala, and J.L. Duband. 2014. Junctional neurulation: a unique developmental program shaping a discrete region of the spinal cord highly susceptible to neural tube defects. *J Neurosci*. 34:13208-13221.

Dagher, S.F., J.L. Wang, and R.J. Patterson. 1995. Identification of galectin-3 as a factor in pre-mRNA splicing. *Proceedings of the National Academy of Sciences*. 92:1213-1217.

Dallol, A., A. Agathanggelou, S.L. Fenton, J. Ahmed-Choudhury, L. Hesson, M.D. Vos, G.J. Clark, J. Downward, E.R. Maher, and F. Latif. 2004. RASSF1A interacts with microtubule-associated proteins and modulates microtubule dynamics. *Cancer Res*. 64:4112-4116.

Dammann, R., C. Li, J.H. Yoon, P.L. Chin, S. Bates, and G.P. Pfeifer. 2000. Epigenetic inactivation of a RAS association domain family protein from the lung tumour suppressor locus 3p21.3. *Nat Genet*. 25:315-319.

Davis, J.R., and N. Tapon. 2019. Hippo signalling during development. *Development*. 146:dev167106.

De Los Angeles, A., F. Ferrari, R. Xi, Y. Fujiwara, N. Benvenisty, H. Deng, K. Hochedlinger, R. Jaenisch, S. Lee, H.G. Leitch, M.W. Lensch, E. Lujan, D. Pei, J.

Rossant, M. Wernig, P.J. Park, and G.Q. Daley. 2015. Hallmarks of pluripotency. *Nature*. 525:469-478.

De Paepe, C., M. Krivega, G. Cauffman, M. Geens, and H. Van de Velde. 2014. Totipotency and lineage segregation in the human embryo. *Mol Hum Reprod*. 20:599-618.

Deininger, M.H., K. Trautmann, R. Meyermann, and H.J. Schluesener. 2002. Galectin-3 labeling correlates positively in tumor cells and negatively in endothelial cells with malignancy and poor prognosis in oligodendroglioma patients. *Anticancer Res*. 22:1585-1592.

Delacour, D., C.I. Cramm-Behrens, H. Drobecq, A. Le Bivic, H.Y. Naim, and R. Jacob. 2006. Requirement for galectin-3 in apical protein sorting. *Curr Biol*. 16:408-414.

Delacour, D., A. Koch, W. Ackermann, I. Eude-Le Parco, H.P. Elsasser, F. Poirier, and R. Jacob. 2008. Loss of galectin-3 impairs membrane polarisation of mouse enterocytes in vivo. *J Cell Sci*. 121:458-465.

Delacour, D., A. Koch, and R. Jacob. 2009. The Role of Galectins in Protein Trafficking. *Traffic*. 10:1405-1413.

Delaune, E., P. Lemaire, and L. Kodjabachian. 2005. Neural induction in Xenopus requires early FGF signalling in addition to BMP inhibition. *Development*. 132:299.

Demetriou, M., M. Granovsky, S. Quaggin, and J.W. Dennis. 2001. Negative regulation of T-cell activation and autoimmunity by Mgat5 N-glycosylation. *Nature*. 409:733-739.

Donato, R., E.A. Miljan, S.J. Hines, S. Aouabdi, K. Pollock, S. Patel, F.A. Edwards, and J.D. Sinden. 2007. Differential development of neuronal physiological responsiveness in two human neural stem cell lines. *BMC Neuroscience*. 8:36.

Dumic, J., S. Dabelic, and M. Flögel. 2006. Galectin-3: an open-ended story. *Biochim Biophys Acta*. 1760:616-635.

Dvorak, H.F. 1986. Tumors: Wounds That Do Not Heal. *New England Journal of Medicine*. 315:1650-1659.

Ekdahl, C.T., J.H. Claasen, S. Bonde, Z. Kokaia, and O. Lindvall. 2003. Inflammation is detrimental for neurogenesis in adult brain. *Proc Natl Acad Sci U S A*. 100:13632-13637.

Elad-Sfadia, G., R. Haklai, E. Balan, and Y. Kloog. 2004. Galectin-3 augments K-Ras activation and triggers a Ras signal that attenuates ERK but not phosphoinositide 3-kinase activity. *Journal of Biological Chemistry*. 279:34922-34930.

Eom, D.S., S. Amarnath, and S. Agarwala. 2013. Apicobasal polarity and neural tube closure. *Dev Growth Differ*. 55:164-172.

Eom, D.S., S. Amarnath, J.L. Fogel, and S. Agarwala. 2012. Bone morphogenetic proteins regulate hinge point formation during neural tube closure by dynamic modulation of apicobasal polarity. *Birth Defects Res A Clin Mol Teratol*. 94:804-816.

Eriksson, P.S., E. Perfilieva, T. Björk-Eriksson, A.-M. Alborn, C. Nordborg, D.A. Peterson, and F.H. Gage. 1998. Neurogenesis in the adult human hippocampus. *Nature Medicine*. 4:1313-1317.

Evans, M.J., and M.H. Kaufman. 1981. Establishment in culture of pluripotential cells from mouse embryos. *Nature*. 292:154-156.

Fan, S., T.W. Hurd, C.-J. Liu, S.W. Straight, T. Weimbs, E.A. Hurd, S.E. Domino, and B. Margolis. 2004. Polarity Proteins Control Ciliogenesis via Kinesin Motor Interactions. *Current Biology*. 14:1451-1461.

Fedorova, V., T. Vanova, L. Elrefae, J. Pospisil, M. Petrasova, V. Kolajova, Z. Hudacova, J. Baniariova, M. Barak, L. Peskova, T. Barta, M. Kaucka, M. Killinger, J. Vecera, O. Bernatik, L. Cajanek, H. Hribkova, and D. Bohaciakova. 2019. Differentiation of neural rosettes from human pluripotent stem cells in vitro is sequentially regulated on a molecular level and accomplished by the mechanism reminiscent of secondary neurulation. *Stem Cell Res*. 40:101563.

Feil, R. 2007. Conditional somatic mutagenesis in the mouse using site-specific recombinases. *Handb Exp Pharmacol*:3-28.

Fernandez, M.E., S. Croce, C. Boutin, H. Cremer, and O. Raineteau. 2011. Targeted electroporation of defined lateral ventricular walls: a novel and rapid method to study fate specification during postnatal forebrain neurogenesis. *Neural Dev*. 6:13.

Feuk-Lagerstedt, E., E.T. Jordan, H. Leffler, C. Dahlgren, and A. Karlsson. 1999. Identification of CD66a and CD66b as the major galectin-3 receptor candidates in human neutrophils. *The Journal of Immunology*. 163:5592-5598.

Fietz, S.A., I. Kelava, J. Vogt, M. Wilsch-Bräuninger, D. Stenzel, J.L. Fish, D. Corbeil, A. Riehn, W. Distler, R. Nitsch, and W.B. Huttner. 2010. OSVZ progenitors of human

and ferret neocortex are epithelial-like and expand by integrin signaling. *Nature Neuroscience*. 13:690-699.

Fiorelli, R., K. Azim, B. Fischer, and O. Raineteau. 2015. Adding a spatial dimension to postnatal ventricular-subventricular zone neurogenesis. *Development*. 142:2109-2120.

Flowers, S.A., K.A. Thomsson, L. Ali, S. Huang, Y. Mthembu, S.C. Regmi, J. Holgersson, T.A. Schmidt, O. Rolfson, L.I. Björkman, M. Sundqvist, A. Karlsson, G.D. Jay, T. Eisler, R. Krawetz, and N.G. Karlsson. 2019. Core-2 O-glycans are required for Galectin-3 interaction with the osteoarthritis related protein lubricin. *bioRxiv*:2019.2012.2020.884148.

Fortier, L.A. 2005. Stem cells: classifications, controversies, and clinical applications. *Vet Surg*. 34:415-423.

Fortuna-Costa, A., A.M. Gomes, E.O. Kozlowski, M.P. Stelling, and M.S.G. Pavão. 2014. Extracellular Galectin-3 in Tumor Progression and Metastasis. *Frontiers in Oncology*. 4.

Fowlis, D., C. Colnot, M.A. Ripoche, and F. Poirier. 1995. Galectin-3 is expressed in the notochord, developing bones, and skin of the postimplantation mouse embryo. *Dev Dyn*. 203:241-251.

Frigeri, L.G., R.I. Zuberi, and F.T. Liu. 1993. Epsilon BP, a beta-galactoside-binding animal lectin, recognizes IgE receptor (Fc epsilon RI) and activates mast cells. *Biochemistry*. 32:7644-7649.

Fritsch, K., M. Mernberger, A. Nist, T. Stiewe, A. Brehm, and R. Jacob. 2016. Galectin-3 interacts with components of the nuclear ribonucleoprotein complex. *BMC Cancer*. 16:502.

Fukumori, T., Y. Takenaka, N. Oka, T. Yoshii, V. Hogan, H. Inohara, H.-o. Kanayama, H.-R.C. Kim, and A. Raz. 2004. Endogenous galectin-3 determines the routing of CD95 apoptotic signaling pathways. *Cancer research*. 64:3376-3379.

Funayama, N. 2018. The cellular and molecular bases of the sponge stem cell systems underlying reproduction, homeostasis and regeneration. *Int J Dev Biol*. 62:513-525.

Furtak, V., F. Hatcher, and J. Ochieng. 2001. Galectin-3 Mediates the Endocytosis of β-1 Integrins by Breast Carcinoma Cells. *Biochemical and Biophysical Research Communications*. 289:845-850.

Garner, Omai B., and Linda G. Baum. 2008. Galectin–glycan lattices regulate cell-surface glycoprotein organization and signalling. *Biochemical Society Transactions*. 36:1472-1477.

Gee, S.T., S.L. Milgram, K.L. Kramer, F.L. Conlon, and S.A. Moody. 2011. Yes-associated protein 65 (YAP) expands neural progenitors and regulates Pax3 expression in the neural plate border zone. *PLoS One*. 6:e20309.

Genevet, A., and N. Tapon. 2011. The Hippo pathway and apico–basal cell polarity. *Biochemical Journal*. 436:213-224.

Gerdes, J.M., E.E. Davis, and N. Katsanis. 2009. The Vertebrate Primary Cilium in Development, Homeostasis, and Disease. *Cell*. 137:32-45.

Goings, G.E., D.A. Kozlowski, and F.G. Szele. 2006. Differential activation of microglia in neurogenic versus non-neurogenic regions of the forebrain. *Glia*. 54:329-342.

Goletz, S., F.-G. Hanisch, and U. Karsten. 1997. Novel alphaGalNAc containing glycans on cytokeratins are recognized invitro by galectins with type II carbohydrate recognition domains. *Journal of cell science*. 110:1585-1596.

Gomes, W.A., M.F. Mehler, and J.A. Kessler. 2003. Transgenic overexpression of BMP4 increases astroglial and decreases oligodendroglial lineage commitment. *Dev Biol*. 255:164-177.

Gordower, L., C. Decaestecker, Y. Kacem, A. Lemmers, J. Gusman, M. Burchert, A. Danguy, H. Gabius, I. Salmon, R. Kiss, and I. Camby. 1999. Galectin-3 and galectin-3-binding site expression in human adult astrocytic tumours and related angiogenesis. *Neuropathol Appl Neurobiol*. 25:319-330.

Gould, E., P. Tanapat, B.S. McEwen, G. Flugge, and E. Fuchs. 1998. Proliferation of granule cell precursors in the dentate gyrus of adult monkeys is diminished by stress. *Proc Natl Acad Sci U S A*. 95:3168-3171.

Graham, V., J. Khudyakov, P. Ellis, and L. Pevny. 2003. SOX2 functions to maintain neural progenitor identity. *Neuron*. 39:749-765.

Gray, Ryan S., I. Roszko, and L. Solnica-Krezel. 2011. Planar Cell Polarity: Coordinating Morphogenetic Cell Behaviors with Embryonic Polarity. *Developmental Cell*. 21:120-133.

Greene, N.D., and A.J. Copp. 2014. Neural tube defects. *Annu Rev Neurosci*. 37:221-242.

Griffith, C.M., M.J. Wiley, and E.J. Sanders. 1992. The vertebrate tail bud: three germ layers from one tissue. *Anat Embryol (Berl)*. 185:101-113.

Grivennikov, S.I., F.R. Greten, and M. Karin. 2010. Immunity, inflammation, and cancer. *Cell*. 140:883-899.

Gueneau, G., A. Privat, J. Drouet, and L. Court. 1982. Subgranular zone of the dentate gyrus of young rabbits as a secondary matrix. A high-resolution autoradiographic study. *Dev Neurosci*. 5:345-358.

Guhr, A., S. Kobold, S. Seltmann, A.E.M. Seiler Wulczyn, A. Kurtz, and P. Loser. 2018. Recent Trends in Research with Human Pluripotent Stem Cells: Impact of Research and Use of Cell Lines in Experimental Research and Clinical Trials. *Stem Cell Reports*. 11:485-496.

Guo, C., S. Tommasi, L. Liu, J.-K. Yee, R. Dammann, and Gerd P. Pfeifer. 2007. RASSF1A Is Part of a Complex Similar to the Drosophila Hippo/Salvador/Lats Tumor-Suppressor Network. *Current Biology*. 17:700-705.

Gupta, T., V. Nair, and R. Jalali. 2014. Stem cell niche irradiation in glioblastoma: providing a ray of hope? *CNS oncology*. 3:367-376.

Gurusamy, N., A. Alsayari, S. Rajasingh, and J. Rajasingh. 2018. Adult Stem Cells for Regenerative Therapy. *Prog Mol Biol Transl Sci*. 160:1-22.

Habbig, S., M.P. Bartram, R.U. Müller, R. Schwarz, N. Andriopoulos, S. Chen, J.G. Sägmüller, M. Hoehne, V. Burst, M.C. Liebau, H.C. Reinhardt, T. Benzing, and B. Schermer. 2011. NPHP4, a cilia-associated protein, negatively regulates the Hippo pathway. *The Journal of cell biology*. 193:633-642.

Habbig, S., M.P. Bartram, J.G. Sägmüller, A. Griessmann, M. Franke, R.-U. Müller, R. Schwarz, M. Hoehne, C. Bergmann, C. Tessmer, H.C. Reinhardt, V. Burst, T. Benzing, and B. Schermer. 2012. The ciliopathy disease protein NPHP9 promotes nuclear delivery and activation of the oncogenic transcriptional regulator TAZ. *Human Molecular Genetics*. 21:5528-5538.

Haegele, L., B. Ingold, H. Naumann, G. Tabatabai, B. Ledermann, and S. Brandner. 2003. Wnt signalling inhibits neural differentiation of embryonic stem cells by controlling bone morphogenetic protein expression. *Mol Cell Neurosci*. 24:696-708.

Hafsia, N., M. Forien, F. Renaudin, D. Delacour, P. Reboul, P. Van Lent, M. Cohen-Solal, F. Lioté, F. Poirier, and H.K. Ea. 2020. Galectin 3 Deficiency Alters Chondrocyte

Primary Cilium Formation and Exacerbates Cartilage Destruction via Mitochondrial Apoptosis. *International journal of molecular sciences*. 21:1486.

Han, Y.-G., and A. Alvarez-Buylla. 2010. Role of primary cilia in brain development and cancer. *Current Opinion in Neurobiology*. 20:58-67.

Hanahan, D., and Robert A. Weinberg. 2011. Hallmarks of Cancer: The Next Generation. *Cell*. 144:646-674.

Hao, Y., A. Chun, K. Cheung, B. Rashidi, and X. Yang. 2008. Tumor suppressor LATS1 is a negative regulator of oncogene YAP. *Journal of Biological Chemistry*. 283:5496-5509.

Harrington, M.J., E. Hong, and R. Brewster. 2009. Comparative analysis of neurulation: first impressions do not count. *Mol Reprod Dev*. 76:954-965.

Harvey, K.F., C.M. Pfleger, and I.K. Hariharan. 2003. The Drosophila Mst ortholog, hippo, restricts growth and cell proliferation and promotes apoptosis. *Cell*. 114:457-467.

Haudek, K.C., P.G. Voss, J.L. Wang, and R.J. Patterson. 2016. A 10S galectin-3-U1 snRNP complex assembles into active spliceosomes. *Nucleic Acids Res*. 44:6391-6397.

Heallen, T., M. Zhang, J. Wang, M. Bonilla-Claudio, E. Klysik, R.L. Johnson, and J.F. Martin. 2011. Hippo pathway inhibits Wnt signaling to restrain cardiomyocyte proliferation and heart size. *Science*. 332:458-461.

Hedgepeth, C.M., L.J. Conrad, J. Zhang, H.C. Huang, V.M. Lee, and P.S. Klein. 1997. Activation of the Wnt signaling pathway: a molecular mechanism for lithium action. *Dev Biol*. 185:82-91.

Herbst, S., P. Campbell, J. Harvey, E.M. Bernard, V. Papayannopoulos, N.W. Wood, H.R. Morris, and M.G. Gutierrez. 2020. LRRK2 activation controls the repair of damaged endomembranes in macrophages. *The EMBO Journal*. 39:e104494.

Higginbotham, H., J. Guo, Y. Yokota, N.L. Umberger, C.-Y. Su, J. Li, N. Verma, J. Hirt, V. Ghukasyan, and T. Caspary. 2013. Arl13b-regulated cilia activities are essential for polarized radial glial scaffold formation. *Nature neuroscience*. 16:1000-1007.

Hillis, J.M., J. Davies, M.V. Mundim, O. Al-Dalahmah, and F.G. Szele. 2016. Cuprizone demyelination induces a unique inflammatory response in the subventricular zone. *Journal of Neuroinflammation*. 13:190.

Hirabayashi, J., T. Hashidate, Y. Arata, N. Nishi, T. Nakamura, M. Hirashima, T. Urashima, T. Oka, M. Futai, W.E.G. Muller, F. Yagi, and K.-i. Kasai. 2002. Oligosaccharide specificity of galectins: a search by frontal affinity chromatography. *Biochimica et Biophysica Acta (BBA) - General Subjects*. 1572:232-254.

Hirate, Y., S. Hirahara, K.-i. Inoue, A. Suzuki, Vernadeth B. Alarcon, K. Akimoto, T. Hirai, T. Hara, M. Adachi, K. Chida, S. Ohno, Y. Marikawa, K. Nakao, A. Shimono, and H. Sasaki. 2013. Polarity-Dependent Distribution of Angiomotin Localizes Hippo Signaling in Preimplantation Embryos. *Current Biology*. 23:1181-1194.

Ho, M.-K., and T. Springer. 1982. Mac-2, a novel 32,000 Mr mouse macrophage subpopulation-specific antigen defined by monoclonal antibodies. *The Journal of Immunology*. 128:1221-1228.

Hong, M.-H., W.-H. Lin, I.-C. Weng, Y.-H. Hung, H.-L. Chen, H.-Y. Chen, P. Chen, C.-H. Lin, W.Y. Yang, and F.-T. Liu. 2019. Intracellular galectins control cellular responses commensurate with cell surface carbohydrate composition. *Glycobiology*. 30:36-48.

Honig, E., K. Ringer, J. Dewes, T. von Mach, N. Kamm, G. Kreitzer, and R. Jacob. 2018. Galectin-3 modulates the polarized surface delivery of beta1-integrin in epithelial cells. *J Cell Sci*. 131.

Hoyos, H.C., M. Rinaldi, S.P. Mendez-Huergo, M. Marder, G.A. Rabinovich, J.M. Pasquini, and L.A. Pasquini. 2014. Galectin-3 controls the response of microglial cells to limit cuprizone-induced demyelination. *Neurobiology of Disease*. 62:441-455.

Hrdlickova-Cela, E., J. Plzak, K. Smetana, Jr., Z. Melkova, H. Kaltner, M. Filipec, F.T. Liu, and H.J. Gabius. 2001. Detection of galectin-3 in tear fluid at disease states and immunohistochemical and lectin histochemical analysis in human corneal and conjunctival epithelium. *Br J Ophthalmol*. 85:1336-1340.

Hribkova, H., M. Grabiec, D. Klemova, I. Slaninova, and Y.M. Sun. 2018. Calcium signaling mediates five types of cell morphological changes to form neural rosettes. *J Cell Sci*. 131.

Hsu, D.K., R.-Y. Yang, Z. Pan, L. Yu, D.R. Salomon, W.-P. Fung-Leung, and F.-T. Liu. 2000. Targeted Disruption of the Galectin-3 Gene Results in Attenuated Peritoneal Inflammatory Responses. *The American Journal of Pathology*. 156:1073-1083.

Huflejt, M.E., C.W. Turck, R. Lindstedt, S.H. Barondes, and H. Leffler. 1993. L-29, a soluble lactose-binding lectin, is phosphorylated on serine 6 and serine 12 in vivo and by casein kinase I. *J Biol Chem*. 268:26712-26718.

Hughes, R.C. 1999. Secretion of the galectin family of mammalian carbohydrate-binding proteins. *Biochimica et Biophysica Acta (BBA) - General Subjects*. 1473:172-185.

Hussain, S.P., L.J. Hofseth, and C.C. Harris. 2003. Radical causes of cancer. *Nat Rev Cancer*. 3:276-285.

Hynes, R.O. 2002. Integrins: Bidirectional, Allosteric Signaling Machines. *Cell*. 110:673-687.

Ihrie, R.A., and A. Alvarez-Buylla. 2011. Lake-front property: a unique germinal niche by the lateral ventricles of the adult brain. *Neuron*. 70:674-686.

Inohara, H., and A. Raz. 1995. Functional evidence that cell surface galectin-3 mediates homotypic cell adhesion. *Cancer Research*. 55:3267-3271.

Jackson, E.L., J.M. Garcia-Verdugo, S. Gil-Perotin, M. Roy, A. Quinones-Hinojosa, S. VandenBerg, and A. Alvarez-Buylla. 2006. PDGFR alpha-positive B cells are neural stem cells in the adult SVZ that form glioma-like growths in response to increased PDGF signaling. *Neuron*. 51:187-199.

Jacques, T.S., J.B. Relvas, S. Nishimura, R. Pytela, G.M. Edwards, C.H. Streuli, and C. ffrench-Constant. 1998. Neural precursor cell chain migration and division are regulated through different beta1 integrins. *Development*. 125:3167-3177.

Jafri, N.F., J.L. Clarke, V. Weinberg, I.J. Barani, and S. Cha. 2013. Relationship of glioblastoma multiforme to the subventricular zone is associated with survival. *Neuro-oncology*. 15:91-96.

James, D., A.J. Levine, D. Besser, and A. Hemmati-Brivanlou. 2005. TGFbeta/activin/nodal signaling is necessary for the maintenance of pluripotency in human embryonic stem cells. *Development*. 132:1273-1282.

James, R.E., J. Hillis, I. Adorjan, B. Gration, M.V. Mundim, A.J. Iqbal, M.M. Majumdar, R.L. Yates, M.M. Richards, G.E. Goings, G.C. DeLuca, D.R. Greaves, S.D. Miller, and F.G. Szele. 2016. Loss of galectin-3 decreases the number of immune cells in the subventricular zone and restores proliferation in a viral model of multiple sclerosis. *Glia*. 64:105-121.

Jeng, K.C.G., L.G. Frigeri, and F.-T. Liu. 1994. An endogenous lectin, galectin-3 (εBP / Mac-2), potentiates IL-1 production by human monocytes. *Immunology Letters*. 42:113-116.

Jia, J., A. Claude-Taupin, Y. Gu, S.W. Choi, R. Peters, B. Bissa, M.H. Mudd, L. Allers, S. Pallikkuth, K.A. Lidke, M. Salemi, B. Phinney, M. Mari, F. Reggiori, and V. Deretic. 2020. Galectin-3 Coordinates a Cellular System for Lysosomal Repair and Removal. *Developmental Cell*. 52:69-87.e68.

Jia, J., W. Zhang, B. Wang, R. Trinko, and J. Jiang. 2003. The Drosophila Ste20 family kinase dMST functions as a tumor suppressor by restricting cell proliferation and promoting apoptosis. *Genes Dev*. 17:2514-2519.

Jiang, K., C.R. Rankin, P. Nava, R. Sumagin, R. Kamekura, S.R. Stowell, M. Feng, C.A. Parkos, and A. Nusrat. 2014. Galectin-3 regulates desmoglein-2 and intestinal epithelial intercellular adhesion. *J Biol Chem*. 289:10510-10517.

Johannes, L., C. Wunder, and M. Shafaq-Zadah. 2016. Glycolipids and Lectins in Endocytic Uptake Processes. *Journal of Molecular Biology*. 428:4792-4818.

Jope, R.S. 2003. Lithium and GSK-3: one inhibitor, two inhibitory actions, multiple outcomes. *Trends Pharmacol Sci*. 24:441-443.

Joven, A., A. Elewa, and A. Simon. 2019. Model systems for regeneration: salamanders. *Development*. 146.

Kalamakis, G., D. Brüne, S. Ravichandran, J. Bolz, W. Fan, F. Ziebell, T. Stiehl, F. Catalá-Martinez, J. Kupke, S. Zhao, E. Llorens-Bobadilla, K. Bauer, S. Limpert, B. Berger, U. Christen, P. Schmezer, J.P. Mallm, B. Berninger, S. Anders, A. Del Sol, A. Marciniak-Czochra, and A. Martin-Villalba. 2019. Quiescence Modulates Stem Cell Maintenance and Regenerative Capacity in the Aging Brain. *Cell*. 176:1407-1419.e1414.

Kanai, F., P.A. Marignani, D. Sarbassova, R. Yagi, R.A. Hall, M. Donowitz, A. Hisaminato, T. Fujiwara, Y. Ito, L.C. Cantley, and M.B. Yaffe. 2000. TAZ: a novel transcriptional co-activator regulated by interactions with 14-3-3 and PDZ domain proteins. *Embo j.* 19:6778-6791.

Kang, H.G., D.-H. Kim, S.-J. Kim, Y. Cho, J. Jung, W. Jang, and K.-H. Chun. 2016. Galectin-3 supports stemness in ovarian cancer stem cells by activation of the Notch1 intracellular domain. *Oncotarget*. 7:68229-68241.

Karaman, R., and G. Halder. 2018. Cell Junctions in Hippo Signaling. *Cold Spring Harb Perspect Biol*. 10:a028753.

Kaszuba, K., M. Grzybek, A. Orłowski, R. Danne, T. Róg, K. Simons, Ü. Coskun, and I. Vattulainen. 2015. N-Glycosylation as determinant of epidermal growth factor receptor conformation in membranes. *Proceedings of the National Academy of Sciences*. 112:4334-4339.

Kelava, I., and M.A. Lancaster. 2016. Stem Cell Models of Human Brain Development. *Cell Stem Cell*. 18:736-748.

Kettenmann, H., U.-K. Hanisch, M. Noda, and A. Verkhratsky. 2011. Physiology of Microglia. *Physiological Reviews*. 91:461-553.

Kim, M., M. Kim, M.-S. Lee, C.-H. Kim, and D.-S. Lim. 2014. The MST1/2-SAV1 complex of the Hippo pathway promotes ciliogenesis. *Nature Communications*. 5:5370.

Knecht, A.K., and M. Bronner-Fraser. 2002. Induction of the neural crest: a multigene process. *Nat Rev Genet*. 3:453-461.

Knoblich, J.A. 2010. Asymmetric cell division: recent developments and their implications for tumour biology. *Nature Reviews Molecular Cell Biology*. 11:849-860.

Kobayashi, T., T. Shimura, T. Yajima, N. Kubo, K. Araki, S. Tsutsumi, H. Suzuki, H. Kuwano, and A. Raz. 2011. Transient gene silencing of galectin-3 suppresses pancreatic cancer cell migration and invasion through degradation of β-catenin. *International Journal of Cancer*. 129:2775-2786.

Koch, A., F. Poirier, R. Jacob, and D. Delacour. 2010. Galectin-3, a novel centrosome-associated protein, required for epithelial morphogenesis. *Mol Biol Cell*. 21:219-231.

Kraut, R., W. Chia, L.Y. Jan, Y.N. Jan, and J.A. Knoblich. 1996. Role of inscuteable in orienting asymmetric cell divisions in Drosophila. *Nature*. 383:50-55.

Kriegstein, A., and A. Alvarez-Buylla. 2009. The glial nature of embryonic and adult neural stem cells. *Annu Rev Neurosci*. 32:149-184.

Kuhn, H.G., H. Dickinson-Anson, and F.H. Gage. 1996. Neurogenesis in the dentate gyrus of the adult rat: age-related decrease of neuronal progenitor proliferation. *J Neurosci*. 16:2027-2033.

Kuklinski, S., P. Pesheva, C. Heimann, S. Urschel, S. Gloor, S. Graeber, V. Herzog, T. Pietsch, O.D. Wiestler, and R. Probstmeier. 2000. Expression pattern of galectin-3 in neural tumor cell lines. *J Neurosci Res*. 60:45-57.

Kuo, H.Y., H.T. Hsu, Y.C. Chen, Y.W. Chang, F.T. Liu, and C.W. Wu. 2016. Galectin-3 modulates the EGFR signalling-mediated regulation of Sox2 expression via c-Myc in lung cancer. *Glycobiology*. 26:155-165.

Kuwabara, I., and F.-T. Liu. 1996. Galectin-3 promotes adhesion of human neutrophils to laminin. *The Journal of Immunology*. 156:3939-3944.

Lakshminarayan, R., C. Wunder, U. Becken, M.T. Howes, C. Benzing, S. Arumugam, S. Sales, N. Ariotti, V. Chambon, C. Lamaze, D. Loew, A. Shevchenko, K. Gaus, R.G. Parton, and L. Johannes. 2014. Galectin-3 drives glycosphingolipid-dependent biogenesis of clathrin-independent carriers. *Nature Cell Biology*. 16:592-603.

Lalancette-Hebert, M., G. Gowing, A. Simard, Y.C. Weng, and J. Kriz. 2007. Selective ablation of proliferating microglial cells exacerbates ischemic injury in the brain. *J Neurosci*. 27:2596-2605.

Lalancette-Hébert, M., V. Swarup, J.M. Beaulieu, I. Bohacek, E. Abdelhamid, Y.C. Weng, S. Sato, and J. Kriz. 2012. Galectin-3 is required for resident microglia activation and proliferation in response to ischemic injury. *J Neurosci*. 32:10383-10395.

Lau, K.S., E.A. Partridge, A. Grigorian, C.I. Silvescu, V.N. Reinhold, M. Demetriou, and J.W. Dennis. 2007. Complex N-glycan number and degree of branching cooperate to regulate cell proliferation and differentiation. *Cell*. 129:123-134.

Lawson, C., and D.D. Schlaepfer. 2012. Integrin adhesions: who's on first? What's on second? Connections between FAK and talin. *Cell Adh Migr*. 6:302-306.

Lechler, T. 2012. Adherens junctions and stem cells. *Sub-cellular biochemistry*. 60:359-377.

Lee, C.-G., M.J. Oh, S.-Y. Park, H.J. An, and J.H. Kim. 2018. Inhibition of poly-LacNAc biosynthesis with release of CMP-Neu5Ac feedback inhibition increases the sialylation of recombinant EPO produced in CHO cells. *Scientific Reports*. 8:7273.

Lee, J.L., and C.H. Streuli. 2014. Integrins and epithelial cell polarity. *Journal of Cell Science*. 127:3217-3225.

Levenstein, M.E., T.E. Ludwig, R.H. Xu, R.A. Llanas, K. VanDenHeuvel-Kramer, D. Manning, and J.A. Thomson. 2006. Basic fibroblast growth factor support of human embryonic stem cell self-renewal. *Stem Cells*. 24:568-574.

Levison, S.W., C. Chuang, B.J. Abramson, and J.E. Goldman. 1993. The migrational patterns and developmental fates of glial precursors in the rat subventricular zone are temporally regulated. *Development*. 119:611-622.

Levison, S.W., and J.E. Goldman. 1993. Both oligodendrocytes and astrocytes develop from progenitors in the subventricular zone of postnatal rat forebrain. *Neuron*. 10:201-212.

Li, W., W. Sun, Y. Zhang, W. Wei, R. Ambasudhan, P. Xia, M. Talantova, T. Lin, J. Kim, X. Wang, W.R. Kim, S.A. Lipton, K. Zhang, and S. Ding. 2011. Rapid induction and long-term self-renewal of primitive neural precursors from human embryonic stem cells by small molecule inhibitors. *Proc Natl Acad Sci U S A*. 108:8299-8304.

Li, X., R. Krawetz, S. Liu, G. Meng, and D.E. Rancourt. 2009. ROCK inhibitor improves survival of cryopreserved serum/feeder-free single human embryonic stem cells. *Hum Reprod*. 24:580-589.

Li, X., Y. Tao, R. Bradley, Z. Du, Y. Tao, L. Kong, Y. Dong, J. Jones, Y. Yan, C.R.K. Harder, L.M. Friedman, M. Bilal, B. Hoffmann, and S.-C. Zhang. 2018. Fast Generation of Functional Subtype Astrocytes from Human Pluripotent Stem Cells. *Stem Cell Reports*. 11:998-1008.

Lian, I., J. Kim, H. Okazawa, J. Zhao, B. Zhao, J. Yu, A. Chinnaiyan, M.A. Israel, L.S. Goldstein, and R. Abujarour. 2010. The role of YAP transcription coactivator in regulating stem cell self-renewal and differentiation. *Genes & development*. 24:1106-1118.

Lim, D.A., S. Cha, M.C. Mayo, M.-H. Chen, E. Keles, S. VandenBerg, and M.S. Berger. 2007. Relationship of glioblastoma multiforme to neural stem cell regions predicts invasive and multifocal tumor phenotype. *Neuro-oncology*. 9:424-429.

Lim, D.A., A.D. Tramontin, J.M. Trevejo, D.G. Herrera, J.M. Garcia-Verdugo, and A. Alvarez-Buylla. 2000. Noggin antagonizes BMP signaling to create a niche for adult neurogenesis. *Neuron*. 28:713-726.

Lin, F., T. Hiesberger, K. Cordes, A.M. Sinclair, L.S.B. Goldstein, S. Somlo, and P. Igarashi. 2003. Kidney-specific inactivation of the KIF3A subunit of kinesin-II inhibits renal ciliogenesis and produces polycystic kidney disease. *Proceedings of the National Academy of Sciences*. 100:5286-5291.

Lin, H.-M., R.G. Pestell, A. Raz, and H.-R.C. Kim. 2002. Galectin-3 enhances cyclin D 1 promoter activity through SP1 and a cAMP-responsive element in human breast epithelial cells. *Oncogene*. 21:8001-8010.

Lindstedt, R., G. Apodaca, S.H. Barondes, K.E. Mostov, and H. Leffler. 1993. Apical secretion of a cytosolic protein by Madin-Darby canine kidney cells. Evidence for polarized release of an endogenous lectin by a nonclassical secretory pathway. *J Biol Chem*. 268:11750-11757.

Liu, F.-T., and N. Orida. 1984. Synthesis of surface immunoglobulin E receptor in Xenopus oocytes by translation of mRNA from rat basophilic leukemia cells. *Journal of Biological Chemistry*. 259:10649-10652.

Liu, F.-T., R.J. Patterson, and J.L. Wang. 2002. Intracellular functions of galectins. *Biochimica et Biophysica Acta (BBA) - General Subjects*. 1572:263-273.

Liu, F.-T., and G.A. Rabinovich. 2005. Galectins as modulators of tumour progression. *Nature Reviews Cancer*. 5:29-41.

Liu, F.T., D.K. Hsu, R.I. Zuberi, I. Kuwabara, E.Y. Chi, and W.R. Henderson, Jr. 1995. Expression and function of galectin-3, a beta-galactoside-binding lectin, in human monocytes and macrophages. *The American journal of pathology*. 147:1016-1028.

Liu, L., C. Guo, R. Dammann, S. Tommasi, and G.P. Pfeifer. 2008. RASSF1A interacts with and activates the mitotic kinase Aurora-A. *Oncogene*. 27:6175-6186.

Liu, L., T. Sakai, N. Sano, and K. Fukui. 2004. Nucling mediates apoptosis by inhibiting expression of galectin-3 through interference with nuclear factor kappaB signalling. *Biochemical Journal*. 380:31-41.

Liu, L., S. Tommasi, D.-H. Lee, R. Dammann, and G.P. Pfeifer. 2003. Control of microtubule stability by the RASSF1A tumor suppressor. *Oncogene*. 22:8125-8136.

Liu, S., Y. Wang, X. Fan, J. Ma, W. Ma, R. Wang, and T. Jiang. 2016. Anatomical Involvement of the Subventricular Zone Predicts Poor Survival Outcome in Low-Grade Astrocytomas. *PloS one*. 11:e0154539-e0154539.

Liu, S., Y. Wang, X. Fan, J. Ma, X. Qiu, and T. Jiang. 2017. Association of MRI-classified subventricular regions with survival outcomes in patients with anaplastic glioma. *Clin Radiol*. 72:426.e421-426.e426.

Lowery, L.A., and H. Sive. 2004. Strategies of vertebrate neurulation and a re-evaluation of teleost neural tube formation. *Mech Dev*. 121:1189-1197.

Ludwig, T.E., V. Bergendahl, M.E. Levenstein, J. Yu, M.D. Probasco, and J.A. Thomson. 2006a. Feeder-independent culture of human embryonic stem cells. *Nat Methods*. 3:637-646.

Ludwig, T.E., M.E. Levenstein, J.M. Jones, W.T. Berggren, E.R. Mitchen, J.L. Frane, L.J. Crandall, C.A. Daigh, K.R. Conard, M.S. Piekarczyk, R.A. Llanas, and J.A. Thomson. 2006b. Derivation of human embryonic stem cells in defined conditions. *Nat Biotechnol*. 24:185-187.

Lyck, L., T. Kroigard, and B. Finsen. 2007. Unbiased cell quantification reveals a continued increase in the number of neocortical neurones during early post-natal development in mice. *Eur J Neurosci*. 26:1749-1764.

Macara, I.G. 2004. Parsing the Polarity Code. *Nature Reviews Molecular Cell Biology*. 5:220-231.

Maejima, I., A. Takahashi, H. Omori, T. Kimura, Y. Takabatake, T. Saitoh, A. Yamamoto, M. Hamasaki, T. Noda, Y. Isaka, and T. Yoshimori. 2013. Autophagy sequesters damaged lysosomes to control lysosomal biogenesis and kidney injury. *The EMBO Journal*. 32:2336-2347.

Magescas, J., L. Sengmanivong, A. Viau, A. Mayeux, T. Dang, M. Burtin, U.J. Nilsson, H. Leffler, F. Poirier, F. Terzi, and D. Delacour. 2017. Spindle pole cohesion requires glycosylation-mediated localization of NuMA. *Scientific Reports*. 7:1474.

Maier, O., S.A. Marvin, H. Wodrich, E.M. Campbell, and C.M. Wiethoff. 2012. Spatiotemporal Dynamics of Adenovirus Membrane Rupture and Endosomal Escape. *Journal of Virology*. 86:10821-10828.

Malatesta, P., I. Appolloni, and F. Calzolari. 2008. Radial glia and neural stem cells. *Cell Tissue Res*. 331:165-178.

Marchetti, G., S. Escuin, A. van der Flier, A. De Arcangelis, R.O. Hynes, and E. Georges-Labouesse. 2010. Integrin alpha5beta1 is necessary for regulation of radial migration of cortical neurons during mouse brain development. *Eur J Neurosci*. 31:399-409.

Marshall, C.A., S.O. Suzuki, and J.E. Goldman. 2003. Gliogenic and neurogenic progenitors of the subventricular zone: who are they, where did they come from, and where are they going? *Glia*. 43:52-61.

Matallanas, D., D. Romano, K. Yee, K. Meissl, L. Kucerova, D. Piazzolla, M. Baccarini, J.K. Vass, W. Kolch, and E. O'Neill. 2007. RASSF1A elicits apoptosis through an MST2 pathway directing proapoptotic transcription by the p73 tumor suppressor protein. *Molecular cell*. 27:962-975.

Matarrese, P., O. Fusco, N. Tinari, C. Natoli, F.T. Liu, M.L. Semeraro, W. Malorni, and S. Iacobelli. 2000. Galectin-3 overexpression protects from apoptosis by improving cell adhesion properties. *International journal of cancer*. 85:545-554.

Mauris, J., A.M. Woodward, Z. Cao, N. Panjwani, and P. Argueso. 2014. Molecular basis for MMP9 induction and disruption of epithelial cell-cell contacts by galectin-3. *J Cell Sci*. 127:3141-3148.

Mazurek, N., J. Conklin, J.C. Byrd, A. Raz, and R.S. Bresalier. 2000. Phosphorylation of the beta-galactoside-binding protein galectin-3 modulates binding to its ligands. *J Biol Chem*. 275:36311-36315.

McEwen, A.E., D.E. Escobar, and C.J. Gottardi. 2012. Signaling from the Adherens Junction. *In* Adherens Junctions: from Molecular Mechanisms to Tissue Development and Disease. T. Harris, editor. Springer Netherlands, Dordrecht. 171-196.

McIlwain, D.R., T. Berger, and T.W. Mak. 2013. Caspase functions in cell death and disease. *Cold Spring Harb Perspect Biol*. 5:a008656-a008656.

Medelnik, J.P., K. Roensch, S. Okawa, A. Del Sol, O. Chara, L. McHedlishvili, and E.M. Tanaka. 2018. Signaling-Dependent Control of Apical Membrane Size and Self-Renewal in Rosette-Stage Human Neuroepithelial Stem Cells. *Stem Cell Reports*. 10:1751-1765.

Mehul, B., and R.C. Hughes. 1997. Plasma membrane targetting, vesicular budding and release of galectin 3 from the cytoplasm of mammalian cells during secretion. *Journal of Cell Science*. 110:1169-1178.

Menon, R.P., and R.C. Hughes. 1999. Determinants in the N-terminal domains of galectin-3 for secretion by a novel pathway circumventing the endoplasmic reticulum-Golgi complex. *Eur J Biochem*. 264:569-576.

Merkle, F.T., and A. Alvarez-Buylla. 2006. Neural stem cells in mammalian development. *Current Opinion in Cell Biology*. 18:704-709.

Miller, F.D., and A.S. Gauthier. 2007. Timing is everything: making neurons versus glia in the developing cortex. *Neuron*. 54:357-369.

Miller, M.C., H. Ippel, D. Suylen, A.A. Klyosov, P.G. Traber, T. Hackeng, and K.H. Mayo. 2016. Binding of polysaccharides to human galectin-3 at a noncanonical site in its carbohydrate recognition domain. *Glycobiology*. 26:88-99.

Mistry, A.M., A.T. Hale, L.B. Chambless, K.D. Weaver, R.C. Thompson, and R.A. Ihrie. 2017. Influence of glioblastoma contact with the lateral ventricle on survival: a meta-analysis. *J Neurooncol*. 131:125-133.

Mizrak, D., N.S. Bayin, J. Yuan, Z. Liu, R.M. Suciu, M.J. Niphakis, N. Ngo, K.M. Lum, B.F. Cravatt, A.L. Joyner, and P.A. Sims. 2020. Single-Cell Profiling and SCOPE-Seq Reveal Lineage Dynamics of Adult Ventricular-Subventricular Zone Neurogenesis and NOTUM as a Key Regulator. *Cell Reports*. 31:107805.

Mizrak, D., H.M. Levitin, A.C. Delgado, V. Crotet, J. Yuan, Z. Chaker, V. Silva-Vargas, P.A. Sims, and F. Doetsch. 2019. Single-Cell Analysis of Regional Differences in Adult V-SVZ Neural Stem Cell Lineages. *Cell Rep*. 26:394-406.e395.

Molè, M.A., G.L. Galea, A. Rolo, A. Weberling, O. Nychyk, S.C. De Castro, D. Savery, R. Fässler, P. Ybot-González, N.D.E. Greene, and A.J. Copp. 2020. Integrin-Mediated Focal Anchorage Drives Epithelial Zippering during Mouse Neural Tube Closure. *Dev Cell*. 52:321-334.e326.

Monje, M.L., H. Toda, and T.D. Palmer. 2003. Inflammatory blockade restores adult hippocampal neurogenesis. *Science*. 302:1760-1765.

Moon, R.T., B. Bowerman, M. Boutros, and N. Perrimon. 2002. The promise and perils of Wnt signaling through beta-catenin. *Science*. 296:1644-1646.

Munoz-Sanjuan, I., and A.H. Brivanlou. 2002. Neural induction, the default model and embryonic stem cells. *Nat Rev Neurosci*. 3:271-280.

Nakajima, K., D.H. Kho, T. Yanagawa, Y. Harazono, X. Gao, V. Hogan, and A. Raz. 2014. Galectin-3 inhibits osteoblast differentiation through notch signaling. *Neoplasia*. 16:939-949.

Neder, L., S.K. Marie, C.G. Carlotti, Jr., A.A. Gabbai, S. Rosemberg, S.M. Malheiros, R.P. Siqueira, S.M. Oba-Shinjo, M. Uno, P.H. Aguiar, F. Miura, R. Chammas, B.O. Colli, W.A. Silva, Jr., and M.A. Zago. 2004. Galectin-3 as an immunohistochemical tool to distinguish pilocytic astrocytomas from diffuse astrocytomas, and glioblastomas from anaplastic oligodendrogliomas. *Brain Pathol*. 14:399-405.

Nelson, W.J., and R. Nusse. 2004. Convergence of Wnt, beta-catenin, and cadherin pathways. *Science*. 303:1483-1487.

Ngamukote, S., M. Yanagisawa, T. Ariga, S. Ando, and R.K. Yu. 2007. Developmental changes of glycosphingolipids and expression of glycogenes in mouse brains. *Journal of Neurochemistry*. 103:2327-2341.

Nielsen, M.I., J. Stegmayr, O.C. Grant, Z. Yang, U.J. Nilsson, I. Boos, M.C. Carlsson, R.J. Woods, C. Unverzagt, H. Leffler, and H.H. Wandall. 2018. Galectin binding to cells and glycoproteins with genetically modified glycosylation reveals galectin–glycan specificities in a natural context. *Journal of Biological Chemistry*. 293:20249-20262.

Nikolopoulou, E., G.L. Galea, A. Rolo, N.D. Greene, and A.J. Copp. 2017. Neural tube closure: cellular, molecular and biomechanical mechanisms. *Development*. 144:552-566.

Nishioka, N., K.-i. Inoue, K. Adachi, H. Kiyonari, M. Ota, A. Ralston, N. Yabuta, S. Hirahara, R.O. Stephenson, N. Ogonuki, R. Makita, H. Kurihara, E.M. Morin-Kensicki, H. Nojima, J. Rossant, K. Nakao, H. Niwa, and H. Sasaki. 2009. The Hippo Signaling Pathway Components Lats and Yap Pattern Tead4 Activity to Distinguish Mouse Trophectoderm from Inner Cell Mass. *Developmental Cell*. 16:398-410.

Nurnberger, J., R.L. Bacallao, and C.L. Phillips. 2002. Inversin forms a complex with catenins and N-cadherin in polarized epithelial cells. *Mol Biol Cell*. 13:3096-3106.

Ochieng, J., V. Furtak, and P. Lukyanov. 2002. Extracellular functions of galectin-3. *Glycoconj J*. 19:527-535.

Ochieng, J., M.L. Leite-Browning, and P. Warfield. 1998. Regulation of cellular adhesion to extracellular matrix proteins by galectin-3. *Biochemical and biophysical research communications*. 246:788-791.

Oh, H., and K.D. Irvine. 2008. In vivo regulation of Yorkie phosphorylation and localization. *Development*. 135:1081-1088.

Oh, H.J., K.-K. Lee, S.J. Song, M.S. Jin, M.S. Song, J.H. Lee, C.R. Im, J.-O. Lee, S. Yonehara, and D.-S. Lim. 2006. Role of the Tumor Suppressor RASSF1A in Mst1-Mediated Apoptosis. *Cancer Research*. 66:2562-2569.

Oka, N., S. Nakahara, Y. Takenaka, T. Fukumori, V. Hogan, H.-o. Kanayama, T. Yanagawa, and A. Raz. 2005. Galectin-3 inhibits tumor necrosis factor–related apoptosis-inducing ligand–induced apoptosis by activating Akt in human bladder carcinoma cells. *Cancer research*. 65:7546-7553.

Osumi, N., H. Shinohara, K. Numayama-Tsuruta, and M. Maekawa. 2008. Concise review: Pax6 transcription factor contributes to both embryonic and adult neurogenesis as a multifunctional regulator. *Stem Cells*. 26:1663-1672.

Pan, J., and W. Snell. 2007. The Primary Cilium: Keeper of the Key to Cell Division. *Cell*. 129:1255-1257.

Pantalacci, S., N. Tapon, and P. Leopold. 2003. The Salvador partner Hippo promotes apoptosis and cell-cycle exit in Drosophila. *Nat Cell Biol*. 5:921-927.

Papaspyropoulos, A., L. Bradley, A. Thapa, C.Y. Leung, K. Toskas, D. Koennig, D.-E. Pefani, C. Raso, C. Grou, G. Hamilton, N. Vlahov, A. Grawenda, S. Haider, J. Chauhan, L. Buti, A. Kanapin, X. Lu, F. Buffa, G. Dianov, A. von Kriegsheim, D. Matallanas, A. Samsonova, M. Zernicka-Goetz, and E. O'Neill. 2018. RASSF1A uncouples Wnt from Hippo signalling and promotes YAP mediated differentiation via p73. *Nature Communications*. 9:424.

Paramasivam, M., A. Sarkeshik, I. John R. Yates, M.J.G. Fernandes, and D. McCollum. 2011. Angiomotin family proteins are novel activators of the LATS2 kinase tumor suppressor. *Mol Biol Cell*. 22:3725-3733.

Paredes, M.F., D. James, S. Gil-Perotin, H. Kim, J.A. Cotter, C. Ng, K. Sandoval, D.H. Rowitch, D. Xu, P.S. McQuillen, J.M. Garcia-Verdugo, E.J. Huang, and A. Alvarez-Buylla. 2016. Extensive migration of young neurons into the infant human frontal lobe. *Science*. 354.

Park, J.W., P.G. Voss, S. Grabski, J.L. Wang, and R.J. Patterson. 2001. Association of galectin-1 and galectin-3 with Gemin4 in complexes containing the SMN protein. *Nucleic acids research*. 29:3595-3602.

Park, K.S. 2011. Tgf-Beta family signaling in embryonic stem cells. *Int J Stem Cells*. 4:18-23.

Park, S.M., H.J. Jang, and J.H. Lee. 2019. Roles of Primary Cilia in the Developing Brain. *Frontiers in Cellular Neuroscience*. 13.

Parker, R.B., and J.J. Kohler. 2010. Regulation of intracellular signaling by extracellular glycan remodeling. *ACS chemical biology*. 5:35-46.

Parnavelas, J.G. 1999. Glial cell lineages in the rat cerebral cortex. *Exp Neurol*. 156:418-429.

Paron, I., A. Scaloni, A. Pines, A. Bachi, F.-T. Liu, C. Puppin, M. Pandolfi, L. Ledda, C. Di Loreto, and G. Damante. 2003. Nuclear localization of Galectin-3 in transformed thyroid cells: a role in transcriptional regulation. *Biochemical and biophysical research communications*. 302:545-553.

Partridge, E.A., C. Le Roy, G.M. Di Guglielmo, J. Pawling, P. Cheung, M. Granovsky, I.R. Nabi, J.L. Wrana, and J.W. Dennis. 2004. Regulation of Cytokine Receptors by Golgi N-Glycan Processing and Endocytosis. *Science*. 306:120-124.

Pasquini, L.A., V. Millet, H.C. Hoyos, J.P. Giannoni, D.O. Croci, M. Marder, F.T. Liu, G.A. Rabinovich, and J.M. Pasquini. 2011. Galectin-3 drives oligodendrocyte differentiation to control myelin integrity and function. *Cell Death Differ*. 18:1746-1756.

Passaniti, A., J.L. Brusgard, Y. Qiao, M. Sudol, and M. Finch-Edmondson. 2017. Roles of RUNX in Hippo Pathway Signaling. *Adv Exp Med Biol*. 962:435-448.

Pastrana, E., V. Silva-Vargas, and F. Doetsch. 2011. Eyes wide open: a critical review of sphere-formation as an assay for stem cells. *Cell Stem Cell*. 8:486-498.

Patten, I., and M. Placzek. 2002. Opponent activities of Shh and BMP signaling during floor plate induction in vivo. *Curr Biol*. 12:47-52.

Paz, I., M. Sachse, N. Dupont, J. Mounier, C. Cederfur, J. Enninga, H. Leffler, F. Poirier, M.-C. Prevost, F. Lafont, and P. Sansonetti. 2010. Galectin-3, a marker for vacuole lysis by invasive pathogens. *Cellular Microbiology*. 12:530-544.

Pera, M.F., J. Andrade, S. Houssami, B. Reubinoff, A. Trounson, E.G. Stanley, D. Ward-van Oostwaard, and C. Mummery. 2004. Regulation of human embryonic stem cell differentiation by BMP-2 and its antagonist noggin. *J Cell Sci*. 117:1269-1280.

Pfeffer, S.R. 2013. Rab GTPase regulation of membrane identity. *Current Opinion in Cell Biology*. 25:414-419.

Pinkstaff, J.K., J. Detterich, G. Lynch, and C. Gall. 1999. Integrin subunit gene expression is regionally differentiated in adult brain. *J Neurosci*. 19:1541-1556.

Piroli, M.E., J.O. Blanchette, and E. Jabbarzadeh. 2019. Polarity as a physiological modulator of cell function. *Front Biosci (Landmark Ed)*. 24:451-462.

Platel, J.C., K.A. Dave, V. Gordon, B. Lacar, M.E. Rubio, and A. Bordey. 2010. NMDA receptors activated by subventricular zone astrocytic glutamate are critical for neuroblast survival prior to entering a synaptic network. *Neuron*. 65:859-872.

Poirier, F., and E.J. Robertson. 1993. Normal development of mice carrying a null mutation in the gene encoding the L14 S-type lectin. *Development*. 119:1229.

Postiglione, M.P., C. Jüschke, Y. Xie, G.A. Haas, C. Charalambous, and J.A. Knoblich. 2011. Mouse inscuteable induces apical-basal spindle orientation to facilitate intermediate progenitor generation in the developing neocortex. *Neuron*. 72:269-284.

Potten, C.S., and M. Loeffler. 1990. Stem cells: attributes, cycles, spirals, pitfalls and uncertainties. Lessons for and from the crypt. *Development*. 110:1001-1020.

Pownall, M.E., and H.V. Isaacs. 2010. Neural Induction. *In* FGF Signalling in Vertebrate Development. Morgan & Claypool Life Sciences, San Rafael (CA).

Praskova, M., F. Xia, and J. Avruch. 2008. MOBKL1A/MOBKL1B phosphorylation by MST1 and MST2 inhibits cell proliferation. *Curr Biol*. 18:311-321.

Pugacheva, E.N., S.A. Jablonski, T.R. Hartman, E.P. Henske, and E.A. Golemis. 2007. HEF1-dependent Aurora A activation induces disassembly of the primary cilium. *Cell*. 129:1351-1363.

Qian, B.-Z., and J.W. Pollard. 2010. Macrophage Diversity Enhances Tumor Progression and Metastasis. *Cell*. 141:39-51.

Rabinovich, G.A., M.A. Toscano, S.S. Jackson, and G.R. Vasta. 2007. Functions of cell surface galectin-glycoprotein lattices. *Current Opinion in Structural Biology*. 17:513-520.

Rausch, V., and C.G. Hansen. 2020. The Hippo Pathway, YAP/TAZ, and the Plasma Membrane. *Trends in Cell Biology*. 30:32-48.

Raz, A., L. Meromsky, I. Zvibel, and R. Lotan. 1987. Transformation-related changes in the expression of endogenous cell lectins. *International journal of cancer*. 39:353-360.

Raz, A., D.G. Zhu, V. Hogan, N. Shah, T. Raz, R. Karkash, G. Pazerini, and P. Carmi. 1990. Evidence for the role of 34-kDa galactoside-binding lectin in transformation and metastasis. *Int J Cancer*. 46:871-877.

Rezaie, P., and D. Male. 1999. Colonisation of the developing human brain and spinal cord by microglia: a review. *Microscopy Research and Technique*. 45:359-382.

Rhyu, M.S., L.Y. Jan, and Y.N. Jan. 1994. Asymmetric distribution of numb protein during division of the sensory organ precursor cell confers distinct fates to daughter cells. *Cell*. 76:477-491.

Ribeiro Xavier, A.L., B.T. Kress, S.A. Goldman, J.R. Lacerda de Menezes, and M. Nedergaard. 2015. A Distinct Population of Microglia Supports Adult Neurogenesis in the Subventricular Zone. *J Neurosci*. 35:11848-11861.

Riedl, S.J., and Y. Shi. 2004. Molecular mechanisms of caspase regulation during apoptosis. *Nat Rev Mol Cell Biol*. 5:897-907.

Roff, C., and J. Wang. 1983. Endogenous lectins from cultured cells. Isolation and characterization of carbohydrate-binding proteins from 3T3 fibroblasts. *Journal of Biological Chemistry*. 258:10657-10663.

Rong, R., W. Jin, J. Zhang, M. Saeed Sheikh, and Y. Huang. 2004. Tumor suppressor RASSF1A is a microtubule-binding protein that stabilizes microtubules and induces G2/M arrest. *Oncogene*. 23:8216-8230.

Ryves, W.J., and A.J. Harwood. 2001. Lithium inhibits glycogen synthase kinase-3 by competition for magnesium. *Biochem Biophys Res Commun*. 280:720-725.

Sanai, N., A. Alvarez-Buylla, and M.S. Berger. 2005. Neural Stem Cells and the Origin of Gliomas. *New England Journal of Medicine*. 353:811-822.

Sanai, N., T. Nguyen, R.A. Ihrie, Z. Mirzadeh, H.H. Tsai, M. Wong, N. Gupta, M.S. Berger, E. Huang, J.M. Garcia-Verdugo, D.H. Rowitch, and A. Alvarez-Buylla. 2011. Corridors of migrating neurons in the human brain and their decline during infancy. *Nature*. 478:382-386.

Sano, H., D.K. Hsu, L. Yu, J.R. Apgar, I. Kuwabara, T. Yamanaka, M. Hirashima, and F.-T. Liu. 2000. Human galectin-3 is a novel chemoattractant for monocytes and macrophages. *The Journal of Immunology*. 165:2156-2164.

Sato, N., L. Meijer, L. Skaltsounis, P. Greengard, and A.H. Brivanlou. 2004. Maintenance of pluripotency in human and mouse embryonic stem cells through activation of Wnt signaling by a pharmacological GSK-3-specific inhibitor. *Nat Med*. 10:55-63.

Sato, S., I. Burdett, and R.C. Hughes. 1993. Secretion of the Baby Hamster Kidney 30-kDa Galactose-Binding Lectin from Polarized and Nonpolarized Cells: A Pathway Independent of the Endoplasmic Reticulum-Golgi Complex. *Experimental Cell Research*. 207:8-18.

Sato, S., and J. Nieminen. 2002. Seeing strangers or announcing “danger”: Galectin-3 in two models of innate immunity. *Glycoconjugate Journal*. 19:583-591.

Sato, S., N. Ouellet, I. Pelletier, M. Simard, A. Rancourt, and M.G. Bergeron. 2002. Role of galectin-3 as an adhesion molecule for neutrophil extravasation during streptococcal pneumonia. *The Journal of Immunology*. 168:1813-1822.

Sawyer, J.M., J.R. Harrell, G. Shemer, J. Sullivan-Brown, M. Roh-Johnson, and B. Goldstein. 2010. Apical constriction: A cell shape change that can drive morphogenesis. *Developmental Biology*. 341:5-19.

Schlegelmilch, K., M. Mohseni, O. Kirak, J. Pruszak, J.R. Rodriguez, D. Zhou, Bridget T. Kreger, V. Vasioukhin, J. Avruch, Thijn R. Brummelkamp, and Fernando D. Camargo. 2011. Yap1 Acts Downstream of α-Catenin to Control Epidermal Proliferation. *Cell*. 144:782-795.

Schmid, R.S., and E.S. Anton. 2003. Role of Integrins in the Development of the Cerebral Cortex. *Cerebral Cortex*. 13:219-224.

Schneider, D., C. Greb, A. Koch, T. Straube, A. Elli, D. Delacour, and R. Jacob. 2010. Trafficking of galectin-3 through endosomal organelles of polarized and non-polarized cells. *European Journal of Cell Biology*. 89:788-798.

Schwartz, M.A., and R.K. Assoian. 2001. Integrins and cell proliferation. *regulation of cyclin-dependent kinases via cytoplasmic signaling pathways*. 114:2553-2560.

Scott, C.T., J.B. McCormick, and J. Owen-Smith. 2009. And then there were two: use of hESC lines. *Nat Biotechnol*. 27:696-697.

Seetharaman, J., A. Kanigsberg, R. Slaaby, H. Leffler, S.H. Barondes, and J.M. Rini. 1998. X-ray crystal structure of the human galectin-3 carbohydrate recognition domain at 2.1-A resolution. *J Biol Chem*. 273:13047-13052.

Seguin, L., M.F. Camargo, H.I. Wettersten, S. Kato, J.S. Desgrosellier, T. von Schalscha, K.C. Elliott, E. Cosset, J. Lesperance, S.M. Weis, and D.A. Cheresh. 2017. Galectin-3, a Druggable Vulnerability for KRAS-Addicted Cancers. *Cancer Discovery*. 7:1464-1479.

Seguin, L., S. Kato, A. Franovic, M.F. Camargo, J. Lesperance, K.C. Elliott, M. Yebra, A. Mielgo, A.M. Lowy, H. Husain, T. Cascone, L. Diao, J. Wang, Wistuba, II, J.V. Heymach, S.M. Lippman, J.S. Desgrosellier, S. Anand, S.M. Weis, and D.A. Cheresh. 2014. An integrin β_3-KRAS-RalB complex drives tumour stemness and resistance to EGFR inhibition. *Nat Cell Biol*. 16:457-468.

Shalom-Feuerstein, R., T. Cooks, A. Raz, and Y. Kloog. 2005. Galectin-3 regulates a molecular switch from N-Ras to K-Ras usage in human breast carcinoma cells. *Cancer research*. 65:7292-7300.

Sharon, N., and H. Lis. 2004. History of lectins: from hemagglutinins to biological recognition molecules. *Glycobiology*. 14:53R-62R.

Shigemoto-Mogami, Y., K. Hoshikawa, J.E. Goldman, Y. Sekino, and K. Sato. 2014. Microglia enhance neurogenesis and oligodendrogenesis in the early postnatal subventricular zone. *J Neurosci*. 34:2231-2243.

Shimura, T., Y. Takenaka, T. Fukumori, S. Tsutsumi, K. Okada, V. Hogan, A. Kikuchi, H. Kuwano, and A. Raz. 2005. Implication of galectin-3 in Wnt signaling. *Cancer Res*. 65:3535-3537.

Shimura, T., Y. Takenaka, S. Tsutsumi, V. Hogan, A. Kikuchi, and A. Raz. 2004. Galectin-3, a novel binding partner of beta-catenin. *Cancer Res*. 64:6363-6367.

Silvis, M.R., B.T. Kreger, W.-H. Lien, O. Klezovitch, G.M. Rudakova, F.D. Camargo, D.M. Lantz, J.T. Seykora, and V. Vasioukhin. 2011. α-Catenin Is a Tumor Suppressor That Controls Cell Accumulation by Regulating the Localization and Activity of the Transcriptional Coactivator Yap1. *Science Signaling*. 4:ra33-ra33.

Smith, C.A., K.M. Lau, Z. Rahmani, S.E. Dho, G. Brothers, Y.M. She, D.M. Berry, E. Bonneil, P. Thibault, and F. Schweisguth. 2007. aPKC-mediated phosphorylation regulates asymmetric membrane localization of the cell fate determinant Numb. *The EMBO journal*. 26:468-480.

Smith, J.R., L. Vallier, G. Lupo, M. Alexander, W.A. Harris, and R.A. Pedersen. 2008. Inhibition of Activin/Nodal signaling promotes specification of human embryonic stem cells into neuroectoderm. *Developmental Biology*. 313:107-117.

Song, M.S., S.J. Song, N.G. Ayad, J.S. Chang, J.H. Lee, H.K. Hong, H. Lee, N. Choi, J. Kim, H. Kim, J.W. Kim, E.-J. Choi, M.W. Kirschner, and D.-S. Lim. 2004. The tumour suppressor RASSF1A regulates mitosis by inhibiting the APC–Cdc20 complex. *Nature Cell Biology*. 6:129-137.

Song, S., N. Mazurek, C. Liu, Y. Sun, Q.Q. Ding, K. Liu, M.-C. Hung, and R.S. Bresalier. 2009. Galectin-3 Mediates Nuclear β-Catenin Accumulation and Wnt Signaling in Human Colon Cancer Cells by Regulation of Glycogen Synthase Kinase-3β Activity. *Cancer Research*. 69:1343-1349.

Sowers, J.L., K.M. Johnson, C. Conrad, J.T. Patterson, and L.C. Sowers. 2014. The role of inflammation in brain cancer. *Adv Exp Med Biol*. 816:75-105.

Spalding, K.L., O. Bergmann, K. Alkass, S. Bernard, M. Salehpour, H.B. Huttner, E. Boström, I. Westerlund, C. Vial, B.A. Buchholz, G. Possnert, D.C. Mash, H. Druid, and J. Frisén. 2013. Dynamics of hippocampal neurogenesis in adult humans. *Cell*. 153:1219-1227.

Sparrow, C., H. Leffler, and S. Barondes. 1987. Multiple soluble beta-galactoside-binding lectins from human lung. *Journal of Biological Chemistry*. 262:7383-7390.

Steed, T.C., J.M. Treiber, K. Patel, V. Ramakrishnan, A. Merk, A.R. Smith, B.S. Carter, A.M. Dale, L.M. Chow, and C.C. Chen. 2016. Differential localization of glioblastoma subtype: implications on glioblastoma pathogenesis. *Oncotarget*. 7:24899-24907.

Stemple, D.L. 2005. Structure and function of the notochord: an essential organ for chordate development. *Development*. 132:2503-2512.

Straube, T., T. von Mach, E. Hönig, C. Greb, D. Schneider, and R. Jacob. 2013. pH-Dependent Recycling of Galectin-3 at the Apical Membrane of Epithelial Cells. *Traffic*. 14:1014-1027.

Streit, A., A.J. Berliner, C. Papanayotou, A. Sirulnik, and C.D. Stern. 2000. Initiation of neural induction by FGF signalling before gastrulation. *Nature*. 406:74-78.

Strik, H.M., M.H. Deininger, B. Frank, H.J. Schluesener, and R. Meyermann. 2001. Galectin-3: Cellular Distribution and Correlation with WHO-grade in Human Gliomas. *Journal of Neuro-Oncology*. 53:13-20.

Strous, G.J. 1986. Golgi and secreted galactosyltransferase. *CRC Crit Rev Biochem*. 21:119-151.

Stupack, D.G., and D.A. Cheresh. 2002. Get a ligand, get a life: integrins, signaling and cell survival. *Journal of Cell Science*. 115:3729-3738.

Sulik, K., D.B. Dehart, T. Iangaki, J.L. Carson, T. Vrablic, K. Gesteland, and G.C. Schoenwolf. 1994. Morphogenesis of the murine node and notochordal plate. *Dev Dyn*. 201:260-278.

Swarte, V.V., R.E. Mebius, D.H. Joziasse, D.H. Van den Eijnden, and G. Kraal. 1998. Lymphocyte triggering via L-selectin leads to enhanced galectin-3-mediated binding to dendritic cells. *European journal of immunology*. 28:2864-2871.

Taha, Z., H.J. Janse van Rensburg, and X. Yang. 2018. The Hippo Pathway: Immunity and Cancer. *Cancers (Basel)*. 10.

Takahashi, K., K. Tanabe, M. Ohnuki, M. Narita, T. Ichisaka, K. Tomoda, and S. Yamanaka. 2007. Induction of pluripotent stem cells from adult human fibroblasts by defined factors. *Cell*. 131:861-872.

Takahashi, K., and S. Yamanaka. 2006. Induction of pluripotent stem cells from mouse embryonic and adult fibroblast cultures by defined factors. *Cell*. 126:663-676.

Takenaka, Y., T. Fukumori, T. Yoshii, N. Oka, H. Inohara, H.R. Kim, R.S. Bresalier, and A. Raz. 2004. Nuclear export of phosphorylated galectin-3 regulates its antiapoptotic activity in response to chemotherapeutic drugs. *Mol Cell Biol*. 24:4395-4406.

Taulman, P.D., C.J. Haycraft, D.F. Balkovetz, and B.K. Yoder. 2001. Polaris, a Protein Involved in Left-Right Axis Patterning, Localizes to Basal Bodies and Cilia. *Mol Biol Cell*. 12:589-599.

Taylor, M.E., K. Drickamer, R.L. Schnaar, M.E. Etzler, and A. Varki. 2015. Discovery and Classification of Glycan-Binding Proteins. *In* Essentials of Glycobiology. rd, A. Varki, R.D. Cummings, J.D. Esko, P. Stanley, G.W. Hart, M. Aebi, A.G. Darvill, T. Kinoshita, N.H. Packer, J.H. Prestegard, R.L. Schnaar, and P.H. Seeberger, editors, Cold Spring Harbor (NY). 361-372.

Thakurela, S., N. Tiwari, S. Schick, A. Garding, R. Ivanek, B. Berninger, and V.K. Tiwari. 2016. Mapping gene regulatory circuitry of Pax6 during neurogenesis. *Cell Discov*. 2:15045.

Thomas, L., and L.A. Pasquini. 2018. Galectin-3-Mediated Glial Crosstalk Drives Oligodendrocyte Differentiation and (Re)myelination. *Front Cell Neurosci*. 12:297.

Thomson, J.A., J. Itskovitz-Eldor, S.S. Shapiro, M.A. Waknitz, J.J. Swiergiel, V.S. Marshall, and J.M. Jones. 1998. Embryonic stem cell lines derived from human blastocysts. *Science*. 282:1145-1147.

Thomson, J.A., and V.S. Marshall. 1998. Primate embryonic stem cells. *Curr Top Dev Biol*. 38:133-165.

Topal, T., Z. Fan, L.Y. Deng, P.H. Krebsbach, and C.X. Deng. 2019. Integrin-Targeted Cyclic Forces Accelerate Neural Tube-Like Rosette Formation from Human Embryonic Stem Cells. *Advanced Biosystems*. 3:1900064.

Torkko, J.M., A. Manninen, S. Schuck, and K. Simons. 2008. Depletion of apical transport proteins perturbs epithelial cyst formation and ciliogenesis. *Journal of Cell Science*. 121:1193.

Trichas, G., J. Begbie, and S. Srinivas. 2008. Use of the viral 2A peptide for bicistronic expression in transgenic mice. *BMC Biol*. 6:40.

Udan, R.S., M. Kango-Singh, R. Nolo, C. Tao, and G. Halder. 2003. Hippo promotes proliferation arrest and apoptosis in the Salvador/Warts pathway. *Nat Cell Biol*. 5:914-920.

Vallier, L., S. Mendjan, S. Brown, Z. Chng, A. Teo, L.E. Smithers, M.W. Trotter, C.H. Cho, A. Martinez, P. Rugg-Gunn, G. Brons, and R.A. Pedersen. 2009. Activin/Nodal signalling maintains pluripotency by controlling Nanog expression. *Development*. 136:1339-1349.

Van den Brûle, F.A., P.L. Fernandez, C. Buicu, F.T. Liu, P. Jackers, R. Lambotte, and V. Castronovo. 1997. Differential expression of galectin-1 and galectin-3 during first trimester human embryogenesis. *Dev Dyn*. 209:399-405.

van der Weyden, L., A. Papaspyropoulos, G. Poulogiannis, A.G. Rust, M. Rashid, D.J. Adams, M.J. Arends, and E. O'Neill. 2012. Loss of *Rassf1a* Synergizes with Deregulated Runx2 Signaling in Tumorigenesis. *Cancer Research*. 72:3817-3827.

Van Hateren, N.J., R.M. Das, G.M. Hautbergue, A.-G. Borycki, M. Placzek, and S.A. Wilson. 2011. FatJ acts via the Hippo mediator Yap1 to restrict the size of neural progenitor cell pools. *Development*. 138:1893-1902.

Varelas, X. 2014. The Hippo pathway effectors TAZ and YAP in development, homeostasis and disease. *Development*. 141:1614-1626.

Varelas, X., R. Sakuma, P. Samavarchi-Tehrani, R. Peerani, B.M. Rao, J. Dembowy, M.B. Yaffe, P.W. Zandstra, and J.L. Wrana. 2008. TAZ controls Smad nucleocytoplasmic shuttling and regulates human embryonic stem-cell self-renewal. *Nat Cell Biol*. 10:837-848.

Varelas, X., P. Samavarchi-Tehrani, M. Narimatsu, A. Weiss, K. Cockburn, B.G. Larsen, J. Rossant, and J.L. Wrana. 2010. The Crumbs complex couples cell density sensing to Hippo-dependent control of the TGF-β-SMAD pathway. *Developmental cell*. 19:831-844.

Vassilev, A., K.J. Kaneko, H. Shu, Y. Zhao, and M.L. DePamphilis. 2001. TEAD/TEF transcription factors utilize the activation domain of YAP65, a Src/Yes-associated protein localized in the cytoplasm. *Genes & development*. 15:1229-1241.

Vergani, F., J. Martino, C. Gozé, V. Rigau, and H. Duffau. 2011. World Health Organization Grade II gliomas and subventricular zone: anatomic, genetic, and clinical considerations. *Neurosurgery*. 68:1293-1298; discussion 1298-1299.

Vernay, A., and P. Cosson. 2013. Immunofluorescence labeling of cell surface antigens in Dictyostelium. *BMC Res Notes*. 6:317.

Vieira, O.V., K. Gaus, P. Verkade, J. Fullekrug, W.L.C. Vaz, and K. Simons. 2006. FAPP2, cilium formation, and compartmentalization of the apical membrane in polarized Madin–Darby canine kidney (MDCK) cells. *Proceedings of the National Academy of Sciences*. 103:18556.

Viguier, M., T. Advedissian, D. Delacour, F. Poirier, and F. Deshayes. 2014. Galectins in epithelial functions. *Tissue Barriers*. 2:e29103.

Villa-Diaz, L.G., A.M. Ross, J. Lahann, and P.H. Krebsbach. 2013. Concise review: The evolution of human pluripotent stem cell culture: from feeder cells to synthetic coatings. *Stem cells (Dayton, Ohio)*. 31:1-7.

Villa-Verde, D.M.S., E. Silva-Monteiro, M.G. Jasiulionis, D.A. Farias-de-Oliveira, R.R. Brentani, W. Savino, and R. Chammas. 2002. Galectin-3 modulates carbohydrate-dependent thymocyte interactions with the thymic microenvironment. *European journal of immunology*. 32:1434-1444.

Vos, M.D., A. Martinez, C. Elam, A. Dallol, B.J. Taylor, F. Latif, and G.J. Clark. 2004. A Role for the RASSF1A Tumor Suppressor in the Regulation of Tubulin Polymerization and Genomic Stability. *Cancer Research*. 64:4244-4250.

Wang, H., X. Song, Q. Huang, T. Xu, D. Yun, Y. Wang, L. Hu, Y. Yan, H. Chen, D. Lu, and J. Chen. 2019. LGALS3 Promotes Treatment Resistance in Glioblastoma and Is Associated with Tumor Risk and Prognosis. *Cancer Epidemiology Biomarkers & Prevention*. 28:760.

Wang, J.L., R.M. Gray, K.C. Haudek, and R.J. Patterson. 2004. Nucleocytoplasmic lectins. *Biochimica et Biophysica Acta (BBA) - General Subjects*. 1673:75-93.

Wang, L., H. Inohara, K.J. Pienta, and A. Raz. 1995. Galectin-3 Is a Nuclear Matrix Protein Which Binds RNA. *Biochemical and Biophysical Research Communications*. 217:292-303.

Wang, R.N., J. Green, Z. Wang, Y. Deng, M. Qiao, M. Peabody, Q. Zhang, J. Ye, Z. Yan, S. Denduluri, O. Idowu, M. Li, C. Shen, A. Hu, R.C. Haydon, R. Kang, J. Mok, M.J. Lee, H.L. Luu, and L.L. Shi. 2014a. Bone Morphogenetic Protein (BMP) signaling in development and human diseases. *Genes & Diseases*. 1:87-105.

Wang, W., J. Huang, and J. Chen. 2011. Angiomotin-like proteins associate with and negatively regulate YAP1. *Journal of Biological Chemistry*. 286:4364-4370.

Wang, Y., J. Gao, X. Guo, T. Tong, X. Shi, L. Li, M. Qi, Y. Wang, M. Cai, J. Jiang, C. Xu, H. Ji, and H. Wang. 2014b. Regulation of EGFR nanocluster formation by ionic protein-lipid interaction. *Cell Research*. 24:959-976.

Watanabe, K., M. Ueno, D. Kamiya, A. Nishiyama, M. Matsumura, T. Wataya, J.B. Takahashi, S. Nishikawa, S. Nishikawa, K. Muguruma, and Y. Sasai. 2007. A ROCK inhibitor permits survival of dissociated human embryonic stem cells. *Nat Biotechnol*. 25:681-686.

Watters, A.K., S. Rom, J.D. Hill, M.K. Dematatis, Y. Zhou, S.F. Merkel, A.M. Andrews, J. Cena, R. Potula, A. Skuba, Y.-J. Son, Y. Persidsky, and S.H. Ramirez. 2015. Identification and dynamic regulation of tight junction protein expression in human neural stem cells. *Stem cells and development*. 24:1377-1389.

Weissman, I.L. 2000. Stem cells: units of development, units of regeneration, and units in evolution. *Cell*. 100:157-168.

Wilson, S., A. Rydström, T. Trimborn, K. Willert, R. Nusse, T.M. Jessell, and T. Edlund. 2001. The status of Wnt signalling regulates neural and epidermal fates in the chick embryo. *Nature*. 411:325-330.

Wilson, S.I., and T. Edlund. 2001. Neural induction: toward a unifying mechanism. *Nat Neurosci*. 4 Suppl:1161-1168.

Wilson, S.I., E. Graziano, R. Harland, T.M. Jessell, and T. Edlund. 2000. An early requirement for FGF signalling in the acquisition of neural cell fate in the chick embryo. *Curr Biol*. 10:421-429.

Woo, H.J., L.M. Shaw, J.M. Messier, and A.M. Mercurio. 1990. The major non-integrin laminin binding protein of macrophages is identical to carbohydrate binding protein 35 (Mac-2). *Journal of Biological Chemistry*. 265:7097-7099.

Wu, S., J. Huang, J. Dong, and D. Pan. 2003. hippo encodes a Ste-20 family protein kinase that restricts cell proliferation and promotes apoptosis in conjunction with salvador and warts. *Cell*. 114:445-456.

Xu, C., E. Rosler, J. Jiang, J.S. Lebkowski, J.D. Gold, C. O'Sullivan, K. Delavan-Boorsma, M. Mok, A. Bronstein, and M.K. Carpenter. 2005a. Basic fibroblast growth factor supports undifferentiated human embryonic stem cell growth without conditioned medium. *Stem Cells*. 23:315-323.

Xu, R.-H., T.L. Sampsell-Barron, F. Gu, S. Root, R.M. Peck, G. Pan, J. Yu, J. Antosiewicz-Bourget, S. Tian, R. Stewart, and J.A. Thomson. 2008. NANOG Is a Direct Target of TGFβ/Activin-Mediated SMAD Signaling in Human ESCs. *Cell Stem Cell*. 3:196-206.

Xu, R.H., X. Chen, D.S. Li, R. Li, G.C. Addicks, C. Glennon, T.P. Zwaka, and J.A. Thomson. 2002. BMP4 initiates human embryonic stem cell differentiation to trophoblast. *Nat Biotechnol*. 20:1261-1264.

Xu, R.H., R.M. Peck, D.S. Li, X. Feng, T. Ludwig, and J.A. Thomson. 2005b. Basic FGF and suppression of BMP signaling sustain undifferentiated proliferation of human ES cells. *Nat Methods*. 2:185-190.

Yamamoto, H., C. Awada, H. Hanaki, H. Sakane, I. Tsujimoto, Y. Takahashi, T. Takao, and A. Kikuchi. 2013. The apical and basolateral secretion of Wnt11 and Wnt3a in polarized epithelial cells is regulated by different mechanisms. *Journal of Cell Science*. 126:2931-2943.

Yamaoka, A., I. Kuwabara, L.G. Frigeri, and F.T. Liu. 1995. A human lectin, galectin-3 (epsilon bp/Mac-2), stimulates superoxide production by neutrophils. *The Journal of Immunology*. 154:3479.

Yanagisawa, M., and R.K. Yu. 2007. The expression and functions of glycoconjugates in neural stem cells. *Glycobiology*. 17:57R-74R.

Yang, R.-Y., D.K. Hsu, and F.-T. Liu. 1996. Expression of galectin-3 modulates T-cell growth and apoptosis. *Proceedings of the National Academy of Sciences*. 93:6737-6742.

Ybot-Gonzalez, P., C. Gaston-Massuet, G. Girdler, J. Klingensmith, R. Arkell, N.D.E. Greene, and A.J. Copp. 2007. Neural plate morphogenesis during mouse neurulation is regulated by antagonism of Bmp signalling. *Development*. 134:3203.

Ying, Q.L., M. Stavridis, D. Griffiths, M. Li, and A. Smith. 2003. Conversion of embryonic stem cells into neuroectodermal precursors in adherent monoculture. *Nat Biotechnol*. 21:183-186.

Yoshida, N., S. Hishiyama, M. Yamaguchi, M. Hashiguchi, Y. Miyamoto, S. Kaminogawa, and T. Hisatsune. 2003. Decrease in expression of α5β1 integrin during neuronal differentiation of cortical progenitor cells. *Experimental Cell Research*. 287:262-271.

Young, G.S., E.A. Macklin, K. Setayesh, J.D. Lawson, P.Y. Wen, A.D. Norden, J. Drappatz, and S. Kesari. 2011. Longitudinal MRI evidence for decreased survival among periventricular glioblastoma. *J Neurooncol*. 104:261-269.

Yu, F., R.L. Finley, A. Raz, and H.-R.C. Kim. 2002. Galectin-3 translocates to the perinuclear membranes and inhibits cytochrome c release from the mitochondria A role for synexin in galectin-3 translocation. *Journal of Biological Chemistry*. 277:15819-15827.

Yu, J., M.A. Vodyanik, K. Smuga-Otto, J. Antosiewicz-Bourget, J.L. Frane, S. Tian, J. Nie, G.A. Jonsdottir, V. Ruotti, R. Stewart, Slukvin, II, and J.A. Thomson. 2007. Induced pluripotent stem cell lines derived from human somatic cells. *Science*. 318:1917-1920.

Yu, R.K., and Y. Itokazu. 2014. Glycolipid and Glycoprotein Expression During Neural Development. *In* Glycobiology of the Nervous System. R.K. Yu and C.-L. Schengrund, editors. Springer New York, New York, NY. 185-222.

Zaltsman, Y., S. Masuko, J.J. Bensen, and L.L. Kiessling. 2019. Angiomotin Regulates YAP Localization during Neural Differentiation of Human Pluripotent Stem Cells. *Stem Cell Reports*. 12:869-877.

Zhang, D., Z.G. Chen, S.H. Liu, Z.Q. Dong, M. Dalin, S.S. Bao, Y.W. Hu, and F.C. Wei. 2013. Galectin-3 gene silencing inhibits migration and invasion of human tongue cancer cells in vitro via downregulating beta-catenin. *Acta Pharmacol Sin*. 34:176-184.

Zhang, H., M. Deo, R.C. Thompson, M.D. Uhler, and D.L. Turner. 2012. Negative regulation of Yap during neuronal differentiation. *Developmental Biology*. 361:103-115.

Zhang, S., and W. Cui. 2014. Sox2, a key factor in the regulation of pluripotency and neural differentiation. *World J Stem Cells*. 6:305-311.

Zhang, X., C.T. Huang, J. Chen, M.T. Pankratz, J. Xi, J. Li, Y. Yang, T.M. Lavaute, X.J. Li, M. Ayala, G.I. Bondarenko, Z.W. Du, Y. Jin, T.G. Golos, and S.C. Zhang. 2010. Pax6 is a human neuroectoderm cell fate determinant. *Cell Stem Cell*. 7:90-100.

Zhao, B., L. Li, Q. Lu, L.H. Wang, C.-Y. Liu, Q. Lei, and K.-L. Guan. 2011. Angiomotin is a novel Hippo pathway component that inhibits YAP oncoprotein. *Genes & development*. 25:51-63.

Zhao, B., L. Li, K. Tumaneng, C.Y. Wang, and K.L. Guan. 2010. A coordinated phosphorylation by Lats and CK1 regulates YAP stability through SCF(beta-TRCP). *Genes Dev*. 24:72-85.

Zhao, B., X. Wei, W. Li, R.S. Udan, Q. Yang, J. Kim, J. Xie, T. Ikenoue, J. Yu, and L. Li. 2007. Inactivation of YAP oncoprotein by the Hippo pathway is involved in cell contact inhibition and tissue growth control. *Genes & development*. 21:2747-2761.

Zihni, C., C. Mills, K. Matter, and M.S. Balda. 2016. Tight junctions: from simple barriers to multifunctional molecular gates. *Nature Reviews Molecular Cell Biology*. 17:564-580.

Zohn, I.E., C.R. Chesnutt, and L. Niswander. 2003. Cell polarity pathways converge and extend to regulate neural tube closure. *Trends Cell Biol*. 13:451-454.

Zywitza, V., A. Misios, L. Bunatyan, T.E. Willnow, and N. Rajewsky. 2018. Single-Cell Transcriptomics Characterizes Cell Types in the Subventricular Zone and Uncovers Molecular Defects Impairing Adult Neurogenesis. *Cell Rep*. 25:2457-2469.e2458.

Appendices

Appendix A. Neural differentiation using EB protocol

H9 cells were induced to commit to the astrocytic fate by using the embryoid body (EB) protocol (Figure 7.1 A). Firstly, H9 pluripotent cells are induced to become neural progenitors through the duals SMAD inhibition protocol in a 3D environment. In order to do that, H9 aggregates were firstly passaged with Versene™ as previously described, counted and centrifuged for 5 min at 300 rcf. Pellet was resuspended in STEMdiff™ Neural Induction Medium supplemented with SMADi (NIM) and 10 μM of Y-27632 and cells were seeded into AggreWell™800 Plate (StemCell Technologies) at a dilution of 7500 cells/microwell. AggreWell™800 Plate were previously treated with Anti-Adherence Rinsing Solution (StemCell Technologies) which was added to the wells, centrifuged at 1300 rcf and aspirated within 5 min. These plates allow homogeneous EB formation by preventing adhesion and promoting equal distribution of cells among the wells. Partial media change (3/4) was performed every day for 4 days. At day 5, EBs were collected and filtered through a 37 μm Reversible Strainer (StemCell Technologies) into a 6-well Matrigel™-coated plate containing NIM supplemented with SMADi and allowed to adhere and grow for 6 days. At the end of this period, fully formed neural rosettes were selected using STEMdiff™Neural Rosette Selection Reagent (StemCell Technologies) and transferred to a new Matrigel™-coated plate in the same media. Neural rosettes were allowed to attached for 24 h and then induced to become astrocytic using STEMdiff™ Astrocyte Differentiation Medium (StemCell Technologies), which was changed every day. Cell were cultured in those conditions for 16 days maximum.

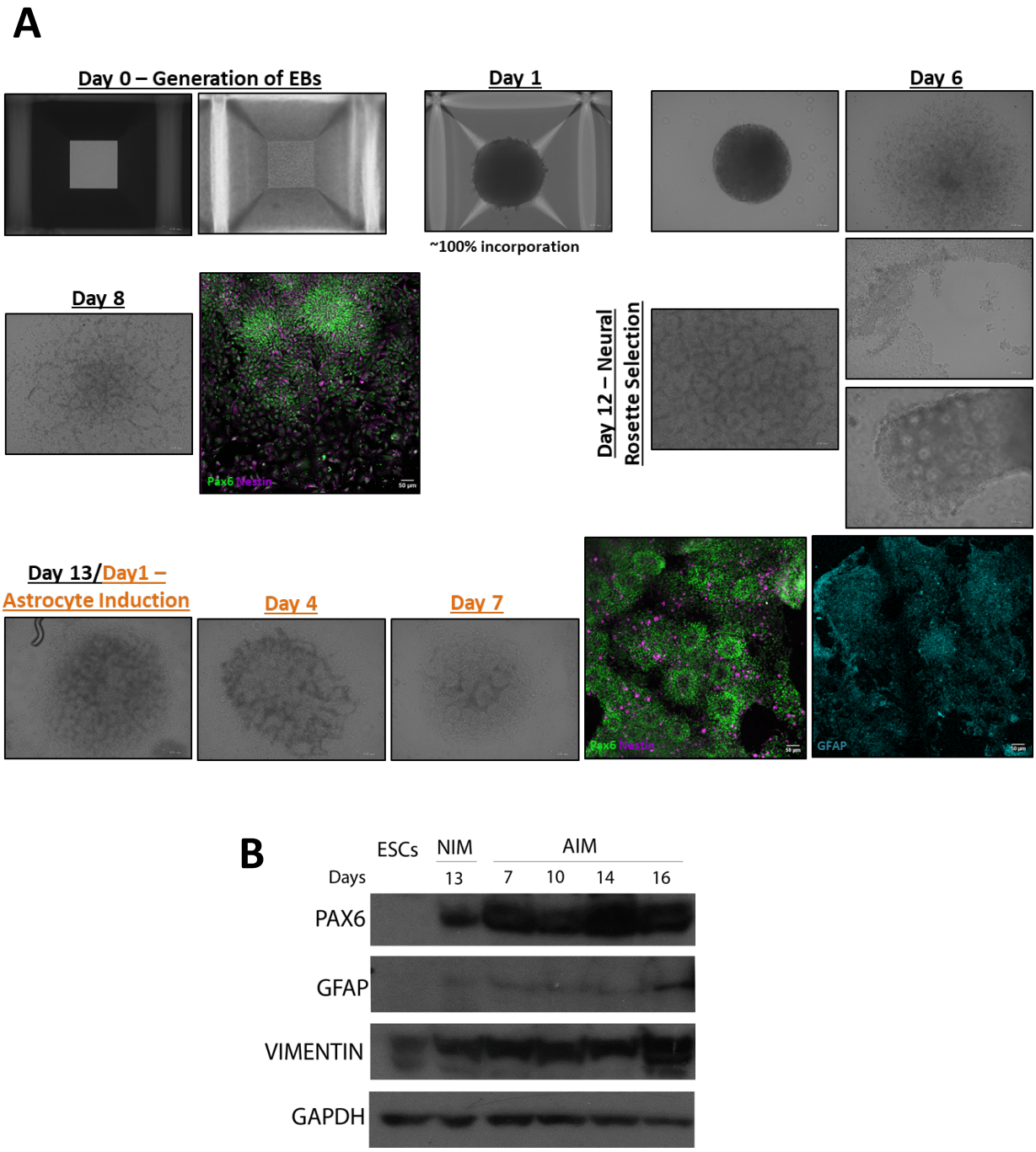


Figure 7.1. Generation of astrocytes using the EB protocol.

A) Brightfield and IF images exemplifying the protocol for generation of astrocytes from EBs. Scale bar: 50 μm. B) Western blotting for markers of NSCs and astrocytes. ESCs: embryonic stem cells; NIM: neural induction media; AIM: astrocyte induction media.
Figure 7.1 B is authored by Viviana Macarelli.

I confirmed the expression of neural markers Pax6 and Nestin after 8 days of neural induction, when cells had adhered to the plate and formed neural rosettes. I also observed that 7 days of astrocyte induction was not enough for detection of GFAP [#130300, Life technologies, Dilutions: 1:1000 (WB), 1:100 (IF)] (Figure 7.1 A). Western blotting analysis showed the expression of Pax6 and the RG marker Vimentin [#5741, Cell Signalling, Dilutions: 1:1000 (WB)] after neural induction. Differently, GFAP only starts to be expressed upon astrocyte induction at Day 16 (Figure 7.1 B).

I have also assessed the expression of R1A during astrocyte induction via immunostaining (n=2). It was possible to see R1A expression in a patter thar resembles the cytoskeleton, similar to what was shown in Chapter 5.

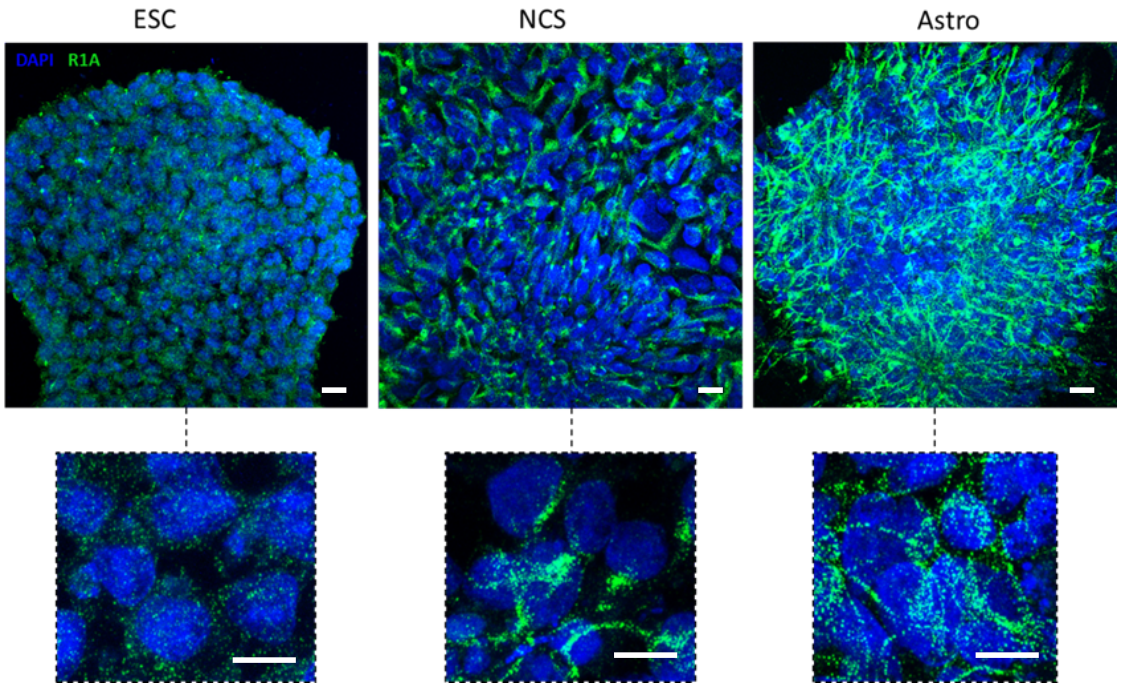


Figure 7.2. R1A during EB neural induction

Confocal images illustrating the expression and localisation of R1A during astrocyte induction using the EBS protocol. Scale bar: 20 μm. ESC: embryonic stem cells; NCS: neural stem cells; Astro: astrocytes.

Appendix B. Gal-3 and YAP at the junctional complex

Immunostaining analysis of Gal-3 and YAP in hESCs-derived NSC showed that both proteins are localised towards the lumen of neural rosettes (Chapter 5). Considering the involvement of both proteins in epithelial polarisation (Argüeso et al., 2015; Genevet and Tapon, 2011; Karaman and Halder, 2018), I analysed the interaction between Gal-3, YAP and components of the junctional complex, including β-catenin [β-catenin rabbit - #9562, Cell Signalling, Dilutions: 1:1000 (WB), 1:100 (IP); β-catenin mouse - #sc-376959, Santa Cruz, Dilutions: 1:1000 (WB)], via co-immunoprecipitation at different time points of neural induction. Gal-3 is known for its interaction with the adherent junction component β-catenin, although this interaction has never been shown in at the cell junction (Al-Dalahmah et al., 2020b; Shimura et al., 2005; Song et al., 2009). Here, Gal-3 did not precipitate with YAP and β-catenin, neither with the tight junction protein ZO-1 (n=1) (Figure 7.3 A). The reverse co-Immunoprecipitation of β-catenin indeed pulled down the adherent junction N-cadherin [#14215, Cell Signalling, Dilutions: 1:1000 (WB)], as expected (Nelson and Nusse, 2004). However, the interaction with Gal-3 was not observed (n=1) (Figure 7.3 B). Therefore, these results demonstrate that Gal-3 is not part of the junctional complex during neural differentiation.

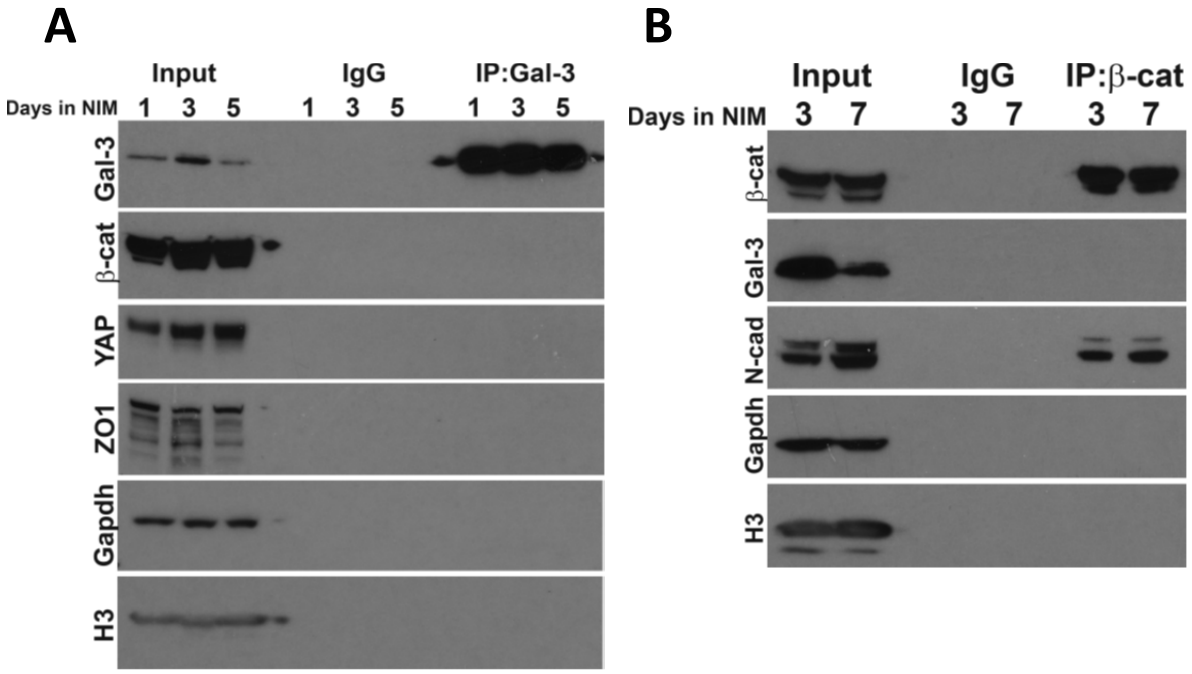


Figure 7.3. Gal-3 is not at the junctional complex.

Western blot to test the interaction between Gal-3 and components of the junctional complex after Gal-3 (A) and β-catenin (B) immunoprecipitation; n=1. Different neural induction time points are shown. Antibody against the IgG of the same species was used as a negative control. NIM: neural induction media.

Appendix C. ReNCell® as an *in vitro* model of neural differentiation

ReNCell® CX were used to study the interaction between Gal-3 and the components of the Hippo pathway YAP and R1A. For that, ReNCell® CX were cultured as described in Chapter 2. They were also allowed to spontaneously differentiate upon withdraw of growth factors (EGF and FGF). In brief, cells were passaged as previously described, counted and pelleted down for 5 min at 300 rcf. The pellet was resuspended in ReNcell® NSC Medium (Merck Millipore) without growth factors and cells were seeded in laminin-coated plates. Media was changed every other day, and cells were allowed to growth and differentiate for a maximum of 7 days. Gal-3 was modulated in ReNCell® CX during differentiation. For that, cells were either treated with 1 μg/ml of carrier-free human recombinant Gal-3 (R&D systems, #1154-GA-050/CF) every 2 days, or transfected with Gal-3 OE plasmid or shorth-hairpin RNA against Gal-3 (shNT, shGal-3 V1), as previous described (Chapter 2).

Firstly, I observed that YAP and R1A increase in ReNCell® CX upon differentiation (Figure 7.4 A). The localisation of R1A at Day 0, when they are progenitors and express Nestin (Donato et al., 2007), was polarised (Figure 7.4 A'). Similar to what observed in hESCs cells (Chapter 5), this pattern resembled the Golgi complex where R1A indeed has been described to localise (Arnette et al., 2014).

Modulation of Gal-3 affected levels of YAP and R1A. While knockdown of Gal-3 decreased levels of YAP and R1A (Figure 7.4 B), the upregulation with either transfection of Gal-3 OE plasmid or treatment with recombinant Gal-3 had the opposite effect and increased their levels (Figure 7.4 B').

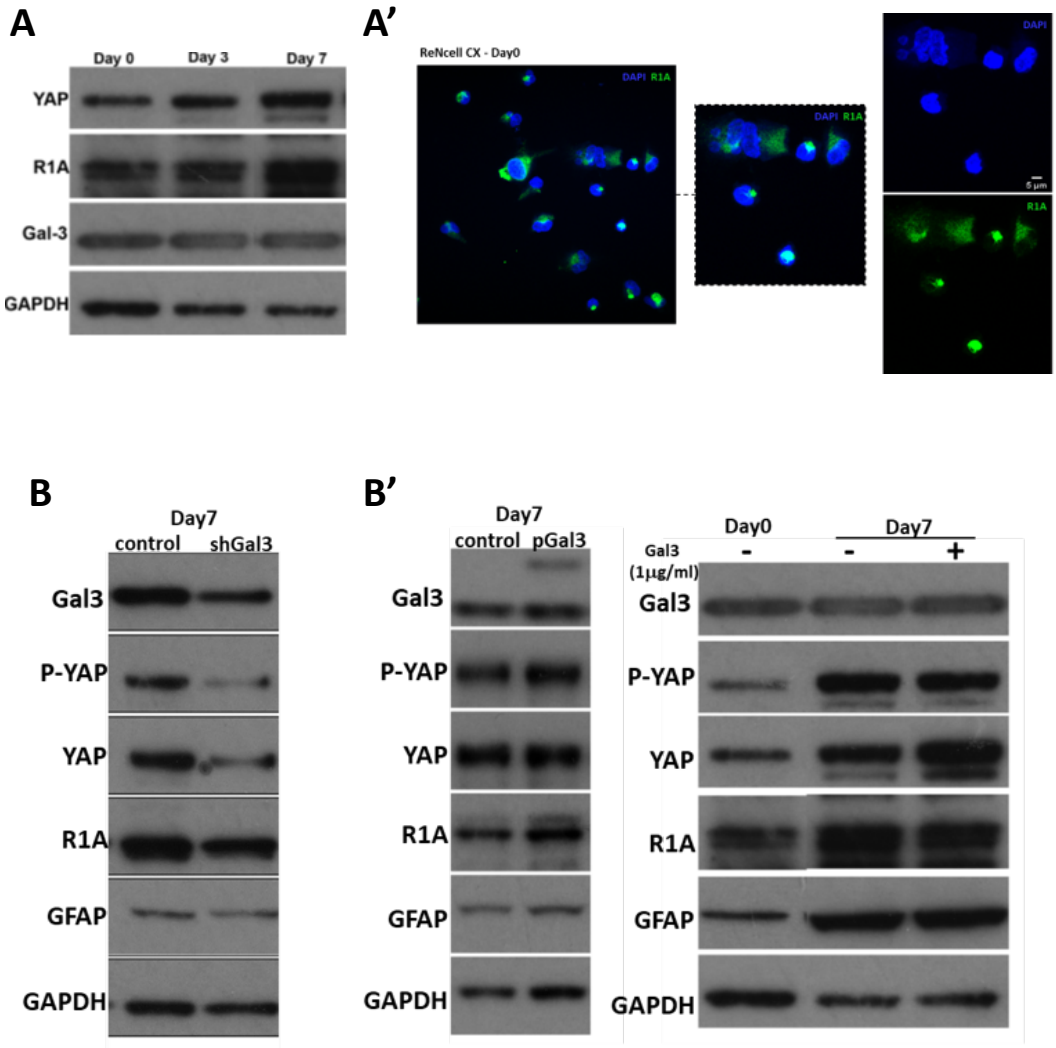


Figure 7.4. Gal-3 and the Hippo pathway in ReNCell®

A) Representative western blotting showing that endogenous levels of YAP and R1A increase during differentiation of ReNCell®. A') Immunofluorescence image exemplifying R1A localisation at Day 0. B) Representative Western blotting of the effect of Gal-3 depletion in the Hippo pathway. B') Representative Western blotting showing the Hippo pathway after upregulation of Gal-3, either upon transfection with Gal-3 OE plasmid (pGal3) or treatment with recombinant Gal-3 (+).

Appendix D. Galectin-3 and cancer

Cancer is a multifactorial disease that present several hallmarks, which support cell survival, proliferation, as well as promoting tumor spread (Hanahan and Weinberg, 2011). Among these hallmarks, inflammation predispose cancer development through the recruitment of immune cells and secretion of cytokines in a host attempt to control tumor growth that will result instead in further tumorigenesis and genomic instability (Colotta et al., 2009; Dvorak, 1986; Grivennikov et al., 2010; Hussain et al., 2003; Qian and Pollard, 2010; Sowers et al., 2014). Moreover, cytokines released activate developmental pathways that shift the tumor towards a more undifferentiated state and increase the number of cancer stem cells (Arnold et al., 2015). In the brain, the SVZ is a uniquely inflammatory region that predispose cancer by the action of inflammatory regulators such as Gal-3 on stem cells (Bardella et al., 2018). Gliomas in contact with the SVZ are indeed more aggressive, likely to spread and reappear, resulting in a worse prognosis (Adeberg et al., 2014; Chen et al., 2015; Gupta et al., 2014; Jafri et al., 2013; Lim et al., 2007; Liu et al., 2016; Liu et al., 2017; Mistry et al., 2017; Sanai et al., 2005; Steed et al., 2016; Vergani et al., 2011; Young et al., 2011).

Gal-3 has been linked with cancer aggressiveness, not only due its pro-inflammatory role, but because it upregulates several pro-tumorigenic pathways. In brain cancer, Gal-3 positively correlated with tumor grade and worse prognosis, being differentially expressed in different types of gliomas, although there is some contradictory literature (Bresalier et al., 1997; Camby et al., 2001; Gordower et al., 1999; Kuklinski et al., 2000; Neder et al., 2004; Strik et al., 2001; Wang et al., 2019). The discrepancy could be explained by differential roles played by Gal-3 depending on tumor stage, cell type

and subcellular localization, a phenomenon not yet not completely understood in the context of gliomagenesis. For example, endothelial cells are strongly positive for Gal-3 in low grade glioma but almost negative in glioblastoma, possibly related with formation of pathological vasculature (Deininger et al., 2002; Neder et al., 2004; Strik et al., 2001). In glioblastoma, Gal-3 staining is strong in pseudopalisading necrosis, evidencing its importance for migration or survival of those cells (Neder et al., 2004).

As previously described, Gal-3 has several pro-survival roles that are related to tumorigenesis, including activation of proliferative pathways, inhibition of apoptosis and anoikis, facilitation of metastasis through interaction with integrins; and regulation of developmental signalling pathways often dysregulated in cancer. Gal-3 is also well known for its pro-inflammatory role, which can predispose cancer through the recruitment of immune cells and secretion of cytokines in a host attempt to control tumour growth that will result instead in further tumorigenesis and genomic instability (Colotta et al., 2009; Dvorak, 1986; Grivennikov et al., 2010; Hussain et al., 2003; Qian and Pollard, 2010; Sowers et al., 2014). Moreover, cytokines released activate developmental pathways that shift the tumour towards a more undifferentiated state and increase the number of cancer stem cells (Arnold et al., 2015).

Here, I observed that several cell lines of glioblastoma express Galectin-3 (Figure 7.5 A and A'). These levels positively correlated with expression of Pax6 and the component of the developmental Hippo pathway YAP and R1A. Interesting, Gal-3 levels negatively correlated with the markers Nestin and Sox2. Immunostaining analysis showed that the distribution of Gal-3 is not homogenous among the cells (Figure 7.5 A'').

Additionally, a mice model of early gliomagenesis generated through insertion of $IDH1^{R132H}$ in the SVZ, has tumour infiltration in the adjacent tissue (Bardella et al., 2016), and high levels of Gal-3 under immunostaining (Figure 7.5. B and B'), with a consequent microglia overactivation (Figure 7.5 B''). The tumour microenvironment frequently present changes in the glycosylation levels in the due to abnormal function of Mgat5, which can mean differential ability of Gal-3 binding (Fernandes et al., 1991; Fortuna-Costa et al., 2014; Granovsky et al., 2000; Kyselova et al., 2008). In gliomas, levels of Mgat5 and the presence of branched N-glycans are related to early gliomagenesis, regulating proliferation and invasion (Hassani et al., 2017; Padhiar et al., 2015; Yamamoto et al., 2000). These facts suggest a role for Gal-3 in events leading to glioma formation and invasion, which can be related to Mgat5 activity.

The evidenced actions of Gal-3 in promoting many aspects of brain tumorigenesis opens the question of whether it would be a good target for treating gliomas, and at which stage. Gal-3 conferred resistance to traditional treatment with chemotherapy and radiotherapy in glioblastoma (Wang et al., 2019). There are several inhibitors of Gal-3 described, some in clinical trial for cancer (Stegmayr et al., 2019; Wdowiak et al., 2018).

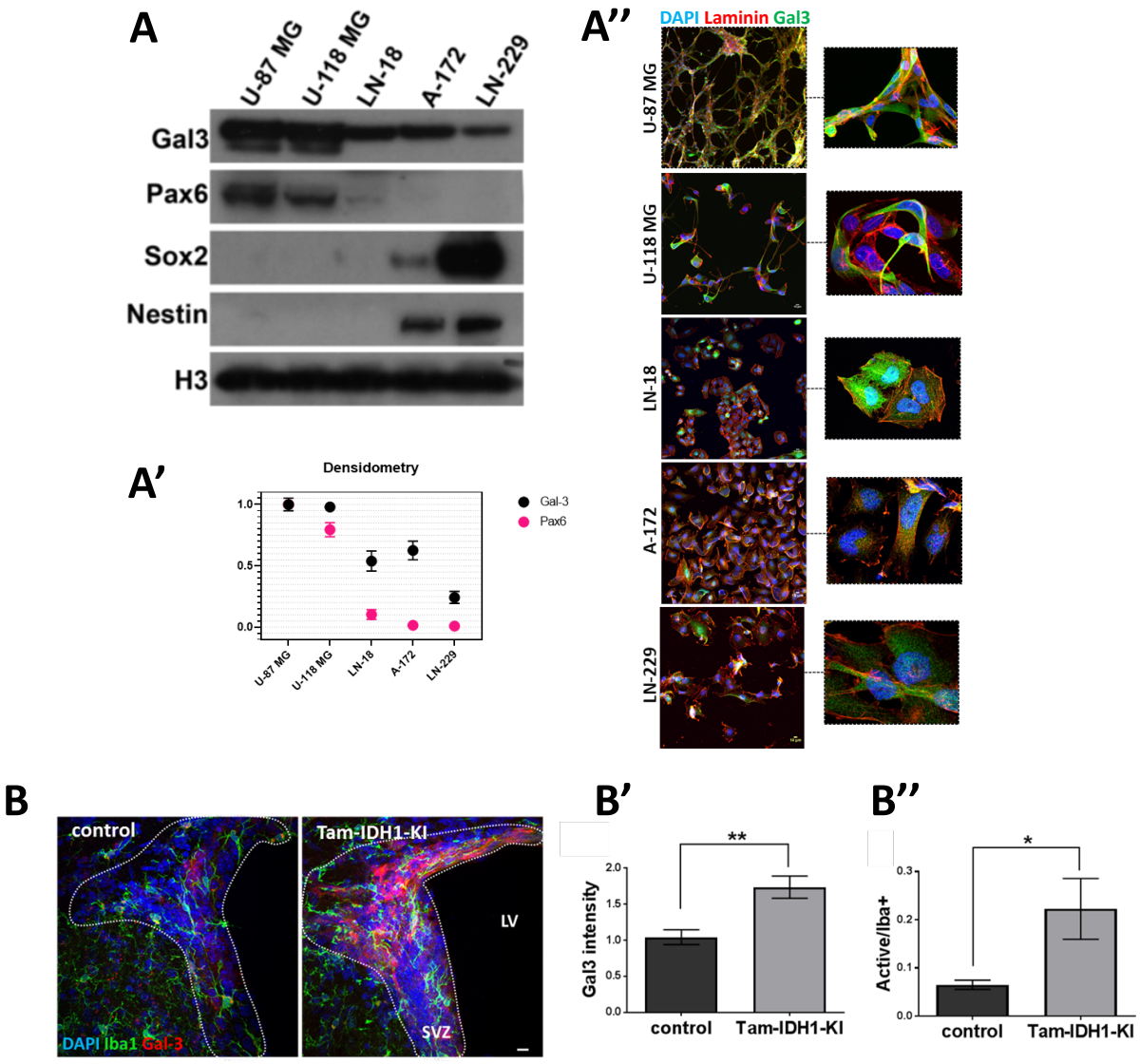


Figure 7.5. Gal-3 and Cancer

A) Representative western blotting showing endogenous levels of Gal-3, components of the Hippo pathway and markers of neural stem cells in different glioblastoma cell lines. Western blots are quantified in (A'), n=3. A'') Immunostaining of Gal-3 in glioblastoma cell lines. Scale bar: 10 μm. B) Confocal image of control and Tam-IDH1-KI (with the insertion of $IDH1^{R132H}$), immune-stained for Gal-3 and Iba1. SVZ is delimited in white dashed lines. LV: lateral ventricle. Scale bar: 10 μm. Gal-3 intensity is quantified in (B') and microglia activation in B'', n=4. Graphs represent mean with SEM; n=4. *$p < 0.05$; **$p < 0.01$.

Appendix E. Free-floating antibodies specificity shown via secondary-only controls

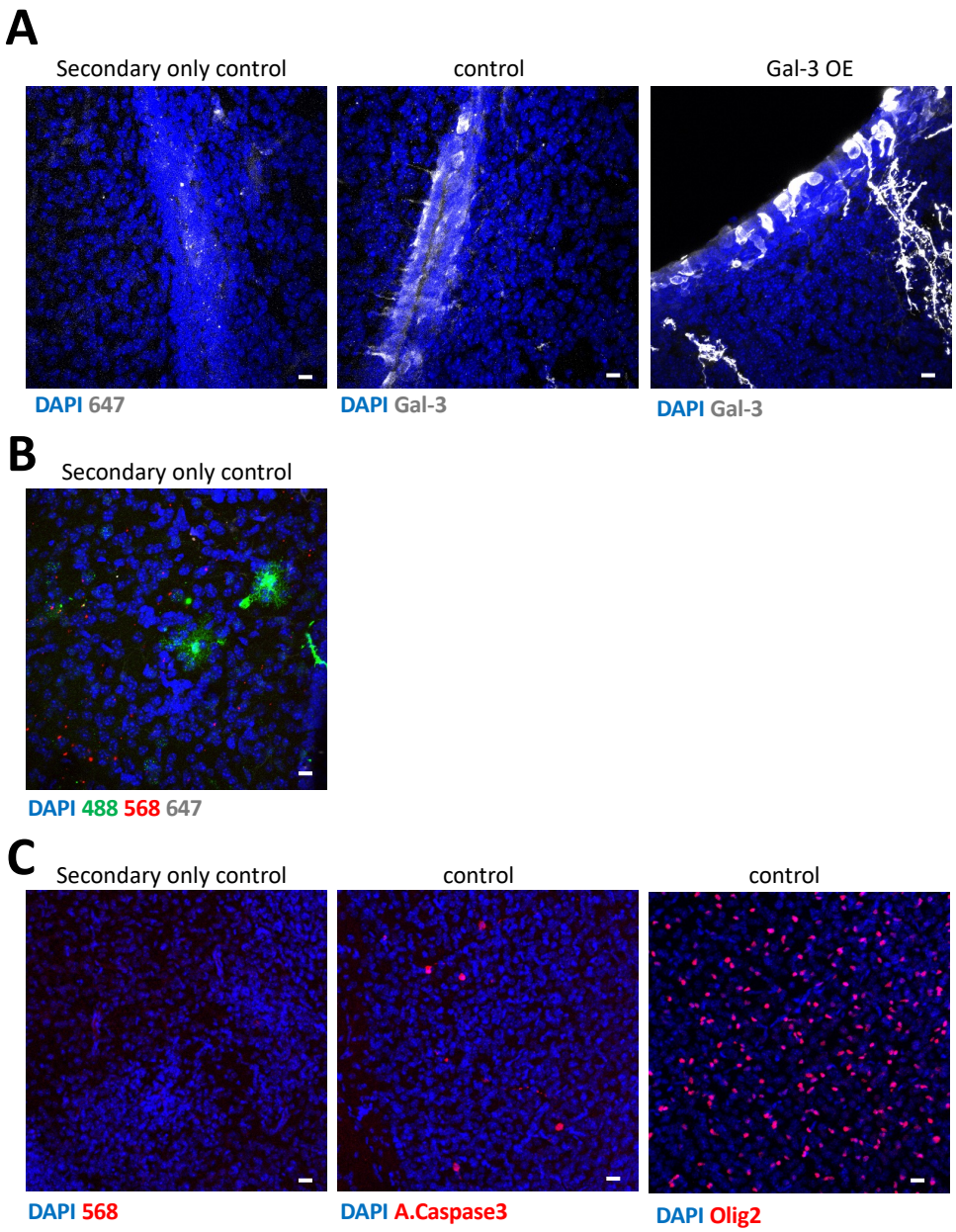


Figure 7.6. Free-floating antibodies specificity.

A) Gal-3 antibody specificity was assessed in 3 DPE control and Gal-3 OE animals. An example of secondary-only control is also shown; referent to Figure 3.3. B) Markers specificity were assessed in 17 DPE mouse via secondary-only control; referent to Figure 3.6. C) A.caspase3 and Olig2 antibodies specificity were assessed in the cortex of control mice via secondary-only control; referent to Figure 3.7. All scale bar 10 μm.